Universidad Politécnica de Cartagena

Depto. de Tecnologías de la Información y las Comunicaciones

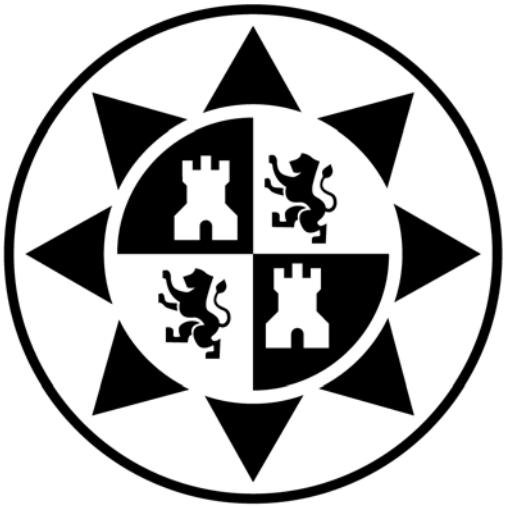

Optimización y Planificación de Redes Ópticas Transparentes WDM

Tesis Doctoral

Ramón Aparicio Pardo

Director:
Pablo Pavón Mariño

Cartagena, 2011

Technical University of Cartagena

Dept. Information and Communication Technologies

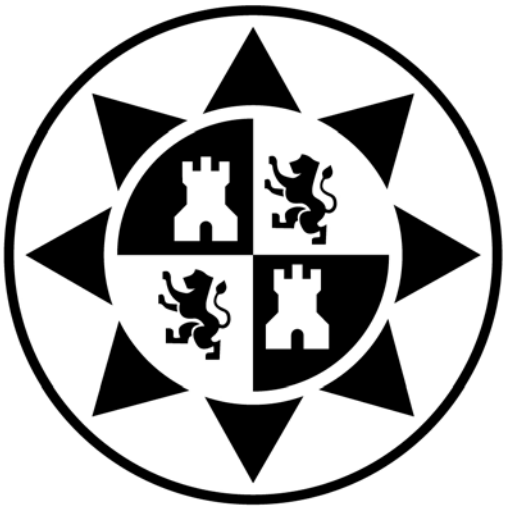

Optimization and Planning of WDM Transparent Optical Networks

Doctoral Thesis

Ramón Aparicio Pardo

Advisor:
Pablo Pavón Mariño

Cartagena, 2011

A mis padres

Resumen

Esta tesis contribuye en el campo de la *optimización y planificación de redes ópticas transparentes WDM*. Las *redes ópticas transparentes* basadas en multiplexación por división de onda (*wavelength division multiplexing*, *WDM*) son las solución tecnológica de las redes troncales de comunicaciones de alta velocidad. En redes transparentes, el tráfico es cursado por medio de conexiones todo-ópticas, llamadas *lightpaths*. Un *lightpath* se origina en un transmisor óptico y termina en un receptor óptico, ocupando un único canal de longitud de onda en cada enlace atravesado. Al ser procesado electrónicamente en los nodos intermedios el tráfico cargado por el lighpath, se pueden conseguir ahorros con respecto al uso de equipamiento de conmutación electrónica. El conjunto concreto de *lighpaths* establecidos sobre la topología física constituye la denominada topología virtual. La planificación de red en estas redes implica resolver un problema multicapa de optimización, al que nos referimos como Diseño de Topología Virtuales (*Virtual Topology Design*, *VTD*): en la capa superior, las demandas de tráfico electrónico son encaminadas a través de la topología virtual, mientras que, en la capa inferior, cada *lightpath* en la topología virtual lo es sobre la topología de red física, al tiempo que se le asigna a una longitud de onda.

El problema de la capa inferior es generalmente denominado Problema de Enrutamiento y Asignación de Longitud de Onda (*Routing and Wavelength Assignment*, *RWA*). El problema completo *VTD* y el problema *RWA* pueden ser modelados exactamente como programas matemáticos, en concreto, como programas de optimización lineal entera mixta (*Mixed Integer Linear Programming*, *MILP*) o programas de optimización lineal entera (*Integer Linear Programming*, *ILP*), respectivamente. En estos modelos matemáticos, algún tipo de coste de la red es minimizado sujeto a restricciones matemáticas que representan la configuración de red. Un diseño *factible* de red corresponde a una solución que satisfaga todas estas restricciones, es decir, una solución contenida en el interior del conjunto definido por estas restricciones. Si la solución es también óptima (p.ej. mínimo coste), el diseño de la red encontrado es el "más barato" posible. Por desgracia, se ha demostrado que los problemas *VTD* y *RWA* son de tipo *NP-hard*, es decir, todavía no se ha encontrado un algoritmo de optimización matemática que sea capaz de resolver el problema en tiempo polinomial. Como consecuencia, problemas de tamaño moderado ya resultan computacionalmente intratables, motivando la necesidad de desarrollar procedimientos

heurísticos subóptimos para proporcionar soluciones aproximadas a las óptimas del problema de planificación. Dado que, para muchos tamaños de red, la solución del modelo exacto no es posible, el planificador de red debe calcular cotas inferiores a los costes mínimos a partir de fórmulas analíticas para estimar la calidad de las soluciones heurísticas subóptimas. Una vez evaluada la "bondad" de los algoritmos heurísticos desarrollados, estos métodos, junto con formulaciones exactas *ILP* o *MILP*, o las mencionadas cotas analíticas pueden ser aplicados a la exploración de compensaciones en los costes de red entre configuraciones alternativas.

En la presente tesis, tres problemas en redes ópticas transparentes son investigados mediante la metodología previamente mencionada: (a) Planificación Estática Multifibra (*Static Multifiber Planning*), (b) Planificación Estática bajo Degradaciones de Capa Física (*Static Physical Layer Impairment Aware*, *PLIA*, *Planning*), y (c) Planificación Multihora (*Multihour Planning*). Algunas conclusiones interesantes se extraen acerca de las mejores configuraciones de red, en términos de costes, y sobre las ventajas y desventajas entre ellas. En los párrafos siguientes se resume el contenido de los capítulos de tesis.

El Capítulo 1 introduce el concepto de redes ópticas WDM, como tecnología para el desarrollo de redes de de comunicación de gran velocidad. Los aspectos de planificación y optimización de estas redes también son presentados. Algunos de los problemas abiertos en esta línea de investigación son destacados, motivando el trabajo realizado en esta tesis. Por último, las contribuciones de esta tesis, elaborada en los capítulos siguientes, se enumeran y resumen.

El Capítulo 2 describe la contribución de esta tesis a la investigación en la planificación multifibra. Es decir, redes en las que más de una fibra puede ser activada en los enlaces entre dos nodos. La contribución de la tesis consiste en un estudio comparativo que evalúa en qué circunstancias la activación de una nueva fibra se prefiere con respecto a la instalación de conversores de longitud de onda, como un medio para aumentar la capacidad de la red. Sorprendentemente, los resultados niegan la utilidad de de la instalación de conversores de longitud de onda, ya que no se encontraron soluciones en las cuales el uso de estos conversores sustituye a la activación de fibras extra.

El Capítulo 3 desarrolla las principales aportaciones de esta tesis en la Planificación Estática bajo Degradaciones de Capa Física o planificación *PLIA*, es decir, cuando las consideraciones de capa física son introducidas en la planificación de redes WDM. En este escenario más realista, el planificador de la red tiene en cuenta los fenómenos físicos que degradan la calidad de la señal óptica. En las primeras secciones del capítulo, presentamos los fenómenos físicos que afectan con mayor severidad a la calidad de la señal, así como algunos métodos para estimar su impacto. Por lo general, dos familias de estrategias se utilizan para determinar si la señal óptica en el receptor cumple la llamada Calidad de Transmisión (*Quality of Transmission*, *QoT*): (i) calcular individualmente el efecto de cada de fenómeno en la *QoT*, o

(ii) elaborar un evaluador global de calidad de la señal, contando todos los fenómenos físicos. Según el método de estimación *QoT*, varias técnicas para incorporar las degradaciones físicas están disponibles para el planificador de red: en el primer caso, las estimaciones individuales de cada efecto se pueden añadir como restricciones a los modelos *MILP* o *ILP*; mientras, en el segundo, se pueden desarrollar algoritmos heurísticos que alternen etapas de planificación de red con evaluaciones globales *QoT*. También, en las primeras secciones, se presentan el conjunto de problemas de planificación *PLIA* abordados en esta tesis. A continuación, las principales contribuciones de esta tesis en este tema se detallan, junto con un breve estado de la técnica. En primer lugar, se proponen dos algoritmos heurísticos para resolver el problema *PLIA-RWA* en redes de 10 Gbps: una búsqueda de optimización global llevada a cabo por las formulaciones *BILP* cuya complejidad es controlada heurísticamente a lo largo de la búsqueda, y un enfoque secuencial, donde las demandas de establecimiento de *lightpaths* se procesan de forma secuencial siguiendo un orden precalculado. En segundo lugar, se estudia el diseño de la topologías virtuales en redes mixtas 10/40 Gbps, teniendo en cuenta interferencias no lineales entre canales. En este estudio, los transceptores de 10 Gbps proporcionan alcances transparentes mayores, mientras que los de 40 Gbps, mayor capacidad y mejores costes por bps. Como consecuencia de ello, estamos interesados en investigar las compensaciones en el coste total de transceptores entre ambos tipos. El problema se formula como un modelo MILP, antes de proponer un algoritmo heurístico basado en una descomposición de la formulación. Finalmente, para concluir las contribuciones en planificación *PLIA*, el autor ha contribuido en el problema relacionado de Colocación de Regeneradores (*Regenerator Placement*, *RP*). La contribución a este problema de planificación, colateral a esta tesis, también se indica.

El Capítulo 4 detalla las contribuciones de esta tesis a la planificación multihora en redes ópticas *WDM*. En contraste con los dos problemas de planificación anteriores en los que se consideraba la demanda de tráfico constante a lo largo del tiempo y la lightpaths se establecían semi-permanentemente sobre la base de este tráfico constante; en la planificación multihora, los cambios de la demanda de tráfico a lo largo de tiempo se suponen conocidos suficiente con precisión de antemano. Entonces, la planificación se lleva a cabo a lo largo de varios periodos de tiempo, tales como las horas o días, modelando la demanda de tráfico entre los nodos de la red como una secuencia de matrices, donde cada una corresponde a un periodo dado. Las ventajas y desventajas presentes en diferentes escenarios de red multihora fueron evaluados: (a) topología virtual reconfigurable o no, suponiendo encaminamiento variable de los flujos de tráfico sobre la topología virtual, (b) encaminamiento fijo o variable sobre los lightpaths, suponiendo topología virtual no reconfigurable, y (c) encaminamiento divisible o indivisible, también asumiendo topología virtual no reconfigurable. De acuerdo con estas configuraciones de red, los problemas *VTD* multihora considerados en esta tesis puede clasificarse en dos grandes familias: (i)

Diseño de Topologías Virtuales Reconfigurables (*Reconfigurable Virtual Topology Design, R-VTD*), done se supone que los componentes ópticos son reconfigurables, y (ii) Diseño de Topologías Virtuales No Reconfigurables (*Non-Reconfigurable Virtual Topology Design*, *NR-VTD*), cuando se consideran *lightpaths* no reconfigurables. En este último grupo, podemos distinguir varias versiones en función de las hipótesis sobre el enrutamiento del tráfico de capa superior sobre la lightpaths: fijo o variable, divisible o indivisible. En todas estas variantes del problema, se evalúa la reducción en el número de transmisores-receptores necesarios para configurar la topología virtual. En la primera sección del capítulo, estos problemas multihora se presentan. En segundo lugar, se resume el trabajo relacionado en la literatura. A continuación, los problemas *VTD* considerados se modelan como formulaciones *MILP*. Después de eso, varios métodos heurísticos son propuestos para manejar problemas de gran tamaño. Algunas de las propuestas heurísticas se corresponden a técnicas clásicas de optimización, como la búsqueda tabú, algoritmos voraces o métodos basados en relajación *lagrangiana*; en cambio, otros algoritmos son nuevos enfoques que hacen uso del concepto de dominación de tráfico para elaborar técnicas eficaces de reducción de la complejidad. Por último, dos estudios sobre los balances de coste entre los antes mencionados diseños de red multihora concluyen el capítulo. En el primer estudio, en un escenario de topología virtual no reconfigurable (problema *NR-VTD*), los balances de coste, en primer lugar, entre encaminamientos fijos y variables, y, a continuación, entre indivisibles y divisibles, son evaluados. El heurístico propuesto para realizar este estudio hace uso de la variante de la dominación de tráfico entre dos matrices de tráfico con el fin de reducir el número de matrices necesarias para resolver el problema. Es decir, el algoritmo heurístico encuentra una única matriz, ya que la dominación del tráfico determina algunas condiciones para eliminar las matrices del problema, pero garantizando que no se elimina ninguna solución factible del espacio de soluciones. Los diferentes tipos de dominación se utilizan para tratar cada uno de los problemas antes mencionados NT-VTD: la *dominación débil* en problemas de enrutamiento variable, y, la *dominación total* en problemas de enrutamiento fijo. Por otra parte, los casos de enrutamiento indivisible se resuelven mediante la llamada *dominación respecto flujos indivisibles*. En el segundo estudio, se asume como variable en el tiempo el enrutamiento de flujos de tráfico, para explorar las ventajas e inconvenientes que surjan entre topologías virtuales reconfigurable y no reconfigurables. Por lo tanto, las soluciones de problemas *R-VTD* y *NR-VTD* se comparan. Con este objeto, todos los algoritmos heurísticos propuestos en el capítulo se utilizan: para el caso no reconfigurable, los algoritmos basados en la dominación del tráfico; para el caso reconfigurable, una búsqueda tabú (*TS*), un algoritmo de de subgradiente basado en una relajación *lagrangiana* (*LRvSG*) y un algoritmo voraz (*GARF*). Además, esta último heurístico fue empleado para analizar el impacto de la frecuencia con la que se reconfiguran *lightpaths* sobre el coste de transceptores.

Por último, el Capítulo 5 concluye la tesis, resumiendo los principales resultados y sugiriendo

posibles líneas futuras de investigación. De los dos problemas de planificación más intensamente investigados en la tesis, Planificación Estática bajo Degradaciones de Capa Física (Planificación *PLIA*) y Planificación Multihora, algunas conclusiones importantes pueden ser extraídas. En cuanto a la Planificación *PLIA*, los efectos físicos que degradan la calidad de transmisión fueran investigados tanto en redes de una única tasa binaria como en redes mixtas. En primer lugar, el estudio de las redes de una única tasa de 10 Gbps nos sugiere que reencaminar los *lightpaths* encontrados lo largo de la búsqueda en el espacio de soluciones, y conducir dicha búsqueda utilizando información precalculada sobre la capa física son estrategias válidas para diseñar algoritmos *PLIA RWA* eficientes y escalables. En segundo lugar, el estudio de redes mixtas con varias tasas binarias 10/40 Gbps apunta a que las interferencias no lineales entre señales moduladas en intensidad a tasas de 10 Gbps y señales moduladas en fase a tasas de 40 Gbps disuade de mezclarlos en redes altamente cargadas, a pesar de los posibles balances entre los mayores alcances transparentes de transmisores-receptores de 10 Gbps y la mayor capacidad y mejor coste por bps de los transceptores de 40 Gbps puede justificar la coexistencia de tasas binarias diferentes en la misma línea de transmisión. Con respecto a la planificación *Multihora*, los balances de coste mencionados en el párrafo anterior fueron evaluados, obteniendo resultados interesantes. En las redes donde la reconfiguración de la topología virtual no está permitida, la utilización de enrutamiento variable en lugar de fijo introduce una moderada reducción de costes en términos del número de transceptores necesarios para establecer la topología virtual. Del mismo modo, el más flexible enrutamiento divisible no supone una reducción significativa del coste total de transceptores en comparación con la opción indivisible. Los balances de costes en topologías virtuales totalmente reconfigurables también fueron estudiados. En este caso, una vez más, la reducción del número de transceptores fue muy limitada. Incluso, algunos resultados indican que una "red casi no reconfigurable" (por ejemplo, permitiendo una sola reconfiguración por hora en toda la red) podría proporcionar una reducción de costes similares a los de una red totalmente reconfigurable.

Además, dos anexos completan la tesis con algunas contribuciones colaterales obtenidas a lo largo de la misma. En el anexo A, la herramienta de planificación de redes ópticas *MatPlanWDM*, desarrollada por la Universidad Politécnica de Cartagena (UPCT) con fines educativos y de investigación se describe brevemente. Parte del proceso de desarrollo de la herramienta se llevó a cabo en el marco de esta tesis. Además todos los algoritmos propuestos en esta tesis fueron desarrollados y probados en esta herramienta. A su vez, el anexo B resume algunas de definiciones relevantes para esta tesis en el ámbito de la dominación de tráfico. En primer lugar, se introduce la dominación entre dos matrices, junto con sus variantes empleadas en el algoritmo utilizado para explorar las ventajas y desventajas de las redes no reconfigurables. A continuación, se presenta la generalización de los tipos anteriores de dominación a los conjuntos de matrices. Finalmente, se describe un esquema general para aplicar la dominación entre

conjuntos de matrices en problemas de redes generales de comunicación.

Abstract

The present thesis contributes in the field of the *optimization and planning of WDM transparent optical networks*. *Transparent optical networks* based on *wavelength division multiplexing* (*WDM*) are the enabling technology for high-speed backbone networks. In transparent networks, traffic is carried over all-optical connections, called *lightpaths*. A lightpath originates at an optical transmitter and terminates at an optical receiver, occupying a single wavelength channel in each traversed link. Since the traffic carried over a lightpath is not processed electronically at intermediate nodes, savings with respect to electronic switching equipment can be achieved. The particular set of lightpaths established over the physical topology constitutes the so-called virtual topology. The network planning in these networks implies solving a multilayer optimization problem named *Virtual Topology Design* (*VTD*): in the upper layer, electronic traffic demands are routed over the virtual topology; whereas, in the lower layer, each lightpath in the virtual topology is routed over the physical network topology and assigned to a wavelength. The lower layer problem is generally called *Routing and Wavelength Assignment* (*RWA*) *problem*. The overall *VTD* and the *RWA* problem can be modeled exactly as Mixed Integer Linear Programming (MILP) or Integer Linear Programming (ILP) formulations, respectively. In these mathematic models, some kind of network cost is minimized subject to the constraints representing the network configuration. A *feasible* network design corresponds to a solution meeting all the constraints, that is, a solution contained inside the *feasible* set defined by these constraints. If the solution is also optimal (e.g. minimal cost), the network design found is the "cheapest" possible. Unfortunately, *VTD* and *RWA* problems have been proved as NP-Hard, that is, a mathematical optimization algorithm able to solve the problem in a polynomial time has still not been found. As a consequence, moderate-sized problems are computationally intractable, motivating the need of developing suboptimal heuristic procedure to provide approximate solutions to the optimal ones of the planning problem. Since, for many network sizes, solving the exact model is not possible, the network planner must devise lower bounds on the minimal costs from analytical formulae to estimate the quality of the suboptimal heuristic solutions. Once assessed the "goodness" of the developed heuristic algorithms, these methods along with exact ILP or MILP formulations or the referred analytical bounds can be applied to explore tradeoffs on network costs among different network configurations.

In the present thesis, three problems in transparent optical networks are investigated using methodology previously mentioned: (a) *Static Multifiber Planning*, (b) *Static Physical Layer Impairment Aware (PLIA) Planning*, and (c) *Multihour Planning*. Some interesting conclusions are extracted about the best network configurations to minimize the network costs and about the cost tradeoffs among them. The next paragraphs summarize the content of the thesis chapters.

Chapter 1 introduces the optical WDM network concept, as an enabling technology for high capacity communication networks. The planning and optimization aspects of these networks are also introduced. Some of the open problems in this research line are highlighted, motivating the work carried out in this thesis. Finally, the contributions of this thesis, elaborated in subsequent chapters, are listed and summarized.

Chapter 2 describes the contribution of the present thesis to the research in the *multifiber planning*. That is, networks in which more than one fiber can be activated in the links between two nodes. The contribution of the thesis consists of a comparative study which evaluates in what circumstances activating a new fiber is preferred with respect to installing wavelength converters, as a medium to increase the network capacity. Surprisingly, results neglect the utility of the installing wavelength converters, since solutions where the use of wavelength converters replaces the activation of extra fibers were not found.

Chapter 3 develops the main contributions of the present thesis in *Physical Layer Aware Planning (PLIA) planning*, that is, when physical layer considerations are introduced in the planning of WDM networks. In this more realistic scenario, the network planner takes into account those physical phenomena which degrade the quality of the optical signal. In the first sections of the chapter, we introduce those impairments that impact more severely on the signal quality, as well as some methods to estimate this impact. Generally, two families of strategies are used to determine if the optical signal at the receiver satisfies the Quality of Transmission (QoT) requirements: (i) computing individually each impairment effect on the QoT; or (ii) devising a global QoT performance evaluator accounting all the impairments. According to QoT estimation method, several alternate techniques to incorporate the physical later impairments are available for the network planner: in the first case, individual estimations of the impairments can be added as constraints to ILP or MILP models; whereas, in the second one, heuristic algorithms alternating network planning stages with global QoT evaluations can be devised. In addition to this, the set of Physical Layer Impairment Aware (PLIA) planning problems addressed in this thesis are presented. Next, the major contributions of this thesis in this topic are detailed, along with a brief state of the art. First, two heuristic algorithms to solve the PLIA-RWA problem in 10 Gbps single line rate networks are proposed: a global optimization search conducted by BILP formulations whose

complexity is controlled heuristically along the search, and a sequential approach where the lightpath demands are processed sequentially according to a precomputed ordering. Secondly, the virtual topology design in 10/40 Gbps mixed line rate networks considering non linear inter-channel interferences is studied. In this study, the 10 Gbps transceivers provide longer transparent reaches, whereas the 40 Gbps ones, higher capacities and better costs per bps. As a consequence, we are interested in investigating the tradeoffs on the total transceiver cost between both types of transceivers. The problem is formulated as a MILP model, before proposing a heuristic algorithm based on a decomposition of the formulation. Finally, to conclude the PLIA planning contributions, the author has contributed in the related field of Regenerator Placement problem in semi-transparent optical networks. The contribution in this planning problem, collateral to this thesis, is also outlined.

Chapter 4 details the contributions of this thesis to the *multihour planning* in optical WDM networks. In contrast to the two previous planning problems where the traffic demand was considered constant along time and the lightpaths were established semi-permanently based on this constant traffic, in multihour planning, the traffic demand changes along time following a variation assumed to be accurately known in advance, i.e., the traffic demand can be seen as scheduled. Then, the planning is performed along several time epochs, such as hours or days, modeling the scheduled traffic demands between the network nodes as a sequence of matrices, corresponding each one of them to a given time epoch. Different tradeoffs in multihour networks were evaluated considering different network scenarios: (a) reconfigurable or non-reconfigurable *virtual topology*, assuming time-variable flow routing on top of the virtual topologies; (b) fixed or variable flow routing, assuming non-reconfigurable virtual topology; and (c) *splittable* or *unsplittable* flow routing over the *virtual topology*, also assuming non-reconfigurable virtual topology. According to these network configurations, the multihour VTD problems considered in this thesis can classified into two big families: (i) Reconfigurable Virtual Topology Design (*R-VTD*), when optical components are assumed to be reconfigurable; and, (ii) Non-Reconfigurable Virtual Topology Design (*NR-VTD*), when non-reconfigurable lightpaths are considered. In this last group, we distinguish several variants depending on assumptions about the routing of the higher layer traffic over the lightpaths: time-fixed or time-variable, splittable or unsplittable. In all these problem variants, we evaluate the reduction on the number of transceivers required to set up the virtual topology. In the first section, these multihour VTD problems are stated. Second, a survey of the topic is described. Next, the considered VTD problems variants are modeled as MILP formulations. After that, the heuristic approaches proposed in the framework of the thesis to handle large sized problems are enumerated. Some of the heuristic proposals correspond to classical optimization techniques, such as tabu searches, greedy algorithms or lagrangean relaxation based methods; meanwhile, other ones are novel approaches that make use of the traffic domination concept to devise efficient complexity reduction techniques. Finally,

two studies exploring the aforementioned cost tradeoffs among different multihour network designs conclude the chapter. In the first study, in a non-reconfigurable virtual topology scenario (NR-VTD problems), the cost tradeoffs between, first, fixed versus time-variable traffic routing; and, then, splittable versus unsplittable routing are evaluated. The heuristic proposed used to perform this study makes use of the traffic domination variant between two traffic matrices in order to reduce the number of matrices required to solve the problem. Namely, the heuristic algorithm finds one unique matrix, since the traffic domination determines some conditions to eliminate matrices from the problem, but ensuring that we do not remove any feasible solution from the solution space. Different types of domination are used to address each one of them aforementioned non reconfigurable multihour virtual topology designs problems: *weak domination* in time-variable flow routing problems; and, *total domination* in fixed flow routing ones. Moreover, usplittable routing cases are solved using the so-called *domination with respect unsplittable flows.* In the second study, we assume as time-varying the traffic flow routing to explore the tradeoffs arising between reconfigurable and non-reconfigurable virtual topologies. Therefore, solutions from R-VTD and NR-VTD problems are compared. For this is study, all the heuristic algorithms proposed in the chapter are used: for the non reconfigurable case, the traffic domination based algorithms; for the reconfigurable case, a Tabu Search (TS), a Lagrangean Relaxation via Subgradient Optimization (LRvSG) technique and a Greedy Approach with Reconfiguration Flattening (GARF). Finally, this last heuristic was employed to analyze the impact on the transceiver cost of the lightpath reconfiguration frequency.

Finally, Chapter 5 concludes the thesis, summarizing the main results, as well as, suggesting possible future research lines. From the two planning problems more intensely investigated, that is, *Physical Layer Aware* (*PLIA*) *Planning* and *Multihour Planning*; some important conclusions are extracted. Concerning *PLIA Planning*, the physical impairments in single line rate and mixed line rate networks were studied. First, the study in 10 Gbps single line rate networks suggests us that rerouting the found lightpaths along the search space and driving the search using precomputed physical layer information are valid strategies to design efficient and scalable PLIA-RWA algorithms. Secondly, the 10/40 Gbps mixed line rate study points out that non linear interferences between 10 Gbps intensity modulated signals and 40 Gbps phase modulated signals dissuade to mix them in high loaded networks, although the tradeoffs between longer transparent reach of 10 Gbps transceivers, versus higher capacity and better cost per bps of 40 Gbps transceivers, could justify the coexistence of both different bit rates in the same transmission line. With Respect to the *Multihour Planning*, the tradeoffs mentioned in the previous paragraph were assessed, obtaining interesting results. In networks where reconfiguration along the time of the virtual topology is not allowed, the utilization of variable routing instead fixed over the lightpaths introduces moderate network cost reduction in terms of the number of transceiver required to set up the virtual topology.

Similarly, more flexible spittable routing does not suppose a significant transceiver cost reduction too in comparison with the unsplittable option. The cost tradeoffs in fully reconfigurable virtual topologies were also studied. In this case, once again the transceiver reduction was very limited. Even some results indicate that an “almost non- reconfigurable network” (e.g. allowing one lightpath reconfiguration in the whole network per hour) might provide still a similar transceiver cost reduction than a fully-reconfigurable network.

Furthermore, two annexes complete the thesis with some collateral contributions. In the Annex A, the optical network planning tool MatPlanWDM, developed by the Technical University of Cartagena (*Universidad Politécnica de Cartagena*, *UPCT*) for educational and research purposes is briefly described. Part of the development process of the tool was carried out in the framework of the thesis. Besides, all the algorithms proposed in this thesis were developed and tested in this tool. In its turn, Annex B summarizes some relevant definitions in the field of the traffic domination. First, the domination between two matrices is introduced, along its variants employed in the algorithm used to explore the tradeoffs in non-reconfigurable networks. Next, the generalization of the previous domination types to apply to sets of traffic matrices is presented. Finally, a general scheme to apply the domination between sets of matrices in general communication network problems is outlined.

Agradecimientos

En estos últimos cuatro años muchas personas han contribuido a que esta tesis se haga realidad. A todos ellas, me gustaría expresarles mi agradecimiento.

En primer lugar, a Pablo, mi director, mentor y amigo, al que debo lo que soy como investigador. Sin su dirección exigente, pero, también, honesta, comprometida y brillante, esta tesis no habría sido posible. De él he aprendido mucho, y sigo aprendiendo, y no sólo de investigación.

Una mención muy especial merece Belén, compañera inigualable y generosa, que ha compartido conmigo gran parte de este camino. Amiga y confidente de sinsabores, pero, también, de alegrías en estos años. ¡Ánimo, que en unos meses tú también estarás aquí!

A Joan, por sus buenos consejos y ayuda inestimable en múltiples ámbitos, desde la propia investigación hasta el papeleo administrativo.

A Nina, por su trabajo y colaboración a lo largo de esta tesis, así como por su esfuerzo y tiempo dedicado a hacerme sentir como en casa en Zagreb. En esto último, también quiero mencionar a Marija y a Masa, mis queridas compis croatas.

También me gustaría dar mi más sincero agradecimiento a Michal, por acogerme en su grupo y darme la oportunidad de ampliar mis conocimientos de optimización multihora.

Quiero dedicar también unas líneas a Gonzalo, viejo amigo y compañero de armas, con el que empecé esta aventura en tierras mucho más frías. Su trabajo y apoyo leal e incondicional tienen parte de culpa de que ahora esté escribiéndolas.

No quiero olvidarme de mis compañeros de los laboratorios de telemática, a los que están y a los que se han ido, con los que he compartido momentos inolvidables, dentro y fuera del laboratorio, y a muchos de los cuales puedo llamar también "amigos".

También me gustaría expresar mi agradecimiento sincero a la gente del Departamento, tanto técnicos como investigadores, que siempre han estado dispuestos a echarme una mano cuando lo he necesitado.

Finalmente, quiero darles las gracias a mis padres, que lo han dado y siguen dando todo por mí, y a los que debo todo lo que soy y tengo, y gran parte de lo que seré. Quiero dedicarles a ellos muy especialmente esta tesis, que es algo tan suyo como mío. Ellos han soportado mis días duros de trabajo, se han alegrado con mis éxitos y siempre me han apoyado incondicionalmente. Gracias, Papá y Mamá.

Índice

List of Contents

List of Figures

List of Tables

Chapter 1

1 Introduction

ABSTRACT: This Chapter introduces the optical WDM network concept, as an enabling technology for high capacity communication networks. The planning and optimization aspects of these networks are also introduced. Some of the open problems in this research line are highlighted, motivating the work carried out in this thesis. Finally, the contributions of this thesis, elaborated in subsequent chapters, are listed and summarized.

1.1 Optical WDM Networks

In the last decade, the tremendous growth of the Internet along with the appearance of new bandwidth intensive applications (video-on-demand or multimedia conferencing) have increased the volume of the traffic in the communication backbone networks. The forecasts maintain this trend in the near future. Therefore, it is clear the necessity to provide larger capacities to the long haul backbone networks to meet the increasing traffic demands. In this scenario, ***optical fiber networks based on Wavelength Division Multiplexing*** (***WDM***) [1] have shown to be the winner technology. The optical fiber has a set of potentially limitless capabilities [1], such as huge bandwidth (e.g. a 69.1 Tbps transmission in a single fiber has been proved) [2], low signal attenuation (e.g. 0.2 dB/km), low signal distortion and low power requirement. As an example of the superiority of the optical fiber technology for building high-capacity links, it is interesting to note that the potential bandwidth in optical fibers is more than 1000 times the bandwidth available in the radio communications spectrum. The ***Wavelength Division Multiplexing*** (***WDM***) technique exploits this enormous bandwidth by splitting it into smaller bandwidth channels centered at a wavelength (color) of laser light. Of course, the information is transmitted like optical signals in these wavelength channels.

Unfortunately, there exists a serious limitation on the use of all the potential bandwidth in the ***WDM optical networks***. While the transmission capacity of the fiber media is in the order of tens of Tbps, the processing speed of the electronic switching equipment at the ends of the fibers is in the order of tens of Gbps (3 orders of magnitude smaller). This speed mismatch supposes that the data transmitted optically at higher rates in the fibers must be converted into the electronic format before being processed in the switching equipment at lower electronic rates. Once done that, the data must be returned to the optical domain to continue travelling in the network. All this process is generally referred as to ***OEO conversion***.

As a consequence, the network capacity is not limited by the "faster" transmission media (optical fiber), but the "slower" electronic equipment, constituting, indeed, an "electronic bottleneck" [1] on the network speed. Besides the "electronic bottleneck", additional reasons to reduce as much as possible the *OEO conversions* are the more expensive costs of the electronic equipment in terms of market price, space or power consumption [3]. An illustrative example is that 80 Cisco Carrier Routing Systems CRS-1 (for which each chassis weights up to 795 kg) are required to switch 90 Tbps [4].

In order to address the "electronic bottleneck", several alternatives have been proposed to perform the data switching in the optical domain, gapping the electronic processing. These optical switching paradigms are: Optical Packet Switching (OPS), Optical Burst Switching (OBS) and Optical Circuit Switching (OCS) [5]. However, the only one technologically matured and commercially available is the last, the *Optical Circuit Switching*, also known as *Wavelength Routing* (*WR*) [5]. The optical WDM networks based on this switching paradigm are, generally, referred as to *Wavelength Routed Networks* (*WRNs*), and also *transparent optical networks*.

In Wavelength Routed Networks, fiber optical links interconnect switching nodes, some of them are also local access nodes, constituting an optical switching network. A switching node is a point in the network where the data can be "moved" from an incoming fiber to an outgoing one or, if the node is a local access point, drawn from the net or injected into it. The fiber links, that start or terminate in the nodes, are usually called *physical links*. The interconnection graph composed of nodes and fiber links is known as *physical topology* (*PT*).

Switching nodes in WR networks consist of both optical and electronic equipment able to switch the data at optical and electronic rates, respectively. In the Fig. 1.1 the typical architecture of a WR node is shown. The optical equipment is represented by the *Optical Add-Drop Multiplexer* (*OADM*) block. Optical Add Drop Multiplexers add optical signals to output ports tuned at certain wavelengths channels or drop the signals from input ports also tuned at certain WDM channels. The core of the optical equipment in the *OADM* block is a device named *Wavelength Crossconnect* (*WXC*). A Wavelength Crossconnect (WXC) switches individual wavelength channels, simultaneously, from any input port to any output port. If the wavelength channel in the output port is the same as the wavelength in the output port, the crossconnect is called *Wavelength Selective Crossconnect* (*WSXC*). Conversely, when the wavelength in the output port is different from the one in the output port, the device is called *Wavelength Interchanging Crossconnect* (*WIXC*). In the latter case, the Wavelength Crossconnect is equipped with *Wavelength Converters* (*WC*) which adds the capability of changing the wavelengths used. In this thesis, we assume that the internal architecture of the *OADMs* and *WXCs* enable any wavelength to be added to any outgoing port or dropped from any incoming port, switching optically WDM channels from input to

output ports without any internal blocking constraint.

The *OADM* input ports may be tuned at wavelength channels of incoming fibers or be connected directly to electro-optical conversers (also denoted as *optical transmitters* and referred in Fig. 1.1 as *T*). Analogously, output ports may be tuned at wavelength channels of outgoing fibers or be connected directly to opto-electronic conversers (also denoted as *optical receivers* and referred in Fig. 1.1 as *R*). Therefore, whenever the wavelengths switch from any input to any output port without using optical transmitters or receivers (named jointly as transceivers), *OEO conversions* are avoided. That is the main advantage of *OADMs* which Wavelength Routed Networks take profit from to overcome the electronic bottleneck. In fixed *OADMs*, the connections from input to output ports are hard-wired. Conversely in *Reconfigurable Optical Add-Drop Multiplexers* (*ROADMs*), all the arrangements can be dynamically reconfigured in tens of milliseconds.

The other main block of a WR node in Fig. 1.1 is the *electronic equipment*. This block is devoted to perform all electronic processing and switching in the network. Therefore, optical signals (from or to the *OADM* block) must experience *OEO conversions* in optical transceivers to pass through the *electronic equipment*. In addition to this, these electronic processing blocks are responsible for adding or dropping local data in electronic format, constituting the access points of the information in the network.

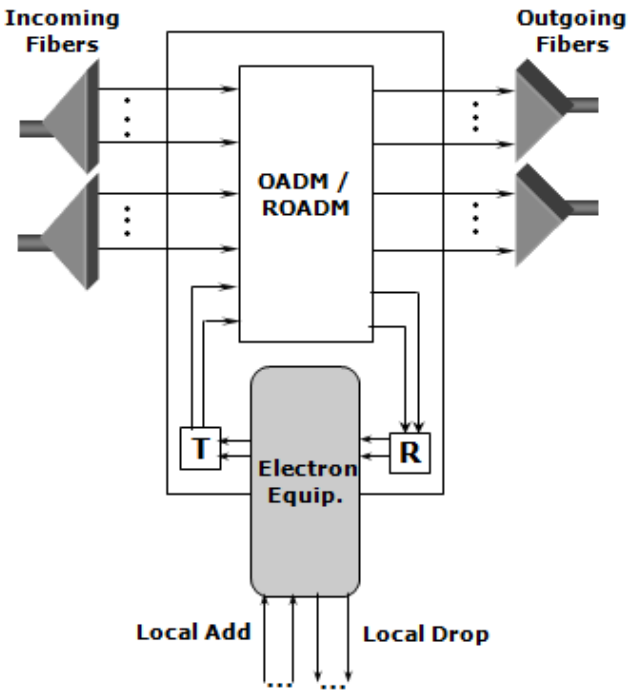

Fig. 1.1. Architecture of a Wavelength Routing node.

A Wavelength Routed Network uses all-optical paths to serve the traffic demands between the node pairs. These all-optical paths are named as **"lightpaths"**, since the *light signals* generated at optical transmitters (*T*) at origin nodes reach optical receivers (*R*) at destination nodes by traversing, without leaving the optical domain, network links and nodes. At the intermediate nodes, the OADMs optically switch the data from a WDM channel in an input port to a WDM channel in an output port, bypassing electronic signal processing and OEO conversions (like data path 1 shows in the Fig. 1.2). A *lightpath* is defined by selecting a path, that is, a sequence of fiber links, and reserving a particular WDM channel on each of these links. If the WR nodes traversed by the *lightpath* are equipped with *Wavelength Converters* (*WCs*), the wavelength reserved on each fiber link can be different. Otherwise, it must be the same and, then, it is said that the *lightpath* meets the *wavelength continuity constraint*. Since the *lightpaths* are actually virtual connections which connect end nodes masking the underlying *physical topology*, they are also referred as to *virtual links* and, thus, the particular network topology graph composed by them is named as *virtual topology* (*VT*). One remarkable fact is that a WDM network based on *lightpaths* constitutes a ***transparent optical network***. *Transparency*, in the strict sense, means that the physical medium (an optical WDM channel in our case) supports end-to-end communication of data, independent of bit rates and signal formats [6]. In our case, a *lightpath* establishes a transparent communication between the end nodes bypassing optically the intermediate ones.

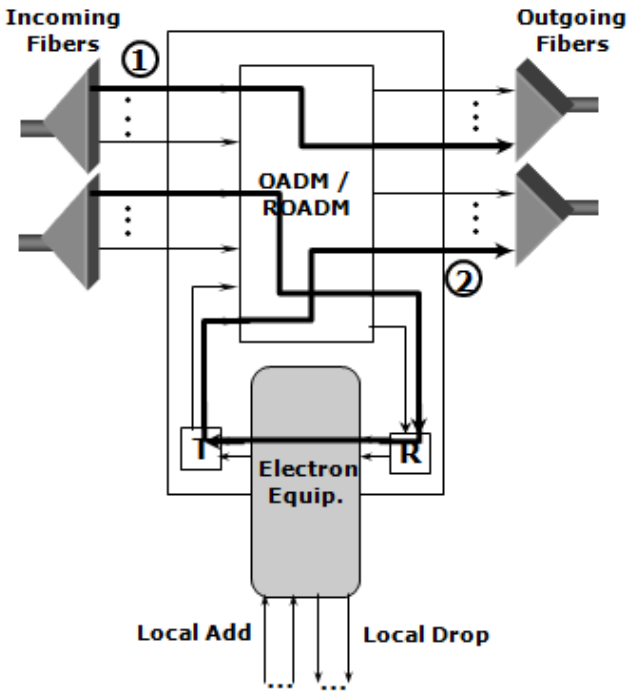

Fig. 1.2. Optical (1) and electronic (2) data paths in a WR node.

In an ideal *transparent optical network*, a traffic demand between any pair of nodes can be supported by a direct *transparent lightpath*. Unfortunately, in the real case, some demands cannot be served through transparent connections since it is not possible to set up a lightpath between their end nodes. There exist several reasons for this *lightpath blocking*: (i) the lack of network resources sufficient to establish the *lightpath*, such as available WDM channels in the fibers or optical transceivers (transmitters or receivers) at the nodes; (ii) the absence of a path with the same available wavelength channel between the end nodes, or (iii) the degradation on the quality of the signal as it travels through several optical components along its lightpath. The first type of blocking is named as *network capacity blocking* and its unique viable solution is to increase the network capacity, e.g., adding more fibers to the physical links or installing mores transceivers at the nodes. The second type, denoted as *wavelength blocking*, appears solely in networks with wavelength converters and can be solved either equipping the nodes with *WCs* or also adding more fibers to the physical links. Finally, the third type is referred as to *signal regeneration blocking* and can be solved by using regenerator equipment. Some of these solutions can break the optical network transparency, since some wavelength converters and signal regenerators process electronically the data to perform their functionality. For example, in the Fig. 1.2, the data path 2 can exemplifies this situation, since signal regeneration can be carried out by the *electronic processing equipment*. Then, *OEO conversion* must be introduced, breaking the *lightpath* into several all-optical transparent fragments. Depending on the number of all-optical fragments in a single *lightpath*, we can enumerate three different scenarios: ***transparency***, ***opacity***, and ***translucency*** [6]. The first one is the paradigm already explained: every *lightpath* is an all-optical path. Conversely, in ***opaque networks***, there are as many all-optical fragments as fiber links in the lightpath, that is, the optical signal carrying traffic terminates at each node to undergo an *OEO conversion* and an electronic processing. This approach simplifies the network design and control since there is a full independence between the network and the physical layer. Finally, ***translucent (or semitransparent) networks*** are an intermediate alternative to both fully *transparent* and fully *opaque* networks. In *translucent networks*, a *lightpath* traverses several all-optical fragments. In each one of them, an optical signal travels "as far as possible" before its quality (say, bit-error rate (BER)) degrades, thereby requiring it to be electronically regenerated. The *transparent optical WDM networks* and *its relaxed translucent version* are the technological framework of the present thesis.

If a direct *lightpath* between a pair of nodes demanding a connection cannot be set up and none of the above commented solutions to the *lightpath blocking* is available, the offered traffic to the end nodes must be carried from the source node of the communication to the destination one by traversing several indirect *lightpaths*. In other words, if some traffic must be served between a pair of nodes *a* and *b*, and *b* is not reachable in one *virtual hop* (direct *lightpath* between *a* and *b*), then, the traffic must be routed through an intermediate node *c* using, e.g., two *virtual hops* (or *indirect lightpaths*), the first one between *a* and *c*,

and the second one, between *c* and *b*. At the intermediate node *c*, the information must be switched electronically from the incoming *lightpath* to the outgoing one, what implies *OEO conversion* and *electronic processing* (like data path 2 shows in the Fig. 1.2). Consequently, this multihop approach also breaks the optical transparency in the network, but in contrast to electronic regenerators, here the electronic equipment allows *traffic grooming*, i.e., to add small local data flows to the traffic in a outgoing *lightpath*. These data will be dropped from the groomed traffic in the incoming *lightpaths*, also, by the electronic equipment at destination node of the communication.

Before concluding this Section, it is important to note the inherent *multilayer* structure described in the previous paragraphs. Firstly, we have an underlying *physical* (*topology*) *layer* composed by the fiber links. Above, the *lightpaths* establishes a *optical layer* or *virtual* (*topology*) *layer* over the fiber links. And, finally, if single virtual hop solutions are not feasible, higher layer traffic flows (e.g. IP connections) are routed over the *lightpaths* of the *virtual topology*. The Fig 1.3 depicts the multilayer scheme of the ***optical WDM networks***, technological scenario of the present thesis, along with one example. A higher layer traffic flow (black arrow) is routed over two *lightpaths* (grey arrows) to connect nodes *2* and *6*. One *lightpath* is set up directly between the nodes *2* and *3* on the wavelength w_2, while the second one connects the nodes *3* and *6* via the node *5* occupying the WDM channel w_1. In the node *3*, the data are electronically switched (see data path 2 in Fig. 1.2). Conversely, in the node *5*, the data are optically switched (see data path 1 in Fig. 1.2).

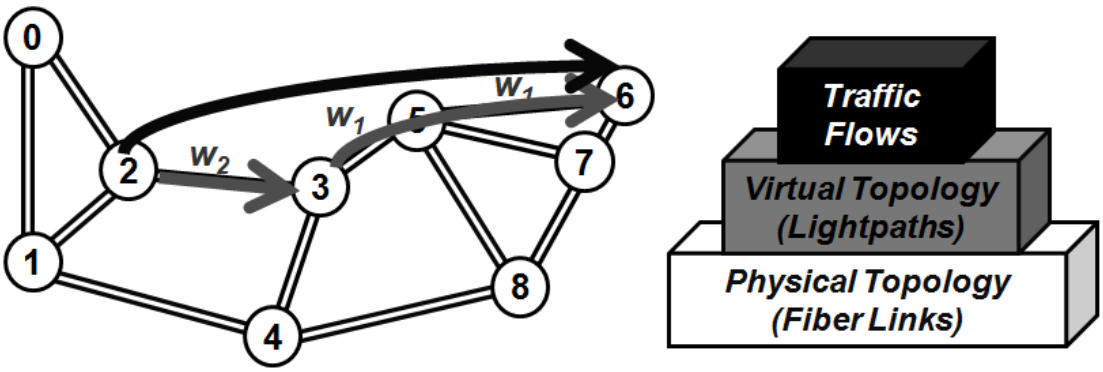

Fig 1.3. Multilayer scheme of optical WDM networks

1.2 Network Planning in Optical Transparent Networks

We refer as network planning to the iterative process, encompassing different stages, devoted to design new networks or enlargements of these ones, ensuring that the subscriber services requirements are met with minimal cost for the network operator. This is an extremely important process which must be performed before the deployment of new telecommunications networks. This design and optimization process must be adapted to each network technology. In the present thesis, we focused on the planning of optical transparent networks. In these networks, the expensive costs of optical components and systems encourage to invest time in their design, planning and optimization. Moreover, aspects from different network layers must be considered jointly during the planning process, introducing a high level of complexity in the design of these networks and stressing the importance of the research in optimization techniques that allow minimizing the total network costs.

The planning in transparent WDM networks implies to solve the so-called ***Virtual Topology Design (VTD) Problem***. The general problem receives as input data the *physical topology* and the estimated (or known) *traffic* among the nodes. The *physical topology* $Gp(V, E_p)$ consists of a network graph, where set V represents both switching and access nodes and set E_p denotes the physical links composed of bunches of fiber cables. The traffic is usually expressed as a *traffic matrix h*, where a element h_{sd} in the matrix is the average traffic offered from a node *s* to a node *d*. Typical additional input data are the number of wavelength channels carried by each fiber, the number of transceivers/wavelength converters/regenerators installed at each node or the technical data of the installed equipments.

The solution of the *VTD* problem is to find a feasible *virtual topology* $G_v(V, E_v)$ along with the routing of the *traffic matrix h* over the virtual topology, optimizing some network cost. The *virtual topology* $G_v(V, E_v)$ is the network graph composed by the nodes set V and the set of *virtual links* E_v, where a *virtual link* groups all the *lightpaths* configured between the same node pair, in the same manner as a *physical link* groups all the *fiber cables* installed between the same node pair. In the *virtual topology*, each *lightpath* must be perfectly characterized in three aspects: (i) origin and destination nodes; (ii) sequence of fibers traversed (*lightpath routing*); and, (iii) sequence of wavelengths selected on each of the fibers (*wavelength assignment*). Traditionally, for a *lightpath* defined in terms of (i), the two latter aspects constitute the solution of the so-called ***Routing and Wavelength Assignment*** (***RWA***) problem [7]. Finally, the solution of the *VTD* problem has to include how the traffic offered from an ingress node *s* to an egress node *d* is routed over the virtual topology, i.e., the *lightpaths* traversed by each traffic flow from *s* to *d (traffic flow routing)* and the amount of routed traffic on them. Fig. 1.4 depicts the overall scheme of the solving process of *VTD* problem.

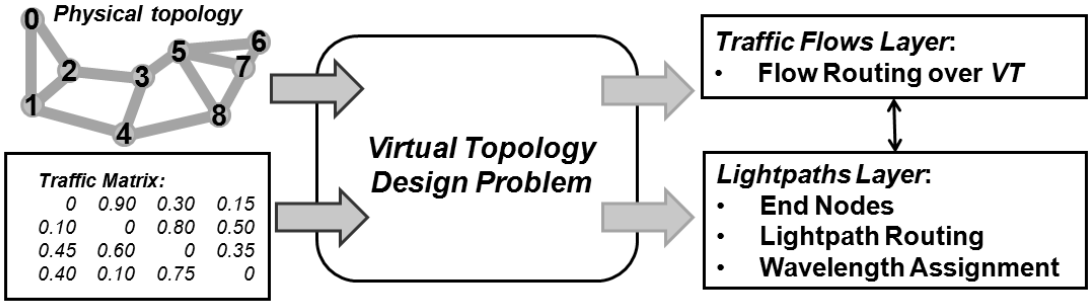

Fig. 1.4. Scheme of the solving process of *VTD* problem

We must note that the *VTD* problem is a multi-layer problem since the solution consists of two layers: an upper layer (traffic flows over *lightpaths*) and a lower layer (*lightpaths* over fiber links). Moreover, the *VTD* problem is also a cross-layer optimization problem: the two layers have to be found jointly as they are bound through the characterization of the *lightpaths.*

In general, there exists an infinity of variations of the above introduced multilayer problem, where additional planning aspects are taken into account, for example, protection and restoration considerations in *fault-tolerant networks planning*, physical layer models in *physical layer impairment aware (PLIA) planning* or the traffic variability along the time in the *multihour planning.*

The *VTD* problem may be formulated as a mathematical optimization program called *Mixed Integer Linear Program* (*MILP*) [1]. A *MILP* mathematical optimization problem intends to find a solution (some values on the so-called *decision variables*) which optimizes some *objective function* subject to some planning *constraints*. The objective function, generally, is a linear function that models the network costs (to minimize); meanwhile, the planning constraints are linear functions representing technological or physical limitations to the feasible space of solutions (values allowed to the decision variables). These decision variables define our planning decisions, i.e., *lightpath routing*, *wavelength assignment* or *traffic flow routing*, and in *VTD* problems can be constrained (or not) to be integer numbers

The planning problems addressed in this thesis, related to multilayer optical WDM networks, are NP-hard [8]. When a problem is NP-hard, we know that all the existing algorithms that solve the problem have a running complexity which grows at least exponentially with the problem size, and thus becoming computationally intractable at medium-sized networks. As a consequence, larger problems will be solved by other methods, such as *heuristic algorithms*. The heuristic methods suppose a good option to generate approximate solutions in a reasonable time. A heuristic algorithm searches for a sub-optimal solution in the space of solutions defined by the problem constraints. The inexact solutions provided by the heuristic must be close enough to the optimal solution, if we want to consider them as valid solutions. This implies

that is necessary to assess the quality of the heuristic results. There are two main alternatives: first, comparing them with optimal ones provided by exact *MILP* approaches for a tractable size; and, second, evaluating them with bounds on the optimum attained by analytical methods. If the heuristic computes solutions with sub-optimal costs nearby either to the *MILP* optimal cost or to the analytical bound on the optimal cost, we can accept them. In other words, the sub-optimality gap (difference between heuristic cost and bound / optimal cost) should be small and not very slack. Although the heuristic algorithms may seem an approach with a reasonable trade-off between running time and optimality on the solutions, some potential drawbacks of these techniques should be mentioned. It may be hard to compute optimality bounds accurate enough to be useful to to evaluate the quality of the heuristic solutions, i.e., very slack bounds which does not provide too much information about the quality of the solution.

The basic *MILP* scheme of the general *VTD* problem is adapted according to the considered type of planning problem. These adaptations may increase the problem complexity with respect to the general *VTD* version. For example, the *physical layer impairment aware (PLIA) planning* adds non-linear constraints to include the physical layer issues, or the *multihour planning* replicates some constraints as many times as time epochs used to model the traffic variability. These modified network problems may suppose a challenge for the planner, since solving them optimally is not something trivial. Thus, the development of efficient optimization algorithms able to find an optimal or an acceptable sub-optimal solution with the existing computing resources becomes critical in the network planning.

On the other hand, *VTD* problems can be classified according to the associated traffic demand variations along time, as *static*, *scheduled* or *dynamic* [9]. The first two assume offline planning, while the third infers online provisioning. In the static traffic case, the traffic demand is constant along time. Therefore, the virtual topology obtained by solving the VTD problem is also constant where the lightpaths are established semi-permanently based on the estimated constant traffic. In the scheduled traffic case, the traffic demand varies along time, but its variation is assumed to be accurately known in advance. The problem can be solved either by finding a static virtual topology capable of handling all the given traffic variations over time, or by finding a succession of virtual topologies dynamically reconfigured in accordance with the traffic changes. The former can be realized using non-reconfigurable components, while the latter requires reconfigurable WXCs. Finally, in the dynamic traffic case, lightpaths are established as the connection requests arrive, with no a priori deterministic knowledge of connection request arrival time.

Among the aforementioned variety of *VTD* problems, this thesis is focused on the next three problem variants:

1) ***Static Multifiber planning,*** which consist of a *static* problem where *physical links* are

considered as composed by bundles of several fiber cables instead assuming single fiber links.

2) ***Static Physical Layer Impairment Aware (PLIA) planning,*** where the physical layer and its degrading effects on the signal quality are introduced in the planning problem, assuming static traffic demands.

3) ***Scheduled Multihour planning,*** where the planning is performed along several time epochs, such as hours or days, modeling the scheduled traffic demands between the network nodes as sequence of matrices, corresponding each one of them to a given time epoch.

1.2.1 Multifiber Planning

In real networks, nodes are connected by *physical links* which contain a number of fiber cables in the order of one hundred. In the planning studios, it is common to see that at most one fiber is active between each two nodes. This is because, activating a fiber means allocating amplification, dispersion compensation and other equipment. In the *multifiber planning* [10], [11], [12], the option of activating more fibers in a physical link to increase the network capacity, is included in the optimization. The *multifiber planning* encompasses a broad field of different families of problems depending on the purpose of the study. For example, some works [10], [12] are focused on the design of fault-tolerant networks under the *multifiber* assumption. In [10], it is analyzed how the availability of multifiber links affects to extra network capacity that must be reserved for protection; whereas, in [12] restoration mechanisms guarantying no service disruption are proposed when the links are composed by bunches of fibers.

Other type of multifiber studies [10], [11], [13] evaluate the tradeoffs of the (i) deployment of several fibers in the *physical links* with (ii) the installation of *wavelength converters* at the nodes. Both approaches are proposed as alternatives to reduce the *lightpath blocking*. A node can change the WDM channel of a traversing *lightpath* using one wavelength converter (*WC*). *WCs* can avoid wavelength clashing, unblocking *lightpath* requests, and, thus, reducing the need of installing additional fiber cables in the links. On the other hand, multifiber cables can relax the *wavelength continuity constraint* in networks without wavelength conversion, since more WDM channels are added to the network capacity.

In the work included in the present thesis [13], the above mentioned tradeoff is studied when not all the fibers deployed in the links are active, assuming static traffic, Surprisingly, the results neglect the utility of the installing *WCs*: solutions where the use of *WCs* replaces the activation of extra fibers seem to be very infrequent.

1.2.2 Physical Layer Impairment Aware (PLIA) Planning

Other research topic addressed in this thesis is the ***Physical Layer Impairment Aware*** (***PLIA***) ***planning*** in transparent optical networks. If our target is to design real optical networks, physical layer considerations must be introduced into the planning process. The degradation on the signal quality due to *physical (layer) impairments* cannot be ignored by the network planner. The *physical layer impairments* (*PLIs*) are accumulated trough the path of the optical signal (fibers and nodes traversed by a *lightpath*), supposing a real limitation on the effective transparent reach, i.e., the maximal reach of the optical signal without requiring electronic regeneration [5]. The *PLIA planning* incorporates these aspects to the classical *VTD* problem in WDM networks. In the present thesis, we focus on the static variant of the general PLIA planning.

The *physical impairments* degrading the optical signal quality become more significant when factors, such as, the length of the span fibers, the number of traversed nodes, the number of used WDM channels in the fibers, the bit rate per wavelength channel or the launch power, are increased. Then, signal regeneration is required. We can distinguish different types of signal regeneration depending on the tasks performed to compensate the *physical impairments*: ***1R regeneration*** (*re-amplification*), *2R* ***regeneration*** (*re-amplification*, *re-shaping*) and ***3R regeneration*** (*re-amplification*, *re-shaping*, *re-timing*) [5]. In ***1R regeneration***, the degradation on the quality signal is compensated by merely increasing its optical power level by optical *re-amplification*. Conversely, in ***2R*** and ***3R regeneration***, *re-shaping* and *re-timing* are conducted using electronic processing of the optical signal, what introduces OEO conversion breaking the optical network transparency. Therefore, in ideal transparent networks, *1R regeneration* is only used; meanwhile in translucent networks, we can find *2R* or *3R regenerators* [6].

The impairments can be classified into linear and nonlinear [14]-[17]. The linear impairments are independent of the signal power. Conversely, non-linear impairments are very sensitive with the power level (usually, become larger with the launch power), introducing perturbations and interferences between different wavelength channels. Examples of linear impairments linear impairments [17] are *fiber attenuation* [14], [18], *amplified spontaneous emission* (*ASE*) *noise* [14], [15], [16], *chromatic dispersion (CD*) [14], [15], [16] or *polarization mode dispersion* (*PMD*) [14], [15], [16]. On the other hand the most non-linear impairments [17] are the Kerr effect impairments [14], [16], [18]: *self phase modulation* (*SPM*), *cross phase modulation* (*XPM*) and *four wave mixing* (*FWM*).

Although the classification linear/non linear is broadly used, the impairments can be categorized in a different manner, more suitable for network planning considerations: (i) those that affect the same *lightpath*; and, (ii) those that are generated by the interference among *lightpaths* [21], [72]. These categories are also named as *static* or *dynamic*, respectively, in our contribution [21]; or, *Class 1* or *Class*

2, respectively, in [72]. Both categories almost correspond to linear and non linear classes, respectively. For this reason, the terms *linear* and *non-linear* sometimes are used with a sense slightly different from their physical meaning [20]. That will be discussed in detail in Chapter 3.

Two main techniques have been used to determine the signal Quality of Transmission (QoT) at the end node of a *lightpath*: (i) computing individually the degradation on the QoT caused by each impairment; or (ii) estimating a global QoT evaluator that collects all the PLIs (e.g., Q- Personick [19]) . Depending on the technique used to estimate the QoT, a different approach to incorporate the PLIs into the planning problem arises. For example, in [20], a wavelength assignment problem is formulated as an ILP model where the the PLIs are estimated individually and incorporated directly as model constraints. Conversely, in [21], heuristic algorithms based on *network planning stages* alternating with *performance evaluation stages*, where global *QoT* estimators are employed, are proposed.

One of the preferred global *QoT* estimators is the so-called called Q factor [18],[19], that accounts all the above mentioned impairments by accumulating them along the path. Two models of Q factors [20] can be distinguished based on the strategy to include the *dynamic* impairments (denoted as *non-linear* in [20]):

- *Static (or Linear* in [20]*) QoT estimators*: The *dynamic* (or non-linear in [20]) impairments are over-estimated and summed to the linear ones, without considering interactions between neighboring lightpaths. In this case, the *QoT* estimation of a *lightpath* depends solely on its own route.
- *Dynamic* (or *Non-Linear* in [20]) *QoT estimators*: The *dynamic* (or non-linear in [20]) impairments are computed explicitly considering interactions between neighboring *lightpaths*. Therefore, the *QoT* obtained for a *lightpath* is dependent on the routing and wavelength assignment of other *lightpaths* in the network.

The Q factor is directly related to the bit error rate (BER) signal, justifying its use as QoT estimator of the digital signal generated by the receiver of the lightpath, since direct estimation of *BER* is difficult due to long data frame required to compute it. For a modulation On-Off this relation is [19]:

$$BER = \frac{1}{2}\operatorname{erfc}\left(\frac{Q}{\sqrt{2}}\right) \tag{1.1}$$

By calculating the Q factor at the end of a *lightpath*, we can estimate the feasibility of a *lightpath* in terms of optical signal quality. For example, if the QoT requirement to accept a digital signal at the output of an optical receiver is a BER lower than 10^{-9} [18], the formula (1.1) say us that the factor Q must be larger than a quality threshold (Q_{thr}) of 15.5 dB for the optical signal at the *lightpath* output. Therefore, any *lightpath* whose Q factor at its destination node is less than 15.5 dB may not be *QoT feasible*. This will add a new constraint to our planning problem: besides finding a route in the physical topology of available wavelength channels at the fibers and free optical transceivers at the end nodes, the accumulation of the physical impairments along the path should not degrade the optical signal quality below a minimum Q factor threshold so as to establish a QoT feasible *lightpath*. This version of the classical routing and wavelength assignment problem is called ***Physical Layer Impairment Aware RWA*** (***PLIA-RWA***) ***problem*** [17],[21]. This thesis investigated this network problem in [21], where two algorithmic approaches, using a common *dynamic QoT estimator*, are proposed. A *dynamic* QoT estimator introduces more realism into the planning problem, since they consider explicitly the possible interactions between *lightpaths*. But, for this same reason, the PLIA problem becomes more complex to face.

If the *PLIA-RWA* fails for a *lightpath*, the *lightpath* cannot be set up in a transparent manner, without electronic processing and OEO conversion (*transparent network*). Instead, *2R* or *3R* regenerators should be placed at some intermediate nodes of the *lightpath* to meet the QoT requirements at the receiver (*translucent networks*). Selecting which nodes must have regeneration capabilities and how many signals can be regenerated at these nodes constitutes a different problem planning called *Regenerator Placement* (*RP*) [22],[23]. In translucent networks, the two aforementioned planning problems can be solved jointly, in the so-called problem *PLIA-RWA-Regenerator Placement* (*IA-RWA-RP*) [20],[24]. In this type of planning problem, this thesis has a small contribution in the work developed in [20].

Traditionally, the most spread bit rate in optical communications was 10 Gbps. However, the enlargement of capacity of the optical networks is forcing to use 40 Gbps or, even, 100 Gbps. These high bit rates supposes a challenge, since, as we have pointed out before, many of the physical impairments, particularly the non-linear, become more severe for higher bit rates than 10 Gbps [16],[18], [25]. When the classical *VTD* problem as stated in Subsection 1.2 takes into account the PLIs in networks operating at several data rates (10/40/100 Gbps) is generally called *mixed line rate virtual topology design*. This is still a novel research topic [26],[27], where this thesis contributes with the work in [27].

1.2.3 Multihour planning

The third main research area a variant of the offline scheduled VTD problem, denoted as *Multi-Hour*

Virtual Topology Design (*MH-VTD*) [28]-[30], where *multihour planning* is applied to transparent optical networks.

The term *multihour planning* describes a classical network planning [31], where the demand takes the form of a temporal sequence of traffic matrices, reflecting the traffic variation along a given period of time (typically days or weeks). The periodic nature of the traffic has been confirmed with real traffic traces in numerous experiments, such as the Abilene backbone network [32], making the traffic load in the network fairly predictable. Moreover, in networks spanning over multiple time zones, like Abilene, the existence of different demand peaks between different node pairs at different times, i.e., the non-coincidence of busy-hours, suggests the possibility of taking profit of the unused capacity in the network. For example, a traffic demand between two towns placed at US east coast (e.g. New York and Washington) at 8:00 am (offices opening hour) could be routed easier via a US midwestern (e.g. Chicago), where the time is 7:00 am and the network is less busy. The *multihour planning* explores the reduction on network costs by exploiting the traffic periodicity and the busy-hours non-coincidence of the *multihour* traffic in continental long-haul networks.

In optical *WDM* networks, the number of optical transceivers is commonly referred as a network cost criterion in planning studies [33], [34], [35]. Consequently, one of the objective functions *Multi-Hour Virtual Topology Design* (*MH-VTD*) can minimize the number of optical transceivers required to meet all the traffic demand along time, since, in a given time slot, those transceivers with lower usage can be used to serve part of the traffic between the most loaded node pairs.

The author has collaborated in several works which investigate different MH-VTD problem [30],[36]-[40]. Some of the contributions in these papers are a part of the present thesis.

In [30],[36]-[40] the tradeoffs existing in *Multi-Hour Virtual Topology Design* are investigated according to the several criteria:

- Considering reconfigurable or non-reconfigurable *virtual topology* [36],[37],[38],[40], when assumed time-variable flow routing on top of the virtual topologies. In the first case, one unique virtual topology design is obtained for all the multihour traffic demand. Then, the optical components are assumed to be non-reconfigurable. We name this problem as *NR-VTD* (*-Non Reconfigurable Virtual Topology Design*). In the second case, denoted as *R-VTD* (*Reconfigurable Virtual Topology Design*), reconfigurable switching nodes are assumed, i.e., the virtual topology design can change along time.
- Considering fixed or variable flow routing [30],[39], when assumed non-reconfigurable virtual topology. A fixed flow routing indicates that the traffic from a source node to a destination node

is always transmitted via the same set of *lightpaths*. This problem is called *NR-VTD-FR* (*NR-VTD with Fixed Flow Routing*). On the contrary, variable routing imposes no such constraints, but at a cost of higher signaling and network management complexity. This problem is denoted as the *NR-VTD-VR* (*NR-VTD with Variable Flow Routing*).

- Considering *splittable* or *unsplittable* flow routing over the *virtual topology* [30]. *Unsplittable* routing means that all the traffic between a pair of nodes is forced to traverse an unique path of nodes. Conversely, if the routing is *splittable*, the traffic between two nodes may be split into several paths, each one of them carries a fraction on the total offered traffic to the pair. Obviously, the *splittable* routing allows to perform a better load balancing, although with the cost of increasing the signaling overload.

In the *MH-VTD* problem, the number of some constraints is dependent on the number of traffic matrices (one matrix per considered time interval). Consequently, the reduction on the total number of matrices used to solve the problem could be a valuable technique to decrease the problem complexity. The concept of ***domination*** between matrices [41] and matrices sequences [42],[43] provides a theoretical basis allowing us to devise a set of complexity reduction techniques which transform the original multihour sequence into smaller set of matrices.

The relation of domination between traffic matrices was introduced by Oriolo in [41], and it can be defined roughly as *one traffic matrix h^1 dominates other matrix h^2 if h^1 (considered as capacity matrix) can support h^2*. In other words, h^1 dominates h^2 if a network with links capacitated according to h^1 (the capacity in a direct link between nodes *s* and *d* is h_{sd}^{1} traffic units) can carry all the offered traffic h^2. Trivially, it is easy to realize that if h^1 dominates h^2, we can use solely h^1 to find a link capacity assignment sufficient to support both matrices h^1 and h^2. This is the basic idea which we can use to build more or less sophisticated reduction methods on the number of matrices required to model the planning problem.

We refer to the above mentioned domination concept as *weak domination* to distinguish it from other variants also introduced by Oriolo in [41]: *strong domination, total domination, domination with respect to unsplittable flows, domination between sets of matrices…* Moreover, the generalization to several matrices (domination between sets of matrices) was also studied more deeply by [42],[43]. Depending on the network planning problem, we can apply a given type of domination, for instance, *domination with respect to unsplittable flows* can be used to solve problems where the traffic demands must be routed on unique path. In the present thesis, several problem reduction techniques based on the domination are developed to assess of aforementioned the tradeoffs at the *MH-VTD* problem variants. The basic notions

required to understand the domination variants used in this thesis are summarized in the Annex B, at the end of the thesis. Furthermore, in this annex, a novel scheme to apply the traffic domination between sets of matrices to the multihour planning in general communication network is outlined.

1.3 An academic Network Planning Tool: *MatPlanWDM*

Part of the works of the present thesis were carried out in the framework of the development process of *MatPlanWDM*. *MatPlanWDM* [44], [45], [46] tool is an academic network planner developed by the Technical University of Cartagena (*Universidad Politécnica de Cartagena, UPCT, Spain*), and devoted to design and plan multilayer transparent and translucent WDM Networks. The tool consists of four modes that allow to solve different *VTD* problem variants and perform different analysis: (i) *Static Planning Mode*, (ii) *What-If Analysis Mode*, (iii) *Multi-hour Analysis Mode* and (iv) *Dynamic Analysis Mode*.

The *MatPlanWDM* project has its origin in the author's MSc Final Year Project [47] together with the MSc Final Year Project [48]. The first version, including solely the *Static Planning* and *What-If Analysis* modes, was distributed in January 2007 and introduced in the work [49]. After that, new versions of the tool were released, including additional functionalities and the remaining modes. The expansions where the other two modes were added generated some publications:

a) *Multihour planning mode* was presented in [50].

b) *Dynamic Analysis Mode* was presented in [51]. This enlargement was implemented as part of the MSc Final Year Project [52].

MatPlanWDM has been specifically designed to permit the users to extend it by adding their own planning algorithms. This is a particularly useful feature in the research and academic world. These new planning algorithm can be added either i) starting from any of the classical algorithms included in libraries distributed with the tool; or, ii) starting from scratch by developing an own planning algorithm. Beside this, the user can also select a MILP (Mixed Integer Linear Programming) search of the optimum solution instead of a heuristic planning algorithm by using an The MILP-optimization algorithm integrated in the tool can be solved by two different *solvers*: a commercial *solver* (*TOMLAB™/CPLEX*) [53] or an open-source one (GLPK, GNU Linear Programming Kit, included in the MatPlanWDM distribution) [54].

In the annex A, the main contributions of this thesis to the *MatPlanWDM* project are detailed. These contributions are focused on (i) *Static Planning Mode*, (ii) *What-If Analysis Mode* and (iii) *Multi-hour*

Analysis Mode, whose implementation give arise to the publications [49] and [50]. On the other hand, *MatPlanWDM* has also served as development and simulation framework in all the research works constituting the present thesis. The optimization models and algorithms presented in the thesis were implemented and tested with the tool.

Beside the research utilization, we must note that *MatPlanWDM* has also been used for teaching purposes in several courses in Technical University of Cartagena (Spain) and in Faculty of Electronics and Computation (*FER*), University of Zagreb (Croatia).

Finally, the tool is still being developed and updated with new versions in the context of other two Ph D Thesis still in progress. Current version of the tool (v0.60) can be freely downloaded from [46].

1.4 Overview of the thesis and structure of chapters.

The present thesis consists of six chapters, including this one, and two annexes.

In this introductory Chapter (Chapter 1), a brief introduction to the planning of WDM networks is provided. The thesis is motivated, justifying its research interest. The different problem variants studied in the thesis are exposed and the main contributions of the thesis are introduced.

In Chapter 2, the ***multifiber planning*** study conducted in the thesis is described. This work consists of a cost comparative study of the tradeoffs between two approaches to reduce blocking situations: (i) *multifiber links* and (ii) *wavelength converters.* The outcomes of this work has been published in [13].

Chapter 3 collects the thesis' contributions to the ***physical layer impairments aware planning***. First, the Chapter describes the research in the *physical layer impairment aware routing and wavelength assignment* (*PLIA-RWA*) problem, assuming traditional single line rate scenarios at 10 Gbps. The results of this work have been published in [21]. Second, the investigations on the planning of novel mixed line rate networks (10/40 Gbps), where the impairments are more severe, are described. These results has been also presented in [27]. Finally, as epilogue of the Chapter, the work [20] in the context of regenerator placement (*Non-Linear PLIA-RWA-RP*) is briefly explained, since the author's thesis has collaborated in this study.

In Chapter 4, the investigations in the ***multihour planning*** (*Multi-Hour Virtual Topology Design*) encompassing the papers [30] and [36]-[40], are detailed. In all these works, the number of optical transponders (transceivers and receivers) is used as the network cost to minimize. The tradeoffs on the transceiver cost exiting in non-reconfigurable virtual topologies (*NR-VTD*) and reconfigurable ones (*R-VTD*), assuming time-variable flow routing on top of the *VTs*, are studied in [36], [37], [38] and [40].

Meanwhile, the reductions on the transceiver cost in non reconfigurable VTDs, under different assumptions on flow routing on top of the *VT*: fixed or variable; and, *splittable* or *unsplittable* are assessed in [30]. In this work, complexity reduction techniques based on the traffic domination concept [41] are applied to the design of algorithms solving *NR-VTD* problems. This thesis has also contributed in the work in [39] where more advanced domination based techniques are developed and applied to *multihour* problems with time-fixed capacities assignment general in communication networks. This collaboration is briefly commented in the Annex B, where the basic notions about traffic dominations used along the thesis are also outlined.

Finally, Chapter 6 presents the main conclusions extracted in this thesis carried and suggests some possible future research lines.

Additionally, the Annexes A and B summarize some collateral results generated in the framework of the present thesis. First, Annex A introduces the *MatlPlanWDM* tool commented in the previous section. Then, Annex B outlines some contributions in traffic dominations: (i) the theoretical basis required for a better understanding of domination concept; and, (ii) a novel scheme, where the author contributed, to apply domination among sets of matrices to general multhour planning in optical networks.

Chapter 2

2 Multifiber Planning

ABSTRACT: This Chapter describes the contribution of the present thesis to the research in the multifiber planning. That is, networks in which more than one fiber can be activated in the links between two nodes. The contribution of the thesis consists of a comparative study which evaluates in what circumstances activating a new fiber is preferred with respect to installing wavelength converters, as a medium to increase the network capacity.

2.1 Problem statement

In real optical networks, the network operators deploy bundles of fiber wires between the nodes. As a consequence, a physical link connecting two nodes is composed by several fibers, usually, in the order of one hundred. However, the number of *active* fibers in the *physical links* is solely the figure required to satisfy the current traffic demand (generally one), since the costs of the equipment required to activate the remaining fibers may be quite expensive. Therefore, a growth in the demanding traffic will force the network operator to enlarge the network capacity by activating extra fiber wires. Selecting carefully these fibers among the installed cables may be an effective method of minimizing the capacity expansion cost. This is the purpose of the *multifiber planning*, where the benefit-cost ratio of activating additional fiber cables in the *physical links* are analyzed.

This Chapter develops the research in the ***static multifiber planning*** performed in the present thesis. This research consists of a comparative study between two alternatives to assume the traffic growths: (i) installing *wavelength converters* at the nodes to alleviate the wavelength continuity constraint or (ii) activating more fibers in the *physical links*. The results of this case-study of *multifiber planning* were published in the work [13].

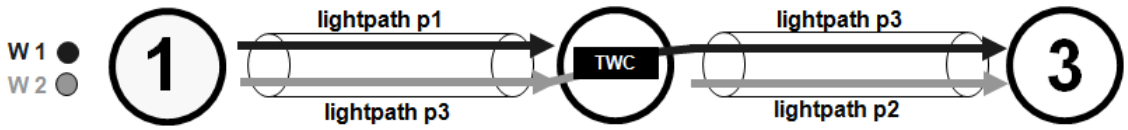

Fig. 2.1. Wavelength Conversion Approach

In the wavelength converter approach, shown in Fig. 2.1, a node can change the WDM channel of a traversing lightpath using one wavelength converter (*WC*), like lightpaths *p3* in Fig. 2.1. *WCs* can avoid wavelength clashing, unblock lightpath requests, and, thus, increase network capacity, reducing the need of activating additional fiber cables. Conversely, in the multifiber approach, depicted in Fig. 2.2, the wavelength continuity constraint is relaxed in a different manner: as many lightpaths as active fibers in a bundle between two nodes, can be assigned to the same wavelength, since they occupy different fibers in the bundle. This is the case of lightpaths *p1* and *p3* tuned at the wavelength *w1* in Fig. 2.2.

Unfortunately, the multifibre approach adds the cost of amplifying, equalizing, monitoring, switching, etc. more fibers, and the WC approach involves the cost of one WC device per wavelength conversion (we assume that the WCs are shared per node). The balance between the cost of extra activated fibers and the cost of the wavelength converters is analyzed through a binary ILP (Integer Linear Programming) formulation, which simultaneously includes the cost of both alternatives. Then, we obtain the minimum cost solution under different conditions, and evaluate the actual use of WCs and/or activated fibers. Surprisingly, the results neglect the utility of the installing *WCs*: solutions where the use of *WCs* replaces the activation of extra fibers seem to be very infrequent.

The next Section consists of a state of art in the planning problem. The Section2.3 describes the proposed ILP formulation. Section 2.4 presents the results obtained. Finally, Section2.5 concludes the chapter.

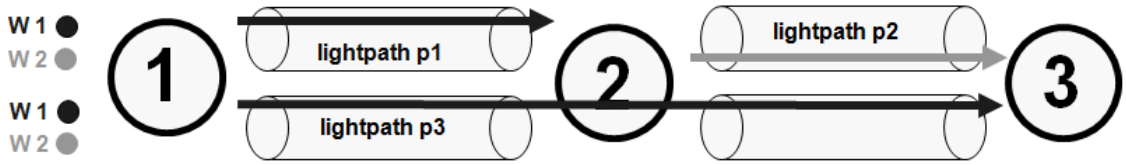

Fig. 2.2. Multifiber Approach

2.2 Related Work

In the framework of the planning in multifiber WDM network, many works have been published, encompassing a broad field of different problems. First, the studies addressed in the literature may be grouped into two main categories, depending on the time-variability of the traffic: dynamic works [11],[55]-[60] and static ones [10],[12],[61]-[69]. In the former works [11],[55]-[60], the blocking performance of several dynamic *RWA* algorithms is evaluated. These algorithms attempt to allocate dynamically as many *lightpath* requests as possible, using different criteria to select for each connection

request a free path with available wavelength channels. Since the contribution in this thesis pertains to the static case, we will not concentrate on these dynamic investigations, but comment some remarkable results. In the works [11],[55],[57]-[59], the wavelength conversion was introduced to the multifiber problem, although with two different approaches: (i) in [55] and [58], considering explicitly wavelength converters placed at the nodes, and (ii), in [11],[57] and [59], assuming the full wavelength conversion as a special multifiber case where the number of wavelength channels per fiber is solely one. The results in these works point out that a multifiber network without wavelength converters can have a similar blocking performance to that of a full-wavelength convertible network, being a limited number of fibers per fibers per physical link is sufficient to guarantee a low lightpath blocking probability.

In the static multifiber planning, a variety of investigations have been performed under different assumptions: (a) different objective costs to optimize (maximizing the carried traffic [12],[66], minimizing the number of required wavelengths [61], [62], [68], minimizing the network congestion [65], minimizing the total number of fiber wires [10],[63],[64],[67],[69], minimizing the lightpath lengths [62],[64],[69]), (b) wavelength convertible networks [10],[63],[64],[67],[69]; or, (c) survivability and resiliency considerations [10], [12], [61],[63],[67],[69].

In [10],[63],[64],[67],[69], the wavelength conversion is considered in the multifiber planning, assuming nodes with *Wavelength Interchanging Crossconnect* (*WIXC*) with full conversion range. In all these works, the network cost function to minimize is the total number of fibers cables that must be activated, without considering any realistic cost model of activating a fiber (costs of in-line amplifiers, dispersion compensating devices, etc). In some of these works [64],[69], the links lengths are also used as cost weights.

The exhaustive research published in [10] presents four ILP link-path formulations to study multifiber protected and non-protected networks with and without wavelength converters at the nodes. In the fault-tolerant case, three protection strategies are evaluated: dedicated path protection, shared path protection and single link failure protection. Furthermore, for non-wavelength convertible networks, two types of transceiver configurations are compared: wavelength-agility and fixed-wavelength. This variety of technological scenarios, along with the large number of tested network topologies, are the strengths of this work. Conversely, its main drawback is that traffic demands are limited to one lightpath request between a node pair. Finally, the study concludes that, solely, in protected networks with fixed-wavelength transceivers, a significant reduction on the number of required fiber wires can be achieved with the introduction of wavelength conversion. In the works [63],[64],[67] and [69], similar studies to [10] are carried out and similar results are obtained, neglecting the utility of wavelength conversion to reduce the number of fibers to enable in the network. These papers are mainly focused on the

computational tractability of the NP-hard ILP formulation, proposing ILP models ([64],[67] and [69]) or heuristic methods ([63] and [67]). The ILP formulations consider more than one *lightpath* demand between a pair of nodes, increasing the complexity problem. Therefore, several complexity reduction techniques are applied: in [64], two source node formulations for both wavelength convertible networks and wavelength non-convertible networks are proposed to dimension the fiber requirements, ignoring the exact *RWA* of the *ligthtpaths*; in [67] a "standard" node-link formulation considering both terminal nodes is presented, also for wavelength conversion and non wavelength conversion; and, in [69], the formulation in [67] for the wavelength conversion case is relaxed by collapsing all connection requests relative to the same source-destination couple in a single variable. Additionally, in [67] and [69], the formulations are modified to include dedicated path protection. Finally,in the works [63] and [67], a general heuristic method is applied to protected and unprotected networks. The method consists of two stages: (i) a greedy VT mapping, where multiple heuristic criteria are proposed to perform the *lightpath* routing and wavelength assignment, (ii) a reoptimization cycle, where solutions obtained in (i) are improved by rerouting some connections. In the whole design procedure the network state is represented by a Multifiber Layered Graph (MLG).

Finally, to conclude this section, the differences and common points between the study described in this section and the works [10],[63],[64],[67],[69] are highlighted. Both these studies and the work in this theses propose exact programming formulations to address the multifiber problem in wavelength convertible networks, but, in our proposal, the tradeoffs between wavelength conversion and multifiber are studied directly through a formulation balancing the wavelength conversion cost and the multifiber activation cost, instead evaluating them indirectly by two different multifiber formulations. Besides, in contrast to these works, we use a realistic cost model [70] to compute the cost of activating a fiber.

2.3 BILP model of the planning problem

This section describes the Binary Integer Linear Program (BILP) modeling the static planning problem. Let N be the set of nodes, M the set of unidirectional links. We denote as $|\cdot|$ the number of elements of a set. Each link $m \in M$ is a pair (i,j), $i \in N$, $j \in N$, composed by a bundle of K fibers. Then, the total number of fibers in the network is given by $|F|=K|M|$. We denote $F_{in}(n)$ and $F_{out}(n)$ as the set of fibers that end and start in node n, respectively. The same spectral grid of W wavelengths is considered in all the fibers. The cost of activating a fiber f is c_f, $f \in F$. The cost of a wavelength converter is given by c_{WC}. Let S be the demand of lightpaths to be established. The decision variables to the problem are:

- $p(s,f,w)$={1 if lightpath s traverses fiber f using wavelength w, 0 otherwise}, $s \in S$, $f \in F$, $w \in W$.

- e_f={1 if fiber f is active, 0 otherwise}, f=1$\in F$
- $c^+(s,n,w)\in\{0,1\}$, $c^-(s,n,w)\in\{0,1\}$. These variables are used to track wavelength conversion in node n, for lighptath s, involving wavelength w. $s\in S$, $n\in N$, $w\in W$.

The ILP cost function (minimize) and constraints are:

$$\min\left\{\sum_{f\in F} c_f e_f + \frac{c_{WC}}{2}\sum_{s\in S, n\in N, w\in W} c^+(s,n,w) + c^-(s,n,w)\right\} \tag{2.1}$$

Subject to

$$\sum_{s\in S} p(s,f,w) \le 1, \forall f \in F, w \in W \tag{2.2}$$

$$\sum_{\substack{f\in Fout(n)\\ w\in W}} p(s,f,w) - \sum_{\substack{f\in Fin(n)\\ w\in W}} p(s,f,w) = \begin{cases} 1, \textit{ if } s \textit{ starts in node } n \\ -1 \textit{ if } s \textit{ ends in node } n, \\ 0 \textit{ otherwise} \end{cases} \quad \forall s \in S, \forall n \in N \tag{2.3}$$

$$p(s,f,w) \le e_f, \forall s \in S, f \in F, w \in W \tag{2.4}$$

$$\sum_{f\in Fout(n)} p(s,f,w) - \sum_{f\in Fin(n)} p(s,f,w) = c^+(s,n,w) - c^-(s,n,w), \tag{2.5}$$
$$\forall w \in W, s \in S, s \text{ neither starting nor ending in node } n$$

First set of constraints (2.2) avoid wavelength clashing. Second set (2.3) are the conservation constraints, allowing wavelength conversion. Third set of constraints (2.4) avoid any lightpath to traverse a fiber, unless it is active. Fourth set of constraints (2.5) tackle the wavelength conversion issue. When a lightpath s converts its wavelength in node n from w_1 to w_2, $c^-(s,n,w_1)$=1 and $c^+(s,n,w_2)$=1. Both are 0 otherwise. As this formulation counts twice each conversion, c_{WC} value is divided by 2 in the cost function.

2.4 Results

We tested three networks of 7 nodes: a mesh network (Fig. 2.3), a ring and a star with centre in node 3 (last two cases with fibres of 100 km length). In all the cases, links have two fibers, and eight

wavelengths per fiber. One fibre in the link is already pre-activated at cost 0. The cost of activation of the other fiber is computed using the CapEx model of the NOBEL project [70] as 20+0.96036(*d*/80)+1.585(*d*/360), where *d* is the link distance in km. This expression is referred to the cost of one 10G LH transponder: the unity cost is the cost of one transmitter plus one receiver. Divisions are rounded to the floor, and correspond to optical line amplifiers, and dynamic gain equalizers per each 80 km and 360 km spans, respectively.

The formulation has been implemented in the MatPlanWDM tool [46], which interacts with a TOMLAB/CPLEX solver [53]. Let *h* be the 7x7 traffic matrix in Fig. 2.3, obtained from traffic forecast studies for a national optical backbone (measured in Gbps). All the traffic matrixes used are calculated multiplying *h*, by a real factor. For each topology we made 20 tests with different traffic matrixes, from the higher traffic carried at 0 cost, to the higher carried traffic feasible found. In each test, we apply the heuristic algorithm in [33] which obtains the minimum set of lightpaths which is able to carry the traffic demand, assuming a capacity of 10 Gbps per lightpath. As the WC technology is not fully mature, WC prices are estimated sweeping the WC cost from 0.01 (1% of a transmitter plus a receiver), to a sufficiently high value. Naturally, as the WC cost grows, a lower preference for WCs can be expected.

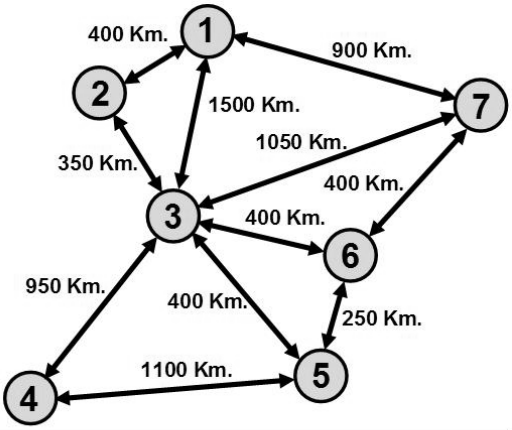

	1	2	3	4	5	6	7
1	0	13.30	23.53	8.10	13.52	22.81	20.59
2	4.28	0	22.91	7.89	13.16	22.24	20.07
3	23.53	73.69	0	43.03	71.88	121.47	109.70
4	8.10	25.28	43.03	0	24.66	41.69	37.67
5	13.52	42.26	71.88	24.66	0	69.66	62.90
6	22.81	71.41	121.47	41.69	69.66	0	106.30
7	20.59	64.50	109.70	37.67	62.90	106.30	0

Fig. 2.3. Mesh topology and its associated traffic matrix *h*

Surprisingly, as it is shown in Table 2.1, wavelength converters are not used in any case, even considering the lower WC cost of c_{WC}=0.01. As traffic grows, a higher number of fibres are activated; but always happens, that given a set of active fibres, if a solution with wavelength converters is found, a solution without WCs and the *same active fibers* is found (obviously at a lower cost). These results neglect the utility of the installing *WCs* in multifiber networks. This conclusion is consistent with the results of previous studies in both dynamic [11],[57] and [59]) and static planning scenarios ([10],[63],[64] and [67]), where the improvement on blocking performance (dynamic experiments) and total number of enabled fibers (static cases) by introducing wavelength conversion in multifiber designs was very limited. However, the results in the work [13], developed in this chapter, are even stronger because of two main reasons: (i) the solutions were obtained by a unique formulation which balances the WCs costs and the multifiber activation costs while performing an optimal search in the solution space; and (ii), only solutions without WCs were found.

Table 2.1. Results when c_{WC}=0.01

	MESH net - 7 nodes			RING net - 7 nodes			STAR net - 7 nodes		
Matrix Index	Carried Traffic (Gbps)	No. Used WCs	No. Extra Activ. Fibres	Carried Traffic (Gbps)	No. Used WCs	No. Extra Activ. Fibres	Carried Traffic (Gbps)	No. Used WCs	No. Extra Activ. Fibres
1	953	0	0	368	0	0	338	0	0
2	1005	0	2	397	0	1	356	0	1
3	1057	0	3	425	0	3	375	0	2
4	1109	0	4	454	0	4	393	0	3
5	1160	0	5	483	0	4	412	0	3
6	1212	0	6	512	0	5	431	0	3
7	1264	0	6	540	0	6	449	0	4
8	1316	0	6	569	0	6	468	0	5
9	1367	0	7	598	0	7	486	0	5
10	1419	0	7	627	0	7	505	0	5
11	1471	0	8	655	0	9	523	0	6
12	1523	0	10	684	0	10	542	0	6
13	1574	0	11	713	0	10	561	0	6
14	1626	0	11	742	0	11	579	0	6
15	1678	0	13	770	0	11	598	0	7
16	1730	0	13	799	0	11	616	0	7
17	1781	0	15	828	0	12	635	0	7
18	1833	0	16	857	0	13	653	0	7
19	1885	0	16	885	0	14	672	0	7
20	1937	0	18	914	0	14	691	0	7

2.5 Conclusion

In the study carried out in [13], two approaches to expand the capacity in multifiber optical networks were compared: (i) installing wavelength converters at the WR nodes; or, (ii), activating additional fiber in the physical links. A novel ILP formulation which explicitly balance the WC cost and the multifiber cost was proposed to perform the cost comparative study.

The ILP formulation was tested for a realistic mesh network (Fig. 2.3) based on a national optical backbone with an associated traffic matrix from traffic forecast studies. In addition, experiments were conducted on a ring and a star network. In the solutions, for increasing traffic loads, WCs were not required. These results neglect the utility of the installing *WCs*: solutions where the use of *WCs* replaces the activation of extra fibers were not found. This conclusion is coherent with previous results suggesting that the reduction on the activation of additional fiber wires by introducing wavelength conversion is not significant.

Chapter 3

3 Physical Layer Impairment Aware Planning

ABSTRACT: This chapter develops the main contributions of the present thesis to the planning of WDM networks when physical layer are introduced in the optimization problem. In this more realistic scenario, the network planner takes into account those physical phenomena which degrade the quality of the optical signal. In the first sections of the chapter, we introduce those impairments that impact more severely on the signal quality, as well as some methods to account them to determine if the optical signal at the receiver satisfies the Quality of Transmission (QoT) requirements. Then, the set of Physical Layer Impairment Aware (PLIA) planning problems addressed in this thesis are presented. Next, the contributions of this thesis in this topic are detailed: first, several heuristic algorithms to solve the PLIA-RWA problem in 10 Gbps single line rate networks are proposed; secondly, the planning in 10/40 Gbps mixed line rate networks considering non linear inter-channel interferences is modeled and a problem-decomposition-based heuristic to solve it is presented. Finally, this thesis has also contributed in the related field of Regenerator Placement problem in optical networks. The contributions in this topic are commented.

3.1 Physical Layer Impairment Aware Planning in WDM networks

In the real optical networks, the degradation on the signal's quality along a *lightpath* is one of the most critical limitations to the virtual topology design. Although, there exist sufficient free resources, such as WDM channels, optical transponders or input/ouput ports in the WXCs, a *lightpath* establishment may be infeasible, as the physical impairments accumulated along the optical path may degrade the signal's quality below the minimal *Quality of Transmission* (*QoT*) required at the *lightpath* receiver node. Conversely, a *lightpath* meeting these QoT requirements at the optical receiver is called as *QoT feasible*.

Introducing these impairments due to the physical layer into the optical network planning defines the so-called ***Physical Layer Impairment Aware (PLIA) Planning***. These planning problems can be classified, like many WDM network problems, depending on the time-variability of the estimated traffic demand in [17] *dynamic* and *static PLIA planning*. In this thesis, we focused on the latter one, i.e., the PLIA problem variant where the estimated traffic demand is assumed as known, and constant along the time. With the term of *PLIA planning*, we refer in this thesis to several WDM network planning problem

variants which consider explicitly the physical layer:

1) ***Physical Layer Impairment Aware VTD*** (***PLIA-VTD***) ***problem*****.** This problem is the version of the overall multilayer VTD problem detailed in Section 1.2. The problem receives the traffic matrices and the physical topology description in order to perform, in the lower layer, the RWA of the lightpaths, guarantying the *QoT* requirements; and, in the upper layer, the flow routing of the traffic matrices over the *QoT feasible lightpaths.*

2) ***Physical Layer Impairment Aware RWA*** (***PLIA-RWA***) ***problem***. This is the lower layer subproblem of the previous PLIA planning variant. In this problem, the *virtual topology* (number of lightpaths to establish between each node pair) is received as input parameter. The PLIA-RWA problem searches for each lightpath a valid route and wavelength (RWA), so that the *QoT* of the lightpaths are satisfied.

3) ***Regenerator Placement* (*RP*) *problem.*** This problem receives as an input a virtual topology along with the RWA of the *lightpaths*. Some of the *lightpaths* in the *VT* may be *QoT infeasible* requiring that signal regenerators must be placed at some intermediate nodes. Therefore, the objective of the RP is to find the optimal allocation of signal regenerators at the nodes to guaranty the *QoT feasibility* in all the *VT*.

4) ***PLIA-RWA-Regenerator Placement* (*PLIA-RWA-RP*) *problem*** [20]**.** The last two above mentioned problems ***PLIA-RWA*** and ***RP*** can be solved jointly, in the so-called problem *PLIA-RWA-Regenerator Placement* (*PLIA-RWA-RP*) [20].

The major contributions of this thesis in *PLIA planning* pertains to the framework of the **(i) *PLIA-RWA problem*** with the work **[21]**, and **(ii) *PLIA-VTD* problem** with the work **[27]**. In the first study, the *PLIA-RWA* is investigated in optical communications systems using the classical 10 Gbps bit rate and standard OOK format modulation. In contrast, [27] studies the overall *PLIA-VTD* problem in the context of optical systems employing higher bit rates (40 Gbps) and more advanced modulation formats (DQ-PSK) along with classical 10 Gbps OOK signals. Finally, this thesis has also contributed to the work [20] on *PLIA-RWA-RP*.

Several techniques have been proposed in the literature to introduce the physical impairments into the planning problem. These techniques require estimating the impact of the physical layer impairments on the *lightpath QoT feasibility.* Obviously, this *QoT* estimation depends on the list of physical impairments taken as relevant to degrade the optical signal and the way how to compute them. Moreover, according to the bit rate and the modulation format, the list of most relevant impairments and the procedure to estimate

them may change. Therefore, we comment these aspects in the next subsections before going further into the PLIA planning investigations.

3.2 Main physical layer impairments

The physical layer impairments (PLIs) that affect the quality of the optical signal are usually classified into ***linear*** and ***nonlinear*** [14]-[17]. According to [17], a *linear impairment* is independent of the signal power and, generally, but not always, affect each one of the WDM channels individually; whereas a *nonlinear impairment* are very sensitive with the power level (usually, become larger with the launch power) and affect not only each optical wavelength channel individually (they also cause disturbance and interference between them).

The main linear impairments affecting optical communications are [14]-[18]:

- *Fiber Attenuation* [14], [18]. In a natural way, the power level of an optical signal diminishes when propagating along a fiber. This power attenuation is caused by different reasons such as, material absorption (both intrinsic and extrinsic), *Rayleigh* scattering or waveguide imperfections (like macro- and micro- bending losses).
- *Component Insertion Losses* [17]. Since perfect insertion between optical components (e.g. an optical fiber and an optical amplifier) is impossible, some part of the optical power is not transmitted through the interface between them.
- *Amplified Spontaneous Emission* (*ASE*) *noise* [14], [15], [16]. The optical signal requires a minimum power level to be detected by the receiver. Therefore, losses along the optical path have to be compensated through a proper amplification. Unfortunately, optical amplification is not possible without the generation of *amplified spontaneous emission* (*ASE*) *noise* at each amplifier. The total *ASE* accumulated along the amplifier chain is the fundamental noise term at the receiver.
- *Chromatic Dispersion (CD*) [14], [15], [16]. *Chromatic dispersion* (or also called, *group velocity dispersion*, *GVD*) causes an optical pulse to broaden in time, since the different frequency components of the pulse travel at different group velocities. This pulse broadening results in inter-symbol interference (ISI), limiting the transmission distance. The *CD* can be compensated by Dispersion Compensation Fibers (DCF), special optical filters or some kind of pre- or post-process at the nodes. However, the total compensation of the *CD* can be counterproductive, as the dispersion alleviates other effects, such as *Cross Phase Modulation (XPM*).

- *Polarization Mode Dispersion* (*PMD*) [14], [15], [16]. In this dispersion, the pulse broadening is caused by the difference in the group velocities of the two orthogonal polarization modes, resulting from a mechanical stress induced birefringence in the fiber. Again, the dispersion limits the maximum reach of the optical signal. *PMD* is especially sensitive with the bit rate, being the most important polarization effect for systems with high bit rates (40 Gbps and above [16],[71]).
- *Polarization Dependant Losses* (*PDL*) [15]. This effect combined with PMD causes optical power variation, waveform distortion and signal-to-noise ratio fading, being accumulated with the components on the transmission path.
- *Crosstalk* (*XT*) [14], [15], [16]. Crosstalk is caused by power leakage from other signals to the desired signal. In a WDM system, crosstalk can be originated in the filters, mux/demux and WXCs. Crosstalk can be classified into intra-channel or inter-channel. The former is when the interfering signal is at the same wavelength as the desired signal, whereas, in the latter case the interfering signal uses a different wavelength. Intra-channel crosstalk is much more severe compared to inter-channel crosstalk. For this reason, PLIA planning usually considers only the intra-channel one.
- *Filter Concatenation* (*FC*) [14], [15], [16]. In a *lightpath*, the optical signal must traverse multiple WDM filters between source and receiver nodes. This concatenation of filters narrows the effective spectral transfer function, since individual filters' function does not match perfectly. The narrowing of the total filter pass-band can lead to a time-domain distortion and a distortion-induced eye closure penalty. This effect becomes significant the more filters are traversed, supposing a serious limitation on the *lightpath* length. Moreover, since traffic at lower bit rates can tolerate a narrower passband, the *FC* effect can increase dramatically at higher bit rates.

On the other hand, the most important *non-linear impairment*s [17] are grouped in two categories:

- Kerr effect impairments [14], [16], [18]: *self phase modulation* (*SPM*), *cross phase modulation* (*XPM*) and *four wave mixing* (*FWM*).
- Inelastic scattering mechanisms [14], [16], [18]: *stimulated Brillouin scattering* (*SRS*) and *stimulated Raman scattering* (*SRS*).

The optical Kerr effect results in an intensity dependent phase shift of the optical signal, usually manifested as a phase modulation. By contrast, inelastic scattering mechanisms are responsible for

intensity dependent gain or loss.

The optical Kerr effect is caused by an intensity dependent refractive index with optical power, responsible for an intensity dependent phase shift of the optical signal. This nonlinear phase shift usually is manifested as a phase modulation. The nonlinearities stemming from the Kerr effect occur due to the nonlinear relationship between the induced polarization and the applied electric field when higher powers and/or bit rates are applied. Therefore, these non linear impairments constraint seriously the optical launch power, becoming also a major issue on higher bit rate systems.

In the inelastic scattering mechanisms, a original photon scatters to a lower energy photon such that the energy difference appears in the form an acoustic phonon (in *SBS*) or an optical phonon (in *SRS*). Both scattering process results in a loss of power at the incident frequency, and, *stimulated Raman scattering* causes power increases in short-wavelength channels and power decreases in long-wavelength channels. These effects can be prevented by keeping low the optical power level when launched into the fiber.

Assuming the launch power in low levels, the impairments caused by the optical Kerr effect are the non-linear ones affecting more seriously to the quality of the optical signal. The main non linear impairments caused by Kerr effect are [14],[16],[18],[71]:

- *Self Phase Modulation* (*SPM*) and *Cross Phase Modulation* (*XPM*). Both effects consist of the change of the optical phase of a channel induced by either its own pulse (*SPM* case) or other optical pulses in other channels (*XPM* case). The effect of *SPM* combined with chromatic dispersion results in the reduction of the pulse broadening. However, *SPM* and its interaction with *CD* are usually ignored because of its negligible contribution as indicated in [71]. Conversely, *XPM* can impair more severely the network performance. Similarly to *SPM*, *XPM* also interacts with *CD*, but *XPM* is relevant only when pulses in the other channels are superimposed in time with the signal of interest. If the *CD* is significant, the different group velocities of the pulses in each channel reduces the length of the distance (*walk-off distance*) where two pulses in different channels are superimposed, decreasing the *XPM* effect.

- *Four Wave Mixing* (*FWM*). In this phenomenon three waves (or two waves) are mixed during the propagation in the fiber to generate a new fourth wave (or third wave), which may fall into other busy channels and cause in-band crosstalk. FWM takes place when some wavelength channels satisfies a particular phase relationship called phase matching:

$$f_{ijk} = f_i + f_j - f_k \, (i, j \neq k) \tag{3.1}$$

The influence of *FWM* is larger when the optical channels are equally spaced, and, particularly, when WDM systems operate in the zero dispersion region. Therefore, *FWM* is more important in Dispersion Shifted Fibers (DSF) and, like *SPM* and *XPM*, can be reduced by increasing *CD*.

Although the previous classification into *linear* and *nonlinear* impairments is the most widely used in the literature, when considering PLIA planning algorithms, it is useful to categorize the PLIs into those that affect the same *lightpath* and those that are generated by the interference among *lightpaths* [21], [72]. These categories are also named as *static* or *dynamic*, respectively, in our contribution [21]; or, *Class 1* or *Class 2*, respectively, in [72]. According to this categorization, a *static* or *Class 1 impairment* is solely topology-dependent, and independent from the routing and wavelength assignment state of the network; whereas, a *dynamic* or *Class 2 impairment* depends on the presence and characteristics (RWA) of other *lightpaths* already established in the network. With this classification, the most relevant PLIs in WDM network planning can be regrouped into:

- *Static (*or *Class 1) impairments*: amplified spontaneous emission noise (ASE), polarization mode dispersion (PMD), chromatic dispersion (CD), filter concatenation (FC), self-phase modulation (SPM);
- *Dynamic* (*or Class 2*) *impairments*: crosstalk (XT) (intrachannel and interchannel crosstalk), cross-phase modulation (XPM), four-wave mixing (FWM).

We must note that the many of the linear impairments can be classified as *static*, and many of the non-linear, as *dynamic*. For example, the *crosstalk* impairment is, indeed, a linear, but a dynamic (Class 2) impairment, since its effect on a given lightpath depends on the *RWA* of the other lightpaths, but, however, is independent with the launch power. On the contrary, the SPM modulation, a non-linear Kerr effect impairment, is, indeed, a static (Class 1) impairment. This aspect has motivated that many works uses the *non-linear term* to refer to *crosstalk*, cross-phase modulation (XPM) and four-wave mixing (FWM) [20]. In the sequel, we will use the denominations *static*/*dynamic* and *linear*/*non-linear* according to the criterions exposed above, excepting in Section 3.6, where the work [20] is summarized. Then, we will use the *non-linear* term to refer to the *dynamic* impairments.

3.3 Introducing the Physical Layer Impairments in the Planning Problem

In order to incorporate the physical layer impairments (PLIs) in the optimization process, we must estimate its impact on the quality of the optical signal. The effects of PLIs can be estimated in two different manners: (i) computing each impairment effect individually; or, (ii) accounting all the impairments in a global *QoT* performance evaluator.

The first approach is more natural and intuitive, since each impairment is directly computed by analytical closed formula or estimated from laboratory measurements or simulation results. Then, for each impairment, we must consider a *QoT* independent criterion to determine if the *lighpath* is *QoT feasible* at the receiver node. For example, when the polarization mode dispersion (PMD) is evaluated, a normal criterion used is that the total Differential Group Delay (DGD) ΔT^{PMD}_{Tot} between the two polarization modes at the *lightpath* receiver node should be less than a fraction (ε) of the bit duration T (usually a 10%) [73]. This condition is expressed in (3.2), where B is the bit rate, M is the number of fibers in the lightpath, $D_{PMD}(k)$ is the PMD parameter in the kth fiber of the lightpath and $L(k)$ is the length of the kth fiber.

$$\Delta T_{Tot}^{PMD} = \sqrt{\sum_{k=1}^{M}\left(D_{PMD}^{2}(k)\cdot L(k)\right)} < \varepsilon \cdot T \;\Rightarrow\; B\cdot\sqrt{\sum_{k=1}^{M}\left(D_{PMD}^{2}(k)\cdot L(k)\right)} < \varepsilon \tag{3.2}$$

Assuming all the fibers in the network with D_{PMD} = 0.1 ps/√km and ε = 0.1 [73], the equation (3.2) becomes into a constraint on the total lightpath length whose value depends on the bit rate: 10,000 km for bit rates of 10 Gbps; and 625 km, for 40 Gbps. Therefore, in 40 Gbps communications, any lighpath longer than 625 km would not satisfy the QoT requirements at the receiver node.

In contrast to the previous approach, a *global QoT performance evaluator* accumulates all the impairment effects into one unique metric. Several global *QoT* performance evaluators have been proposed in the literature: *Bit Error Rate* (*BER*) [74], *Optical Signal to Noise Ratio* (*OSNR*)[75],[76],[77] and the so-called *Q-factor* [19],[21],[24],[78]-[82]. Since the ***BER*** is the main performance metric for digital optical receivers, the other two performance evaluators will be usually referred to the *BER* of the digital signal detected at the decision circuit of the receiver. A commonly criterion used for digital receivers requires the BER to be below than 10^{-9} [18]. Then, direct BER computation requires to count errors over very long, even absurdly long simulation time intervals, since errors are very infrequent.

Other QoT metric used to estimate the impact of channel noises in the optical signal is the ***OSNR***.

As the dominant noise along the optical path is the cumulated ASE noise, the OSNR results a good measurement of the ASE effect on the signal's quality [73],[76]. However, OSNR is an optical performance ratio, whereas BER is an electrical metric, therefore, the relation between both figures of merit will depend on how the optoelectronic conversion is performed by the optical receiver (dominant terms in the electrical noise at the receiver, receiver technology, quality of the receiver, existence of FEC, bit rate, threshold current, …). For example, in [73], a minimal OSNR of 20 dB for 10 Gbps communications without FEC at the receiver is proposed.

Finally, among the previous quality evaluators, the most widely accepted *global QoT estimator* is the ***Q factor***. Some of the reasons of this success are [17]: (i) its close correlation with BER (since direct measurement of BER is really difficult), (ii) its capability to account various PLIs effects as an integrated metric, and (iii) its flexibility to evaluate the quality of transmission using analytical [79] or experimental based models [80],[81]. The Q-factor may be considered as a special electrical signal-to-noise ratio defined at the input of the decision circuit in the receiver node. The Q factor is defined according to the formula (3.3) [19], [29]:

$$Q = \frac{\mu_1 - \mu_0}{\sigma_0 + \sigma_1} \tag{3.3}$$

where μ_0 and μ_1 are the mean values of the "zeros" and the "ones" currents or voltages, and σ_0 and σ_1 are their standard deviations in the decision circuit at the sampling time.

Under the assumptions that: (i) the probabilities of the received samples corresponding to sent "one" and "zero" bits posses a Gaussian distribution and their standard deviations are equal, (ii) the decision threshold is optimum, and (iii) the sample point at the decision circuit is also optimum, assumptions usually met in On-Off Keying (OOK) communications; the relation between Q factor and BER modulation format is:

$$BER = \frac{1}{2}\operatorname{erfc}\left(\frac{Q}{\sqrt{2}}\right) \tag{3.4}$$

By calculating the Q factor at the end of a *lightpath*, we can estimate the feasibility of a *lightpath* in terms of optical signal quality. For example, if the QoT requirement to accept a digital signal at the output

of an optical receiver is a BER lower than 10^{-9} [18], the formula (3.4) tells us that the factor Q must be greater than a quality threshold (Q_{thr}) of 15.5 dB for the optical signal at the *lightpath* output. Therefore, any *lightpath* whose Q factor at its destination node is less than 15.5 dB may not be *QoT feasible*.

The Q-factor can be classified in two categories [20] according to the strategy to include the *dynamic* impairments (denoted as *non-linear* in [20]):

- *Static (or Linear* in [20]*) QoT estimators*: The *dynamic* (or *non-linear* in [20]) impairments are over-estimated and summed to the linear ones, without considering interactions between neighboring lightpaths. In this case, the *QoT* estimation of a *lightpath* depends solely on its own route.
- *Dynamic* (or *Non-Linear* in [20]) *QoT estimators*: The *dynamic* (or *non-linear* in [20]) impairments are computed explicitly considering interactions between neighboring *lightpaths.* Therefore, the *QoT* obtained for a *lightpath* is dependent on the routing and wavelength assignment of other *lightpaths* in the network.

Several techniques have been proposed to introduce the PLIs into the planning problem. The technique selected by the network planner will depend on the approach used to estimate the impact of the impairments onto the QoT. In some works [27], [72], [83], the PLIs are estimated individually and incorporated, directly, [72], [83] or indirectly [27],[72], to mathematical programs (MILP or ILP) as model constraints. Whereas, in other ones [19],[21],[24],[75]-[82], heuristic algorithms based on *network planning stages* alternating with *global QoT performance evaluation stages* are proposed. In the *QoT performance evaluation stages*, one of the aforementioned global estimators is used to verify the *QoT feasibility* of the candidate lightpaths found in the *network planning stages.*

In a direct estimation approach, for each impairment individually, the contribution of its source along the route of the lightpath (WXCs at the nodes for crosstalk, amplifiers at the links and nodes for ASE noise, interfering wavelengths at the fibers for XPM, SPM and FWM, etc) is introduced in the formulation. Usually, for each impairment, its contribution to the total lightpath noise variance is computed for each candidate path and wavelength. Then, an upper bound on the total variance which can tolerate a lightpath to be accepted is computed. Finally, this upper bound is used in the formulation to constrain the sum of noise variance contributions along the candidate paths and wavelengths. An example of this direct estimation approach is used in the work [19], where this thesis has contributed. In [19], an ILP formulation constraining the lightpath noise variance related to *dynamic impairments* (as we define in this thesis) *intrachannel crosstalk*, *XPM* and *FWM* is applied to perform a wavelength

assignment. The upper bound on the maximum *"dynamic"* noise variance to still meet the QoT requirements is estimated after accounting for the *static* impairments which do not depend on the other used lightpaths and can be precomputed.

In opposite to the aforementioned direct approach, the PLIs can be introduced indirectly in the mathematical formulations as design limitations on factors such as 1) the length and the number of hops of a path (e.g. due to ASE noise and optical dispersions); 2) the number of adjacent (and second adjacent) WDM channels over all links of the lightpath (e.g. due to XPM); and 3) the number of intrachannel generating sources along the optical path (e.g. due to intrachannel crosstalk). For example, in the above mentioned PMD case, according to [73], a constraint on the total lightpath length (625 km) could be introduced in the planning of 40 Gbps networks, assuming in all the fibers D_{PMD} = 0.1 ps/√km, in order to keep the Differential Group Delay at the receiver below 10% of the bit duration. We find other application of the indirect estimation approach in the mixed line rate study [27], which forms part of this thesis, broadly developed in the Section 3.5. In this study, we assume that the accumulation of all the PLIs limit the lightpath transparent reach to 2000 km for 10 Gbps optical communications; and 600 km for 40 Gbps systems, whereas the XPM interferences between 10 and 40 Gbps lightpaths is incorporated as the obligation of leaving a guard WDM channel between them.

Apart from the above mentioned formulation based approaches, the physical impairments can be introduced in the PLIA planning by heuristic methods where *network planning stages* alternate with *QoT verifications stages*. In the planning stages, the main planning decisions (i.e. lightpath routing, wavelength assignment, regenerator placement, traffic routing onto the virtual topology, …) are taken, considering or not the physical layer [17]; whereas, in the QoT verifications stages, the quality of the lightpaths decided to establish in the planning stages is evaluated with different QoT metrics, such as OSNR [75],[76],[77] or Q factor [19],[21],[24],[78]-[82]. If the lightpath quality does not overcome a minimal threshold (e.g. 15.5 dB for the Q factor), it is not *QoT feasible*, and removed from the current solution. Generally, the *network planning stages* alternate with *QoT verifications stages* until some stopping criterion is met, e.g. a number of iterations or a minimum number of *QoT feasible* lightpaths. In [17], the different approaches published under this alternating scheme are categorized in two: a) *network planning stages* ignoring physical layer impairments with *QoT verifications stages*, and; b) *network planning stages* considering physical layer impairments also with *QoT verifications stages*. This last approach is the applied in one of the single line rate PLIA-RWA algorithms [21] presented in the next section.

In the next chapter sections, the main author's contributions, where examples of all the mentioned procedures to incorporate the physical layer into the network planning are used, are broadly detailed. In

all these works, dynamic impairments were considered explicitly, increasing the problem complexity, since all the possible mutual interferences between lightpaths constraint the solution space.

First, we develop the heuristic algorithms proposed for 10 Gbps single line rate networks in [21]. These proposals employ the same *dynamic* QoT estimator. Then, in the Section 3.5, the 10/40 mixed line rate study conducted in [27] is explained. The two aforementioned works constitute the main contributions of the present thesis to the PLIA planning, but the author has also collaborated in the work [19] where the joint PLIA-RWA-RP is investigated. This research is summarized in the brief Section 3.6 that concludes this chapter.

3.4 Single Line Rate PLIA-RWA Algorithms

3.4.1 Problem statement

In next subsections, we describe the contributions of this thesis in the single line rate PLIA-RWA planning. It mostly corresponds to the material published in [21]. This work contributes in the field of the single line rate (SLR) network planning problem by the proposal and comparative evaluation of two novel static PLIA-RWA algorithms for multilayer WDM optical networks, which share a common dynamic QoT evaluation function, indeed a Q factor. In the PLIA-RWA, the physical impairments are considered during the cross-layer planning of optical WDM networks. The selection of a route of free WDM channels to establish the set of lightpaths in the virtual topology will depend on (i) how the upper layer traffic demands are translated to lightpath demands, and (ii) the degradation on the signal's quality caused by the physical layer impairments (PLIs). The estimation of the degrading impact of the PLIs is complicated by the diversity of modulation formats, transmission rates, amplification and compensation equipments, or deployed fiber links. In this study, the optical signals are transmitted at 10 Gbps by using the traditional intensity modulation format On Off Keying (OOK). The physical impairments in 10 Gbps OOK optical communications are well known [71],[73],[74],[84]-[89], allowing the implementation of Q factors embracing the major PLIs. This is the case of the Q-tool used in the two proposed algorithms. This Q-tool function models a Q-factor of the lightpaths in a virtual topology. The Q-factor can be directed related to the signal Bit Error Rate (BER) performance according to the formula (3.4) and it us used to estimate the degradation on the transmitted signal Quality of Transmission caused by the accumulation of the PLIs along the lightpath. In this case, if the Q factor of a lightpath drops beyond a predetermined threshold of15.5 dB (corresponding to BER = 10^{-9}), then this lightpath will be blocked, an event called "QoT blocking".

Two main types of optimization strategies exist when dealing with the network planning process. They are commonly called as offline (static) and online (dynamic) planning**.** In offline planning, the traffic demand is assumed as fixed and known in advance, while online planning designs the reactions to the arrival of lightpath establishment requests along time. Thus, the online planning problem is commonly addressed by processing individual requests one by one, examining the feasibility of the possible lightpaths for each connection request. In fact, in the online planning scenario we can always calculate (through appropriate analytical models) or measure (by optical performance/impairment monitoring) the interference of the other channels to the lightpath under investigation, since other lightpaths have already been established when the algorithm is executed. This maybe explains why the most of the first algorithms proposed in the open literature address the online version of the PLIA-RWA problem (Comprehensive surveys can be found in [17] and [90]). In contrast to this, the work in [21] is focused on the static PLIA-RWA planning problem, where the investigations are less. This is mainly due to the fact that even the classical static RWA problem, ignoring physical layer is NP-complete, and it becomes more complicated when considering signal impairments, which imply cross-layer optimization techniques. Then, planning algorithms have to make use of techniques where network planning stages alternate with *QoT* verifications stages, such as, (i) a network planning modules which intends to perform smartly a global exploration of the solutions space (e.g. by using some QoT evaluator), or (ii) dynamic approaches used to address the static traffic sequentially following different pre-orderings. In both approaches, the heuristic takes tentative decisions in planning steps, followed by QoT sanity steps to verify its QoT feasibility. Then, new planning and QoT steps can alternate to improve the solutions. In the first approach, the information about the constraints that physical layer impairments imposes on the lightpath feasibility can be used to reduce severely the solutions space where a optimal solution is searched. Consequently, this reduction will depend on the QoT performance valuator used to model the impact of the PLIs on the signal's quality. In the second approach, based on online algorithms adapted for the offline case, the connection requests are served sequentially, checking the QoT of each connection request before going on with the next one. In this case, the order in which the connections are served becomes particularly important for the final solution. Therefore, to improve the performance, an ordering phase can be used before sequentially serving the connections. The two algorithms presented in [21] are based on these two approaches.

The first proposed algorithm heuristically combines a set of Binary Integer Linear Programming (BILP) formulations. It is designed to allow a global search of the solutions space, but limiting the complexity of the BILP formulations to guarantee its scalability. As far as the author knows, this was one of the first proposals following this approach. Then, two variations of a heuristic algorithm are proposed which explore the solutions space by first sequencing the traffic demand in different manners, and then

processing the demands one by one. The proposed schemes are compared in different scenarios, evaluating their lightpath blocking rate performance. Also, the scalability of the algorithms is assessed by evaluating the algorithms' response time in diverse situations. Results reveal great scalability properties of the global search algorithm, and a performance similar to or better than the sequential schemes.

The rest of the section is organized as follows. In Subsection 3.4.2, a review on existing offline PLIA-RWA algorithms is provided. Subsection 3.4.3 presents the used dynamic QoT performance evaluator (Q-tool). Subsection 3.4.4 presents our PLIA-RWA algorithm based on the global optimization approach and is followed by the traffic demand sequencing approach in Subsection 0. Comparative simulation results, along with the study on the algorithms scalability are compiled in Subsection 3.4.6. Finally, Subsection 3.4.7 concludes.

3.4.2 Related work

This section surveys a set of relevant contributions in the field of PLIA planning in multilayer WDM networks. Comprehensive reviews can be found in [17] and [90]. Most of these studies consider the online (dynamic) version of the problem [74],[76],[91]-[95], whereas the offline (static) case has received less attention by the researchers. Before we will focus on the own static works related to the present work, it is worth mentioning that online algorithms can be used to solve the offline problem. This can be done by considering the offline connections sequentially and serve them on a one-by-one basis. In order to use an online algorithm for solving the offline problem the algorithm has to be able to take into account the effect of the existing connections [81]. In general, these approaches do not optimize the utilization of wavelengths for all connections requests jointly and thus their performance is suboptimal.

In [96] a link-path Integer Linear Programming (ILP) formulation for the classical RWA problem is proposed. Impairment constraints are taken into account by appropriately pre-processing the data which feed the RWA formulation. This is done by pre-calculating a set of k paths with the assistance of a shortest path algorithm, which uses either a single physical impairment [96] or a Q-penalty [78] as the link cost parameter. Then, the virtual topology is calculated by the ILP formulation, considering only the set of candidate paths. Finally, the virtual topology resulting from the RWA formulation is post-processed by evaluating the QoT feasibility of its lightpaths. For the lightpaths with unacceptable transmission performance, new solutions are searched by excluding lightpaths that were previously considered from the original set of candidate paths.

An impairment-aware offline RWA algorithm that assigns Q-factor costs to the links before solving the problem is proposed in [79]. In this work, k-shortest routes are computed considering Q-penalty values as the links costs. Finally the wavelength that maximizes the Q value is selected for each

connection request. Since the wavelength assignment is not performed jointly for all connections, a worst case scenario for the interference among lightpaths is used. Therefore, the proposed algorithm does not take into account the interference among lightpaths and does not optimize the solution in order to avoid inter-lightpath interferences.

Some more specific proposals that introduce physical layer impairment constraints into the optimization problem were studied as well. A Mixed Integer Linear Programming (MILP) formulation for the RWA problem of multicast connections, while considering optical power constraints, is presented in [97]. The authors formulate the RWA problem considering the optical power in order to ensure that the power level at the beginning of each optical amplifier, and also at the end of each fiber is above a certain threshold.

An ILP formulation for the problem of traffic grooming in optical virtual private networks with the BER constraint is presented in [98]. The physical layer impairments and the BER are indirectly taken into account in the ILP formulation through the length of the path.

In [99] the implementation of an LP solver in a Path Computation Element (PCE) is reported. The implemented objective function minimizes the maximum link bandwidth utilization. As a result the routes satisfying the required constraint in terms of bandwidth and optical signal quality can be found. However, it should be noted that it does not propose an algorithm but a general architecture to consider physical impairments in a Path Computation Element (PCE).

Finally, one of the most recent studies in offline PLIA planning was published in [72]. This work proposes two novel PLIA-RWA algorithms, extending the method for solving the classical RWA problem (ignoring impairments) based on a linear programming (LP) relaxation formulation presented in [100], [101]. The first algorithm consider the physical layer indirectly by adding to the formulation constraints on the path length, the hop account, the number of neighboring channels in path's links, or the number of intrachannel crosstalk sources. By way of contrast, the second algorithm uses noise variance-related parameters to directly account for the most important physical impairments, incorporating to the model constrains on the maximal noise variance tolerable to accept a lightpath.

The work presented in this section contributes to the offline PLIA-RWA planning field in several forms. First, as far as the author knows, the global searching algorithm proposed was one of the first attempt to heuristically combine BILP formulations for the PLIA-RWA problem, in a manner which limits the complexity to guarantee algorithm scalability at common network sizes. In addition, a family of algorithms is proposed to investigate the benefits of optimization techniques which pre-orders the traffic demand following some suitable criteria, and processes each connection request sequentially. All approaches share a common dynamic *Q*-factor evaluation function, to make a fair comparison and extract

useful conclusions about the most suitable optimization approaches. Also, the scalability of the algorithms is studied.

3.4.3 Q-tool: Physical Layer performance evaluator

In this work, we categorize the impairments into *static* and *dynamic* ones, following a similar taxonomy to [72], where the *static* impairments correspond to the *Class 1* impairments in [72] (impairments that affect the same lightpath); and the *dynamic* ones, to the *Class 2* impairments (impairments generated by the interference among lightpaths).

Static impairments are topology-dependent, and independent from the routing state of the network. The static impairments considered in this work are Amplifier Spontaneous Emission (ASE) noise, filter concatenation (FC), and Polarization Mode Dispersion (PMD). Self Phase Modulation (SPM) (and its interaction with chromatic dispersion) was not included because of its negligible contribution (as indicated in [71]) and its static nature that renders it independent of the traffic. Dynamic impairments depend on the presence and characteristics of other lightpaths already established in the network. This work accounts for the following dynamic impairments: node intrachannel crosstalk, originating from signal leaks at nodes, and nonlinear effects: Cross Phase Modulation (XPM) and Four Wave Mixing (FWM).

The Quality of Transmission (QoT) of a lightpath is evaluated by so-called *Q*-tool. *Q*-tool is indeed a *Q*-factor of the lightpaths. The *Q*-factor, defined as (3.3), is related to the signal's Bit-Error Rate (BER) for an On-Off modulated signal according to (3.4), assuming Gaussian distributions of the received "zeros" and "ones" bit samples. Although the Gaussian assumption may not always be accurate, there is always a strong correlation between *Q* factor and BER and hence we use *Q* factor as a Quality of Transmission estimator to represent BER performance.

In this study, the formula (3.3) is simplified considering that the mean value for "zero" bit sample (μ_0) is negligible compared with the mean value for "one" bit sample (μ_1) . Then, the *Q*-tool actually computes the following quantity:

$$Q = \frac{\eta_{PMD} P_1^{'}}{\sigma_0 + \sigma_1} \tag{3.5}$$

where σ_1 and σ_0 are the standard deviations of the received samples corresponding to sent "one" and "zero" bits. As suggested in [89], we model filter concatenation (FC) impairment as an eye closure penalty, yielding the term P_1'. The PMD effect is modeled as a penalty on the *Q*-factor as in [88] through the multiplicative factor η_{PMD}.

Other impairments are accounted for through noise variances:

$$\sigma_1^2 = \sigma_{1,ASE}^2 + \sigma_{1,XT}^2 + \sigma_{1,XPM}^2 + \sigma_{1,FWM}^2 \tag{3.6}$$

$$\sigma_0^2 = \sigma_{0,ASE}^2 + \sigma_{0,XT}^2 \tag{3.7}$$

ASE noise is modeled as a noise variance according to [18] and contributes to both σ_1 and σ_0 via $\sigma_{1,ASE}^2$ and $\sigma_{0,ASE}^2$, respectively. Since P_1', $\sigma_{1,ASE}^2$ and $\sigma_{0,ASE}^2$ only depend on the network topology and physical parameters (as η_{PMD} does), they can be pre-computed for a fast *Q*-factor estimation. Other noise terms such as the receiver thermal noise and shot noise are limited compared to the dominant ASE noise generated in such transmission distances, and therefore disregarded here. We also model node intrachannel crosstalk as a noise variance affecting "one" and "zero" bits according to [74] via the quantities $\sigma_{1,XT}^2$ and $\sigma_{0,XT}^2$. The XPM effect is modeled according to [84] and included in σ_1 via $\sigma_{1,XPM}^2$. Similarly the FWM effect is modeled as indicated by [86],[87] and is accounted for within σ_1^2 via $\sigma_{1,FWM}^2$. We refer the reader to [18], [74],[84], [86]-[89] for additional details about the modeling of each physical impairment.

Finally, we must indicate that this *Q-tool* is a *dynamic Q*-factor, since dynamic impairments (node intrachannel crosstalk, XPM and FWM) are explicitly computed, considering interactions between neighboring *lightpaths*. Therefore, the *QoT* obtained for a *lightpath* is dependent on the routing and wavelength assignment of other *lightpaths* in the network.

3.4.4 Global optimization approach

This subsection describes the global search algorithm proposed. It is based on an iterative search of PLIA-solutions, in which each iteration rearranges parts of the lightpath demand carried through a BILP approach.

Definitions

Let *N* be the set of nodes in the network, and *M* the set of unidirectional links. We denote as |.| the number of elements of a set. The same spectral grid of *W* wavelengths is considered in all the fibers. We define the set *S* as $S=\{(p,w),\ p$ path in the physical topology, $w \in W\}$. Each element in *S* is a path and wavelength assignment. We denote as $Q^*(p,w)$ the *Q* factor of a lightpath occupying path *p* in wavelength *w*, considering only static impairments. That is, in the absence of other lightpaths in the networks which

could degrade its signal quality. This is calculated by calling the *Q*-tool function with a virtual topology composed of only that lightpath. We are only interested in those (*p*,*w*) pairs which could be PLIA-valid, that is, for which $Q^*(p,w)$ is above a $Q_{Threshold}$ value corresponding to the maximum tolerable BER as defined by the network designer. We denote as $S_{IA}=\{(p,w),\ p \text{ path},\ w\in W,\ Q^*(p,w)\geq Q_{Threshold}\}$. Note that for the physical topologies of interest, significantly affected by impairment constraints, the number of elements in S_{IA} is relatively low. Furthermore, $|S_{IA}|$ grows linearly with the number of links in the network, as the impairments commonly end up limiting the maximum number of hops and the maximum distance of the paths.

We denote $S_{IA}\{m\}$, $m\in M$ as the set of PLIA-valid (*p*,*w*) pairs which traverse link *m*. We denote $S_{IA}\{i\rightarrow j\}$, $i,j\in N$ as the set of (*p*,*w*) pairs corresponding to paths initiated in node *i*, and ending at node *j*.

The lightpath demand is defined by the lightpath demand matrix $T=\{T_{i,j},\ i,j=1...|N|\}$, being T_{ij} the number of lightpaths to be established from node *i* to node *j*. We define a virtual topology *V*, as a set of lightpaths established and their routes, where each lightpath is subject to the wavelength continuity constraint. Thus, a lightpath is defined by its route *p* and its wavelength *w*. Given a virtual topology *V*, containing the lightpath (*p*,*w*) we denote $Q_{ev}((p,w),V)$ as the *Q*-factor of the lighptath (*p*,*w*), evaluated in the presence of the other lightpaths in the virtual topology *V*, and thus considering both static and dynamic impairments.

We define the *degradation matrix D*, as a ($|S_{IA}|$ x $|S_{IA}|$) matrix composed of one row and one column for each PLIA-valid (*p*,*w*). Given two lightpaths, $h_1=(p_1,w_1)$, $h_2=(p_2,w_2)$, a degradation value $D(h_1,h_2)$ measures the degradation caused in h_1, when lightpath h_2 is established, assuming that no other lightpaths apart from h_1 and h_2 occupy the network:

$$D(h_1,h_2) = Q^*(h_1) - Q_{ev}(h_1,V=\{h_1,h_2\}) \tag{3.8}$$

Of course, this measure has sense only if both lightpaths are not simultaneously unfeasible because of wavelength clashing. Note also that this degradation measure does not include effects like four-wave mixing, which appear in the presence of more than two lightpaths.

Algorithm overview

The algorithm is organized in 4 sequential phases. Fig. 3.1 includes a pseudocode describing the overall phases. Three different types of Binary Integer Linear Programming (BILP) formulations are applied in different phases of the algorithm. We denote them BILP-1, BILP-2 and BILP-3.

Phase 1 is a preprocessing stage, where S_{IA} set and degradation matrix D are calculated. Both calculations depend only on the physical topology (e.g. do not depend on the traffic demand). Note that computing all the possible paths in the network is not needed, but only the PLIA-valid paths. As mentioned before, this implies a relatively low number of different (p,w) pairs in typical backbone networks. Regarding the D matrix, the potential number of values to calculate grows with the square of $|S_{IA}|$. Fortunately, only a small subset of coordinates in the matrix have significant values. For the cases studied, a relevant degradation appears only between lightpaths sharing at least one node (which includes the lightpaths sharing one link), and with a difference in the wavelength index of at most 2. This reduces the calculations to practical values.

Phase 2 searches for the feasible solution which carries the maximum number of lightpaths, without considering dynamic impairment constraints, but just wavelength clashing. It is conducted by solving BILP-1 formulation. The QoT of the lightpaths in the virtual topology found V is evaluated invoking the Q-tool function. Let V_{best} be the subset of lightpaths evaluated to be over the signal quality threshold. Along the algorithm, V_{best} will store the Q-feasible virtual topology found at this moment with the maximum number of lightpaths. This defines an upper bound (L_{ub}) and a lower bound (L_{lb}) to the number of lightpaths of the optimum Q-feasible virtual topology: $L_{ub}=|V|$, $L_{lb}=|V_{best}|$.

Phase 3 and 4 try to find solutions with an improved number of Q-feasible lightpaths. This is done by searching solutions in which the number of established lightpaths is forced to be exactly L, for different values of L. For a given L value, the *CoreAlgorithm* module is executed, which returns the best virtual topology found V, carrying L lightpaths, and its Q-factor evaluation vector Q_v. This vector contains the Q-factor values of the lightpaths in the virtual topology. The details of the *CoreAlgorithm* module will be described later in this section. The L values should be selected carefully: increasing values of L yield to solutions with more lightpaths established, that may interfere each other and decrease the number of Q-feasible lightpaths.

During phase 3, solutions are searched for decreasing values of L. Each phase 3 iteration, searches for a solution with an L value in the middle of the range $[L_{last},L_{lb}]$, where L_{last} is the L value tested in the last iteration of phase 3, and L_{lb} is the number of Q-feasible lightpaths in the best solution found up to this moment. Phase 3 ends when the L value is equal to or lower than L_{lb}. During phase 3, the list of L values already tested are stored (in order that they are not repeated during the phase 4), and the best solution found is updated.

Phase 4 starts with an initial value of L equal to the Q-feasible lightpaths in the best solution found, plus 1. Its objective is try to find better solutions, increasing 1 by 1 the L values to test, skipping the L values that have been already tested (as they provided worse solutions in the past). The procedure stops if

after G_L consecutive tests of increasing L values, the solutions found did not improve the best existing solution. G_L stands for L-gap. If G_L=1, the algorithm stops if an L value tested in phase 4, does not improve the best existing solution. Intuitively, a G_L value of 1 is logical in the sense that if no solution with L lightpaths established is found with more lightpaths Q-feasible than our best solution, a higher value of L could add more mutual degradation, and even give worse solutions. However, as the solutions space is not exhaustively searched, it happens that in some occasions better solutions are found with an L-gap greater than one. After some tests, we tuned the G_L value to be one tenth of the gap between the number of Q-feasible lightpaths in the best solution after phase 3 (current L_{lb}), and the number of lightpaths in the virtual topology found in the phase 2 (L_{ub}). Afterwards, G_L is bounded to be between 5 and 10. This has proved to be a good balance, suitable for different network load conditions.

Core algorithm

The *CoreAlgorithm* module is the fundamental part of the global search scheme. Given a total demand value L, it provides a virtual topology with exactly L lightpaths, trying to optimize the number of lightpaths among L that are Q-feasible. Fig. 3.2 displays a pseudocode for this algorithm.

The core algorithm starts from an initial solution calculated by BILP-2 formulation. Then, it iteratively searches for a solution improvement, with a bounded number of iterations M_{it}. In each iteration, the previous virtual topology obtained is modified by using a BILP formulation (BILP-3). BILP-3 is designed to:

- Force some active (p,w) pairs (existing lightpaths in the previous solution), to remain active in the next solution. This is denoted as the S_{IA}{r.a} set. The lightpaths to maintain are those whose Q-factor in the previous virtual topology is greater than or equal to current value of the U_1 threshold. Then, by using lower values of the U_1 threshold, we increase the number of lightpaths to maintain unchanged, and thus decrease the complexity of the underlying optimization problem.
- Force some inactive (p,w) pairs to remain inactive in the next solutions. This is denoted as the S_{IA}{r.i} set. The lightpaths to maintain are those which (i) if were activated would clash with lightpaths in S_{IA}{r.a}, or (ii) if were activated, would by its own degrade the Q-factor of a lightpath in S_{IA}(r.a} below the U_2 limit. That is, they are potentially harmful. A simplification is used, estimating at this point the Q-factor of a lightpath as the current Q-factor value minus the degradation calculated in the D matrix. Note that although not exact, this estimation is used inside the heuristic to limit the solutions space adaptively, as the U_2 threshold controls the complexity of the underlying optimization problem. Higher values of U_2 imply that more (p,w)

pairs are considered as potentially harmful, and forced to remain inactive in next iteration.

- Force to find a solution with a minimum number K of changes (K is always greater or equal to 1), respective to the previous iteration solution. Details about how changes between iterations are computed, are included in the BILP-3 explanation.

The BILP-3 formulation returns a solution constrained to previous conditions. It can happen that the BILP-3 formulation cannot find a feasible solution: meeting a minimum number of changes can be impossible if at the same time the number of (p,w) pairs that must remain unchanged is high. When this occurs, U_1 and U_2 thresholds are softened to reduce the number of (p,w) pairs forced to be unchanged, until a feasible solution is found by BILP-3. After a solution is obtained, the best solution stored is updated, if necessary.

The algorithm includes a mechanism to avoid a large number of consecutive iterations to explore a narrow solutions space. The K value is used for this purpose. When a solution is returned which is equal to one that was previously explored, the next iteration is forced to vary greatly, setting K to L/10, rounded to the upper integer. This means that at most 90% of the lightpaths can be left unchanged in the subsequent iteration. We can name this as a “hyper-jump” in the solutions space. Also, if the best stored solution is not improved after $MaxN_{ui}$ iterations since the last “hyper-jump”, one more “hyper-jump” occurs. The details about how the hyper-jump functionality is implemented are clarified in the next section.

The size of the “hyper-jump” could be modified using a simulated annealing technique, where the K values are selected randomly, with the average K decreasing as the number of iterations grows. This would imply a more global-oriented search in the solution space during the first algorithm iterations, which is smoothly converted into a more local-oriented search along algorithm execution. This technique is left to be explored in the future.

Global Search Algorithm overview

Phase 1: Preprocessing
Calculate the S_{IA} set.
Calculate the path degradation matrix D.

Phase 2: Find the first feasible solution
V = BILP-1(physical topology, T, S_{IA})
Q_v = Q-tool (V)
// extract the Q-feasible lightpaths from V
V_{best} = {(p,w) in V, $Q_v(p,w) \geq Q_{Threshold}$ }
L_{lb} = $|V_{best}|$; L_{ub} = $|V|$.

Phase 3: Down search of improving IA solution
$L = L_{ub}$
init loop phase 3:
L = floor ((L+L_{lb})/2)
if ($L_{lb} \geq L$)
  goto phase 4
end
[V,Q_v] = CoreAlgorithm (L,S_{IA},D)
V_{PLIA} = {(p,w) in V, $Q_v(p,w) \geq Q_{Threshold}$ }
add L to the list of L values tested
if $|V_{PLIA}| > |V_{best}|$ // improving solution
  $V_{best} = V_{PLIA}$
end
L_{lb} = max (L_{lb}, $|V_{PLIA}|$)
goto *init loop phase 3*
  .
Phase 4: Up search of optimum IA solution
$L = L_{lb} + 1$
G_L = min(10,max(5,floor((L_{ub}-L_{lb})/10]))
unimprLvalues = 0;

init loop phase 4:
while L value already tested in phase 3
  $L = L + 1$
end
[V,Q_v] = CoreAlgorithm (L,S_{IA},D)
add L to the list of tested L values
V_{PLIA} = {(p,w) in V, $Q_v(p,w) \geq Q_{Threshold}$ }
if $|V_{PLIA}| > |V_{best}|$ // improving solution
  $V_{best} = V_{PLIA}$
  unimprovedLvalues = 0;
else
  unimprovedLvalues ++;
end
if *unimprovedLvalues* == G_L
  end algorithm // V_{best} is the best solution found
else
  $L = L + 1$
  goto init *loop phase 4*
end

Fig. 3.1. Pseudocode for the general scheme of the global search algorithm

BILP formulations

The proposed algorithm solves three different types of BILP formulations along its execution named respectively BILP-1, BILP-2 and BILP-3. All three share the decision variables, and a part of the constraints, but their objective function differs.

The decision variables in BILP-1, BILP-2 and BILP-3 are:

- $x(p,w)$ = {1 path p is being used by a lightpath, using wavelength w, 0 otherwise}, $(p,w) \in S_{IA}$.

BILP-1 formulation (3.9) is devoted to calculate the virtual topology which maximizes the carried lightpaths, not considering impairment constraints. Constraints in (*c1*) are the wavelength clashing constraints. They avoid that two lightpaths occupy the same wavelength in the same link. Set of constraints (*c2*) defines the traffic demand constraints. They limit the number of lightpaths established between two nodes, to the lightpath demand between these nodes.

$$\begin{aligned} &\max \sum_{p,w \in S_{IA}} x(p,w), s.t. \\ &(c1) \sum_{(p,w) \in S_{IA}\{m\}} x(p,w) \le 1, \forall m \in M, w \in W \\ &(c2) \sum_{(p,w) \in S_{IA}\{i \to j\}} x(p,w) \le T_{i,j}, \forall i, j \in N \end{aligned} \tag{3.9}$$

In the BILP-2 formulation (3.10), the objective is to maximize the sum of the $Q^*(p,w)$ values of the carried lightpaths, without considering dynamic impairments. The set of constraints (*c1*) and (*c2*) are similar to the one in BILP-1. The constrain (*c3*) forces to carry exactly L lightpaths among the lightpath demand.

$$\begin{aligned} &\max \sum_{p,w \in S_{IA}} Q^*(p,w) x(p,w), s.t. \\ &(c1), (c2)\ like\ BILP-1 \\ &(c3) \sum_{(p,w) \in S_{IA}} x(p,w) = L \end{aligned} \tag{3.10}$$

In the BILP-3 formulation (3.11), the objective function intends to minimize the sum of the Q-

degradation values of the solution lightpaths, over the lightpaths that are forced to remain active from previous iteration. The *Q*-degradation suffered by a lightpath (*p*,*w*) is estimated as the sum of the *Q*-degradations of the other existing lightpaths over (*p*,*w*). Notice that this scheme does not expect to be a way to estimate the new *Q* factor of the lightpaths, but just a method to choose a solution which rearranges the carried demand in a way which minimizes a measure of *Q*-degradation on the lightpaths that remain unchanged. The sets of constraints (*c1*-*c3*) are the same as in BILP-2. The set of constraints (*c4*) forces some selected active lightpaths in previous iteration, to remain active in this iteration. The set of constraints (*c5*) forces some (*p*,*w*) pairs which were inactive in the previous iteration, to remain inactive in the current one. Constraint (*c6*) determines the minimum solution variation condition. This constraint forces to find a solution with a minimum number of changes *K* in the virtual topology, respective to previous iteration. A change is accounted as the number of (*p*,*w*) pairs that were active in the previous iteration, and are not active at present. Then, a lightpath reroute, a new lightpath establishment and an old lightpath tear down count as one change. This is an effective way to force large rearrangements in the virtual topology when desired, and to avoid ineffective continuous local explorations in the solutions space.

$$
\begin{aligned}
&\min \sum_{\substack{p_1,w_1 \in S_{IA}\{r.a\} \\ p,w \in S_{IA}}} D((p_1,w_1),(p,w))x(p,w), s.t. \\
&(c1),(c2),(c3)\ like\ BILP-2 \\
&(c4)x(p,w)=1,\ p,w \in S_{IA}\{r.a\} \\
&(c5)x(p,w)=0,\ p,w \in S_{IA}\{r.i\} \\
&(c6)L - \sum_{(p,w)\in S_{IA}\{act\}} x(p,w) \geq K
\end{aligned}
\tag{3.11}
$$

Core algorithm (L, S_{IA}, D)
/* L: fixed number of lighptaths to establish */
N_{ui} = 0 ; K = 1 ; it = 0;
$U_1^n = Q_{Threshold}$; $U_2^n = Q_{Threshold}$; M_{it} = 20; $MaxN_{ui}$ = 3

/* Search for starting solution */
V = BILP-2 (L); Q_v = Q-tool (V)
V_{opt} = {(p,w) in V, $Q_v(p,w) \geq Q_{Threshold}$ }; $Q_{v\text{-}opt}=Q_v$

/* Global virtual topology reconfiguration loop */
while ($it < M_{it}$) and ($|V_{opt}| <$ L)
  loop 1:
  S_{IA}{act}=(p,w) active in previous solution V
  S_{IA}{in}= (p,w) inactive in previous solution V
  S_{IA}{r.a}= (p,w)$\in S_{IA}${act}, $Q(V,(p,w)) \geq U_1$
  S_{IA}{r.i}= (p,w)$\in S_{IA}${in} that remain inactive.
    They are the ones for which:
    1. (p,w) clashes with any lightp. in S_{IA}{r.a.}, or
    2. $Q_{ev}((p_{ra},w_{ra}),V)$-$D((p_{ra},w_{ra}), (p,w)) < U_2$,
      for any $(p_{ra},w_{ra}) \in S_{IA}${r.a.}
  V = BILP-3 (L, S_{IA}{r.a}, S_{IA}{r.i}, K)
  if unfeasible, $U_1=U_1$+0.5; $U_2=U_2$-0.5; goto *loop 1*
  Q_v = Q-tool (V)
  V_{PLIA} = {(p,w) in V, $Q_v(p,w) \geq Q_{Threshold}$ }
  $U_1 = U_1^n$; $U_2 = U_2^n$
  if (V_{PLIA} solution repeated from previous iterations)
    K = ceil (L/10)
  else
    if $|V_{PLIA}| > |V_{opt}|$ // improving solution
      K = 1; N_{ui} = 0; V_{opt} = V_{PLIA}; $Q_{v\text{-}opt}=Q_v$
    else
      $N_{ui} = N_{ui} + 1$
      if ($N_{ui} == MaxN_{ui}$), K = ceil (L/10), end
    end
  end
  $it = it + 1$
end
return V_{opt}, $Q_{v\text{-}opt}$

Fig. 3.2. Pseudocode of the CoreAlgorithm module.

3.4.5 Sequential heuristic approaches

This section describes two algorithms based on a pre-processing ordering of the traffic demand, and a subsequent sequential processing of individual lightpath demands. The algorithms are described in pseudocode in Fig. 3.3.

The first stage in the sequential algorithms is a *demand pre-processing ordering* module. We propose two different strategies to order the demands. Both are based on assessing the a-priori distance between two nodes *i* and *j* by the length of the shortest path between *i* and *j*. Then, we order (*i*,*j*) node pairs according to the aforementioned shortest distance, multiplied by the number of lightpaths to be established between *i* and *j*, T_{ij}. Ties are broken randomly in this pre-processing step. Two orderings are considered: ascending and descending order. Ascending order prioritizes (*i*,*j*) node pairs with shortest paths and smaller demands, while descending order prioritizes (*i*,*j*) node pairs with longest paths and larger demands.

The sequential processing stage processes one by one the ordered list of (*i*,*j*) pairs. For each (*i*,*j*) pair, the T_{ij} lightpath demands are processed sequentially. If a route and wavelength assignment is found for the lightpath demand, so that all the previously established lightpaths and the new one are *Q*-feasible, then the lightpath and its associated route are added to the current virtual topology *V*. If not, the lightpath is blocked.

A lightpath demand is processed by first finding a candidate list of possible routes and wavelength assignments for the lightpath (*pwc* variable in the pseudocode). For each candidate route, a candidate virtual topology *V*' is constructed, composed of the current virtual topology, and the new lightpath demand traversing the candidate route. *V*' is evaluated by means of the *Q*-tool function. If any lightpath in *V*' is below the QoT threshold, the candidate route is discarded. When all the candidate routes are checked, if none of them passed the QoT test the lightpath is blocked. If more than one route passes the QoT test, the route chosen is the one with the maximum worst *Q*-factor (the *Q*-factor of the lightpath with the lowest *Q*-factor).

The *pwc* list for the node pair (*i*,*j*) is constructed in our tests as follows. For each wavelength we find the *k*-shortest paths which fulfill two constraints: (i) they do not clash with existing lightpaths in *V*, (ii) they are in $S_{IA}\{i \rightarrow j\}$, which means that their static impairments do not already classify them as unfeasible paths. Note that increasing the size of the set of candidates can be controlled with parameter *k*, and has an adverse effect on the algorithm running time: all candidate routes are checked for QoT adequacy, and QoT computations are time-consuming.

Sequential algorithms

```
/* Pre-processing stage */
for each (i,j)
   k(i,j)=kilometers of the shortest path i→j
   d(i,j)=k(i,j)·T_ij
end
sort (i,j) pairs in increasing/decreasing d(i,j) order

/* Sequential processing stage */
/* V: Virtual topology */
for each (i,j) pair taken in sequence in the list
   T_ij = lightpath demand i→j
   for each lightpath demand 1...T_ij
      pwc = {} // path-wavelength candidates
      for each wavelength λ
         pwc = (p,λ), such that p∈S_IA{i→j}
         remove from pwc the (p,λ) pairs which imply
         wavelength clashing in V for wavelength λ
         order pwc (p,λ) pairs in ascending order of the
         distance (Km) of p. Paths with the same
         distance are ordered by the number of hops
         for k=1...max_k // max_k is 10 in the tests
            (p',λ) = k-th shortest path in pwc list.
            V' = V plus a lightpath in (p',λ)
            Q_v = Q-tool (V')
            Q_worst = min {Q_v}
            if (Q_worst < Q_Threshold)
               remove (p,λ) as a candidate in pwc list
            end
         end
      end
      if (pwc list is empty)
         block the lightpath
      else
         carry the lightpath through the (p,w) pair with
         higher Q_worst value
      end
   end
end
```

Fig. 3.3. Pseudocode of the sequential schemes.

3.4.6 Results

This subsection describes the results obtained for validation and testing of the proposed PLIA algorithms. All the algorithms have been implemented in MATLAB code, integrated and tested in the MatPlanWDM tool [46], which interfaces with the TOMLAB/CPLEX solver [53].

Firstly, we explain the assumptions about network topologies, traffic demands, and physical layer characterization considered in our simulation studies. Secondly, we introduce the simulation model employed. Thirdly, we expose extensive simulation results comparing the PLIA algorithms presented in this Section together with a variation of the well known LERP algorithm [80], used for comparison. Finally we discuss the scalability of the proposed algorithms, attending to the evolution of the running time of the different tests

Assumptions

The algorithms have been tested for two different network topologies displayed in Fig. 3.4. They correspond to the Internet2 network [102] (9 nodes, 26 unidirectional links, average node degree 2.89) and the European Optical Network (EON) [103] (18 nodes, 66 unidirectional links, average node degree 3.67).

Fig. 3.5 depicts the distribution of the distances of the shortest paths between every pair of nodes, for both network topologies. The average shortest path length is 1266 km for Internet2 and 1203 km for EON topology respectively.

The traffic demand is calculated as follows. For the Internet2 topology, a base traffic matrix was calculated from a population-distance model [104]: the traffic in Gbps between two nodes grows with the product of the population between both nodes, and decreases with the square of the distance between them. The base matrix is normalized, so that the sum of the offered traffic equals to 1 Tbps. Table 3.1 shows these traffic matrix values. The base matrix for the EON topology is obtained from [103], and normalized to match a total offered traffic of 5 Tbps (Table 3.2). Note that all the traffic matrices are symmetric. These matrices feed the performance tests shown in this section. Other results, not included in this Section, have been obtained considering asymmetric traffic matrices, which yield the same conclusions.

The PLIA algorithms proposed do not consider traffic grooming. They receive the lightpath demand as an input parameter, measured as the number of lightpaths to be established between every pair of nodes. In order to fairly evaluate the PLIA algorithms, they are tested considering a common algorithm which converts a traffic matrix (Gbps) into a lightpath demand matrix. It is based on a MILP formulation, which works as follows. First, it calculates, for every input-output node pair, the *Q* factor of a lightpath in

the shortest path between those nodes, considering only static impairments. If the lightpath is QoT-feasible (or *Q*-feasible), the input-output pair is considered as admissible. Then, a MILP path-flow formulation calculates the lightpath demand with the minimum number of lightpaths, which is able to carry the traffic matrix, considering only the admissible paths and an infinite number of wavelengths per fiber (that is, without considering wavelength clashing constraints).

The parameters that characterize the physical layer in all the tests for the common QoT calculation, assume a transmitter bit rate of 10 Gbps, spans of standard single mode fiber (SMF) compensated with dispersion compensation (DC) modules. The dispersion management scheme that is utilized in our studies is a pre-compensation module, to achieve better transmission reach. Every SMF span is under-compensated to a value of 30 ps/nm/km in order to alleviate the non-linear effects, and the accumulated dispersion at each node becomes 0 with the use of an appropriate post-compensation module in the end of the link. The pre-compensation is set to -400 ps/nm/km. Other parameters used to characterize the physical layer are the input power (-4 dBm at the input of the DC modules, 3 dBm at the input of the fiber spans), grid spacing (50 GHz), type of modulation (NRZ pulses), and switch crosstalk ratio (randomly distributed between 32 and 38 dB). The span length of the physical links (fibers) are set at 80km. The value of PMD parameter is 0.1 ps/$\sqrt{km}$ and the fiber attenuation is 0.25 dB/km. We set $Q_{Threshold} = 15.5dB$, corresponding to a BER of 10^{-9} when no Forward Error Correction (FEC) is utilized.

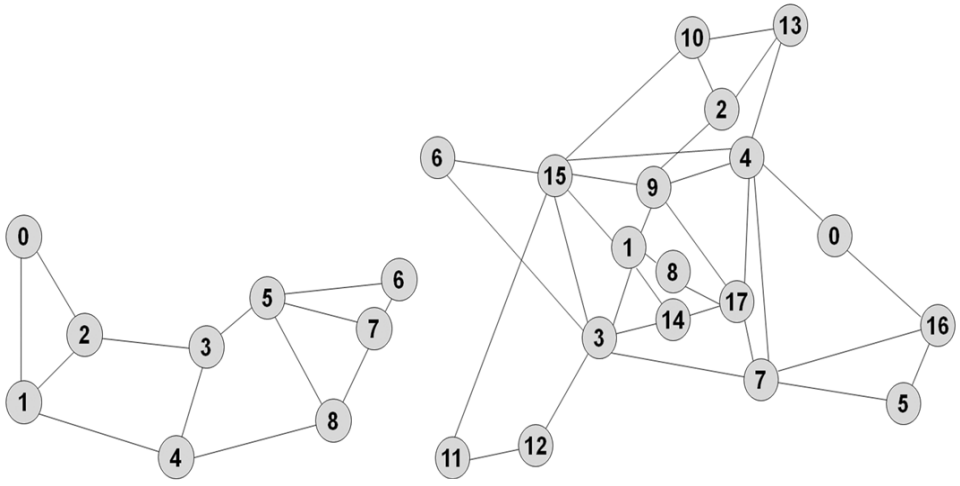

Fig. 3.4. Internet2 (left side) and EON (right side) physical topologies.

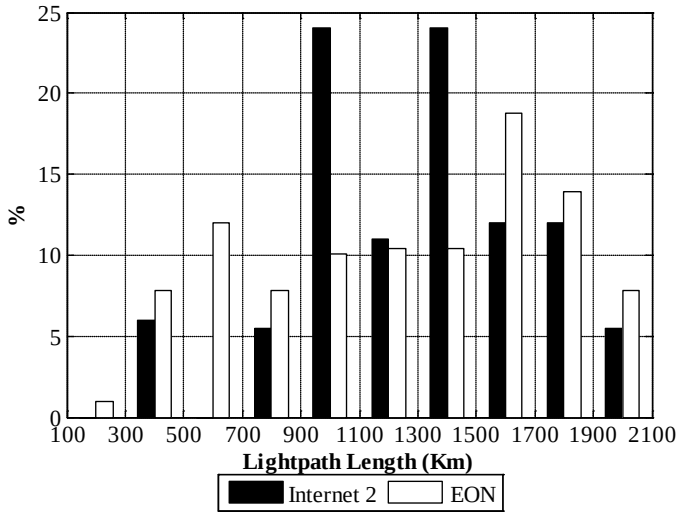

Fig. 3.5. Lightpath length distribution for all-pair connection demand set.

Table 3.1. Internet2 Traffic Matrix in Gbps (Upper Triangular Part) and Link Distances in Km (Lower Triangular Part)

	0	**1**	**2**	**3**	**4**	**5**	**6**	**7**	**8**
0		16.1	13.8	8.7	8.5	8.5	7.4	6.2	7.0
1	1342		16.3	10.9	14.2	14.2	16.5	8.9	10.5
2	913	1303		11.7	11.2	10.1	7.5	7.5	8.8
3	-	1330	-		16.0	17.8	12.9	12.2	14.8
4	-	1705	-	818		16.9	16.2	12.4	16.3
5	-	-	-	690	-		29.5	18.6	20.0
6	-	-	-	-	-	1400		30.5	22.2
7	-	-	-	-	-	905	278		17.7
8	-	-	-	-	1385	1045	-	700	

Table 3.2. Table of EON Traffic Matrix in Gbps (Upper Triangular Part) and Link Distances in Km (Lower Triangular Part)

	0	**1**	**2**	**3**	**4**	**5**	**6**	**7**	**8**	**9**	**10**	**11**	**12**	**13**	**14**	**15**	**16**	**17**
0		8.5	8.5	17.0	76.5	8.5	8.5	42.5	8.5	8.5	8.5	8.5	8.5	8.5	25.5	17.0	8.5	8.5
1	-		8.5	51.0	68.0	8.5	8.5	17.0	8.5	34.0	8.5	8.5	8.5	8.5	25.5	34.0	8.5	8.5
2	-	-		8.5	25.5	8.5	8.5	8.5	8.5	8.5	8.5	8.5	8.5	8.5	8.5	8.5	8.5	8.5
3	-	261.2	-		93.5	8.5	8.5	42.5	8.5	42.5	8.5	8.5	34.0	17.0	51.0	85.0	8.5	8.5
4	523.6	-	-	-		17.0	8.5	76.5	17.0	68.0	17.0	8.5	34.0	51.0	93.5	68.0	17.0	17.0
5	-	-	-	-	-		8.5	17.0	8.5	8.5	8.5	8.5	8.5	8.5	8.5	8.5	8.5	8.5
6	-	-	-	857	-	-		8.5	8.5	8.5	8.5	8.5	8.5	8.5	8.5	8.5	8.5	8.5
7	-	-	-	1102	735.1	1052	-		8.5	17.0	8.5	8.5	25.5	8.5	51.0	25.5	8.5	8.5
8	-	115.8	-	-	-	-	-	-		8.5	8.5	8.5	8.5	8.5	8.5	8.5	8.5	8.5
9	-	205	730	-	680	-	-	-	-		8.5	8.5	17.0	8.5	25.5	42.5	8.5	8.5
10	-	-	550	-	-	-	-	-	-	-		8.5	8.5	8.5	8.5	8.5	8.5	8.5
11	-	-	-	-	-	-	-	-	-	-	-		17.0	8.5	8.5	8.5	8.5	8.5
12	-	-	-	1100	-	-	-	-	-	-	-	583		8.5	17.0	8.5	8.5	0.0
13	-	-	561	-	811	-	-	-	-	-	418.8	-	-		8.5	8.5	8.5	8.5
14	-	488.7	-	302.9	-	-	-	-	-	-	-	-	-	-		25.5	8.5	8.5
15	-	380	-	484	934.3	-	570	-	-	401	1154	1597	-	-	-		8.5	8.5
16	320	-	-	-	-	1073	-	590	-	-	-	-	-	-	-	-		8.5
17	-	-	-	-	379	-	-	1200	371.2	714.5	-	-	-	-	530.4	-	-	

Simulation results

We have conducted two experiments to compare the performance of the proposed approaches. In the first experiment, the blocking rate (percentage of blocked lightpath demands versus total number of offered lightpath demands) is evaluated for each physical topology (Internet2 and EON) considering 8 and 16 wavelengths per fiber (Fig. 3.6 - Fig. 3.9). The graphs illustrate the evolution of the blocking rate, varying the traffic load. The traffic matrices used as input parameters in each simulation point, are the ones shown in Table I and II (Internet2 and EON respectively), normalized to match the value of total offered traffic, shown in the horizontal axis.

Each plot in Fig. 3.6 - Fig. 3.9 includes five curves. Three curves correspond to the three algorithms described in this Section (global search, and the two sequential approaches: the shortest path first (SPF) and longest path first (LPF) ordering). In addition, one more algorithm, named sLERP, is added to the comparison. The sLERP algorithm is a simplification of the LERP algorithm (Lightpath Establishment and Regenerator Placement) proposed in [80]. sLERP adapts the RWA phase of the original LERP algorithm, and skips its regenerator placement phase. In sLERP algorithm, the lightpath demand is ranked randomly, producing a randomly ordered list of 3-tuples (*i*: source node; *j*: destination node, *s*: number of lightpath demands between *i* and *j*). The list of 3-tuples is processed one by one. For each 3-tuple, *k*-shortest paths are computed (*k*=10) which are again processed in order. For each path, wavelengths are assigned to the lightpath demand following a First-Fit scheme. If there are not enough path-free wavelengths in all the *k*-shortest paths for a certain (*i*,*j*,*s*) tuple, the exceeding lightpaths are rejected. When the random sequence is processed, the QoT of the virtual topology obtained is evaluated. The

algorithm stores the best solution found: that is, the one with a higher number of Q-feasible lightpaths. The algorithm continues testing random sequences until the best solution found has not been improved for ten consecutive random orderings. As in the original LERP algorithm, a Black List with the previously tested sequences is kept, to avoid evaluating twice the same demand ordering.

The fifth curve named as *stat-PLIA* in the graphs, is included also for comparison. It is the blocking rate of a MILP algorithm that solves the RWA problem, maximizing the number of lightpaths carried, but including only static signal impairments. That is, the solution calculated is *impairment aware* in the sense that the MILP is forced to assign to the lightpaths, only those paths and wavelengths for which $Q^*(p,w)$ is above the quality threshold. Therefore, all the lightpaths would be valid if only static impairment were considered. The *stat-PLIA* algorithm is employed as an upper bound to the optimum solution.

Results show that the blocking rate obtained by the global optimization and the sequential algorithms considered are similar in the smaller topology Internet2 (Fig. 3.6-Fig. 3.7). However, the global optimization algorithm outperforms the sequential schemes in the EON topology. Both approaches are in a significant number of occasions far from the upper bound calculated, also for small topologies. No strict conclusion can be extracted from this, as the tightness of this bound cannot be calculated. Finally, the comparison between the sequential approaches shows a better behavior in most of the situations with the shortest path ordering. The sLERP algorithm exhibited the worst performance in all the tests.

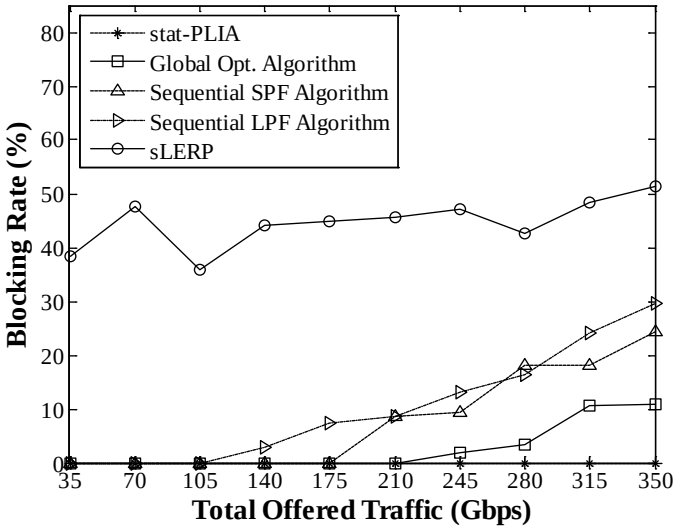

Fig. 3.6. Blocking Rate vs. Load Internet2 8 wavelengths

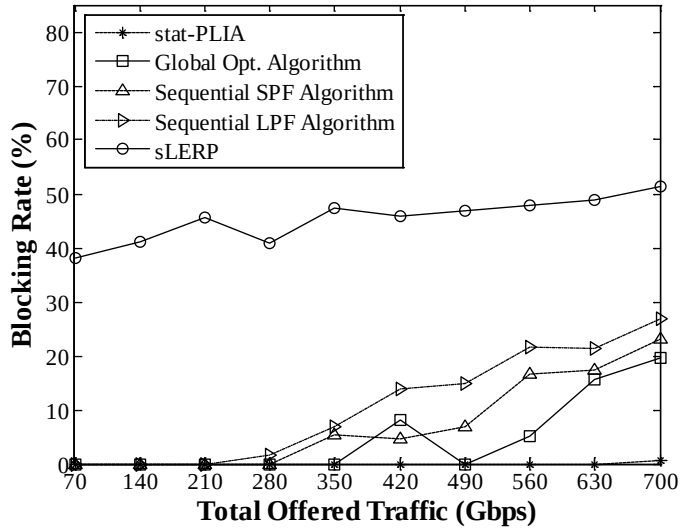

Fig. 3.7. Blocking Rate vs. Load Internet2 16 wavelengths.

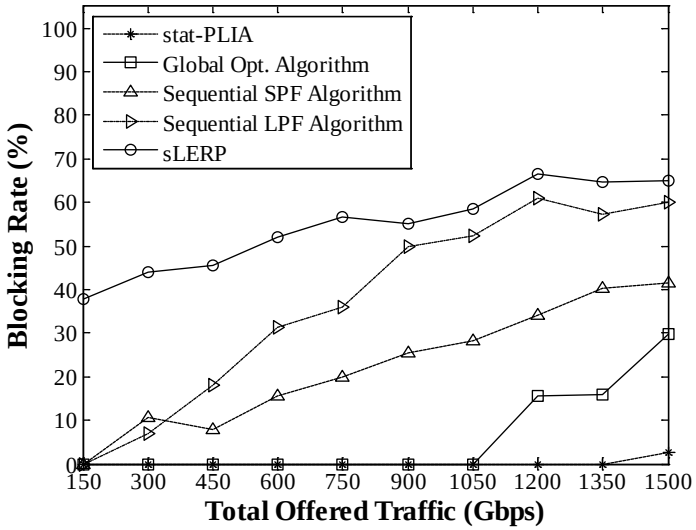

Fig. 3.8. Blocking Rate vs. Load EON 8 wavelengths.

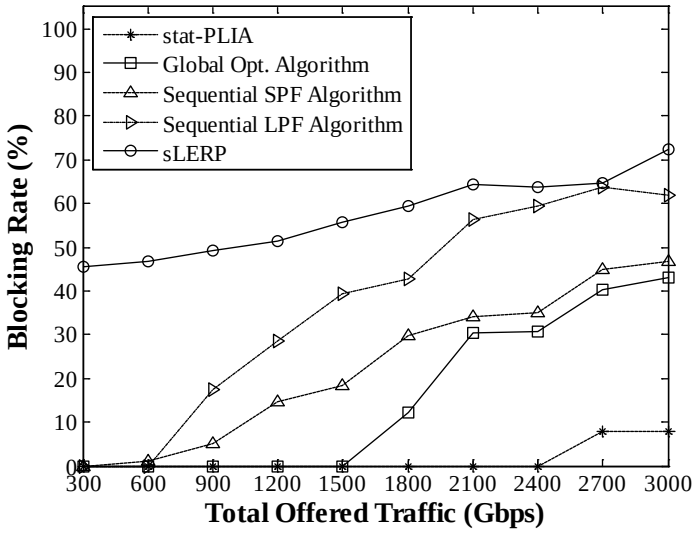

Fig. 3.9. Blocking Rate vs. Load EON 16 wavelengths.

The second experiment consists of an evaluation of the blocking rate when the number of wavelengths per fiber is increased from 8 up to 32. This experiment is repeated for the Internet2 topology and a total offered traffic of 490 Gbps, and the EON topology for a total offered traffic of 2100 Gbps. The results from this experiment are presented in Fig. 3.10 and Fig. 3.11. They can be interpreted in the same way as in previous graphs. The performance of the sequential algorithms is similar to the global search in Internet2. For EON, a significant performance gap appears favoring the global search algorithm. This performance gap is slightly decreasing for a growing number of wavelengths per fiber.

An important conclusion can be drawn from the results in the sequential approaches. Initially, the size of the set of candidates could be seen as a tuning parameter for the trade-off between blocking probability and running time. The parameter k in the k-shortest path search controls this aspect. Nevertheless, our results are calculated for a value of k=10. This implied that, in all the cases tested, given a lightpath demand, *all* the possible paths which could carry a Q-feasible lightpath were tested. This prioritizes the lightpaths which are up in the sequence even more strongly, as they are rejected only if previous lightpaths eliminate any feasible route for the new one. However, our results show that the blocking rate performance of the sequential approaches with this exhaustive search was lower than the one of the global search, which also required a much lower number of QoT evaluations. Therefore, the results suggest that more complex sequencing strategies are needed, combined with processing schemes which allow the rerouting of existing lightpaths.

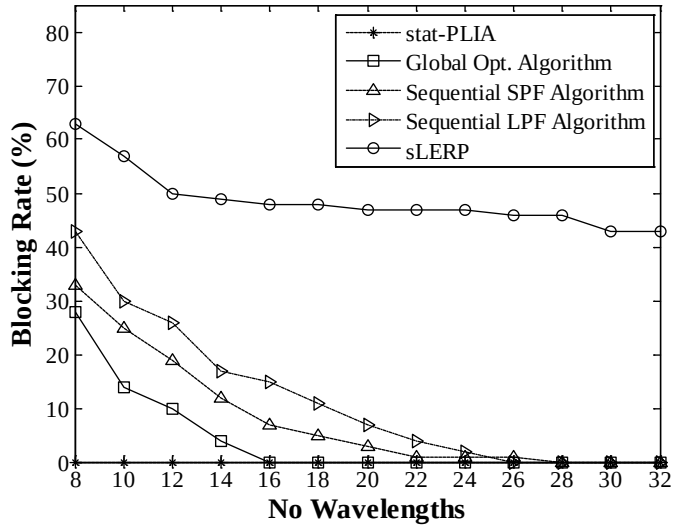

Fig. 3.10. Blocking Rate vs. Number of wavelengths Internet2

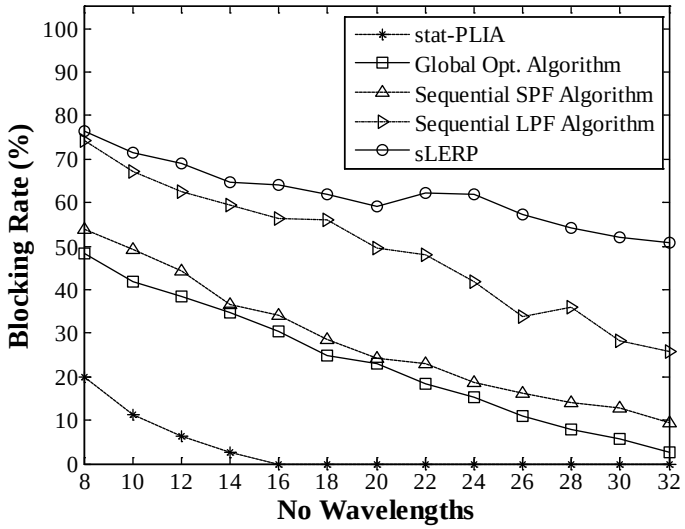

Fig. 3.11. Blocking Rate vs. Number of wavelengths EON.

Scalability study of the algorithms

This section is aimed at discussing the scalability of the proposed algorithms, attending to the

evolution of the running time of the different tests presented in the previous section. In Fig. 3.12 and Fig.3.13 the running times of the algorithms are compared when the traffic load is increased from the 10% of the maximum load to the 100% for the four simulation scenarios (EON and Internet2, 8 and 16 wavelengths).

In the global search algorithm, the execution time is quite small for low loads, and has an abrupt rise at medium to high loads. This is because for low loads the algorithm can find a solution which carries all the traffic demand during its phase 1. For medium and highs loads the algorithm enters in the iterations inside phases 2 and 3, which are more time consuming. It is quite noticeable that at this moment, algorithm response time remains approximately constant, independent from the traffic load, the number of wavelengths, and the topology size. The small unpredictable variations observed are based on the particular conditions that define the algorithm stop.

Regarding also to the global search algorithm, it is relevant to know which part of the response time of the global optimization algorithm, is caused by the BILP sub-algorithms execution, and which part is caused by the QoT evaluation function. Our results are quite clear in this aspect: the average execution times of BILP sub-algorithms in the tests performed are *below one second* for every traffic and topology situation tested a negligible value in static planning. Thus, these results validate our assert that the algorithm designed effectively limits the inherent complexity problem in BILP formulations, by an appropriate control in the number of changeable decision variables.

In the end, close to the 100% of the execution time of both global search and sequential approaches is devoted to the QoT estimation of virtual topology candidates. Then, Fig. 3.12 and Fig.3.13 illustrate the rationale of the better scalability of the global search algorithm. It shows that the number of *Q*-tool evaluations in the sequential schemes tested, grows with the traffic load, number of wavelengths and topology size. Internally, all of them contribute to the growth in the path candidate lists to evaluate. In contrast to this, the number of QoT evaluations of the global search approach depends mainly on the number of iterations performed inside each *CoreAlgorithm* module. The good results obtained with the small constant value of 20 iterations proves the efficiency of the solutions space exploration. Furthermore, the iterative operation of the global search algorithm opens the way to optimization strategies that stop the search after a given execution time, returning the best solution found. That time based stop procedures are not natural for sequential schemes.

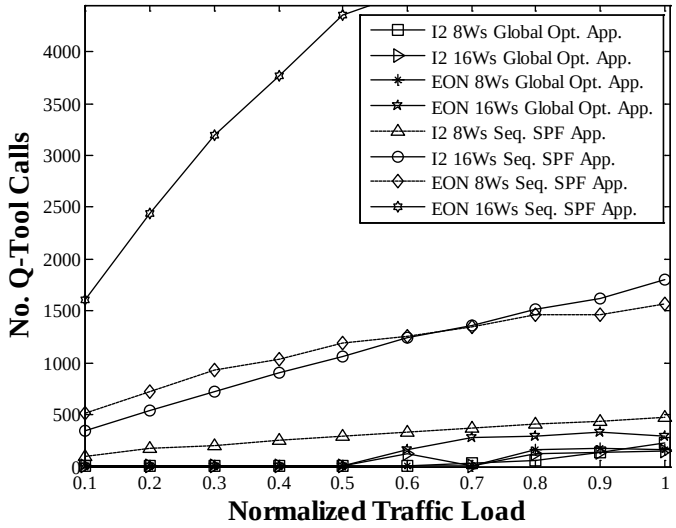

Fig. 3.12. Number of Q-Tool Calls vs. Normalized Traffic Load.

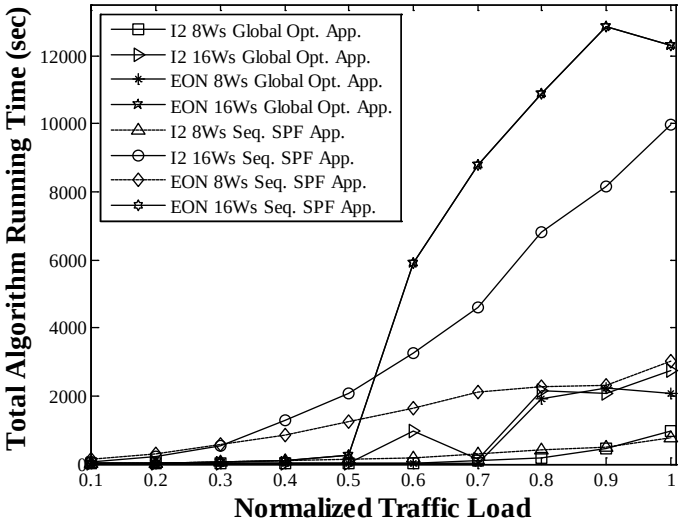

Fig.3.13. Total Algorithm Running Time (sec) vs. Normalized Traffic Load.

3.4.7 Conclusion

The PLIA-RWA algorithms proposed in this section have been compared trough extensive experiments. These algorithms makes use of a common dynamic QoT evaluation function *Q*-tool. The global search approach is based on an iterative method which tries to effectively explore the solutions space. Changes between iterations are controlled by a set of BILP formulations, which favor limited rearrangements in the virtual topology searching for better solutions. The size of the rearrangement is controlled, limiting the BILP complexity. Also, the method allows to force large rearrangements between consecutive iterations to avoid a continuous local exploration of the solutions space. Both sequential and global search approaches showed a similar performance in small topologies. However, results show that this global exploration algorithm outperforms the sequential schemes tested in larger topologies. Furthermore, the time complexity of the global search algorithm remains low, and approximately constant with network size and traffic demand. The impact of BILP executions on the total execution time is negligible, in comparison to the running time of the QoT evaluation function. It can be concluded that the global search method proposed is both effective and scalable. In contrast the sequential approaches are penalized by the excessive utilization of time-consuming QoT evaluations. Results suggest that sequential algorithms should combine rerouting techniques to increase their blocking rate performance.

3.5 Multi Line Rate Virtual Topology Design under Non Linear Effects

3.5.1 Problem statement

Initially, the migration from traditional 10 Gbps based optical transmission systems to higher (40/100 Gbps) bit rates based ones was proposed as a clear strategy to increase the total capacity in WDM optical networks. Besides this capacity enlargement, the higher bit rate systems allow to support more lower bit rate services in one unique wavelength channel, decreasing the number of wavelengths entering a node and relaxing the wavelength switching requirements [105]. On the other hand, the expected cost for a non coherent 40 Gbps transceiver is only 2.5 to 3 times more than a 10 Gbps transceiver, what introduces a volume discount on the cost *per bps* for 40 Gbps transceiver: the cost per bps estimated for 40 Gbps transceivers is between 62.5% and 75% of the same cost for 10 Gbps transceivers [105],[106]. A similar volume discount on the *per bps* cost is expected for 100 Gbps transceivers, however in this case the coherent technology might increase the price. Conversely, physical layer impairments affect more severely to higher bit rate signals. To illustrate that, in 40 Gbps channels with respect to 10 Gbps ones, the dispersion tolerance decreases (by a factor of 16 for Chromatic Dispersion, CD, and by 4 for

Polarization Mode Dispersion, PMD), the OSNR has to be improved by 6 dB to maintain the same BER, and the non linear impairments become more relevant [25],[106]. The situation is very similar in case of 100 Gbps transmission. As a consequence, the maximum distance without electronic regeneration (transparent reach) is shorter for 40/100 Gbps than for 10 Gbps communications.

Summing up the above commented advantages and drawbacks, a tradeoff appears between the higher capacity and lower cost per bps (volume discount) of 40/100 Gbps transceivers and the longer transparent reach of 10 Gbps signals. Therefore, the deployment of mixed line rate systems taking advantage of the good qualities of both options, can be more cost-effective than the pure migration to higher bit rates and replacement of the 10 Gbps transceivers [26],[107].

This section is focused on the Mixed Line Rate Virtual Topology Design (MLR-VTD), a variant of the PLIA-VTD problem when the physical later impairments are considered under several transmission bit rates for the optical connections. Namely, we study the MLR-VTD problem in a realistic scenario where 10 Gbps NRZ-OOK and 40 Gbps RZ-DQPSK lightpaths share a 50 GHz grid on the optical fiber spectrum. In this scenario, non linear impairments (particularly, cross phase modulation, XPM) induced by 10 Gbps (intensity modulated) channels affect seriously to neighboring 40 Gbps (phase modulated) ones [108],[109]. A solution to prevent these non linear interferences is to establish “guard-bands” between 10 and 40 Gbps channels.

In this study, we concentrate on 10 and 40 Gbps, excluding 100 Gbps systems, to stress the tradeoffs between low bit rate (10 Gbps) channels and higher bit rate (40/100 Gbps) channels. Anyway, many of the considerations for the 10/40 Gbps interferences are also valid for 10/100 Gbps ones.

In this section, since the effects of the aforementioned non linear interactions are considered when planning the network, the investigated mixed line rate problem is denoted as MLR-VTD-uNLE (Mixed-Rate Virtual Topology Design under Non Linear Effects). The MLR-VTD-uNLE problem is modeled as a MILP formulation. As the problem is clearly NP-hard, like the general VTD problem [8], it becomes intractable for large sized instances. Therefore, we devise from the MILP formulation a heuristic algorithm, named Heur-MR-uNLE, to solve large size instances of the problem. In both approaches, the PLIs are estimated individually and incorporated indirectly to the formulations as model constraints, using one of the techniques commented in Section 3.3.

To conclude this subsection, we will detail below the main issues to address when 10/40/100 Gbps bit rates coexist on optical networks.

Issues on MLR networks: spectral width and guard bands

The joint utilization of 10 Gbps and 40/100 Gbps channels on the existing infrastructure brings

several challenges. The main issues to solve are related to: (i) the spectral width of the 40/100 Gbps signals and (ii) the non linear effects between 10 Gbps and 40/100 Gbps neighboring channels.

Nowadays, one of the most wide-spread grid spacing in optical communications is the ITU G.694.1 50 GHz grid. The spectral efficiency of the traditional 10 Gbps on-off keying (OOK) signals is 0.2 bits/Hz [106], what easily permits to fit them into the 50 GHz grid. Conversely, 40/100 Gbps OOK signals would need to be accommodated in a grid spacing even larger than 100 GHz. That forced the market to look for more spectral efficient modulation formats for 40/100 Gbps transceivers.

Several formats for 40 Gbps communications have been proposed. The most well-known candidates are the phase shaped binary (PSBT) [110],[111], differential phase shit keying (DPSK) [110],[112], partial DPSK (p-DPSK) [110], [112], return-to-zero differential quaternary phase shift keying (RZ-DQPSK) [110], [112]. In the last years thanks to the successful development of the coherent technology and digital signal processing (DSP) two other modulation formats has been proposed, namely polarization-division multiplexed quaternary phase shift keying (PDM-QPSK) [110], [112],[113] and polarization-division multiplexed binary phase shift keying (PDM-BPSK) [114].

In case of 100 Gbps transmission the situation is simpler, since the feasible only solution is the coherent transmission combined with DSP. Considering the modulation formats here the two candidates are: the PDM-QPSK [113] and the frequency division multiplexed PDM-QPSK (FDM PDM-QPSK) [115].

With the exception of 40 Gbps DPSK, that requires 100GHz spacing, most of the previously mentioned formats fit into 50 GHz grid, what solves the issue of the grid spacing in high bit rate signals.

Other limiting factor to use phase modulated channels together with OOK channels (e.g. 10 Gbps together with 40/100 Gbps), are the nonlinear effects. As it is well known the OOK channels highly deteriorates the quality of phase modulated channels due to the cross phase modulation (XPM). Several papers have been published investigating the nonlinear tolerance of different modulation formats. In [116] the performance of 40 Gbps channel DPSK, p-DPSK, RZ-DQPSK and coherent PDM-QPSK surrounded by 10Gbps are compared. In [117] it was shown that the closer is the symbol rate of 40 Gbps channels to 10 Gbps the higher is the nonlinear penalties due to XPM. In case of polarization multiplexed channels besides the XPM also the cross-polarization modulation (XPolM) limits the optical transmission [118],[119]. In [119] it was shown that for dispersion managed networks the XPolM has higher impact on the signal quality than the XPM.

It is technically possible to have 10 Gbps and 40 Gbps channels in 50 GHz spacing. However in this case an extra OSNR penalty for the 40/100 Gbps channels must be considered. The amount of the OSNR

penalty depends on the modulation format, launch power of the channels and guard bands [120]. In most of the deployed networks it is not possible to change the modulation format as well as the launch powers. Therefore, in these cases the only option is to use guard bands between 40/100 Gbps and 10 Gbps channels, to have the optimal working conditions.

In the following subsections we will consider only 40 Gbps RZ-DQPSK modulation. The RZ-DQPSK (Return to Zero Differential Quadrature Phase Shift Keying) is one of the candidates for 40 Gbps signaling [26], [113], since its spectral efficiency of 0.8 bits/Hz is sufficient to allocate 40 Gbps channels on 50-GHz grids, and presents a tolerable OSNR resilience and a good dispersion tolerance [106], [110],[113]. The counterpart is that is strongly impacted by XPM induced by 10 Gbps intensity modulated channels [108], [109]. For this reason, we adapt the network planning to prevent that 10 Gbps and 40 Gbps channels sharing a fiber link, are allocated neighboring wavelengths.

The rest of the section is organized as follows. Subsection 3.5.2 consists of a brief survey on the topic. In Subsection 3.5.3 we provide an optimal MILP (Mixed Integer Linear Programming) formulation for the MLR-VTD-uNLE problem. Subsection 3.5.4 presents a heuristic algorithm. Results of exhaustive tests are presented in Subsection 3.5.5. Finally, Subsection 3.5.6 concludes the Section.

3.5.2 Related work

In this subsection a brief state of the art in mixed line rate VTD is conducted. In general, mixed line rate problems have scarcely been explored in optical communications. In [121], a dynamic RWA algorithm called DIRWA (Dispersion-optimized Impairment-aware RWA) is proposed. DIRWA incorporates CD information to minimize the lightpath blocking rate in a multi-rate line dynamic case where the lightpath requests arrive randomly.

The MLR-VTD problem has been also studied in [26],[107], where non linear effects between neighboring channels were not considered. In these studies, the transparent reach of a lightpath is computed through analytical models that compute the linear impairments. In [107], a unique modulation format (duobinary) is assumed; whilst, in [26], multiple modulation formats (duobinary and DQPSK) are considered. In both papers, the problem is modeled as an ILP formulation. A heuristic algorithm is proposed in [107].

Finally, network protection aspects in MLR planning are investigated in [122],[123]. In [122], Ethernet is used as transport technology over WDM for backbone networks, whereas [123] extends the study in [107] towards survivability considerations. In contrast to the present study, these works also ignore possible interfering effects between adjacent wavelengths.

3.5.3 MILP model of the planning problem

In this subsection, the MLR-VTD-uNLE problem is characterized as a MILP (Mixed Integer Linear Programming) formulation. In the sequel, we name this model as OPT-MR-uNLE.

Let $G(N,E)$ be the graph of the physical topology being N the set of nodes and E the set of unidirectional fiber links. We denote as $a(e)$ and $b(e)$ the initial and end nodes of fiber $e \in E$, respectively. We assume that a common wavelength grid is used in all the network links, being W the set of wavelengths channels. We denote as D the set of traffic demands, and $a(d)$ and $b(d)$ denote the initial and end nodes of demand $d \in D$, respectively. For each demand d, $h(d)$ represents the volume of the demand in bit rate units (Gbps).

Nodes are equipped with two types of transceivers which we denote as r_{10} and r_{40}. r_{10} represents the 10 Gbps transceiver type that uses NRZ-OOK modulation; and r_{40}, the 40 Gbps transceiver type that uses RZ-DQPSK modulation. The set $R=\{r_{10}, r_{40}\}$ represents the two available types of transceivers. For each transceiver type $r \in R$, BR_r denotes its bit rate in Gbps (that is, $BR_{r10}=10$, $BR_{r40}=40$), and c_r represents the cost of a transmitter plus a receiver of that type.

We denote as P the set of paths p that can support a lightpath meeting the Quality of Transmission (QoT) requirements, i.e., a QoT feasible lightpath. This set can be precomputed in different fashions depending on how the planner decides to estimate the lightpaths' QoT. In this work, a path p is included in set P, if the sum of the lengths of the fibers traversed in the path p does not exceed the transparent reach. Then, any lightpath following this route would be QoT feasible. However, the approach followed in this study is compatible with any other form of defining set P. For instance, the set P can be defined using a linear QoT estimator [20][82] that collects the physical layer impairments to determine the signal quality. This type of QoT estimator computes explicitly the linear impairments (e.g. ASE noise), whereas, it overestimates the non linear ones (e.g. XPM) and accumulates them to the linear ones. By doing so, the QoT estimation of a lightpath would not depend on the copropagating lightpaths, and thus could be precomputed. A lightpath over a path $p \in P$ would be QoT feasible if the value of its QoT value is lower than a given threshold associated to a given bit error rate.

In our case, since we have two transceivers types with two different transparent reaches, two subsets of paths according to QoT considerations are defined: (i) P_{r10} and (ii) P_{r40}, corresponding lightpaths equipped with transceivers r_{10} or r_{40}, respectively. The set of paths traversing fiber $e \in E$ is denoted as P_e. The initial and end nodes of path $p \in P$ are referred to as $a(p)$ and $b(p)$, respectively. Finally, the set of paths initiated and ending at node $n \in N$ are named as $\delta^+(n)$ and $\delta^-(n)$, respectively.

The decision variables of the problem are:

- $x_{dpw} \in [0,\infty)$: fraction of the traffic volume associated to demand $d \in D$ carried onto a lightpath established on $p \in P$ using wavelength $w \in W$.
- $y_{pwr} = \{0,1\}$. y_{pwr} takes the value 1 if a lightpath is established on $p \in P$ using wavelength $w \in W$ and transceiver type $r \in R$.

Then, the problem can be formulated as:

$$\text{Minimize} \sum_{p\in P, w\in W, r\in R} c_r y_{pwr} \tag{3.12}$$

Subject to

$$\sum_{p\in\delta^+(n), w\in W} x_{dpw} - \sum_{p\in\delta^-(n), w\in W} x_{dpw} = \begin{cases} h_d, \text{if } n = a(d) \\ -h_d, \text{if } n = b(d), \\ 0 \text{ otherwise} \end{cases} \quad d \in D, n \in N \tag{3.13}$$

$$\sum_{d\in D} x_{dpw} \le \sum_{r\in R} BR_r y_{pwr}, \qquad p \in P, w \in W \tag{3.14}$$

$$\sum_{p\in P_e, r\in R} y_{pwr} \le 1, \quad e \in E, w \in W \tag{3.15}$$

$$\sum_{r\in R} y_{pwr} \le 1, \qquad p \in P, w \in W \tag{3.16}$$

$$\begin{aligned} y_{pwr} &= 0, w \in W, r \in r_{10}, p \notin P_{r_{10}} \\ y_{pwr} &= 0, w \in W, r \in r_{40}, p \notin P_{r_{40}} \end{aligned} \tag{3.17}$$

$$\begin{aligned} \sum_{p\in P_e} \left[y_{pwr_{10}} + y_{p(w+1)r_{40}} \right] &= 0, \quad e \in E, w \in W - \{w_{|W|}\} \\ \sum_{p\in P_e} \left[y_{pwr_{10}} + y_{p(w-1)r_{40}} \right] &= 0, \quad e \in E, w \in W - \{w_1\} \end{aligned} \tag{3.18}$$

The objective function (3.12) minimizes the total transceiver network cost. The flow conservation constraints (3.13) ensure that all the traffic volume of demands $d \in D$ is carried. The lightpath capacity constraints (3.14) guarantee that traffic allocated in a lightpath does not exceed the bit rate of the transceivers. The wavelength clashing constraints (3.15) prevent assigning the same wavelength to different lightpaths sharing the same fiber. The fact that one unique transceiver type can be assigned to a lightpath is considered in (3.16). Constraints (3.17) forbid that a lightpath exceeds the transceiver transparent reach. Finally, XPM interferences between adjacent NRZ-OOK and DQPSK modulated channels are avoided by leaving unused a guard channel between them in constraints (3.18)

3.5.4 Heuristic approach

Clearly, the MLR-VTD-uNLE problem is NP-hard, as the general VTD problem [8]. According to our results, it becomes intractable even for moderate sized instances (v.g. $|N|=4$, $|W|=6$). In this subsection, we propose a heuristic algorithm, named Heur-MR-uNLE, to solve large size instances of the problem.

General Algorithm Structure

In this subsection, we describe the general structure of the heuristic. The algorithm has an iterative operation. A pseudocode illustrating the steps in the main algorithm loop is shown in Fig. 3.14. The algorithm processes sequentially the demands $d \in D$, attempting to carry the maximum possible volume of them in each iteration. The algorithm finishes when all the demands are totally served or when it is not possible to allocate more traffic.

The algorithm receives as input parameters the graph $G(N,E)$, the wavelength channel set W, the demand set D and the transceivers set R. In the initialization stage, the virtual topology is created as empty, and the demand set D is set as the so-called *remaining demand set D'*, that stores the demand volumes (Gbps) pending to be carried.

At the beginning of each iteration, the remaining demands (demands $d' \in D'$) are resorted in descending order of their volumes $h(d')$ pending to be carried. Then, the demand d' with higher pending traffic is selected, and a path for connecting the ending nodes $a(d')$ and $b(d')$ is searched for. This path consists of a sequence of lightpaths between $a(d')$ and $b(d')$. The ILP formulation (3.19)-(3.25), described in this Subsection, is used to determine the lightpaths in terms of (i) their routing and wavelength assignment, and (ii) their bit rate, which can be different for different lightpaths in the sequence. Guard bands between 10 Gbps and 40 Gbps channels are enforced by (3.19)-(3.25).

If formulation (3.19)-(3.25) for d' results infeasible and no lightpaths are allocated, the algorithm attempts it again with the next demand in set D'. If infeasibility repeats for all demands in D', the traffic pending to be carried is considered as blocked, and the algorithms terminates.

If model (3.19)-(3.25) is able to find a lightpath sequence between nodes $a(d')$ and $b(d')$, the new lightpaths are added to the virtual topology and the algorithm advances to a *flow allocation stage*. In this stage, as much pending traffic as possible from set D' is carried onto the updated virtual topology. Every demand with zero pending traffic is removed from set D'. The *flow allocation stage* is detailed next.

Algorithm:
Input: *G*(*N*,*E*), *W*, *D*, *R*

Initialize
Virtual Topology *VT*←{}
Pending Demand Set *D'*←*D*
while *D'* is not empty **do**
Step 1: Sort demands *d in D'* in descending order of *h*(*d*).
Step 2: Select as *d'* the first demand in set *D'* .
Step 3: Search a sequence of lightpaths between *a*(*d'*) and *b*(*d'*) solving **ILP formulation (3.19-3.25)**
if sequence of lightpaths is found, **do**
Step 4.a.i: Add found lightpaths to *VT*.
Step 4.a.ii: Carry onto *VT* as much traffic from *D'* set as possible by ***Flow Routing Stage*** and remove from *D'* demands with null pending traffic.
else if *d'* is last demand in *D'*,
break.
else
Step 4.b: Select as *d'* the next demand in set *D'* and **go to Step 3.**
end if
end while

Fig. 3.14. Pseudocode of the general structure of the heuristic

Lightpath sequence determination

This subsection describes the ILP formulation to obtain a lightpath sequence between the initial and end nodes of demand *d*'. The input parameters to the formulation are the same as (3.19)-(3.25) and, additionally:

- $z'_{pwr} = \{0,1\}$. z'_{pwr} takes the value 1 if one lightpath was previously established on $p \in P$ using wavelength $w \in W$ and transceiver type $r \in R$.
- ξ_{pwr}: Virtual cost assigned to establishing a lightpath on $p \in P$ using wavelength $w \in W$ and transceiver type $r \in R$.

The decision variables are:

- $z_{pwr} = \{0,1\}$. z_{pwr} takes the value 1 if a lightpath is established on $p \in P$ using wavelength $w \in W$ and transceiver type $r \in R$.

Then, problem can be formulated as:

$$\text{Minimize} \sum\nolimits_{p\in P, w\in W, r\in R} \xi_{pwr} z_{pwr} \tag{3.19}$$

Subject to

$$\sum_{\substack{p\in\delta^+(n)\\ w\in W\\ r\in R}} z_{pwr} - \sum_{\substack{p\in\delta^-(n)\\ w\in W\\ r\in R}} z_{pwr} = \begin{cases} 1, \text{if } n = a(d) \\ -1, \text{if } n = b(d), \quad n \in N \\ 0 \text{ otherwise} \end{cases} \tag{3.20}$$

$$\sum_{p\in P_e, r\in R} z_{pwr} \le 1, \quad e \in E, w \in W \tag{3.21}$$

$$\sum_{r\in R} z_{pwr} \le 1, \quad p \in P, w \in W \tag{3.22}$$

$$\begin{aligned} z_{pwr_{10}} &= 0, w \in W, p \notin P_{r_{10}} \\ z_{pwr_{40}} &= 0, w \in W, p \notin P_{r_{40}} \end{aligned} \tag{3.23}$$

$$\begin{aligned} &\sum_{p\in P_e} \left[z_{pwr_{10}} + z_{p(w+1)r_{40}} \right] = 0, \quad e \in E, w \in W - \{w_{|W|}\} \\ &\sum_{p\in P_e} \left[z_{pwr_{10}} + z_{p(w-1)r_{40}} \right] = 0, \quad e \in E, w \in W - \{w_1\} \end{aligned} \tag{3.24}$$

$$z_{pwr} = 1, \quad (p, w, r) / z'_{pwr} = 1 \tag{3.25}$$

The "lightpath sequence" conservation constraints (3.20) guarantee that the set of lightpaths established composes a path on the physical topology connecting the demand ending nodes $a(d)$ and $b(d)$. The constraints (3.21)-(3.24) are the equivalent to the constraints (3.15)-(3.18) by replacing the decision variables y_{pwr} for z_{pwr}. The constraints (3.25) tie to one the decision variables corresponding to lightpaths set up in previous iterations.

The objective function (3.19) minimizes the virtual cost of the sequence of lightpahs. The particular values used for the cost coefficients ξ_{pwr} becomes critical in the algorithm performance. We have tested the two options given in (3.26) and (3.27):

$$\xi_{pwr} = \frac{c_r}{BR_r}, \; p \in P, w \in W, r \in R \tag{3.26}$$

$$\xi_{pwr_{10}} = M, \xi_{pwr_{40}} = 1, \ p \in P, w \in W \tag{3.27}$$

In (3.26), the relative cost per bps of the transceiver is used as the objective function. Whilst, in (3.27), a large cost value M (e.g. $M=|W||P|$) is chosen so that 40 Gbps lightpaths are always preferred. The performed experiments reveal us that the algorithm generates solutions with lower network costs when (3.26) cost function is used. However, for some of these experiments under high traffic loads, solutions presented blocked traffic. The heavy loaded cases were repeated by using the values (3.27) as coefficient costs, obtaining solutions with null blocking rate, but paying a higher network cost than before for weights (3.26). The rationale behind this algorithm behavior is that high bit rate transceivers are in these cases the only choice to reduce the traffic blocking, because of its higher capacity.

Finally, the new lightpaths to add to current virtual topology are computed as the difference $z_{pwr} - z'_{pwr}$ for each $p \in P$, $w \in W$, $r \in R$.

Flow Routing Stage:
Input: *d', D', VT*
Step 1: Put demand *d'* in the first position in set *D'*.
for $d \in D'$, starting with the first demand **do**
    Step 2: Solve **Max Flow Problem** onto *VT* for demand *d* and subtract carried traffic from *h*(*d*).
    if $h(d) = 0$, $D' \leftarrow D' - \{d\}$; **end if**
end for

Return *D'*

Fig. 3.15. Pseudocode of Traffic Flow Routing Phase

Flow allocation stage

This algorithm stage aims at carrying as much pending traffic as possible onto the upgraded virtual topology design. The pseudocode in Fig. 3.15 illustrates the steps of the algorithm. The input parameters to this stage are: (i) a demand *d'*, (ii) the remaining demand set *D'* and (iii) the established virtual topology *VT*. First of all, the demand *d'* is moved from its current position to the top in the set *D'*, that was previously sorted in descending order of demand volumes. The demands are sequentially fed to an instance of the *MaxFlow* [124] problem, following the order in *D'*. For each demand *d*, the MaxFlow problem intends to carry as much traffic as possible (but limited to *h*(*d*)) using the available capacity in the lightpaths of the *VT*. The Gbps successfully carried in the MaxFlow solution are subtracted from the volume *h*(*d*) pending to route in *D'*. Finally, before continuing on next demand, those demands $d \in D'$ for

which $h(d)=0$ are removed from set D'.

3.5.5 Results

Network scenario

We investigate the MLR planning using as a case of study the Internet 2 network ($|N|=9$ nodes) [102] using 80 wavelengths per fiber and a grid spacing of 50 GHz. The algorithms have been implemented in MATLAB code, integrated and tested in the MatPlanWDM tool [46], which links to the TOMLAB/CPLEX solver [53]. The network cost to minimize is given by the sum of the cost of the transceivers. We assumed the following costs and maximum transparent reachs of the transceivers as shown in Table 3.3.

As a novelty, we study how the MLR systems behave if the lengths of the links in the network are varied. By doing so, we observe the trends in the network performances for different network sizes (e.g. metro, continental network...). Different network sizes are generated by tuning the values of the so-called "link length factor" β. The factor β of a network is computed as the quotient between the longest link length and the transparent reach of 40 Gbps transceivers (600 Km, see table in Table 3.3). Thus, reference factor $\beta_{ref} = 1$ corresponds to a network where the longest link is 600 km. We employ six distance factors $\beta = \{0.25, 0.5, 0.75, 1, 2, 3\}$. In the real link length case, the β factor of Abilene Network is 2.84.

Table 3.3. Transceivers Parameter

Bit Rate (Gbps)	Modulation Format	Transparent Reach (Km)	Cost of one transceiver pair
10	NRZ-OOK	2000	1
40	RZ-DQPSK	600	2.5

Network throughput

First, we are interested on investigating how the maximum network throughput is affected by the link length in MLR networks. In this study we define the maximum network throughput as the maximum traffic which can be carried, according to the Heur-MR-uNLE algorithm, with null traffic blocking. A traffic normalization process is required for this aim. In our tests, a reference traffic matrix T^{BASE} is initially computed by using the distance-population traffic model detailed in [104]. Then, we find the highest factor α_{MAX} for which the traffic matrix $T^{MAX}=\alpha_{MAX}\cdot T^{BASE}$ can be supported with null traffic blocking. The maximum network throughput is then the total volume summing up the coordinates of the

matrix T^{MAX}. Naturally, these values are different for different network size factors β, since larger networks may force the use of 10 Gbps equipment with longer transparent reach but lower capacity. The Table 3.4 collects the results obtained.

As can be observed in Table 3.4, there is an abrupt reduction in the network throughput for those networks with size factor β>1. That is because for these networks some of the links are too long to allow a 40 Gbps lightpath to traverse them. For increasing values of β, more links have a length higher than 600 km (the transparent reach for 40 Gbps transceivers considered), and thus fall into this limitation.

The *Upper Bound* column computes an upper bound to the maximum network throughput. This upper bound is of interest, to assess the quality of the Heur-MR-uNLE algorithm according to its ability to find solutions with null traffic blocking. The upper bound is calculated (i) relaxing the MILP formulation by eliminating the wavelength assignment constraints (3.15) and (3.18), and then (ii) finding the T^{MAX} matrix for which a solution to the relaxed problem is found. The *Gap* column in Table 3.4 shows the optimality gap between the maximum throughput computed by the heuristic and the upper bound. Results reveal that a very small gap is obtained in most of the occasions, confirming the quality of the algorithm to find solutions without traffic blocking.

β	Throughputs	Upper Bound (UB)	Gap (%)
0.25	27.24	27.42	0.67%
0.5	27.24	27.42	0.67%
0.75	27.24	27.42	0.67%
1	26.53	27.42	3.24%
2	7.40	8.93	17.16%
3	6.76	6.84	1.23%

Table 3.4. Maximum network throughput (Tbps)

Network cost

A second set of experiments is devoted to evaluate the evolution of the network cost in MLR networks. Fig. 3.16 collects the results, showing the cost of the network planned with the Heur-MR-uNLE algorithm, as a function of the carried traffic volume. We repeat the tests for ten traffic loads corresponding to fractions of size ρ = {0.1, 0.2, ..., 1} of the maximum network throughput 27.24 Tbps (best case, for link-length factor β=0.25).

Only the cases for which a null lightpath blocking is found, are included. According to Table 3.4, this means that networks with factor β>1 have only cost values for traffic loads <30%. Observing Fig. 3.16, we note that the network cost grows with the traffic volume in a predictive almost linear manner in all the

cases. The slope in the cost variation is significantly steeper for higher network sizes. This result is interesting, since it shows that all the non linear interactions that are introduced in the network plan (RWA constraints, mixed-line-rates, effect of the interferences), still produce an almost perfect linear growth of the cost with the traffic.

To assess the quality of the Heur-MR-uNLE algorithm in terms of cost of the solutions provided, we compare the network cost with a lower bound (LB) to the network cost computed. To compute this cost LB, we make use of the same relaxation, described in the previous *Network Throughput* subsection, of the problem formulation (3.12)-(3.18). In some cases, the CPLEX solver is not able to find a solution to the relaxed problem. However, in all the situations the solver is capable of providing a dual cost to the relaxed problem, which acts as a lower bound on the network cost. Then, we use this dual cost as the lower bound to the original problem. Table 3.5 plots the optimality gaps of the algorithm for the tested cases. Interestingly, the optimality gap is small (2-10 %) in the large majority of the cases, validating the quality of the algorithm. The exceptions occur in some experiments corresponding to middle network loads (ρ) and network size factors β between 0.5 and 1. At the end of the next subsection, we elaborate a possible explanation to this effect. This explanation will suggest that the larger gaps are caused by the slackness of the LB, and not by the quality of the algorithm.

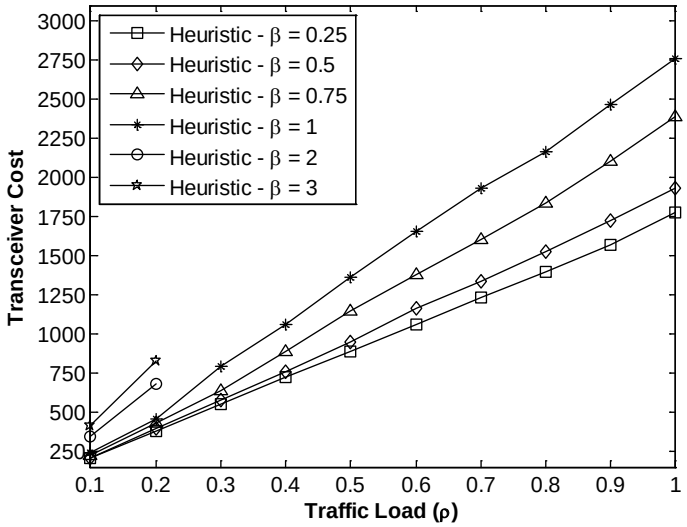

Fig. 3.16. MLR Case. Network Cost.

Table 3.5. Optimality Gap on Total Cost (%)

ρ \ β	0.25	0.5	0.75	1	2	3
0.1	9.7%	9.0%	8.0%	8.2%	9.2%	4.1%
0.2	7.1%	5.6%	6.2%	5.1%	8.0%	4.5%
0.3	6.2%	5.1%	5.1%	18.8%	-	-
0.4	4.5%	3.9%	9.3%	17.0%	-	-
0.5	3.7%	4.6%	11.1%	16.5%	-	-
0.6	3.0%	6.3%	9.6%	13.5%	-	-
0.7	2.6%	5.1%	8.2%	10.3%	-	-
0.8	2.3%	3.5%	7.6%	6.3%	-	-
0.9	2.0%	3.4%	7.5%	5.5%	-	-
1	4.0%	3.6%	7.5%	3.9%	-	-

Usage ratio of 10 Gbps vs 40 Gbps

The usage ratio of 10 Gbps vs 40 Gbps transceivers is analyzed in this subsection. In Fig. 3.17 we show the fraction of the number of 40 Gbps lightpaths in the network, with respect to the total number of lightpaths. These results are extracted from the same experiments (ρ, β) studied in the previous subsection.

Interesting conclusions can be drawn. First, for a given network (fixed β size factor), the use of 40 Gbps transceivers always increases with the traffic load ρ. That means that as traffic grows, the relative number of 10 Gbps decreases due its lower capacity to carry larger demands. Secondly, we can distinguish clearly two different situations depending on the network size factor β. For β values lower than one, it is always possible to find a high capacity virtual topology solely based on 40 Gbps transceivers. This is because in these networks all the links are within the 40 Gbps transparent reach (the 40 Gbps optical connectivity is guaranteed). As a consequence, the 40 Gbps transceivers usage is intense. Naturally, this usage is more intensive for lower β factors, since the availability of 40 Gbps QoT feasible lightpaths is larger (for $\beta = 0.2$, the 40 Gbps transceivers utilization is always close to 100%). Besides, the network planning can profit from the volume cost discount (10 Gbps relative cost per bps is 1, 40 Gbps relative cost per bps is 0.625). Conversely, for β values higher than one, the 10 Gbps transceivers dominate the virtual topology due to the shortage of 40 Gbps paths shorter than its transparent reach (600 Km).

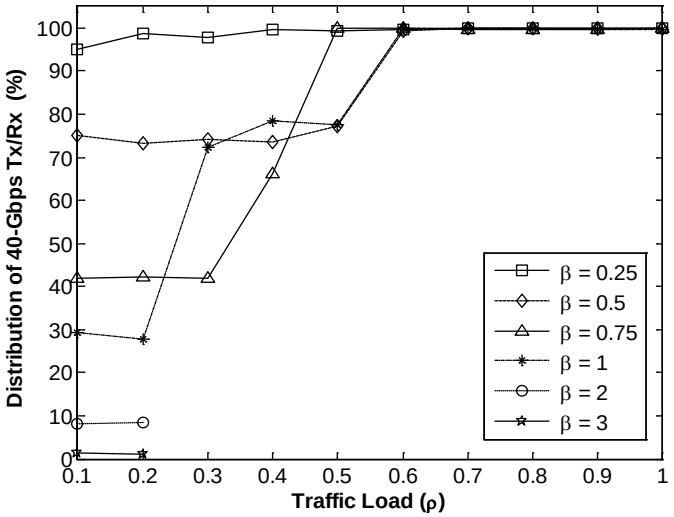

Fig. 3.17. Distribution of 40 Gbps Transceivers (Percentage with respect to the total number)

Finally, the joint analysis of Fig. 3.16 and Fig. 3.17 permits us to guess an explanation on the larger optimality gaps in network cost detected for medium loads. These values appear when the 40 Gbps transceivers utilization is abruptly increased. Moreover, the sharper the 40 Gbps utilization increment is, the worse the optimality gaps are. This abrupt increment cannot be just explained for a major need of higher bit-rate transceivers to face larger traffic loads, and probably is also caused by an extra increment of the number of 40 Gbps lightpaths to avoid to mix them with interacting adjacent 10 Gbps ones. Therefore, this degradation on the gap quality is something expected, since the lower bound is based on a relaxation of the MILP formulation (3.12)-(3.18) that ignores interferences constraints relative to non linear interactions between 10 Gbps amplitude modulated channels and 40 Gbps phase modulated channels.

SLR vs MLR

In this subsection, we repeat for 10 Gbps and 40 Gbps SLR cases (Single Line Rate), the experiments performed for the MLR case in the previous *Network Cost* subsection. In SLR cases, the Heur-MR-uNLE algorithm uses a unique single rate transceiver type. The intention is to compare the benefits of using MLR systems versus SLR ones in the scenarios under test. This type of comparisons has been already addressed in previous studies [26],[107]. The novelty of this study is double: (i) the introduction of the guardband requirements between 10 Gbps and 40 Gbps channels, to mitigate the mutual interferences, and (ii) the comparative analysis for various network sizes.

Fig. 3.18 shows us the costs savings of the MLR approach with respect to the 10 Gbps and 40 Gbps SLR approaches. The savings are computed solely when the heuristic found null lightpath blocking rate solutions for both the MLR case and the SLR case. Obviously, pure 10 Gbps solutions are found just for low traffic loads (up to ρ=0.2). In its turn, pure 40 Gbps solutions are found for short link length factors (up to β=1).

From the observation of Fig. 3.18, it is easy to extract the conclusion that the deployment of MLR systems permits to obtain a lower total network transceiver cost than SLR solutions for low traffic loads. This idea is consistent with the results of previous works [26],[107]. But, in contrast with these studies where non mutual interfering modulation formats are considered; in our work, the requirement of leaving guard bands between 10 Gbps channels and 40 Gbps ones seems to reduce severely the cost savings achieved by mixed systems at middle and high traffic loads.

The magnitude of the MLR savings at low load seems to be very dependent on the network size (β): for pure 10 Gbps cases, it decreases with the growing of β; meanwhile, for 40 Gbps comparisons, increases. These different trends are explained by the tradeoffs between both transceivers types. Increasing the network size (β) means reducing the number of 40 Gbps QoT feasible paths, and using more 10 Gbps paths with longer transparent reaches. Then, MLR solutions become more “10 Gbps pure” and less “40 Gbps pure” on increasing the network size. The transceivers distribution rates shown in Fig. 4 witness this point. As we can expect, the benefits of MLR approaches are lower for those β cases where the MLR design is already basically a SLR one.

At medium and high traffic loads, the 40 Gbps approach is the unique SLR scenario able to find a network design without blocked traffic. In these cases, in comparison with the low load situations, the expected savings due to the presence of cheaper 10 Gbps transponders are negligible or inexistent. Even, in some cases, its presence provokes MLR solutions slightly worse than pure 40 Gbps solutions. This harmful use of lower bit rate transceivers is due to the heuristic nature of the algorithm.

The performance loss appearing in MLR networks for higher traffic loads is caused by higher occupation of the wavelength channels, that seriously limits the possibility of leaving unused guard channels between 10 Gbps and 40 Gbps lightpaths. In these cases, the unique choice to avoid the 10/40 Gbps interferences is utilizing only (or almost only) 40 Gbps lightpaths, becoming MLR designs into pure 40 Gbps SLR ones.

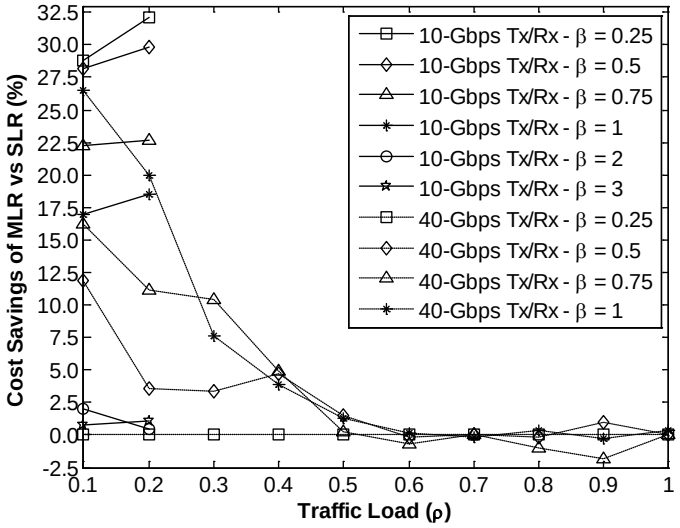

Fig. 3.18. Abilene network. Cost Savings of the MLR approach with respect to the SLR approaches

3.5.6 Conclusion

In this section, we have investigated the planning of multilayer MLR (mixed line rate) optical networks, where 10 Gbps NRZ-OOK modulated signals must share the standard 50 GHz grid with 40 Gbps RZ-DQPSK modulated signals. In this scheme, the intensity modulated signals (10 Gbps) induces non linear impairments over the phase modulated signals (40 Gbps). To cope with this, the network planning should allocate empty wavelengths separating adjacent channels at different bit rates.

The resulting multilayer network planning problem is modeled through a MILP formulation. A heuristic algorithm, that can be easily adapted to any other modulation formats scenario, is presented. The quality of the algorithm has been confirmed by comparison with performance bounds. Finally, several experiments are conducted to analyze under this new light the tradeoffs between longer reach of 10 Gbps transceivers, versus higher capacity and better cost per bps of 40 Gbps transceivers in MLR networks. Results suggest that MLR networks are promising solutions to reduce the transceiver network cost in low loaded networks, where the intensity in the cost reduction is very sensitive with the network size. But, unfortunately, in heavy loaded networks, the interferences between 10 and 40 Gbps channels we have considered, dissuade to mix them, despite the possible benefits of using longer-reach 10 Gbps lightpaths.

3.6 PLIA-RWA and Regenerator Placement Algorithms

This section summarizes the work performed in [20], where the author has a partial contribution. In this paper, the offline problem of Routing and Wavelength Assignment (RWA) and Regenerator Placement (RP) is investigated in translucent networks, minimizing the lightpath blocking and regenerator equipment cost.

The study addresses two variants of the problem corresponding to two different types of Quality of Transmission (QoT) estimators, called Linear and Non-Linear. In the Linear QoT the effects of the non-linear impairments are over-estimated and accumulated to the rest of the impairments in the QoT calculation. As a result, the QoT estimation of a lightpath solely depends on its route. Conversely, in a Non-Linear QoT, non-linear impairments like crosstalk or cross-phase modulation which account for the interferences from neighboring lightpaths in the network are explicitly computed. Then, the QoT estimated for a lightpath depends on the routes of other lightpaths in the network. We must note that this paper uses the terms linear and non-linear to denote to the static (or Class 1) and dynamic (or Class 2) impairments, respectively.

For the linear case, an optimal ILP model of the problem is presented. Its simplicity allows us to test it for small and medium size networks. Also, we propose for larger network problems two heuristic methods, namely *Lightpath Segmentation* and *3-Step*, and a tight lower bound for the regenerator equipment cost. For the non-linear QoT case, we propose a new heuristic called *Iterative Regenerator Placement* (*IRP*). Both the *IRP* and *3-Step* algorithms are designed to guarantee that no lightpath blocking is produced by signal degradation. This is a relevant difference with respect to previous proposals.

The author's contribution in this work was focused on the Non-Linear PLIA-RWA-RP study, namely, on the implementation of a Non-Linear QoT estimator based on analytical models [74],[84]-[88] and the development of the *Iterative Regenerator Placement Heuristic*.

In order to assess the performance and the scalability of the proposals, an extensive battery of tests was conducted. The traffic load in the tests is normalized to fairly assess the ability of the algorithms for minimizing the regeneration cost, without producing any signal-regeneration related to lightpath blocking. The results show that the *LS* and *3-Step* algorithms provide optimal or close-to-optimal solutions in all these tests. They outperform a previous heuristic algorithm presented [80], both in the quality of the solution found and the algorithm execution time. In addition, the 3-Step algorithm guarantees that no signal regeneration lightpath blocking is produced. Consequently, both algorithms can be used to efficiently solve the Linear PLIA-RWA-RP problem (e.g. selecting the best solution provided by both schemes). For solving the Non-Linear PLIA-RWA-RP problem, the *IRP* heuristic is able to provide a zero signal regenerator blocking. It outperforms in both lightpath blocking and regenerator equipment cost the

previous proposals in the literature tested.

In the next subsections, we briefly comment the work carried out in the framework Non-Linear PLIA-RWA-RP problem, where the thesis' author has especially contributed: (i) the Non Linear QoT estimator; and (ii) a PLIA-WA formulation that incorporate the PLIs by directly estimating them. This WA formulation is used in the third step of the *Iterative Regenerator Placement* (*IRP*) algorithm and supposes an interesting example of the indirect estimation approach to introduce PLIs commented in Section 3.3. In the sequel, we skip any detailed explanation of the proposals or the experiment results, recommending to the reader interested to consult the work [20].

3.6.1 Non-Linear QoT estimator

For the Non-Linear PLIA-RWA-RP problem we make use of a Non-Linear QoT estimator called Q-NL. Q-NL factor explicitly considers linear and non-linear effects. Since the physical impairments in 10 Gbps OOK optical communications are well known and modelles [74],[84]-[88], the implementation of Q factors encompassing them is relatively easy. This is the case of the Q-tool used in the Non-Linear PLIA-RWA-RP study.

The main impairments included in this *Q* factor, and modeled according to the references, are: Amplifier Spontaneous Emission (ASE) [74], Intrachannel Crosstalk (XT) [74], Cross-Phase Modulation (XPM)[84]-[86], Four Wave Mixing (FWM) [85]-[87] and Polarization Mode Dispersion (PMD) [88]. Chromatic Dispersion (CD) is considered completely compensated by the transmission system. We refer the reader to [74],[84]-[88] for additional details about the modeling of each physical impairment.

The Q-NL assumes the link and node architectures proposed in [16] and [74], respectively, with spans of standard single mode fiber (SSMF) under-compensated with dispersion compensation fibers (DCF) to a value of 30 ps/nm·km to diminish the non-linear effects. An appropriate post-compensation module in the end of the link compensates the accumulated dispersion. The transmission parameters used are depicted in Table 3.6. A threshold of 17 dB (equivalent to a BER of 10^{-12}) on the acceptable *Q* factor is used to validate the *QoT feasibility*. The resulting maximum link length considering worst-case non-linear impairments (links totally populated with lightpaths) is in the order 3000 km, with slight variations between different topologies and number of wavelengths per fiber.

Table 3.6. Transmission System Parameters

Parameter	Q-NL
Transmitter Bit Rate	10 Gbps
Modulation Type	NRZ-OOK
Grid Spacing	50 Ghz
Maximum Span Length	85 km
Input Power to SSMFs	3 dBm
Input Power to DMFs	-4 dBm
SSMF Attenuation Parameter	0.23 dB/km
DCF Attenuation Parameter	0.5 dB/km
SSMF CD Parameter	17 ps/nm·km
DCF CD Parameter	-80 ps/nm·km
Noise Figure of in-line and pre-amplifiers	5 dB
Noise Figure of boosters	6 dB
PMD Parameter	0.1 ps/$\sqrt{km}$
Switching Power Attenuation	as in [74]
Switch Crosstalk Ratio	32 dB

3.6.2 PLIA-WA used in Iterative Regenerator Placement Heuristic

In the *Non-Linear PLIA-RWA-RP* problem, the interferences between lightpaths are included explicitly in the QoT estimation. In this context, the Q factor of a lightpath depends on the existence of other lightpaths with common links and common nodes. To address this problem we propose the Iterative Regenerator Placement algorithm (IRP), consisting of the three steps. In the last step (*Iterative wavelength re-assignment and regenerator placement*), a wavelength assignment is conducted by using the formulation (3.28)-

(3.31). This formulation follows a direct estimation approach to include the PLIs into the model. This formulation is similar to the proposals in works [72],[83], but eliminating the routing placement, since that has been decided in a previous step of the IRP.

The decision variables of the ILP formulation (3.28)-

(3.31) used to perform the wavelength assignment step are:

- $x_{pw} \in \{0,1\}$, $p \in P_a$, $w \in W$. x_{pw} is equal to 1 if wavelength w is assigned to the one of the transparent segment of lightpath already defined at this step of the algorithm.

Then, the problem can be formulated as:

$$\min \sum_{p \in P_a} S_p \tag{3.28}$$

Subject to

$$\sum_{w \in W} x_{pw} = 1, \forall p \in P_a \tag{3.29}$$

$$\sum_{p \in P_a \cap Q_e} x_{pw} \leq 1, \forall e \in E, w \in W \tag{3.30}$$

$$\sum_{e \in p} \left(\begin{array}{l} s^2_{XT,b(e)} \sum_{p' \mid b(e) \in p'} x_{p'w} + \\ s^2_{XPM-1,e} \sum_{p \in P_a \cap Q_e} (x_{p'w-1} + x_{p'w+1}) \\ + s^2_{XPM-2,e} \sum_{p \in P_a \cap Q_e} (x_{p'w-2} + x_{p'w+2}) \\ + c_{FWM} - S_p \end{array} \right) \leq \sigma^2_{pw,MAX} + B(1 - x_{pw}) \quad p \in P_a, w \in W \tag{3.31}$$

Constraints (3.29) set that one wavelength is assigned per semi-lightpath. The wavelength clashing constraints are defined in (3.30). Constraints

(3.31) include the effects of the non-linear impairments. Left hand side of

(3.31) is an estimation of the noise variance suffered by semi-lightpath p if assigned wavelength w, caused by: (i) XT from other semi-lightpaths with common nodes, and (ii) XPM and (iii) FWM caused by other transparent optical paths with common links. In its turn, $\sigma^2_{pw,MAX}$ represents the maximum noise variance related to non-linear impairments that transparent segment (p,w) could accept while maintaining the required QoT. Worst-case variances s^2 and c_{FWM}, and maximum acceptable variance $\sigma^2_{pw,MAX}$ are calculated according to [74],[84]-[87]. The variables $S_p \geq 0$ are slack variables to permit that some semi-lightpaths exceed the accepted noise variance. The sum of these slack variables is the figure of merit to optimize (3.28).

Chapter 4

4 Multihour Planning

ABSTRACT: This chapter develops the contributions of this thesis to the multihour planning in optical WDM networks. First, the multihour VTD problems studied are stated. In contrast to the two chapters where the traffic demand was considered constant along time and the lightpaths were established semi-permanently based on this constant traffic, in multihour planning, the planning is performed along several time epochs, such as hours or days, modeling the traffic demands between the network nodes as a sequence of matrices, corresponding each one of them to a given time epoch. Second, a survey of the topic is described. Next, the considered VTD problems are modeled as MILP formulations. After that, the heuristic approaches proposed in the framework of the thesis to handle large sized problems are enumerated. Finally, two studies exploring the cost tradeoffs among different multihour network designs conclude the chapter.

4.1 Problem statement

In contrasts to the previous offline works in multifiber and PLIA planning, where static traffic demand was assumed, this chapter is centered on a variant of the offline scheduled VTD problem, denoted as *Multi-Hour Virtual Topology Design* (*MH-VTD*) [28], [29], [30]. In the scheduled problems, the traffic demand varies along time, but its variation is assumed to be known in advance, thanks e.g. by a pervious monitoring campaign. The scheduled VTD problem is denoted as MH-VTD (Multi-Hour Virtual Topology Design) when the traffic demand can be modeled as temporal series of traffic matrices. Then, the problem can be solved either by finding one unique static virtual topology or a succession of virtual topologies capable of handling all the given traffic variations over time. In the MH-VTD problems, the traffic demand takes the form of a temporal sequence of traffic matrices, reflecting the traffic variation along a given period of time (typically days or weeks). This periodic nature of the traffic has been confirmed with real traffic traces in numerous experiments, such as the Abilene network [32] or the GÉANT network [126], making the traffic load in the network fairly predictable.

The *multihour planning* attempts to reduce the network costs by exploiting the traffic periodicity and the busy-hours non-coincidence of the *multihour* traffic in continental long-haul networks [31]. In networks spanning over multiple time zones, like Abilene or GÉANT, the existence of different demand

peaks between different node pairs at different times, i.e., the non-coincidence of busy-hours, suggests the possibility of taking profit of the unused capacity in the network. For example, the traffic demand between two towns placed at US east coast (e.g. New York and Washington) at 8:00 am (offices opening hour) could be routed easier via a US midwestern (e.g. Chicago), where the time is 7:00 am and the network is less busy. In this thesis The *Multi-Hour Virtual Topology Design* works will try to minimize the number of optical transceivers required to meet all the traffic demand along time, since, in a given time slot, those transceivers with lower usage can be used to serve part of the traffic between the most loaded node pairs. In optical *WDM* networks, the number of optical transceivers is commonly referred as a network cost criterion in planning studies [33], [34], [35].

The *Multi-Hour Virtual Topology Design*, like the general *VTD*, implies to solve the multilayer planning problem referred in Section 1.2. In the upper layer, electronic traffic demands or electronic traffic flows (i.e. measured in Gbps) are routed on top of the lightpaths (*Flow Routing on VT subproblem*); whereas, in the lower layer, each lightpath in the virtual topology has to be routed over the physical topology and assigned a free wavelength channel (*Routing and Wavelength Assignment*, *RWA*, *subproblem*). In contrast to the classical VTD problem, in *MH-VTD* problems, both flow routings in the upper layer and lightpaths in the lower one can be modified along the time according to the variations in the traffic demand. The lightpath variations will depend on the presence of reconfigurable optical switching equipment, such as R-OADMs, at the nodes; and, they usually imply increases in signaling complexity and relevant traffic disruptions [127]. For these reasons, the amount of lightpath reconfigurations is also a recommendable metric to reduce in lightpath varying networks. Conversely, the variations on the flow routings over the VT can be performed by reprogramming the switching matrices in the electronic equipment. The tradeoffs on the transceiver cost between these different network configurations will be studied in this chapter.

If we analyze the MH-VTD problem defined above, we realize that the evolution of lightpaths to be established between node pairs totally determines the number of transceivers and reconfigurations in the network, and thus determines the network cost differences and trade-off we intend to evaluate. Of course, solving the RWA problem for the determined set of lightpaths certifies the feasibility of the network plan with respect to wavelength availability and physical impairments. Consequently, if we assume that the links in the network are equipped with a sufficient number of wavelengths and that physical-layer constraints do not apply, the associated RWA constraints can be removed from the network planning optimization problem. Such assumptions can realistically depict several network scenarios, e.g. in metro-area optical networks with an over-dimensioned fiber plant. In this chapter, we consider a network where the previous assumptions hold, and thus eliminate the RWA constraints from our analysis.

Chapter 4. Multihour Planning

This chapter summarizes the main author's contributions to the *Multi-Hour Virtual Topology Design* in the works [30],[36]-[40]. In these works, different tradeoffs were evaluated according to the several criteria:

- Considering reconfigurable or non-reconfigurable *virtual topology* [36],[37],[38],[40], when assumed time-variable flow routing on top of the virtual topologies. In the first case, one unique virtual topology design is obtained for all the multihour traffic demand. Then, the optical components are assumed to be non-reconfigurable. In the second case, reconfigurable switching nodes are assumed, i.e., the virtual topology design can change along time.
- Considering fixed or variable flow routing [30],[39], when assumed non-reconfigurable virtual topology. A fixed flow routing indicates that the traffic from a source node to a destination node is always transmitted via the same set of *lightpaths*. On the contrary, variable routing imposes no such constraints, but at a cost of higher signaling and network management complexity.
- Considering *splittable* or *unsplittable* flow routing over the *virtual topology* [30]. *Unsplittable* routing means that all the traffic between a pair of nodes is forced to traverse an unique path of nodes. Conversely, if the routing is *splittable*, the traffic between two nodes may be split into several paths, each one of them carries a fraction on the total offered traffic to the pair. Obviously, the *splittable* routing allows a better load balancing, although with the cost of increasing the signaling overload.

The criterions described above permit us to categorize the *MH-VTD* problem considered in this thesis according to the Table 4.1 and Table 4.2.

Table 4.1. Classification of MH-VTD problems considered in this thesis

Virtual Topology / **Flow Routing on VT**	**Non Reconfigurable**	**Reconfigurable**
Fixed	Non Reconfigurable VTD with Fixed Flow Routing (NR-VTD-FR)	-
Variable	Non Reconfigurable VTD with Variable Flow Routing (NR-VTD-VR)	Reconfigurable VTD (R-VTD)

Table 4.2. Classification of NR-VTD problems according to the flow routing assumptions

	Unsplittable	**Splittable**
Fixed	NR-VTD with Unplittable Fixed Flow Routing (NR-VTD-FR-u)	NR-VTD with Splittable Fixed Flow Routing (NR-VTD-FR-s)
Variable	NR-VTD with Unplittable Variable Flow Routing (NR-VTD-VR-u)	NR-VTD with Splittable Variable Flow Routing (NR-VTD-VR-s)

Each one of problems shown in Table 4.1 and Table 4.2, have been modeled as exact MILP formulations. Since all the *MH-VTD* problems are NP-Hard, we have also devised heuristic methods to address large sized problems, where the exact programs cannot solve in a reasonable time. For the R-VTD problems, tabu searches, Lagrangean relaxation based algorithms and greedy approaches were proposed. Whereas, for NR-VTD problems, along with the previous algorithms, optimization procedures based on the ***traffic domination*** concept [41] were developed to assess the tradeoffs existing under different assumptions on the flow routing over the non reconfigurable VT. The concept of ***domination*** between matrices [41] and matrices sequences [42],[43] provides a theoretical basis to devise a set of reduction methods on the number of matrices required to model the planning problem, reducing its complexity. In Annex B, the basics about the traffic domination are summarized.

The rest of the chapter is organized as follows. Section 4.2 presents the state-of-the-art on multi-hour virtual topology design. In Section 4.3 we provide optimal MILP formulations for the above described MH-VTD problems variants. Section 4.4 presents the heuristic algorithms proposed to study the multihour planning in transparent optical networks. Finally, in Section 4.5, the heuristic algorithms are assessed and exhaustively evaluated, at the same time as the aforementioned tradeoffs in *MH-VTD* are studied. Some conclusions are drawn.

4.2 Related Work

This section summarizes the state of the art in multihour planning, focusing on the research carried out in optical WDM networks. Dynamic non-hierarchical routing (DNHR) [128] for telephone networks, which can be considered the first case of success of multi-hour network design, appeared in the 1980s. After this, network planning taking into account time-varying traffic demands has been researched for multiple network technologies [28]-[31],[36]-[40],[127]-[153] (see [31] for a comprehensive historical survey in the topic).

The first investigations of MH planning in optical networks were targeted towards the design of virtual topologies in multi-hop networks, based on passive stars [141]. In the last decade, the interest of the optical community has shifted to lightpath-based transparent optical networks. Initial works on virtual topology reconfiguration in lightpath-based networks focus on studying when and how to reconfigure an existing VTD, as a reaction to a variation in the traffic [127],[142]-[145]. The most common design objective considered is minimizing the associated reconfiguration to avoid traffic disruptions. Additional objective criteria include the minimization of (i) the maximum load in the lightpaths [127],[142], (ii) the average virtual hops in the network [143], or (iii) the average propagation delay [144]. A full multilayer approach is given in [145], where VTD reconfiguration is considered in conjunction with RWA reconfiguration. Note that all these approaches only consider a one-time adaptation of a given virtual topology to a known change in traffic, but do not consider periodic (multi-hour) traffic trends.

Incorporating the periodic nature of traffic in transparent optical networks planning has only more recently attracted the interest of the research community [28]-[30],[36]-[40],[146]-[153]. Most research efforts have been focused on planning in the lower layer, i.e. the RWA of a given sequence of virtual topology designs corresponding to MH traffic. This is based on the Scheduled Lightpath Demand (SLD) model proposed in [146] where the evolution of individual lightpaths is known in advance. The planning problem then consists of finding a set of valid RWA solutions for the input VTDs, optimizing several network performances, such as the number of wavelengths used in the highest loaded fiber link. The SLD model enables more efficient utilization of resources by exploiting the temporal relationship between lightpaths. In [146], a branch and bound algorithm and tabu search heuristic were proposed for the Routing and Wavelength Assignment of a set of SLDs. An enhanced tabu search algorithm and efficient greedy algorithms for the same problem were proposed in [147]. Fault tolerant RWA was studied in [148] where the authors propose a Simulated Annealing algorithm using channel re-use and back-up multiplexing. Fault-tolerant RWA SLDs under single component failure was considered in [149]. They develop ILP formulations for the problem with dedicated and shared protection. In [150], the authors indicate some drawbacks in the formulations from [149], and give new ILP formulations for survivable service provisioning in networks with wavelength conversion. Their objective is to minimize the number of wavelength-links used by primary and secondary paths with guaranteed restoration in case of single failures.

A more general model, called the sliding scheduled traffic model was proposed in [151]. In this model, the set-up and holding times of lightpath demands are known in advance, but they are allowed to slide within a predefined window. Consequently, service provisioning consists not only of solving the RWA problem, but also scheduling demands in time subject to the sliding window constraints with the objective to minimize demand overlap. In [151], they solve the problems subsequently: first tackling

scheduling using a demand time conflict reduction algorithm, and then solving RWA with two proposed approaches. Fault tolerant RWA for the sliding scheduled traffic model in networks without wavelength conversion was considered in [152]. They also propose a two-phase approach: time conflict resolution followed by RWA. ILP formulations which jointly solve lightpath scheduling and RWA for the sliding scheduled traffic model are given in [153], along with a faster two-step optimization approach for larger problems.

While the aforementioned approaches deal with a known evolution of virtual topologies, this chapter encompasses studies interested in the problem of determining this evolution from the MH periodic traffic itself (i.e., the R-VTD problem) to plan the upper layer, or, determining a single static virtual topology which can accommodate the traffic at any time (i.e., the NR-VTD problem). To the best of our knowledge, very few works ([28], [29]) exist in the literature, apart from our efforts, focused on the MH-VTD problem variants.

In [28], the multilayer problem of mapping a set of lightpaths onto the physical topology and mapping a set of LSPs (Label Switched Paths) for packet switched traffic over the set of lightpaths is considered. They assume known traffic variations and consider that one LSP is required for each flow. They study the NR-VTD problem with fixed flow routing and unsplittable flows, assuming that a single lightpath capacity is sufficient for each LSP. The authors propose a method, based on a MILP formulation and a decomposition heuristic, for solving the NR-VTD problem. The method is called Joint Configuration with Exact Traffic (JCET) and takes as a set of multihour traffic matrices. The method minimizes a objective function consisting of a combination of the amount of average electronic packet processing along time, the number of optically switched wavelengths and the number of lightpaths in the network.

The JCET method is compared with a simple NR-VTD approach, denoted as Unique Configuration with Maximal Traffic (UCMT). In this alternate method, the temporal sequence of traffic matrices is reduced to one unique maximal matrix where the traffic between nodes (i, j) is assumed to be the maximum along time of the traffic between those nodes. Beside this, the solutions under JCET are also compared with a naïve approach (Independent Configuration with Exact Traffic, ICET) for the R-VTD problem where the VTDs are independently planned in each time interval. In both UCMT and ICET, the proposed MILP formulation is used to solve a single traffic matrix problem: the maximal matrix, for the UCMT; and, each instant traffic matrix, for the ICET. The results of the comparison NR-VTD vs R-VTD approaches indicate that establishing a non reconfigurable virtual topology with fixed routing obtains solutions very close to those in which the virtual topology can be dynamically reconfigured over time.

In [29] the authors address only the NR-VTD problem. They compare the benefits of a variable and

a fixed flow routing (assuming splittable flows) on top of the Non Reconfigurable VTD. They analyze various objectives, such as the average packet hop distance, congestion, and total number of lightpaths, and propose a hybrid one combining all three. The objective to minimize lightpaths is equivalent to minimizing transceivers since each lightpath requires one transmitter at the source node, and one receiver at the destination node. However, the work in [29] assumes a given number of transmitters and receivers per node and, thus, does not investigate the maximal possible savings in this respect. Furthermore, they assume at most one lightpath between each pair of nodes, which is very restrictive. They provide formulations using the various objectives and test on seven and ten node networks for three time slots. In their results, flow rerouting achieved a 7% savings in the number of lightpaths.

In the last years, the author has participated in several works [30],[36]-[40], where the different MH-VTD problem variants are intensively investigated. The work in [36] presents a set of MILP formulations for several NR-VTD and R-VTD problem variants which minimize the number of transceivers. These formulations are extended in [40] to include penalization of VTD reconfiguration. In [37], a set of scalable tabu search based heuristic algorithms solving the previous problems is presented. In [30], different variants of the NR-VTD problem are evaluated, with and without flow routing reconfiguration, with splittable or unsplittable flows. A set of MILP formulations of the problem, together with a 3-step algorithm making use of the concept of traffic domination [41] for problem simplification. Two families of algorithms for the R-VTD problems are presented in [38]. One family of algorithms is based on a tabu search approach, while other is based on a decomposition consisting of a Lagrangean relaxation and a subgradient optimization of the dual problem. Finally, in [40], a greedy algorithm devoted to minimize both transceiver as lightpath reconfigurations is presented. The algorithm, valid for both the NR-VTD and R-VTD variants, is denoted as Greedy Approach with Reconfiguration Flattening (GARF) and strongly improves the performance of the previous proposals.

On the other hand, the author has also contributed in the development of reduction complexity techniques based on traffic domination in [30] and [39]. These works investigate the application of the traffic domination to multi-hour network planning in networks with fixed capacity and static or dynamic traffic routing. In [30], a set of methods based on the domination relation between traffic matrices [41] are used to convert the multihour traffic series into one individual traffic matrix, and plan the optical WDM network according to it. Conversely, in [39], more sophisticated techniques are derived from the traffic domination relation between *sets* of traffic matrices [42],[43]; and, successfully applied to general communication networks. These techniques generate traffic series with a smaller number of matrices from multi-hour traffic demand potentially composed of hundreds of matrices.

4.3 MILP Formulations

In this section, we show the exact MILP formulations proposed for the all the *MH-VTD* problem variants investigated. The formulations for the problems NR-VTD were presented in [30]. In [36], a formulation for the R-VTD was proposed. Finally, [40] extends the previous formulation to include penalization on the number of lightpath reconfigurations.

Let N be the number of nodes in the network, and T the number of time intervals for which the traffic is defined. Let $i,j,s,d,n = \{1\ldots N\}$ be the indices for the nodes, and $t = \{1\ldots T\}$ be the index for the time intervals (since we are dealing with periodic traffic, we assume that the last time interval $t=T$ is followed by the first time interval $t=1$). Let h^t denote the traffic matrix at time slot t, and $h_{sd}{}^t$ denote the traffic demand (measured in Gbps) from node s to node d, during time interval t). Let C denote the lightpath capacity in Gbps. The cost of each transmitter and receiver is considered equal, and is represented by c_1. An artificial cost of reconfiguring a lightpath is denoted as c_2.

4.3.1 NR-VTD-FR-s/u problems

The decision variables of the problem are:

- $\mathbf{f} = (f_{ij}^{sd}) \in [0,1]$. Fraction of the total traffic demand $h_{sd}{}^t$ from node s to node d that is routed on the existing lightpaths from node i to node j.
- $\mathbf{p} = (p_{ij}) = \{0,1,2,...\}$. Number of lightpaths from node i to node j.

The problem formulation is given by (4.1)-(4.4).

$$\min c_1 \sum_{i,j} p_{ij} \tag{4.1}$$

Subject to

$$\sum_{s,d} \left\{ h_{sd}^t \cdot f_{ij}^{sd} \right\} \leq C \cdot p_{ij}, \quad i,j = \{1,...,N\}, \; t = \{1,...,T\} \tag{4.2}$$

$$\sum_j f_{nj}^{sd} - \sum_i f_{in}^{sd} = \begin{cases} 1, if \; n = s \\ -1, if \; n = d, \; n,s,d = \{1,...,N\}, \\ 0 \; otherwise \end{cases} \tag{4.3}$$

Only for NR-VTD-FRu:

$$f_{ij}^{sd} = \{0,1\}, \qquad i, j, s, d = \{1,..., N\} \tag{4.4}$$

The objective function (4.1) searches for a virtual topology that minimizes the number of lightpaths, which is equivalent to minimizing the number of transceivers in the network. Constraints (4.2) force the traffic between two nodes at any time, to be limited by the number of lightpaths planned in the virtual topology between those nodes. Constraints (4.3) are the link-flow conservation constraints. Integrality constraints (4.4) appear only in the unsplittable case (NR-VTD-FRu problem), preventing the flow between two nodes to be fractioned among different paths.

4.3.2 NR-VTD-VR-s/u problems

The decision variables of the problem are:

- $\mathbf{f} = (f_{ij}^{sdt}) \in [0,1]$. Fraction of the total traffic demand $h_{sd}{}^{t}$ from node *s* to node *d* that is routed on the existing lightpaths from node *i* to node *j* during time interval *t*
- $\mathbf{p} = (p_{ij}) = \{0,1,2,...\}$. Number of lightpaths from node *i* to node *j*.

The problem formulation is given by (4.5)-(4.8):

$$\min c_1 \sum_{i,j} p_{ij} \tag{4.5}$$

Subject to

$$\sum_{s,d} \left\{ h_{sd}^{t} \cdot f_{ij}^{sdt} \right\} \leq C \cdot p_{ij}, \quad i, j = \{1,..., N\}, \; t = \{1,..., T\} \tag{4.6}$$

$$\sum_{j} f_{nj}^{sdt} - \sum_{i} f_{in}^{sdt} = \begin{cases} 1, if \; n = s \\ -1, if \; n = d, \; n, s, d = \{1,...,N\}, \; t = \{1,..., T\} \\ 0 \; otherwise \end{cases} \tag{4.7}$$

Only for NR-VTD-VRu:

$$f_{ij}^{sdt} = \{0,1\}, \qquad i, j, s, d = \{1,..., N\}, \; t = \{1,..., T\} \tag{4.8}$$

As in the formulation (4.1)-(4.4), the objective function (4.5) searches for a virtual topology that minimizes the number of lightpaths. Both capacity constraints (4.6) and link-flow conservation constraints (4.7) have been trivially adapted to consider a routing which can change along time, by considering independent constraints in each time slot. Again, integrality constraints (4.8) appear only in the unsplittable case NR-VTD-VRu.

4.3.3 R-VTD problem

The decision variables of the R-VTD problem are:

- $\mathbf{f} = (f_{ij}^{sdt}) \in [0,1]$. Fraction of the total traffic demand $h_{sd}{}^{t}$ from node *s* to node *d* that is routed on the existing lightpaths from node *i* to node *j*.
- $\mathbf{p} = (p_{ij}^{t}) = \{0,1,2,...\}$. Number of lightpaths from node *i* to node *j*, required during time interval *t*.
- $\mathbf{tx} = tx_n = \{0,1,2,...\}$. Number of transmitters installed in node *n*.
- $\mathbf{rx} = rx_n = \{0,1,2,...\}$. Number of receivers installed in node *n*.
- $\mathbf{r}^{+} = (r^{+}{}_{ij}^{t}) = \{0,1,2,...\}$. Number of new lightpaths set up at time *t* with respect to the number of existing lightpaths at time *t*-1 (or time *T* if *t*=1) between the nodes *(i,j).*
- $\mathbf{r}^{-} = (r^{-}{}_{ij}^{t}) = \{0,1,2,...\}$. Number of lightpaths torn down at time *t* with respect to the number of existing lightpaths at time *t*-1 (or time *T* if *t*=1) between the nodes *(i,j)*

The problem formulation is given by (4.9)-(4.15).

$$\min c_1 \sum_n \left(tx_n + rx_n\right) + c_2 \sum_{i,j,t} r^{+}{}_{ij}^{t} \tag{4.9}$$

Subject to

$$\sum_{s,d} \left\{ h_{sd}^{t} \cdot f_{ij}^{sdt} \right\} \le C \cdot p_{ij}^{t}, \quad i, j = \{1,...,N\}, \; t = \{1,...,T\} \tag{4.10}$$

$$\sum_j f_{nj}^{sdt} - \sum_i f_{in}^{sdt} = \begin{cases} 1, if \;\; n = s \\ -1, if \;\; n = d, \;\; n, s, d = \{1,...,N\}, \;\; t = \{1,...,T\} \\ 0 \; otherwise \end{cases} \tag{4.11}$$

$$tx_n \geq \sum_j p_{nj}^t,\ n = \{1,...,N\},\ t = \{1,...,T\} \tag{4.12}$$

$$rx_n \geq \sum_i p_{in}^t,\ n = \{1,...,N\},\ t = \{1,...,T\} \tag{4.13}$$

$$p_{ij}^t - p_{ij}^{t-1} = r^{+}{}_{ij}^t - r^{-}{}_{ij}^t,\ i, j = \{1,...,N\},\ t = \{2...,T\} \tag{4.14}$$

$$p_{ij}^1 - p_{ij}^T = r^{+}{}_{ij}^1 - r^{-}{}_{ij}^1,\ i, j = \{1,...,N\} \tag{4.15}$$

The objective function (4.9) minimizes the total cost of the *transmitters* and *receivers* (c_1) and the artificial *lightpath reconfiguration* cost (c_2). This artificial cost (c_2) can be tuned to a desired value, reflecting its importance to the network planner. Recall that, in contrast to the previous NR-VTD formulations, the number of transmitters (receivers) installed at the network cannot be any more directly derived from the number of lightpaths, since this figure varies along the time. For this reason, the new decision variables **tx** and **rx** replace the lightpath variables **p** in (4.9), and new constraints (4.12) and (4.13) are added to link transceivers with lightpaths.

As in the formulations (4.1)-(4.4) and (4.5)-(4.8), constraints (4.10) force the traffic between two nodes at any time, to be limited by the number of lightpaths planned in the virtual topology between those nodes, but now, the decision variables **p** also varies along the time. Constraints (4.11) are usual the link-flow conservation constraints. New constraints (4.12) and (4.13) ensure that the number of lightpaths originating (terminating) at a given node at any time, must be below the number of transmitters (receivers) installed at that node. And, finally, new constraints (4.14) and (4.15) are used to force the $\mathbf{r}^+$ and $\mathbf{r}^-$variables to account for an absolute increase or decrease, respectively, in the number of lightpaths between nodes *i,j*, at time *t*.

Since lightapath reconfiguration causes temporary service disruption, which can be very significant and expensive due to the high data rates involved, penalizing such reconfigurations might be interesting. That is the rationale behind incorporating the minimization of the lightpath reconfigurations to the objective function (4.9). Note that only variable $\mathbf{r}^+$ is used to compute the number of reconfigurations in (4.9). Naturally, given the periodic nature of the planning, for every node pair, the sum along time of new lightpath establishments ($\mathbf{r}^+$) is equal to the sum along time of lightpath disestablishments ($\mathbf{r}^-$):

$$\sum_t r^{+}{}_{ij}^t = \sum_t r^{-}{}_{ij}^t,\ i, j = \{1,...,N\} \tag{4.16}$$

4.4 Heuristic Algorithms

In this Section, the heuristic approaches proposed in [30],[37],[38] and [40] to address the different *MH-VTD* problem variants are explained. In [30], a three step method based on the domination (3-Step-D) concept is applied to the NR-VTD problems. On the contrary, in [37],[38] and [40], three algorithms valid for solving NR-VTD-VR-s and R-VTD problems are proposed: a tabu search (TS) in [37] and [38], a Lagrangean Relaxation based approach (LRvSG) in [38] and a greedy algorithm (GARF) in [40]. The Table 4.3 classifies the proposals according to the problem variants solved by them.

Before detailing the algorithms a lower bound on the total number of transceivers is presented. These lower bound will be used to assess the performance of all the heuristic algorithms, since is valid for both NR-VTD and R-VTD problems.

Table 4.3. Heuristic proposals in [30],[37],[38] and [40] depending on the problem variant

	NR-VTD				R-VTD
	-FR-u	-FR-s	-VR-u	-VR-s	
3-Step-D	✓	✓	✓	✓	✗
TS	✗	✗	✗	✓	✓
LRvSG	✗	✗	✗	✗	✓
GARF	✗	✗	✗	✓	✓

4.4.1 A Lower Bound on the Number of Transceivers

This Section proposes a lower bound to the optimal number of transceivers required in the network. We define $LB_{TX}(n)$ and $LB_{RX}(n)$, for a node n, as the lower bound on the number of transmitters and receivers, respectively, at that node. Given a sequence of traffic matrices $H = \{h^1,..., h^T\}$, the lower bound on the number of transmitters (receivers) is the minimum number of transmitters (receivers) that a node n requires, that is, the largest number of lightpaths required to add (drop) the total traffic generated by (targeted to) the node in any time slot t. These lower bounds are calculated as follows.

$$LB_{TX}(n) = \max_{t=1...T} \left\{ \sum_{j=1}^{N} \left\lceil \frac{h_{n,j}^t}{C} \right\rceil \right\} \tag{4.17}$$

$$LB_{RX}(n) = \max_{t=1...T} \left\{ \sum_{i=1}^{N} \left\lceil \frac{h_{i,n}^t}{C} \right\rceil \right\} \tag{4.18}$$

Therefore, a lower bound on the total number of transceivers in the network is given by:

$$LB = \sum_{n=1}^{N} \left\{ LB_{TX}(n) + LB_{RX}(n) \right\} \tag{4.19}$$

It is very important to note that the lower bound described above is a lower bound for the *fully reconfigurable* case in which (i) the virtual topology can be reconfigured along time, (ii) the flow routing is variable, and (iii) the flow routing is splittable. Therefore, for cases where the lower bounds are close to the NR-VTD solutions, we can claim that only a small reduction in the number of transceivers can be obtained by allowing the virtual topology to be dynamically reconfigured along time.

4.4.2 3-Steps Domination based algorithm

Herein, we propose a family of heuristic algorithms to solve the four variants of the NR-VTD problem described above. We make use of the concept of domination between traffic matrices introduced in [41], as a foundation for our approach. For a better understanding of the next sections, we provide in the Annex B.1 the notions of the traffic matrix domination concept used in the proposed heuristic approaches.

The four NR-VTD problem variants considered in this chapter have as an input parameter a sequence of T traffic matrices $h^1,..., h^T$, each of them of size NxN, being N the number of nodes in the network. A NxN virtual topology matrix **p** is characterized by planning decision variables p_{ij} as defined in Sections 4.3.1 and 4.3.2. A flow routing matrix **f** denotes the NxNxNxN matrix composed by the decision variables f_{ij}^{sd} as defined in Section 4.3.1. And, if the flow routing pattern varies along the time slots $t = \{1…T\}$, the flow routing matrix at time interval t , is noted as $\mathbf{f}^t$. We must note that the virtual topology matrix **p**, and the flow routing matrix **f** are examples of the generalized capacity vectors u and routing vectors x described in the Annex B.1. Indeed, **p** corresponds to an *integral* capacity vector u.

The heuristic algorithms proposed for each of the four problem variants follow a common scheme, composed of three basic steps.

Step 1: **Replace-with-one matrix**. The initial sequence of traffic matrices $h^1,..., h^T$ is replaced with one unique matrix h, such that matrix h dominates each of the matrices $h^1,..., h^T$. The type of domination depends on the problem variant, and will be described in detail in the subsection below.

Step 2: **Static Virtual Topology Design (VTD)**. Dominating matrix h is used to feed a heuristic algorithm for calculating a static virtual topology **p** (i.e. a capacity vector) and a unique routing vector **f** (unsplittable for problems NR-VTD-FRu and NR-VTD-VRu), which minimizes the number of transceivers, our primary cost measure of interest.

Step 3: **(NR-VTD-VR problems) Per-time-slot flow routing calculation.** For the NR-VTD-VR problem variations, the flow routing **f** calculated in the previous step is not guaranteed to be a feasible routing over all time slots. Consequently, T instances of the multicommodity flow routing problem are solved to individually route the traffic flows in matrices h^t, $t = 1,..., T$ on top of virtual topology **p** for each time slot separately.

The crucial point in the method is that the traffic domination concept guarantees that a virtual topology **p** (a integral capacity vector) calculated in Step 2 supporting the traffic of h, will also be able to support the traffic in all the time slots $h^1,..., h^T$. As such, virtual topology h is a suitable virtual topology for our MH-VTD planning problem.

A more detailed explanation of each individual step in the proposed three-step heuristic follows in the next subsections.

Step 1: Replace-with-one methods

Step 1 is a procedure to replace a sequence of traffic matrices $h^1,..., h^T$ with one dominating matrix h, such that this matrix dominates all matrices in the sequence. Then, matrix it also dominates each matrix h^t, $t = 1,..., T$. Depending on the considered problem variant, different types of domination between matrix h and matrices $h^1,..., h^T$ are applied. For each case, we aim to find that matrix h among all possible matrices h' which dominate the sequence (including for instance, a matrix with all the coordinates set to infinity), yielding the most cost-effective virtual topology **p**. This aspect is described for each problem variant separately.

Total domination for problems NR-VTD-FRs/u

In the NR-VTD-FRs and NR-VTD-FRu problems, flow routing must remain constant along time. Consequently, we must guarantee that a common routing matrix **f** exists, such that (**p**, **f**) supports traffic h^i, for all $i = 1,..., T$. The following lemma proves the validity of the total domination relation as a strategy to solve this problem.

Lemma 1*: Let h be a matrix which totally dominates a sequence of traffic matrices* h^t, $t = 1,..., T$. *Let*

$\mathbf{p}_s$ be a virtual topology and $\mathbf{f}_s$ a routing flow calculated such that ($\mathbf{p}_s$, $\mathbf{f}_s$) supports matrix h with splittable flows. Then, ($\mathbf{p}_s$, $\mathbf{f}_s$) is a solution for the NR-VTD-FRs problem. For the same matrix h, let $\mathbf{p}_u$ be a virtual topology and $\mathbf{f}_u$ a routing flow calculated such that ($\mathbf{p}_u$, $\mathbf{f}_u$) supports matrix h with unsplittable flows. Then, ($\mathbf{p}_u$, $\mathbf{f}_u$) is a solution for the NR-VTD-FRu problem.

Proof: The proof comes immediately from applying the concept of total domination (Definition B.1.2): as *h* totally dominates the sequence, every capacity-routing pair (**p**, **f**) that support *h*, also supports every matrix in the sequence h^t, $t = 1,..., T$. If the routing flow **f** is unsplittable, (**p**, **f**) is a solution to the NR-VTD-FRu problem.

The following lemma provides a method, devised from the Proposition B.1.2, to calculate the total dominating traffic matrix *h* we are searching for.

***Lemma 2**: Given a sequence of traffic matrices $h^1,..., h^T$, the matrix $h = \{h_{ij}\}$, $i,j = 1,..., n$, such that $h_{ij} = max\{h_{ij}^1,..., h_{ij}^T\}$, totally dominates the sequence.*

Proof: As $h_{ij} = \max\{h_{ij}^1,..., h_{ij}^T\}$, then for any $i,j = 1,..., N$, it holds that $h_{ij} \geq h_{ij}^t$ for all $t = 1,..., T$. Then, matrix *h* totally dominates the sequence.

The next lemma states that *any* other matrix which totally dominates the sequence, other than the one above, yields a less cost-effective solution for any cost measure we devise.

***Lemma 3**: Let h^a and h^b be two traffic matrices which totally dominate the same traffic matrix sequence $h^1,..., h^T$. Let h^a be calculated as shown in the previous lemma, while h^b is calculated differently. Let $c(\mathbf{p},\mathbf{f})$ be a cost function which associates a cost to a virtual topology* **p** *and a flow routing* **f**. *Let* ($\mathbf{p}^a$, $\mathbf{f}^a$) *be the virtual topology and routing pair that supports h^a with the minimum cost attending to the cost function c. Let* ($\mathbf{p}^b$, $\mathbf{f}^b$) *be the virtual topology and routing pair that supports h^b with the minimum cost attending to the same cost function c. Then, the cost obtained with h^a is always equal to or lower than the cost obtained with h^b: $c(\mathbf{p}^a,\mathbf{f}^a) \leq c(\mathbf{p}^b,\mathbf{f}^b)$.*

Proof: The proof is based on showing that matrix h^b must totally dominate matrix h^a. This is proved, by reduction to the absurd. Let us assume that h^b does not dominate h^a. Then, there exists a node pair $i,j = 1,..., N$ such that $h_{ij}^b < h_{ij}^a$. Let h^t be the matrix in the sequence such that $h_{ij}^a = h_{ij}^t$, i.e., the matrix associated to the time slot with the maximum value in the position (i, j). Then, it holds that $h_{ij}^b < h_{ij}^t$. Therefore, a contradiction is found, as if matrix h^b does not dominate h^a, then matrix h^b can not dominate matrix h^t, and thus cannot dominate the sequence.

As matrix h^b totally dominates matrix h^a, every $(\mathbf{p}, \mathbf{x})$ pair that supports h^b, also supports h^a. It follows that the $(\mathbf{p}^b, \mathbf{f}^b)$ pair that minimizes the cost figure supports both h^a and h^b. Then, $c(\mathbf{p}^a,\mathbf{f}^a) \leq c(\mathbf{p}^b,\mathbf{f}^b)$, as we wanted to prove.

Note that the method to calculate the totally dominating matrix h is applied to both the NR-VTD-FRs and NR-VTD-FRu problems. As will be shown later, the heuristic algorithms proposed for these two problems differ only in *Step 2* of the approach.

Weak domination for problems NR-VTD-VRs/u

In the NR-VTD-VRs and NR-VTD-VRu problems, we are interested in finding a common virtual topology **p** and a time varying flow routing **f** for the traffic sequence $h^1,..., h^T$. The following lemmas prove the validity of the weak domination relation as a strategy to solve this problem.

Lemma 4*: Let h be a matrix which weakly dominates a sequence of traffic matrices* h^t, $t = 1,..., T$. *Let* **p** *be a virtual topology and* **f** *a flow routing matrix calculated such that* (**p**, **f**) *supports matrix h with splittable flows. Then, there is at least one solution to the NR-VTD-VRs problem which has* **p** *as its common virtual topology, but potentially with different flow routings in different time slots.*

Proof: The proof is based on the definition of weak domination (Definition B.1.1): as matrix *h* (*weakly*) dominates the sequence, and virtual topology **p** supports *h*, then the same virtual topology **p** supports any matrix in the sequence. However, note that the weak domination relation does not guarantee a common flow routing along time.

Lemma 5*: Let h be a matrix which weakly dominates a sequence of traffic matrices* h^t, $t = 1,..., T$ *with respect to unsplittable flows. Let* **p** *be a virtual topology and* **f** *an unsplittable flow routing*

*calculated such that (***p**, **f***) supports matrix h with unsplittable flows. Then, there is at least one solution to the NR-VTD-VRu problem which has U as its common virtual topology, but potentially with different flow routings in different time slots, all of them unsplittable.*

Proof: The proof is analogous to the one for the previous lemma, but replaces the "weak domination" relation with the "weak domination with respect to unsplittable flows" relation by using the Definition B.1.3.

Given a traffic matrix sequence h^1,..., h^T, the method to calculate a matrix *h* which weakly dominates the sequence is based on the application of the Proposition B.1.1. This property states that the traffic matrix *h* we are searching for, seen as a non-integral capacity matrix, should be able to support all the traffic matrices in the sequence. Thus, finding a matrix *h* for the *replace-with-one* step in the NR-VTD-VR case, implies finding a common non-integral capacity matrix *h* which is capable of carrying the traffic over all the time slots in the sequence. In other words, finding a matrix *h* which weakly dominates the sequence, and finding a virtual topology **p** which solves the NR-VTD-VR problem are *almost* equal problems. They can be solved with *almost* the same formulation. The difference between the formulation (4.5)-(4.8), which optimally solves the NR-VTD-VRs/u problems, and the formulation for Step 1 of our heuristic is that in Step 1, the integral constraints for the capacity matrix are removed. Therefore:

- Calculating a matrix *h* which weakly dominates the sequence can be done by solving formulation (4.5)-(4.8) for the NR-VTD-VRs problem, by relaxing the integrality constraints for capacity matrix **p**. The capacity matrix **p** obtained by the relaxed problem is the weakly dominating matrix searched. Note that by relaxing the integrality constraints in variables **p**, an LP (Linear Programming) problem is obtained, which can be solved in polynomial time.
- Analogously, calculating a matrix *h* which weakly dominates the sequence with respect to unsplittable flows can be done by solving formulation (4.5)-(4.8) for the NR-VTD-VRu problem, by relaxing the integrality constraints for capacity matrix **p**. However, for this case, a MILP problem must still be solved since the routing variables remain binary as a consequence of the unsplittable flow constraint.

In summary, the application of the weak domination concept in the *Replace-with-one* step allows us to reduce the complexity of the problem by relaxing the integrality constraints in the capacity variables. Furthermore, the domination concept guarantees that any virtual topology supporting the resulting matrix

will also support the traffic along all the time slots.

Note that the method proposed above for finding matrix h, based on relaxing formulation (4.5)-(4.8), implies finding the weakly dominating matrix which minimizes the sum of its coordinates. This is a reasonable way to produce cost-effective virtual topologies and routings. Unfortunately, the method does not guarantee that any other matrices h' which weakly dominate the same sequence, would yield virtual topologies of equal or higher cost. In contrast to the case for the total dominating relation described in Lemma 3, it is not true that the matrix h calculated by solving the relaxed version of formulation (4.5)-(4.8) is weakly dominated by all other matrices h' which weakly dominate the given sequence. Consequently, finding the matrix which provides the most cost-effective virtual topology is presumably as difficult as optimally solving the NR-VTD-VR problem.

While the *Replace-with-one* step implies a reduction in the complexity with respect to the original problem, calculating the weakly dominating matrix of a long traffic matrix sequence can still be too complex (or intractable in the NR-VTD-VRu case, which involves solving a MILP). As such, we propose two additional complexity-reduction methods which make use of the domination concept and the procedure described in this Section. They can be combined and used together as Step 1 in the heuristic approach for the variable routing problem variants.

Method 1: Reduce to the maximal 'non-dominated set'. This means reduce the original set of matrices to the maximal subset in which no matrix weakly dominates any other.

This method eliminates a subset of matrices from the original sequence of traffic matrices $H = \{h^1,..., h^T\}$ in such a way that the reduced sequence yields an *exactly* equivalent solution to the NR-VTD-VR problem. Thus, the optimal solution remains the same. A matrix h^t is eliminated from the sequence, if it is weakly dominated by other matrix $h^{t'}$ in the sequence. The weak domination relation states that any virtual topology that supports $h^{t'}$ also supports h^t, and thus the set of feasible solutions to the NR-VTD-VR problem is not modified by its removal. Reducing to a maximal non-dominated set can be done by solving a series of small linear formulations where the domination between each pair of matrices is checked. This involves solving a flow routing problem in the NR-VTD-VRs case, and its unsplittable version in the NR-VTD-VRu case.

Method 2: Hierarchical calculation of the weakly dominating matrix.

This method finds a matrix h which weakly dominates sequence $H^1 = \{h^1,..., h^T\}$ as follows. First, the matrices in H^1 are partitioned into groups of two matrices consecutively. Then, for each group of two

matrices, a matrix that weakly dominates both is calculated. This is done by using the relaxed version of formulation (4.5)-(4.8). For the NR-VTD-VRu problem, weak domination with respect to unsplittable flows is used. The calculated matrices form a sequence H^2 comprised of the ceil of $T/2$ matrices (if T is odd, one matrix from H^1 is directly mapped to H^2). The process is repeated, reducing the sequence size by half in each repetition. In the last repetition, a single matrix is obtained. Every virtual topology **p** that supports this matrix also supports the matrices in the original sequence H^1, and in all intermediate sequences. The method is suboptimal in the sense that it cannot guarantee that other matrices *h*' which dominate the original sequence cannot be found, which lead to more cost-effective virtual topologies. However, since there is no guarantee that the weakly dominating matrix solved using formulation (4.5)-(4.8) for the original sequence yields the optimal solution to the NR-VTD-VR, the solution obtained with this approximation technique is not necessarily worse. The complexity reduction obtained by applying this method is quite relevant, as the relaxed version of formulation (4.5)-(4.8) is executed for instances of only 2 matrices. The number of instances solved for a sequence of $T = 2^k$ matrices, equals $2^{k-1} + 2^{k-2} + ... + 2^0 = 2^k - 1 = T - 1$.

Step 2: Virtual topology design calculation

In Step 2, the dominating matrix *h* calculated in the previous step is used to feed an algorithm that calculates a virtual topology which supports traffic *h*. In the study in [30], we have chosen the heuristic algorithm presented in [33] which sub-optimally minimizes the number of transceivers, but any algorithm able to compute a virtual topology from a traffic matrix *h* would be valid. The algorithm in [33] starts with a fully connected virtual topology where all the traffic is carried between node pairs in one direct virtual hop. If the traffic between a node pair exceeds the capacity of a lightpath, multiple lightpaths between the same pair of nodes are assumed. The algorithm iteratively tries to reroute all the traffic on the least loaded lightpath onto its shortest path using the spare bandwidth available in the current virtual topology. If it succeeds, the lightpath under consideration is eliminated from the virtual topology and the corresponding traffic is rerouted. The process is repeated until the traffic in the least loaded lightpath of some iteration can not be rerouted using the available capacity. While the algorithm described in [33] considers only unsplittable flows, we have made a modification which allows us to consider also a splittable routing version. The modification consists of solving a fractional min-cost flow formulation instead a shortest path algorithm for rerouting the traffic on the least loaded lightpath, instead of a shortest-path approach. The algorithm from [33] is used for the unsplittable problem variants NR-VTD-FRu and NR-VTD-VRu, while the adaptation to fractional routing of [33] is used in the splittable problem variants.

In the NR-VTD-FR fixed routing problems, the method guarantees that the common virtual topology

p and the common flow routing matrix **f** obtained in this step, are a feasible solution for the planning problem. However, In the NR-VTD-VR variable routing problem variants, a further step is needed.

Step 3: Variable flow routing calculation

In NR-VTD-VR variable routing problems, the weak domination relation applied in the *replace-with-one* step, does not guarantee that the (**p**,**f**) pair calculated in Step 2, supports the traffic in all time slots. However, the method guarantees that for the obtained virtual topology **p**, there exists at least one routing matrix $\mathbf{f}^t$ for each time slot $t = 1,..., T$, which supports the traffic in that time slot.

Step 3 is responsible of finding such a set of T flow routings $\mathbf{f}^1,..., \mathbf{f}^T$ of interest, where each pair (**p**, $\mathbf{f}^t$) supports traffic matrix h^t, $t = 1,..., T$. If changes in the flow routing along time are not penalized, this can be done by solving T independent conventional multicommodity flow problems. If not, the flow routing problems in different time slots become dependent, yielding to a more complex problem. Some suitable heuristic algorithms have been proposed in the literature which could be then used in this step [151],[154].

Summary

To summarize, Table 4.4 collects the main aspects that define the family of heuristic algorithms proposed for the NR-VTD problem variants.

Table 4.4. Methodology of the three-step heuristic approach according to the planning problem

Planning Problem	**Step 1**	**Step 2**	**Step 3**
NR-VTD-VRs	Weak dommination	Splittable variant of [33]. Obtain **p**.	Required to obtain the flow routings $\mathbf{f}^t$, $t = 1,..., T$
NR-VTD-VRu	Weak dommination (unsplittable)	[33]. Obtain **p**.	Required to obtain the flow routings $\mathbf{f}^t$, $t = 1,..., T$
NR-VTD-FRs	Total dommination	Splittable variant of [33]. Obtain (**p**,**f**).	Not required
NR-VTD-FRu	Total dommination	[33]. Obtain (**p**,**f**).	Not required

4.4.3 Tabu Search approach

In contrast to the previous NR-VTD algorithms, this subsection details the first of three heuristic approaches able to solve as well R-VTD problems, a tabu search heuristic algorithm, denoted as TS in the sequel.

The heuristic iteratively solves smaller MILP formulations with various constraints on transceivers

for independent time intervals in order to jump between neighboring solutions, and thus explore the solution space in a directed manner. In general, tabu search is an iterative meta-heuristic which guides the search through the solution space using a memory structure, called a tabu list, to avoid getting stuck in local optima. It does so by 'memorizing' a certain number of the most recently visited solutions, or some of their attributes, prohibiting the search to reconsider them for as long as they remain in the list. This prevents cycling between neighboring solutions around a local optimum.

A general tabu search algorithm starts with an initial current solution. Next, it explores all its neighboring solutions, and chooses the best neighboring solution (not forbidden by the tabu list) to become the new current solution in the next iteration. Potential solutions are evaluated with a fitness function. After each iteration, the tabu list and the best found solution overall, called the *incumbent* solution, are updated. The algorithm terminates according to a predefined termination criterion, such as the number of iterations run, the achieved solution quality, or the number of iterations without improvement.

In order to describe a specific tabu search algorithm, it is necessary to define (i) the structure of a potential solution, (ii) the initial solution, (iii) the neighborhood, (iv) the fitness function, (v) the tabu list structure, and (vi) the termination criterion.

Structure of potential solutions and the initial solution

A potential solution in TS consists of T virtual topologies, one for each time slot t=1,…,T. For the non-reconfigurable case, post-processing is done to obtain a single virtual topology from the T scheduled ones.

The initial solution is obtained by solving a MILP formulation for static Virtual Topology Design for each time slot separately, referred to as VTD-LT (Virtual Topology Design with Limited Transceivers). This formulation receives as input a single traffic matrix, a physical topology, and a set of upper bounds on the number of transceivers at each node. It calculates a virtual topology and its corresponding flow routing with the objective to minimize electronic switching, i.e., to minimize the number of lightpaths traversed by a unit of traffic in the network. For the initial solution, the upper bounds on the transceivers per node is set to infinity for each time slot. For each of the T executions, the decision variables in the VTD-LT formulation are:

- $\mathbf{f} = (f_{ij}^{sd}) \in [0,1]$. Fraction of the total traffic demand h_{sd} from node s to node d that is routed on the existing lightpaths from node i to node j.
- $\mathbf{p} = (p_{ij}) = \{0,1,2,...\}$. Number of lightpaths from node i to node j.

The objective function and the set of constraints are described in (4.20)-(4.24), for the problem associated with a time slot t=1,..., T:

$$\min \sum_{i,j,s,d} f_{ij}^{sd} \tag{4.20}$$

Subject to

$$\sum_{s,d} \left\{ h_{sd} \cdot f_{ij}^{sd} \right\} \leq C \cdot p_{ij}, \quad i,j = \{1,...,N\} \tag{4.21}$$

$$\sum_{j} f_{nj}^{sd} - \sum_{i} f_{in}^{sd} = \begin{cases} 1, if \ \ n = s \\ -1, if \ \ n = d, \ \ n,s,d = \{1,...,N\} \\ 0 \ otherwise \end{cases} \tag{4.22}$$

$$\sum_{j} p_{nj} \leq UB_{TX}(n), \ \ n = \{1,...,N\} \tag{4.23}$$

$$\sum_{i} p_{in} \leq UB_{RX}(n) \ \ n = \{1,...,N\} \tag{4.24}$$

Constraints (4.21) represent the capacity constraints, and equations (4.22) are the flow conservation constraints. Constraints (4.23) and (4.24) ensure that the number of lightpaths originating (terminating) at a given node, must be below the decided upper bounds on number of transmitters (receivers) at that node.

Neighborhood

First, we introduce some notation and basic concepts for better understanding of the neighborhood of a current solution:

- *Activity matrices*: For a given solution composed of T virtual topologies, we define a (NxT) matrix named *Active Transmitters* (**AT**) *matrix*. $AT(n,t)$={0, 1, 2,…} represents the number of transmitters that are active at node n in time slot t in that solution. In other words, a row n shows how the number of active transmitters at node n varies over time. A column t shows the number of active transmitters at all nodes in time slot t. The necessary number of transmitters per node is shown as a vector $T(n)$ = max(t){$AT(n,t)$}, i.e. the maximum element in each row n. The total number of transmitters needed in the network corresponding to that solution is T_{tot}=sum(n){$T(n)$}. Consider the following example. Suppose there are 3 nodes and 4 time slots,

i.e. N=3, T=4, with an *Active Transmitters matrix* of a potential solution as shown below.

$$\mathbf{AT} = \begin{pmatrix} 3 & 1 & 1 & 2 \\ 2 & 2 & 1 & 1 \\ 1 & 2 & 0 & 4 \end{pmatrix}$$

Fig. 4.1. An example of an **AT** matrix.

In this example, value $AT(1,4)=2$ indicates that in the fourth time slot there are 2 transmitters active at node 1. The number of necessary transmitters per node is: $T(n)$= [3 2 4], while the total number of transmitters required is T_{tot} = 11.

We do the same for receivers to get activity matrix Active Receivers (**AR**), the necessary number of receivers per node **R**(n), and the total required receivers R_{tot}.

- *Utilization matrices*: For a given solution, we define a (NxT) matrix, which we denote as Utilization of Transmitters (**UT**) matrix. It is obtained from matrix **AT** by subtracting from each element in **AT**, the value of the maximal element in its row except itself. In other words,

$$UT(n_i, t_i) = AT(n_i, t_i) - \max_{t|t \neq t_i}(AT(n_i, t)) \tag{4.25}$$

According to the above definition, the utilization matrix for the previous example is:

$$\mathbf{UT} = \begin{pmatrix} 1 & -2 & -2 & -1 \\ 0 & 0 & -1 & -1 \\ -3 & -2 & -4 & 2 \end{pmatrix}$$

Fig. 4.2. An example of an **UT** matrix

The positive elements in this matrix indicate the number of transmitters that are only used in a single time slot, i.e. are not very efficiently utilized. For example, $UT(3,4)=2$ indicates that in time slot 4 at node 3, there are 2 transmitters that are only used in this time slot. Intuitively, trying to rearrange these poorly utilized transmitters may lead to better results.

We do the same for receivers from **AR** to get a matrix Utilization of Receivers (**UR**).

We consider neighboring solutions of a current solution to be all those where the number of transmitters or receivers per node, and the corresponding virtual topology and flow routing, are changed in only one time slot. Since there is a large number of such solutions, we propose a neighborhood reduction technique described below which reduces this set to include those solutions which we think are more likely to give good results.

Firstly, if the number of transmitters or receivers at some node in the current solution is already at its lower bound, there is no need to consider neighboring solutions which decrease the transmitters or receivers, respectively, at that node since such solutions are surely infeasible. Furthermore, recall that our main objective is to find the virtual topologies and flow routings in a way which most efficiently utilizes network resources, i.e., uses the minimum number of transceivers which can carry the given periodic traffic. Thus, reducing the number of transceivers at nodes where they are highly utilized does not seem to make much sense since a reduction of these transceivers will need compensation in several time slots. Conversely, reducing a transmitter (receiver) at nodes where there are transmitters (receivers) that are used only in a single time slot can more easily be compensated for, making it more likely to find feasible solutions of higher quality. In other words, we think eliminating poorly utilized transceivers where feasible should yield better results.

Consequently, we perform neighborhood reduction as follows. For each node, we choose one time slot with poorly utilized transmitters and one time slot with poorly utilized receivers, except for nodes forbidden by the tabu list (as described in *Tabu list structure and termination criterion* subsection).[1] We denote these 'candidates' as triples in the form: (*n*, *t*, 'tr'/ 're'), each corresponding to one neighboring solution. The number of candidates (or neighbors) is thus $2 \cdot n$ - (the size of the tabu list). Note that candidates cannot include nodes at time slots for which the lower bound on transmitters/receivers is reached.

To choose the set of candidates (*n*, *t*, 'tr') *with respect to transmitters*, we consider only *strictly positive***,** i.e. poorly utilized**,** elements in **UT**, for which $AT(n,t) > LB_{TX}(n)$. For each node *n*, we choose one such element at random which is not forbidden by the tabu list. If there are no positive elements in **UT**, we choose at random a time slot corresponding to one of the elements with a value of zero (there is always at least one such element). For each obtained candidate (*n*, *t*, 'tr'), we run the VTD-LT formulation for time slot *t* (i.e. with the traffic matrix at time *t*) but bound the maximum number of transmitters at node *n* to **AT**(*n*,,*t*)-1. Receivers at node *n*, along with transmitters and receivers at all other

[1] The same time slot can be chosen for both poorly utilized transmitters and receivers.

nodes, are bounded to their maximal value along time in the current solution. The new virtual topology obtained by solving the VTD-LT formulation replaces the virtual topology at corresponding time slot *t* in the current solution, giving the new neighboring solution. The same is done to obtain neighbors from candidates (*n*, *t*, 're') *with respect to receivers*, chosen analogously from non-negative elements of **UR** for which $AR(n,t) > LB_{RX}(n)$.

In our example, assuming no violation of the lower bound and tabu list constraints, we would have four neighbors with respect to transmitters obtained from candidates (1, 1, 'tr'), (2, 1 or 2, 'tr') and (4, 3, 'tr'), which correspond to elements *UT*(1,1), *UT*(2,1) or *UT*(2,2), and *UT*(4,3), respectively. If all neighboring solutions in the reduced neighborhood are infeasible in an iteration, the neighborhood is increased to $2 \cdot t \cdot n$ where candidates correspond to *all* nodes and *all* time slots for both transmitters and receivers, and with no constraints imposed by the tabu list.

Fitness function

To choose the best neighboring solution to become the new current solution in the next iteration, we define three different fitness functions for three variations of the algorithm.

- *Non Reconfigurable VTD (NR-VTD) problem:* This fitness function has the objective to minimize the number of transceivers per node in the NR-VTD problem where transmitters and receivers at the same node cannot be used for different lightpaths in different time intervals. Consequently, the number of transceivers per node corresponds to the maximal number of different lightpaths originating and terminating at that node over all time intervals. It follows that the fitness function is:

$$2 \cdot c_1 \sum_{j=1}^{N} \sum_{j=1, j \neq i}^{N} \max_{t} p_{ij}^{t} \tag{4.26}$$

  where p_{ij}^{t} is the number of lightpaths established between nodes *i* and *j* at the time slot *t*, and c_1 is the cost of one transceiver (or receiver).

- *Reconfigurable VTD problem*: This fitness function aims to minimize both the number transceivers and the lightpath reconfigurations, assuming reconfigurable equipment, i.e., the same transceivers can be used for different lightpaths as long as they are in different time slots. The lightpath reconfigurations are computed as the increases or decreases in the number of lightpaths between consecutive time slots. Now, the fitness function is given by:

$$c_1 \sum_n \left\{ \max_t \sum_{j, j \neq n} p_{nj}^t \right\} + c_1 \sum_n \left\{ \max_t \sum_{i, i \neq n} p_{in}^t \right\} + c_2 \sum_{i,j,t} \left| p_{ij}^t - p_{ij}^{t-1} \right| \quad (4.27)$$

Tabu list structure and termination criterion

Each entry in the tabu list is a pair (*n*, 'tr'/'re') representing the node *n* at which either transmitters (tr) or receivers (re) were reduced in order to get the new current solution from the previous one. For as long as this pair remains in the tabu list, the transmitters/receivers at node *n* cannot be further reduced. The tabu list is realized as a FIFO (First In First Out) queue of finite size, updated after each iteration. The termination criterion for the algorithm is defined by the maximum number of iterations which can be run without improvement of the incumbent solution.

Postprocessing

For the non-reconfigurable case, a post-processing step is necessary since the final solution must be in the form of a single virtual topology, while the tabu search algorithm gives a set of *T* virtual topologies. To achieve a single virtual topology *T*, which can handle all the traffic over time from the obtained solution, we establish p_{ij} lightpaths between nodes *i* and *j*, where $p_{ij} = \max(t)\{ p_{ij}^t \}$, $t = 1 \ldots T$, from the solution given by the tabu search. To assign individual traffic flow routings for each time slot over the obtained static virtual topology, we use a multi-commodity flow LP (Linear Programming) formulation yielding optimal solutions.

4.4.4 Lagrangean Relaxation via Subgradient Optimization approach

This subsection describes a application to multihour problems in transparent optical networks of the well-known *Lagrangean Relaxation via Subgradient Optimization* method [155]. The mentioned application was published in [38].

The Lagrangean Relaxation based Dual Subgradient Optimization Algorithm has been applied previously in [31],[135] to solve multihour capacity design problems in dynamically reconfigurable ATM-based broadband networks. In these works, time-fixed modular capacities were assigned to an underlying and given physical topology; whereas, time-varying virtual ATM paths were routed on these modular capacities. This problem is equivalent to the NR-VTD-VRu problem as formulated in Subsection 4.3.2, considering the time-fixed modular capacities as non-reconfigurable lightpaths, and the virtual ATM paths as non-defined higher layer traffic flows. On the contrary, in work [38], the algorithm is applied to the optical R-VTD problem as formulated in Subsection 4.3.3. In this MH-VTD problem

variant, we attempt to minimize the number of optical transceivers and lightpath reconfigurations in a reconfigurable (time-varying) virtual topology.

Since the general procedure used in [38] is the same as described in [31],[135],[155], we refer to these references for a more detailed description. We will focus solely on the distinctive features of the application presented herein: (i) the Lagrangean Relaxation on the formulation (4.9)-(4.15); and, (ii) the Lagrangean Minimization Subproblems that arises on minimizing the relaxed problem.

The *Lagrangean Relaxed Problem* appears when the constraints (4.10), (4.12) and (4.13) are "relaxed" (or "dualized") by adding them (weighted by Lagrangean multipliers) to the objective function (4.9) and eliminating them of the total set of constraints of (4.10)-(4.15). We denote in the remaining subsection as *primal problem* to the formulation (4.9)-(4.15). Let $\boldsymbol{\lambda} = (\lambda_{ij}^t)$, $\boldsymbol{\mu} = (\mu_i^t)$ and $\boldsymbol{\nu} = (\nu_j^t)$ be the Lagrangean (or dual) multipliers associated with the constraints (4.10), (4.12) and (4.13), respectively. Then, the Lagrangean function $L(\boldsymbol{\lambda}, \boldsymbol{\mu}, \boldsymbol{\nu}, \mathbf{f}, \mathbf{p}, \mathbf{tx}, \mathbf{rx}, \mathbf{r}^+)$ resulting of the relaxation is:

$$
\begin{aligned}
&L(\boldsymbol{\lambda},\boldsymbol{\mu},\boldsymbol{\nu},\mathbf{f},\mathbf{p},\mathbf{tx},\mathbf{rx},\mathbf{r}+) = c_1 \sum_n \{tx_n + rx_n\} + c_2 \sum_{i,j,t} r^{+}{}_{ij}^{t} + \\
&+ \sum_{i,j,t} \lambda_{ij}^t \cdot \left\{ \sum_{s,d} \left\{ m_{sd}^t \cdot f_{ij}^{sdt} \right\} - C \cdot p_{ij}^t \right\} + \sum_{i,t} \mu_i^t \cdot \left\{ \sum_j p_{ij}^t - tx_i \right\} + \sum_{j,t} \nu_j^t \cdot \left\{ \sum_i p_{ij}^t - rx_j \right\} = \\
&= \sum_n \left\{ c_1 - \sum_t \mu_n^t \right\} \cdot tx_n + \sum_n \left\{ c_1 - \sum_t \nu_j^t \right\} \cdot rx_n + \sum_{t,i,j} \lambda_{ij}^t \cdot \left\{ \sum_{s,d} \left\{ h_{sd}^t \cdot f_{ij}^{sdt} \right\} \right\} + \\
&+ c_2 \sum_{i,j,t} r^{+}{}_{ij}^{t} + \sum_{t,i,j} \left\{ \mu_i^t + \nu_j^t - C \cdot \lambda_{ij}^t \right\} \cdot p_{ij}^t = \\
&= L_1(\boldsymbol{\mu}, \mathbf{tx}) + L_2(\boldsymbol{\nu}, \mathbf{rx}) + L_3(\boldsymbol{\lambda}, \mathbf{f}) + L_4(\boldsymbol{\lambda}, \boldsymbol{\mu}, \boldsymbol{\nu}, \mathbf{r}^+, \mathbf{p})
\end{aligned}
\tag{4.28}
$$

And the *Lagrangean Relaxed Problem* is:

$$
W(\boldsymbol{\lambda},\boldsymbol{\mu},\boldsymbol{\nu}) = \min_{\mathbf{f},\mathbf{p},\mathbf{tx},\mathbf{rx},\mathbf{r}^+} \left\{ L(\boldsymbol{\lambda},\boldsymbol{\mu},\boldsymbol{\nu},\mathbf{f},\mathbf{p},\mathbf{tx},\mathbf{rx},\mathbf{r}^+) \parallel \text{constraints (4.11), (4.14) and (4.15)} \right\} \tag{4.29}
$$

Where $W(\boldsymbol{\lambda}, \boldsymbol{\mu}, \boldsymbol{\nu})$ is the dual function, and the *dual problem* to solve via subgradient optimization is:

$$\max_{\boldsymbol{\lambda},\boldsymbol{\mu},\boldsymbol{\nu}} \left\{ W(\boldsymbol{\lambda},\boldsymbol{\mu},\boldsymbol{\nu}) \mid \boldsymbol{\lambda} \geq \mathbf{0}, \boldsymbol{\mu} \geq \mathbf{0}, \boldsymbol{\nu} \geq \mathbf{0} \right\} \tag{4.30}$$

The minimization of the Lagrangean function $L(\boldsymbol{\lambda}, \boldsymbol{\mu}, \boldsymbol{\nu}, \mathbf{f}, \mathbf{p}, \mathbf{tx}, \mathbf{rx}, \mathbf{r}^+)$ (4.29) can be decoupled into four sets of separate minimization subproblems since the relaxation of the constraints (4.10), (4.12) and (4.13) have broken the dependencies among some primal decision variables. The first and second sets of subproblems are associated to the variables **tx** and **rx**, respectively. The third set of subproblems corresponds to the variables **f** solely restrained by the constraints (4.11). And, finally, in the fourth set of subproblems the variables **p**, $\mathbf{r}^+$ and $\mathbf{r}^-$ remain linked trough the constraints (4.14) and (4.15).

$$\begin{aligned} W(\boldsymbol{\lambda},\boldsymbol{\mu},\boldsymbol{\nu}) &= \min_{\mathbf{f},\mathbf{p},\mathbf{tx},\mathbf{rx},\mathbf{r}^+} \left\{ L(\boldsymbol{\lambda},\boldsymbol{\mu},\boldsymbol{\nu},\mathbf{f},\mathbf{p},\mathbf{tx},\mathbf{rx},\mathbf{r}^+) \mid \text{constraints (4.11), (4.14) and (4.15)} \right\} = \\ &= \min_{\mathbf{tx}} \left\{ L_1(\boldsymbol{\mu},\mathbf{tx}) \right\} + \min_{\mathbf{rx}} \left\{ L_2(\boldsymbol{\nu},\mathbf{rx}) \right\} + \min \left\{ L_3(\boldsymbol{\lambda},\mathbf{f}) \mid \text{constraints (4.11)} \right\} + \\ &+ \min_{\mathbf{p},\mathbf{r}^+} \left\{ L_4(\boldsymbol{\lambda},\boldsymbol{\mu},\boldsymbol{\nu},\mathbf{p},\mathbf{r}^+ \mid \text{constraints (4.14), (4.15)} \right\} = W_1(\boldsymbol{\mu}) + W_2(\boldsymbol{\nu}) + W_3(\boldsymbol{\lambda}) + W_4(\boldsymbol{\lambda},\boldsymbol{\mu},\boldsymbol{\nu}) \end{aligned} \tag{4.31}$$

If we analyse these subproblems, we can note that solutions **tx*** , **rx*** and **f*** to the first, second and third subproblems, respectively, can be easily computed. For each group (*s*,*d*,*t*), the solutions $f^*_{ij}{}^{sdt}$ is the shortest path between node *s* and *d* in network with link weights λ_{ij}^t. The solutions tx^*_n can be trivially obtained by setting:

$$tx_n^* = \begin{cases} UB_{TX}, & \text{if } c_1 < \sum_t \mu_n^t \\ LB_{TX}, & \text{if } c_1 \geq \sum_t \mu_n^t, \end{cases} \quad n = \{1 \ldots N\} \tag{4.32}$$

where UB_{TX} and LB_{RX} are upper and lower bounds, respectively, on the number of transmitters. The upper bounds may are artificial enough large values; whilst, we can take as lower bunds those one defined in Subsection 4.4.1. The solutions rx^*_n may be computed analogously replacing **tx** and **μ** for **rx** and **ν**, and using proper lower and upper bonds.

Finally, the solution **p*** , **r+*** and **r-*** are obtained by solving the fourth set of ILP subproblems in (4.31). Although solving these subproblems implies to solve ILP formulations, we must note that they suppose an important reduction on complexity with respect to the original unrelaxed primal one.

Once we have found a solution (**f***, **p***, **tx***, **rx***, $\mathbf{r}^{*+}$, $\mathbf{r}^{*-}$) that minimizes the *Lagrangean function* $L(\boldsymbol{\lambda}, \boldsymbol{\mu}, \mathbf{v}, \mathbf{f}, \mathbf{p}, \mathbf{tx}, \mathbf{rx}, \mathbf{r}^{+})$ (4.29), the *dual function* is totally characterized and the *dual problem* (4.30) can be solved via a *subgradient optimization* step. The *subgradient optimization* step generates a new triple (**λ**, **μ**, **v),** that is replaced in the Lagrangean function (4.28), given rise a new instance of the *Lagrangean Relaxed Problem* (4.29). Then, after solving the new *Lagrangean Relaxed Problem*, a new *subgradient optimization* step follows. A more detailed description of a *Lagrangean Relaxation via Subgradient Optimization* method suitable for network dimensioning problems, like this, can be consulted in [155].

Finally, and after concluding this subsection, we must note that the minimal solution (**f***, **p***, **tx***, **rx***, $\mathbf{r}^{*+}$, $\mathbf{r}^{*-}$) that optimizes the *Lagrangean Relaxed Problem* (4.29) might be not feasible from the point of view of the *primal problem* (i.e. *primal feasible*), since we have relaxed some constraints in (4.9)-(4.15). Therefore, we need to find a *primal feasible* solution (**f***, $\mathbf{p}^{pf}$, $\mathbf{tx}^{pf}$, $\mathbf{rx}^{pf}$, $\mathbf{r}^{*+}$, $\mathbf{r}^{+pf}$,$\mathbf{r}^{-pf}$). This solution can be generated from the minimal solution **f*** following the next steps. Unlike the solutions **p***, **tx*** , **rx***, and $\mathbf{r}^{+}$*; the solutions **f*** is also *primal feasible*. For this reason, we may use **f*** in (4.10) to compute a primal-feasible solution $\mathbf{p}^{pf}$. Then, this solution $\mathbf{p}^{pf}$ will be replaced in (4.12) and (4.13) to derivate primal-feasible $\mathbf{tx}^{pf}$ and $\mathbf{rx}^{pf}$; and, in (4.14) and (4.15) to derivate primal-feasible $\mathbf{r}^{+pf}$ and $\mathbf{r}^{-pf}$

4.4.5 Greedy Approach with Reconfiguration Flattening

In this Section, we develop a heuristic algorithm to address both NR-VTD (namely, the NR-VTD-VRs variant) and R-VTD problems. We refer to this algorithm as GARF (Greedy Approach with Reconfiguration Flattening). GARF is divided into three steps. In *Step 1*, a fast greedy approach is run which obtains a good feasible solution with respect to transceivers, without caring for the frequency of reconfiguration. *Step 2* applies a tabu search approach targeted to further reduce the transceiver cost and, finally, *Step 3* is aimed at reducing reconfiguration frequency according to a tunable factor which controls its tradeoff with transceiver cost. We must note that the heuristic tabu search employed in *Step 2* is different from the one detailed in Subsection 4.4.3. A flow chart illustrating the individual steps of GARF is given in Fig. 4.3.

Step 1 - Greedy Approach

In this step, a greedy algorithm creates an initial solution with the objective to minimize the number of transceivers. First, as a preprocessing step, some lower bounds on the number of transceivers, such as the ones proposed in Subsection 4.4.1, are computed.

The basic idea is as follows. Since, at least, the transceivers indicated in the lower bounds will surely be needed at some point in time, these are the ones we want to use up first when planning each time slot.

We call the set of these transceivers as *mandatory transceivers.*

For each time slot, in increasing order of its total traffic, two phases of the algorithm are performed. In phase 1, lightpaths are iteratively established using only transmitters/receivers from the *mandatory transceivers* set in decreasing order of their associated traffic demands, until the set is exhausted. Each time a new lightpath is established, as much of the associated direct traffic as possible is routed over the new lightpath. If this traffic demand exceeds the lightpath capacity, the excess traffic remains unrouted. Then, all remaining unrouted traffic demands between all node pairs are sorted in decreasing order and sequentially fed to a linear program (LP) formulation which models the Minimal Cost Flow Problem (Min Cost Flow Problem) [124]. This formulation is used to route each traffic demand over the available spare capacity. Where the LP is successful, the spare capacity is updated before the next demand is processed.

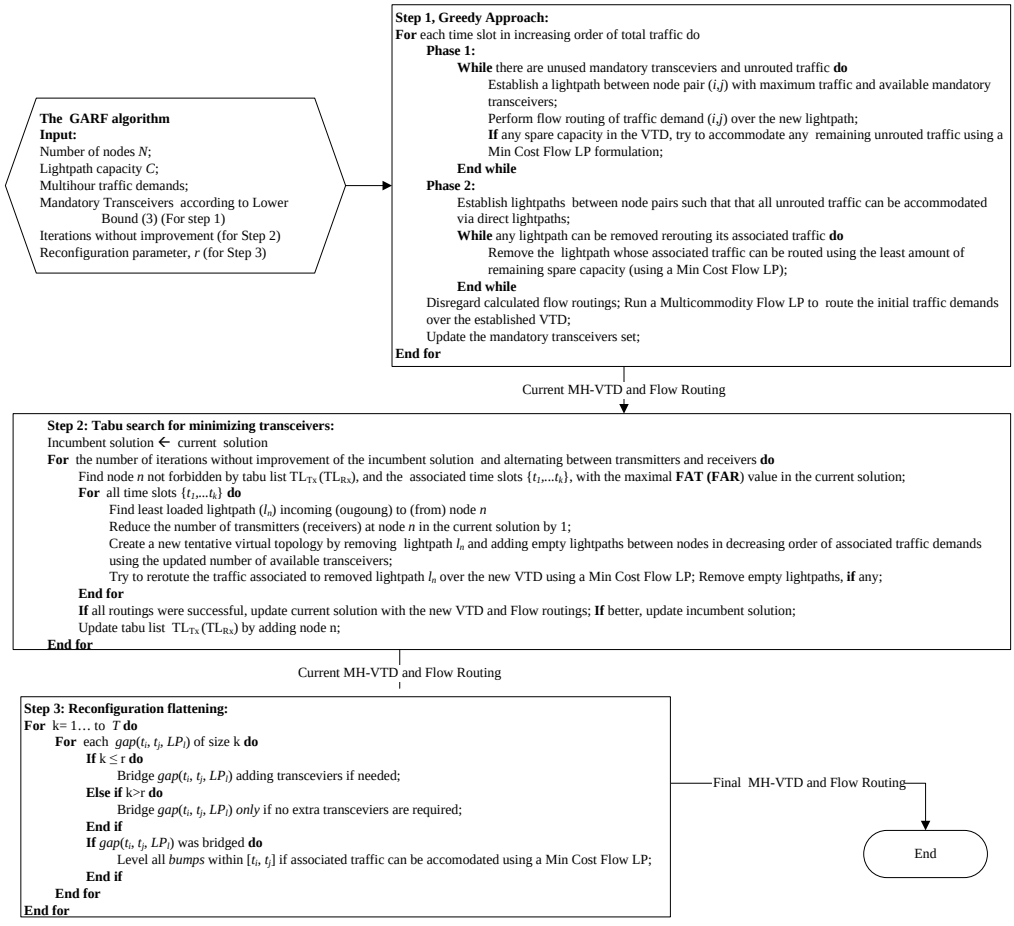

Fig. 4.3. Flow chart of the GARF algorithm

After the mandatory transceivers are exhausted in phase 1, the algorithm moves to the second phase which uses a modified version of the greedy algorithm proposed in [33]. Phase 2 begins by establishing as many lightpaths as necessary between node pairs such that all the remaining unrouted traffic can be routed via direct lightpaths. The algorithm then tries to iteratively remove the lightpath whose traffic can be accommodated by using the least amount of the remaining spare capacity. The algorithm proceeds for as long as such a lightpath removal is possible between any pair of nodes. After Phase 2 terminates, the currently calculated flow routings are disregarded and a Multicommodity flow LP formulation is run to re-route the original traffic demands in the considered time slot over the newly established virtual topology. The *mandatory transceivers* set is then updated to include all the transceivers associated with the new virtual topology to be used in subsequent time slots. This forces the algorithm to first use the transceivers that we have already decided to 'buy', before adding new ones. The algorithm terminates after all time slots are processed.

Step 2 – Tabu Search for Minimizing Transceivers

In this step, we employ a tabu search to improve the solution generated in *Step 1*. In general, tabu search is an iterative meta-heuristic which guides the search through the solution space using a memory structure, called a tabu list, to avoid cycling between neighboring solutions around local optima. It does so by 'memorizing' a certain number of the most recently visited solutions, or some of their attributes, prohibiting the search to reconsider them for as long as they remain in the list.

First we introduce some concepts and notations required for a better understanding of the algorithm:

- *Active Transmitters matrix* (**AT**): an $N \times T$ matrix defined for a given solution to the *MH-VTD* problem, where a element $\mathbf{AT}(n,t) = \{0, 1, 2, \ldots\}$ represents the number of transmitters that are active at node n in time slot t.
- *Fluctuation of Active Transmitters matrix* (**FAT**): an $N \times T$ matrix obtained from matrix **AT** by subtracting from each element in **AT**, the value of the *minimal* element in its row except itself. In other words:

$$\mathbf{FAT}(n_i, t_i) = \mathbf{AT}(n_i, t_i) - \min_{t | t \neq t_i}(\mathbf{AT}(n_i, t)) \tag{4.33}$$

An example **AT,** and corresponding **FAT** matrix, are shown in Fig. 4.4 for a potential solution in a 3 node network with 4 time slots, i.e. N=3, T=4.

$$\mathbf{AT} = \begin{pmatrix} 3 & 1 & 1 & 2 \\ 2 & 2 & 1 & 1 \\ 1 & 4 & 2 & 4 \end{pmatrix} \quad \mathbf{FAT} = \begin{pmatrix} 2 & 0 & 0 & 1 \\ 1 & 1 & 0 & 0 \\ 0 & 3 & 1 & 3 \end{pmatrix}$$

Fig. 4.4. An example of an **AT** and corresponding **FAT** matrix.

AT(1,4)=2, for example, indicates that in the fourth time slot there are 2 transmitters active at node 1. The positive elements in the **FAT** matrix indicate the number of transmitters that are used in each time slot above the minimal value used in the least active time slot. The amplitude or maximal fluctuation of activity per node is the maximal element in each row of **FAT**.

Analogously for receivers, we define the *Active Receivers* (**AR**) matrix and the *Fluctuation of Active Receivers* (**FAR**) matrix.

Step 2 of GARF runs as follows. After obtaining a feasible solution in *Step 1*, tabu search iterations are run alternating between transmitters and receivers until the maximal number of iterations without improvement of the best solution is met. Upon termination, the incumbent (i.e., best visited) solution is deemed the final result. During these iterations, two tabu lists are maintained, realized as FIFO (First In First Out) queues of finite size corresponding to either transmitters (tabu list TL_{TX}) or receivers (tabu list TL_{RX}).

In each iteration, the **FAT (FAR)** matrix is computed to show the fluctuation of active transmitters (receivers) for that solution. A node *n* with the maximal amplitude of fluctuation, i.e. a row containing the maximal element in **FAT (FAR),** which is not forbidden by tabu list TL_{TX} (TL_{RX}) is chosen. In our example, this would correspond to node 3, where for time slots 2 and 4 the corresponding value *FAT*(3,2) = *FAT*(3,4) = 3 is the maximal value in the **FAT** matrix. For the chosen node *n*, we then attempt to remove one transmitter (receiver) from the current solution. This implies checking whether a lightpath initiated (ending) at node *n* could be removed in each of the time slots t_n where $FAT(n, t_n)$ is maximal (in our example, time slots 2 and 4). The check associated with each time slot t_n consists of three steps. First we choose the lightpath l_n originating (terminating) at node *n* which is least loaded during that time slot. Second, we construct the so-called *tentative virtual topology* and, finally, we attempt to reallocate the traffic carried by lightpath l_n onto the *tentative VT* for time slot t_n. The *tentative VT* is constructed from the original one by (i) removing the aforementioned least loaded lightpath l_n and (ii) adding as many new empty lightpaths as the available transceivers in the network permit. Available transceivers assume all those which are allocated to the nodes over time but not used by the current VT in the considered time

slot, with the number of transmitters (receivers) at node *n* reduced by 1. The new empty lightpaths are established between node pairs with available transceivers, in decreasing order of their original traffic demands. This traffic is not routed over the new lightpaths, i.e. the lightpaths remain empty, but is only used as a sorting criterion. After adding a lightpath to the *tentative VT*, the value of the corresponding traffic is decreased by the value of the lightpath capacity and the traffic demands are re-sorted. After constructing a *tentative VT*, the check procedure attempts to reallocate the traffic associated to the removed lightpath on the spare capacities of the *tentative VT*, solving a Min Cost Flow problem. If this rerouting of the traffic in the least loaded lightpath is successful for all the time slots t_n, all empty left-over lightpaths are removed and the new set of virtual topologies and corresponding flow routings become the new current solution in the next iteration. Otherwise, the old current solution remains unchanged and the algorithm proceeds to the next iteration. If the solution in the current iterarion is better than the incumbent solution, it is updated accordingly. In any case, tabu list TL_{TX} (TL_{RX}) is updated to include the considered node *n*.

Step 3 – Reconfiguration flattening

Step 3 of GARF is aimed at minimizing the frequency of reconfiguration of the lightpaths obtained in *Step 2*. A tunable parameter controls the penalization of reconfiguration, allowing the solution to range from the static case (NR-VTD-VRs) to various levels of reconfiguration for the R-VTD problem variant.

First, we introduce some notation and basic concepts for better understanding of the algorithm:

- *Unique lightpath identifier* (LP_i). A feasible solution to a MH-VTD problem consists of a set of lightpaths which are active at a certain interval(s) in time (for the NR-VTD all established lightpaths are always active). We assign to each lightpath a unique identifier in the form of LP_i, i={1, 2, 3, …}. Note: we differentiate between multiple lightpaths established between the same pairs of nodes, but the same unique lightpath can be established and torn down over multiple time intervals.

- *Lightpath activity function* (*LAF*). Each unique lightpath corresponds to one lightpath activity function (LAF) which indicates its activity over time, i.e. is a graphic representation of its schedule. Each transition in a LAF indicates one reconfiguration: A drop in the LAF from 1 to 0 indicates that the associated lightpath was torn down, while a jump from 0 to 1 indicates that the lightpath was established.

- *gap*(t_i, t_j, LP_l). We call a gap any part of a LAF which starts with a 1 to 0 transition and ends with a 0 to 1 transition, while remaining at 0 in-between. We denote a specific gap as *gap*(t_i, t_j, LP_l), where t_i and t_j denote the first and last time slots of the gap and LP_l denotes the

associated lightpath LAF. We define the size of a gap be the number of time slots it covers.

- *bump*(t_i, t_j, LP_l). A bump refers any part of a LAF starting with a 0 to 1 transition and ending with a 1 to 0 transition, while remaining at 1 in-between. Its notation and size is analogous to that of *gaps.*

Fig. 4.5 shows an example of a simple R-VTD solution for a 3 node network with 7 time slots. Fig. 4.5 (a) shows the set of unique lightpath identifiers while Fig. 4.5 (b) indicates at which times the individual lightpaths are active (i.e. their schedule). Note that the time slots are periodic, i.e., after time slot 7, time slot 0 is active again. The LAFs corresponding to each unique lightpath are shown in Fig. 4.5 (c), along with some examples of bumps and gaps and their corresponding sizes. Also note that each transition in a LAF indicates a reconfiguration, incurring service disruption and signaling overhead. Consequently, the flatter the LAFs, the better. Given an algorithm for the R-VTD problem which does not consider the number of reconfigurations, it is possible that a lightpath may be torn down during a few time slots even though the corresponding transceivers are still available, simply because it is not needed to route traffic in those time slots. One of the basic ideas in *Step 3* of GARF is to eliminate such unnecessary reconfigurations.

Note that no matter its size, each gap and bump is associated with exactly two reconfigurations: one to tear down the lightpath and one to set it up (or vice versa). Intuitively, it seems reasonable to try to eliminate smaller gaps or bumps since they require the same number of reconfigurations as larger ones, but require planning a change with respect to flow routing and transceiver utilization in fewer time slots. 'Bridging' a gap implies letting an established lightpath remain active. 'Leveling' a bump implies trying to reroute traffic so that the associated lightpath can remain inactive over that time period.

The main objective of Step 3 is to maximally flatten (bridge/level) the LAF functions in order to reduce the total number of reconfigurations. Herein, we introduce a tunable parameter $r=\{0, 1, \ldots, T\text{-}1\}$, which allows us to control the increase in the overall number of required transceivers as a tradeoff with minimizing reconfiguration frequency. GARF Step 3 runs as follows. For each time slot, all *gaps* of size r or less in the current solution are bridged, even if it is at the expense of additional transceivers. On the other hand, all *gaps* of size greater than r are bridged only if no additional transceivers are required. In the extreme case of $r=0$, minimizing transceiver cost is the primary objective, while only those *gaps* which correspond to inactivity of lightpaths due to lack of traffic and not lack of transceivers are bridged. For $r=T$, all LAFs will be completely flattened no matter the associated transceiver cost, eliminating reconfiguration all together and yielding a static virtual topology, i.e. a solution to the NR-VTD problem. By tuning parameter r, we can tune this trade-off to a desired value.

During execution of Step 3, each time we bridge a gap of size *s* (with or without adding transceivers), we try to 'level' all bumps of size *s* or less within the time slots that have just been bridged. Leveling a bump is feasible only if the associated traffic can be routed over the remaining established lightpaths and the newly bridged one. This not only reduces additional reconfigurations, but in some cases reduces the total number of transceivers if an entire LAF is ultimately flattened to zero. After considering all gaps and bumps of size 1 to *T* for all time slots, the algorithm terminates.

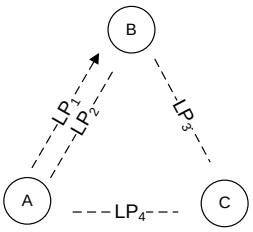

(a)

LP_l	Source	Dest.	Activity	No. of Reconfigs
LP_1	A	B	1:00-3:00; 5:00-6:00	4
LP_2	A	B	2:00-4:00; 5:00-100	4
LP_3	B	C	3:00 – 4:00	2
LP_4	A	C	0:00-0:00	0

(b)

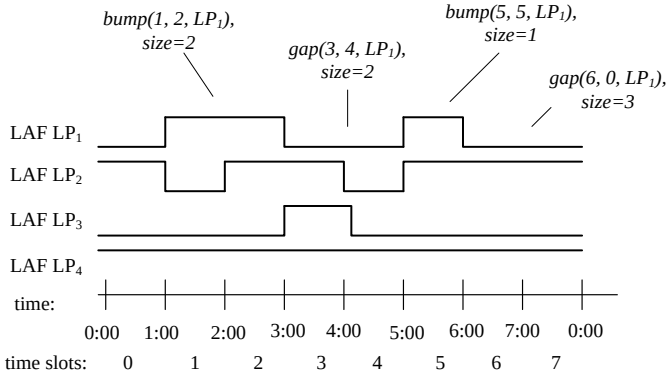

(c)

Fig. 4.5. An example a solution to the R-VTD problem for a 3 node network: (a) the set of unique lightpath identifiers, (b) their schedule and (c) the corresponding lightpath activity functions.

4.5 Results

This Section compiles the major results obtained in multihour planning in the framework of the present Thesis ([30],[36]-[40]). The algorithms presented along the previous Section were used to perform extensive tests with a double purpose: (i) assessing the algorithms performance; and (ii) research the tradeoffs in the different network configurations represented by the MH-VTD variants defined in Section 4.1.

The performance of the algorithms was evaluated by comparing its solutions with those obtained by exact MILP formulations (in small networks), lower bounds to the network cost, and the solutions found by other heuristic algorithms.

In the MH-VTD variants in this thesis, we can distinguish two main tradeoffs whose study is interesting to decide the best cost effective design in terms of total transceiver cost. The following tradeoffs arise:

- between reconfigurable and non-reconfigurable *virtual topology* [36],[37],[38],[40], assuming time-variable flow routing on top of the virtual topologies;
- between fixed and variable flow routing [30],[39], assuming non-reconfigurable virtual topology.

The above mentioned tradeoffs allow us to split the Section into two subsections, where each of them is researched.

4.5.1 Variable vs Fixed Flow Routing in Non Reconfigurable VTDs

This subsection applies the different variants of the *3-Step-D* algorithm explained in Subsection 4.4.2 to analyze the tradeoffs in non reconfigurable VTDs between networks fixed and variable flow routing over the lightpaths. Moreover, for each one of these cases, the tradeoffs when *splittable* and *unsplittable* flow routing is considered were also studied. The algorithms were implemented in the MatPlanWDM tool [46] which links to the TOMLAB/CPLEX library [53] used to solve the MILP formulations in Subsections 4.3.1 and 4.3.2.

Since we follow the assumptions established in Section 4.1 (sufficient number of wavelengths and no application of physical layer constraints), any VTD has a feasible RWA solution, becoming the optimization problem independent of the physical network topology. Therefore, the multihour demand is the only input data to the planning problem. Under these considerations, in this Section two types of traffic data cases are evaluated: synthetic data and data from real traffic traces.

Results for synthetic traffic

In a first step, both the MILP formulations and the heuristic *3-Step-D* approaches were tested for networks consisting of N = {4, 6, 8} nodes, using traffic sequences generated synthetically. Each traffic sequence was composed of T = 12 traffic matrices, each meant to describe the traffic of a two-hour interval over the course of a day. Let $H=\{h^1, h^2, \ldots, h^T\}$ denote a traffic matrix sequence, where $h_{i,j}{}^t$ is the traffic in Gbps from node i to node j during time interval t with i,j = {1,..., N}, t = {1,..., T}. Equations (4.34)-(4.35) describes the traffic synthesis model:

$$m_{ij}^t = b_{ij} \cdot \text{activity}(t) \cdot rf(R), \quad \forall i, j, t. \tag{4.34}$$

$$h_{ij}^t = m_{ij}^t \cdot nf(\rho), \qquad \forall i, j, t \tag{4.35}$$

$$\text{where } nf(\rho) = \frac{n \cdot (n-1) \cdot \rho \cdot C}{\max_t \left\{ \sum_{i,j} m_{ij}^t \right\}}$$

Initially, the traffic between two nodes at a given time $m_{i,j}{}^t$ was calculated as the product of three factors. First, factor $b_{i,j}$ gives the (i,j) coordinate of a base traffic matrix computed for the sequence as follows. 80% of the values in matrix b (randomly chosen) were set to one, while the remaining 20% were set to two. This is meant to capture the effect of non-uniformities in the generated traffic matrices. Secondly, activity factor *activity(t)* in equation (4.34) intends to capture the effect of traffic intensity variation along the day. Our intensity variation scheme is described by equation (4.36), based on the intensity model presented in [156].

$$\text{activity}(t) = \begin{cases} 0.1 \text{ if } t \in [1,6] \\ 1 - 0.9 \cdot \left(\cos\left(\frac{\text{mod}(t,T) - 6}{18} \cdot \pi \right) \right)^{10} \text{ otherwise} \end{cases} \tag{4.36}$$

$$\text{where } t = 1, \ldots, T$$

Finally, factor *rf(R)* in (4.34) is a random value, uniformly distributed over interval [1-R, 1+R]. A new independent sample of the *rf*(R) factor was used for each value $h_{i,j}{}^t$. The purpose of the *rf* factor is to include a randomness effect in the traffic intensity. The random factors used were R = {0.1, 0.2, 0.5}, which correspond to low, medium and high random variation scenarios.

After the full sequence $M=\{m^1, m^2, \ldots, m^T\}$ was calculated, a traffic normalization stage followed.

All the traffic values in the sequence were multiplied by a normalization factor (*nf*). Value *nf* was calculated such that the average traffic between two nodes in the most loaded time slot equals $\rho \cdot C$, where C is the lightpath capacity, and ρ is a value that represents the referred average traffic measured in number of times of the lightpath capacity. The values tested in our study were $\rho = \{0.1, 1, 10\}$. A value of $\rho = 0.1$ corresponds to the case when the average traffic between two nodes in the most loaded time slot is only 10% of a single lightpath capacity. On the contrary, a value of $\rho = 10$ captures cases in which the average traffic between two nodes in the most loaded time slot fills on average 10 full lightpaths.

For each network size N, randomness factor R and normalized load ρ, we generated five independent sequences of traffic matrices, and solved all four variants of the NR-VTD problem. Table 4.5 shows the average number of transceivers used in the solutions obtained for each of the five sequences, using both the exact MILP formulation described in Subsections 4.3.1 and 4.3.2., and the heuristic *3-Step-D* methods presented in Subsection 4.4.2. For the exact MILP formulations, the solver was configured to find a solution within a 5% of optimality gap due to its high complexity. In some cases, this optimality gap has produced solutions in which the cost of the MILP was higher than the solution obtained by the heuristic algorithms, or solutions in which the cost of the more constrained case (such as unsplittable and/or fixed routing) was found to be better than the less constrained case. Note, however, that these situations are a symptom of the small cost differences between both solutions.

For the heuristic methods in the NR-VTD-VR variants, we calculated the matrix which weakly dominates the sequence by applying the two complexity reduction methods described Subsection 4.4.2: first we found the maximal non-dominated set, and then applied the proposed hierarchical scheme to find a matrix which weakly dominates all matrices in the reduced set.

From the obtained MILP solutions, we can extract some interesting conclusions regarding the effect of the different factors on the network cost. As a general rule, and not surprisingly, the number of transceivers used is higher for series of traffic matrices with higher randomness factor R, higher normalized loads ρ and a higher number of nodes N.

With respect to the reduction in the number of transceivers obtained by allowing dynamic reconfiguration of flows, in contrast to the fixed routing case, the following conclusions can be made: (i) the reduction is negligible in the unsplittable routing case, (ii) in the splittable routing case, this reduction is small (a maximum of about 13% at higher loads and higher randomness factors).

Analyzing the same data obtained from the MILP solutions, we can compare splittable vs. unsplittable flow routing. For fixed routing, the cost reduction obtained by allowing the routing to be splittable was only relevant at medium loads $\rho = 1$, increasing for higher randomness factors. The maximum reduction observed was of about 16%. For variable routing, the same trend was found, but with

more intense cost reductions at medium loads (which reached up to about 22%) and non-negligible reductions at higher loads (up to 14%).

Comparison of the variable-splittable routing case, in contrast to the fixed-unsplittable routing case, indicates a significant cost reduction only at medium loads (up to about 25%) and high loads (up to about 17%).

When we compare the results obtained from the exact MILP formulations with the ones obtained by the heuristic algorithms, we can see that, in almost all the cases, the results are fairly similar. The cost gap between the heuristic and the MILP solutions has a significant value (up to 40%) only at low traffic loads. Note that in some cases, the heuristic method gave slightly better solutions for the fixed routing and/or unsplittable case than for the less constrained variable and/or splittable routing. These situations are caused by the inherent inexactitudes in the heuristic algorithms.

The *LBs* (Lower Bounds) column in Table 4.5 shows a lower bound on the number of transceivers in the optimal solution calculated as in Section 4.4.1. It is very important to remind that the lower bound is a lower bound for the *fully reconfigurable* case in which (i) the virtual topology can be reconfigured along time, (ii) the flow routing is variable, and (iii) the flow routing is splittable. Therefore, for cases where the lower bounds are close to the MH-VTD solutions, we can claim that only a small reduction in the number of transceivers can be obtained by allowing the virtual topology to be dynamically reconfigured along time.

The rightmost column in Table 4.5 shows the maximal reduction in the number of transceivers that could be obtained, in the variable and splittable flow routing case, if the virtual topology could change along time. In other words, this column shows the maximal transceiver reduction to be obtained by using reconfigurable equipment over its non-reconfigurable variant. Interestingly enough, results show that only a minor reduction (a maximum of about 7%) can be achieved in all the scenarios tested, except for those with a low load and $N = \{6, 8\}$ nodes. In these cases the maximal cost reduction have shown to be high (about 33% for six nodes, and 65% for eight nodes) and independent of the traffic randomness factor.

Table 4.5. Synthetic traffic. Number of transceivers in the network in the tested scenarios.

N	ρ	R	NR-VTD-VR				NR-VTD-FR				LBs	Cost gap (%)
			Split.		Unsplit.		Split.		Unsplit.			
			Heur. (4.4.2)	Exact MILP	Heur. (4.4.2)	Exact MILP	Heur. (4.4.2)	Exact MILP	Heur. (4.4.2)	Exact MILP		
4	0.1	0.1	10.0	8.0	9.6	8.0	9.6	8.0	9.6	8.0	8.0	0.0
		0.2	9.6	8.0	10.0	8.0	10.8	8.0	10.0	8.0	8.0	0.0
		0.5	10.4	8.0	9.6	8.0	9.2	8.0	9.2	8.0	8.0	0.0
	1	0.1	28.0	28.0	30.4	30.4	28.4	28.0	30.4	30.4	28.0	0.0
		0.2	30.0	28.4	40.4	34.8	34.0	30.8	40.4	34.8	28.2	0.7
		0.5	34.8	32.8	44.0	38.0	36.8	33.6	46.8	38.0	31.4	4.5
	10	0.1	258.4	255.2	270.4	270.4	264.0	262.8	270.4	270.4	253.0	0.9
		0.2	272.8	264.8	294.0	294.0	288.4	285.2	294.0	294.0	260.0	1.9
		0.5	295.2	283.6	319.2	317.2	319.6	309.6	326.8	317.2	274.0	3.5
6	0.1	0.1	18.8	16.0	19.6	16.0	19.6	16.0	19.6	16.0	12.0	33.3
		0.2	19.2	16.0	19.6	16.0	18.8	16.0	19.6	16.0	12.0	33.3
		0.5	20.8	16.0	22.0	16.0	22.0	16.0	22.0	16.0	12.0	33.3
	1	0.1	72.0	71.2	75.6	75.2	72.0	72.0	75.6	75.2	70.6	0.9
		0.2	76.4	71.6	96.8	87.2	80.4	76.0	96.8	88.0	71.0	0.9
		0.5	85.2	76.0	111.6	96.4	95.2	84.8	116.8	102.0	74.2	2.4
	10	0.1	646.8	635.6	686.0	670.0	668.4	670.8	686.0	670.8	627.0	1.4
		0.2	686.4	662.4	747.2	747.2	728.0	726.0	747.2	747.2	647.0	2.4
		0.5	753.6	716.4	847.2	834.0	849.2	817.6	869.6	868.0	693.4	3.3
8	0.1	0.1	32.8	26.4	34.0	26.4	34.8	26.4	34.0	26.8	16.0	65.0
		0.2	33.2	26.0	34.0	26.4	34.8	26.0	34.0	26.4	16.0	62.5
		0.5	34.8	26.8	38.4	27.0	38.4	26.8	40.0	27.6	16.6	61.5
	1	0.1	131.6	127.2	145.2	140.0	134.0	132.8	145.2	142.4	123.0	3.4
		0.2	136.4	130.0	177.6	158.0	148.4	141.6	177.6	160.0	127.6	1.9
		0.5	155.6	140.4	200.8	181.0	179.2	159.2	225.2	188.8	134.8	4.2
	10	0.1	1209.2	1224.8	1301.6	1310.2	1260.8	1261.0	1301.6	1319.6	1166.8	5.0
		0.2	1264.0	1262.8	1397.6	1390.0	1359.2	1359.0	1396.8	1401.2	1196.0	5.6
		0.5	1404.0	1368.8	1536.4	1540.4	1627.6	1586.0	1665.6	1651.2	1275.6	7.3

A realistic case study: the Abilene network

In order to further validate the results and conclusions above commented, we performed a case study on realistic (not synthetically generated) traffic. To do so, we chose the eleven-node Abilene network for which a real traffic trace is publicly available. The traffic matrices used were taken from the measures carried out in the TOTEM project (Toolbox for Traffic Engineering Methods) [32]. The sequence of matrices available in [32] spans several weeks. From this data, we averaged the values taken at the same time and day in the week to obtain a sequence representing the average week in 15-minute time intervals (96 matrices per day, 672 matrices in total). In order to test different traffic intensities, the average week sequence was normalized for values $\rho = \{0.1, 1, 10\}$, in the same manner as in the study on synthetic traffic described above.

Naturally, the exact MILP formulations for such large problem sizes are intractable. Therefore, all tests were conducted using the 3-step-D heuristic approach proposed in Subsection 4.4.2, along with the

two complexity reduction stages described to simplify the first step of the algorithm. First, we applied the reduction to obtain the maximal non-dominated set. This reduced the number of matrices in the set from 672 to 172 in the splittable case, and from 672 to 479 in the unsplittable one. Then, the hierarchical version of the replace-to-one step was applied to the maximal non-dominated sets.

Table 4.6 shows the obtained results for all problem variants. Unfortunately, some parts of the analysis made in the previous Section cannot be repeated here. Namely, the results obtained by the heuristic algorithm for the unsplittable and variable routing case show a higher cost than the ones for the fixed routing case. This comes from the accumulated suboptimalities that appear in the hierarchical reduction method which become very significant with such a large number of matrices.

The analysis of the rest of the data confirms the main trends observed for synthetic traffic, although the cost reductions achieved by allowing variable routing and/or splittable routing are somewhat smaller. First, we can see that for splittable routing, the reduction in the number of transceivers obtained by using variable routing, as opposed to fixed, is minor (a maximal reduction of about 7% was achieved for medium and high loads). In the fixed routing case, the cost reduction obtained by using splittable instead of unsplittable routing is also minor (with a maximal reduction of about 8% at medium loads). Furthermore, if we compare the case of variable-splittable routing with the fixed-unsplittable case, the results show only a moderate cost reduction, with a maximum of about 15% achieved at medium loads.

As before, comparison of the NR-VTD results with the lower bounds indicates the maximal possible reduction in the number of transceivers that could be achieved by using reconfigurable optical equipment − that is, allowing dynamic reconfiguration of the virtual topology. This maximal benefit was shown to be approximately 40%, 15% and 10% for low, medium and high loads, respectively.

Table 4.6. Abilene network. Total number of transceivers

	NR-VTD-VR		NR-VTD-FR			
ρ	**Split.**	**Unsplit.**	**Split.**	**Unsplit.**	**LBs**	**Cost gap (%)**
0.1	62	68	64	68	38	38.7
1	336	402	358	392	286	14.9
10	3046	3556	3292	3360	2739	10.1

Conclusions

Results support interesting conclusions regarding cost reduction (in terms of the number of transceivers used) that network operators can achieve in different circumstances. For instance, in the

scenarios studied the migration from fixed to variable routing is justified only if splittable routing is also allowed in the network, and only for medium or high loads. However, the maximum reduction obtained is still moderate (about 15%) and is a trade-off with increased overhead. Analogously, for network operators evaluating the advantages of splittable routing in constrast to unsplittable routing, our results indicate that the migration is cost-effective for medium load scenarios, with a larger cost reduction if variable routing is allowed. Still, the reductions are moderate (with a maximum of about 20%).

A lower bound to the network cost has been provided for the case in which the network uses variable splittable routing, and the virtual topology can be dynamically reconfigured along time (since it uses reconfigurable optical equipment). The comparison of the lower bounds with our results obtained in the NR-VTD-VRs problem, allows us to measure the maximal benefit that can be achieved in the network with variable and splittable routing if it were to also permit dynamic reconfiguration of the virtual topology. The results show that the maximum cost reduction is not significant except in the low load scenario, where it can reach values of about 40% (in the Abilene case study) and up to 65% (in the studies with synthetic traffic). Nevertheless, it should be noted that in the low load scenario, as the number of lightpaths in the network is low, the reduction in the number of transmitters in absolute value is also small. Therefore, from the perspective of the present non reconfigurable study, it is not possible to definitely state that the increase in cost caused by using reconfigurable optical equipment, at all or some nodes in the network, as well as the extra signaling complexity could not be compensated for by the cost reduction achieved by using fewer transceivers. Namely, this is the topic of the study presented in the next subsection, where the tradeoffs associated with replacing non-reconfigurable equipment with their reconfigurable counterparts are investigated.

4.5.2 Reconfigurable vs Non-Reconfigurable VTDs

This subsection presents the results of extensive tests conducted to compare reconfigurable versus non- reconfigurable VTDs. Our objective is to study whether the introduction of reconfigurable optical equipment (R-VTD problem) implies a reduction on the total transceiver cost to justify its installation versus non-reconfigurable options (NR-VTD problem). We must note that the non reconfigurable problem considered in this subsection is the NR-VTD-VR-s, following the classification in the Section 4.1. In the remaining subsection we will denote this problem simply as NR-VTD. We must note that the most of the results presented in this Section comes from the work [40], where GARF algorithm (Subsection 4.4.5) is proposed as efficient proposal to solve both MH-VTD problems. The GARF is our last proposal to the multihour planning and our most efficient heuristic in terms of quality of the suboptimal solutions found and time required to find them. For instance, solutions with lower transceiver costs have been found by other algorithms in some case, but needing very much larger periods of time.

For this reason, this greedy approach occupies a special position in the analysis of the results.

All the algorithms presented in Section 4.4 are used to perform the experiments. Once again, we follow the assumptions established in Section 4.1 (sufficient number of wavelengths and no application of physical layer constraints) so that every virtual topology design has a feasible RWA solution. Consequently, our algorithms take as input only the multihour traffic demand. As in the previous subsection, the tests are applied to both synthetic traffic data and data from real traffic traces.

Finally, the algorithms performance is also assessed by compare them each other, with the MILP formulations and with the lower bound proposed in Section 4.4.1. The algorithms are implemented in the MatplanWDM tool [46] which links to the TOMLAB/CPLEX library [53] to solve the MILP formulations.

Description of the testing scenarios

The experiments encompass three testing scenarios. The first scenario considers synthetically generated multi-hour traffic for a small 6-node network. Five sequences of $T = 12$ traffic matrices were generated following the MH traffic generation method described in the formulae (4.34)-(4.36). This method synthesizes a sequence of T matrices which capture the effect of traffic intensity variation along the day using the activity model presented in [156] from a single base matrix generated according to a randomness factor R. In out tests R was set to 20%.

The second and third testing scenarios use data from real traffic traces in the eleven-node Abilene network, publicly available at [32]. This data consists of traffic matrices spanning several weeks. Our second testing scenario studies the MH planning for the *average day*. We averaged all values of the trace taken at the same time in the day to obtain a sequence of 24 matrices illustrating typical hourly fluctuations in a day. For the third testing scenario, we applied the same approach for the *average week*. As a result a sequence of 24x7=168 matrices representing the hourly traffic variations along one full week was obtained.

All the sequences of traffic matrices in all three scenarios are normalized to three different traffic intensities or traffic loads $\rho=\{0.1, 1, 10\}$ according to (4.35). The value ρ represents, as in the previous study, the average amount of traffic between two nodes during the highest loaded time slot, measured in the number of lightpaths. Consequently, a value of $\rho=0.1$ corresponds to the case when the highest average traffic equals 10% of a single lightpath capacity. On the contrary, a value of $\rho=10$ captures cases in which the average traffic between two nodes in the highest loaded time slot fills on average 10 full lightpaths.

The sequences of traffic matrices go through an additional pre-processing step to reduce the

complexity of the problem before being applied as an input to the planning algorithms. For each sequence, we make use of the concept of traffic domination [41] to filter out those matrices which are redundant to the planning problem, and thus can be safely eliminated. Informally speaking, if a traffic matrix h^1 dominates a traffic matrix h^2, every network which is able to carry traffic h^1, can also carry traffic h^2. Given a sequence of multihour traffic matrices $H = \{h^t, t = 1..T\}$. we perform two types of traffic demand simplifications, depending on whether the sequence is to be applied to the non-reconfigurable or reconfigurable MH-VTD problem. The traffic demand preprocessing applied in the non-reconfigurable case is the one described in the NR-VTD-VRs version of the *3-Step-D* algorithm (Subsection 4.4.2). The traffic matrices in the sequence which are (weakly) dominated by *any other traffic matrix* in the sequence are filtered out, since they are redundant to the planning problem, i.e. every VTD which is able to carry the original traffic sequence is also able to carry the reduced sequence. In the reconfigurable case, however, a stricter version of such a demand preprocessing is applied: a traffic matrix h^t is filtered out only if it is (weakly) dominated by *the previous traffic matrix* h^{t-1} or by *the subsequent matrix* h^{t+1}. Since the matrix h^{t-1} (or h^{t+1}) dominates h^t, the virtual topology designed for h^{t-1} (or h^{t+1}) can be used without any reconfiguration in the next (or previous) time slot *t*. The reductions in the number of matrices obtained by these preprocessing steps are plotted in Table 4.7. Note that the reductions are very significant in the static case (between 40% and 70%), but negligible in the Abilene networks for the reconfigurable case.

Table 4.7. Reduction in Number of Matrixes In Preprocessing Step

Problem	N = 6; T = 12	Abilene; N = 11; T = 24	Abilene; N = 11; T = 168
NR-VTD	5	14	52
R-VTD	7.8	22	167

The R-VTD problem

Herein we focus on the results obtained by the R-VTD heuristic approaches proposed in Section 4.4, assessing its performance. These results are collected in Table 4.8, whose rows correspond to:

- *LB*: Lower bound on the number of transceivers calculated as shown in Subsection 4.4.1.
- MILP: Exact solution to the MILP formulation to the R-VTD problem presented in Subsection 4.3.3.
- GARF: GARF algorithm presented in Subsection 4.4.5 with parameter $r = 0$. For the Step 2 of

the algorithm, the number of iterations without improvement is set to 20 and the tabu list size to 4 and 7, for the 6-node and Abilene networks, respectively. These values were determined experimentally.

- TS: Tabu Search heuristic approach presented in Subsection 4.4.3 using the fitness function aimed the reconfigurable case. The number of iterations without improvement and the tabu list size are set to the same values as GARF Step 2.
- LRvSG: Lagrangean Relaxation-based approach presented in Subsection 4.4.4. The total number of iterations is set to 50, the initial and the minimal value of the step-size parameter p to 2 and 0.005, respectively, and the maximum number of iterations without improvement to halve p is set to 10.
- ICET: The Independent Configuration with Exact Traffic (ICET) algorithm strategy presented in [28] consists of executing T independent instances of a transceivers minimization problem, one for each time slot. We apply this strategy using the algorithm in [33] for transceivers minimization.
- Gap%: This row shows a bound to the GARF sub-optimality gap. That is, the relative difference between the GARF solution cost, and the cost of the MILP solution (6-node network) or the cost lower bound (Abilene network).

Here, we focus on the case where the number of transceivers is the main objective to minimize and the reconfiguration frequency is a secondary objective. Consequently, parameter r in GARF is set to r=0, while in the MILP, TS and LRvSG algorithms, the cost of reconfiguring a lightpath is set to a sufficiently small fraction of the cost of one transceiver ($\sim 10^{-4}$ and $\sim 10^{-6}$ for 4-node and Abilene networks, respectively) so that the cost of the transceivers dominates the optimization.

Each cell in Table 4.8 shows the number of transceivers of each solution. In parenthesis, we include the number of reconfigurations averaged *per time slot* associated to the plan. This is an intuitive measure of the frequency of the reconfigurations, and thus the relative amount of extra signaling and traffic disruption caused by the VT changes. The heuristic solutions with best results for each objective criterion are printed in bold.

Results reveal that GARF and TS are the best algorithms in terms of minimization of the number of transceivers. The difference between them is not significant in most cases, except for ρ=0.1 in the synthetic traffic scenario, and ρ=0.1 in 24-time slots Abilene case, where TS showed better results (25% and 13% better respectively). However, TS fails with respect to reconfiguration performance. It requires a

much higher amount of lightpath reconfiguration than GARF in all the cases: {7%, 23%, 88%} more in the low load cases, and between 4 and 20 times more in the rest of the scenarios. GARF shows the best results among all the algorithms in terms of reconfiguration frequency.

The GARF algorithm outperforms the ICET approach with respect to both transceiver cost and frequency of reconfiguration in all cases. Also, GARF beats the LRvSG method in the number of transceivers in all cases. In two tests, LRvSG improves the number of reconfigurations of the GARF. Nevertheless, this should not be seen as a true merit of LRvSG since the large number of extra transceivers planned by the LRvSG algorithm in those cases (55% more and 69% more) permits solutions with fewer reconfigurations.

The Gap% row evaluates the quality of the solutions of the GARF algorithm against the optimal MILP solution (in the 6-node network) and the lower bounds (in the Abilene network). The optimality gap results are fairly good: below 1% in the high load scenarios, and below 5% in medium load scenarios. The sub-optimality gap of the GARF algorithm for the low load case, on the other hand, is in the order of 40%. However, it is important to note that this gap is based on the lower bound and may not be a true indication of the real optimality gap for low loads since there are significant disparities between the optimal MILP solutions and the Lower bound for the 6-node network at ρ=0.1. Thus, for the Abilene network and low load, it is difficult to conclude whether the lower bounds are weak or the solutions obtained by GARF are far from optimal. In any case, the GARF solutions in this scenario are the best among the heuristic approaches for the Abilene-168 design and very close to the best heuristic solution (TS) in the Abilene-24 case.

To achieve further insight into the performance of the GARF algorithm, we observe the joint evolution of the number of transceivers and the frequency of the reconfigurations in the GARF designs. Namely, there exists a trade-off between the increase in the number of transceivers and the obtained decrease in the number of reconfigurations, depending on parameter r. To illustrate this relation, we ran the GARF algorithm with parameter r ranging from 0 to T, in $T/8$ increments, for the Abilene-24 and Abilene-168 scenarios. Fig. 4.6, Fig. 4.7 and Fig. 4.8 collect the results for loads ρ=0.1, ρ=1 and ρ=10 respectively, where the frequency of reconfiguration (average number of reconfigurations per time slot) is shown versus the quotient r/T.

We can see that at medium and especially high loads, the number of transceivers slowly, and almost linearly, increases with parameter r. The drop in reconfiguration frequency, on the other hand, is much steeper for small values of r. This suggests that most of the gaps/bumps are of small size, and are removed with the addition of a few transceivers. Consequently, setting r to a small value for medium and high loads can create an advantageous trade-off between transceivers and reconfiguration.

Finally, at low loads, an anomaly is observed where the number of transceivers initially grows with *r* as expected, but is smoothly reduced after a certain *r*. This anomaly is presumably due to the existence of some large gaps, whose "bridging" allows us to permanently tear down some lightpaths along time, reducing the number of transceivers. Namely, at low loads, a gap "bridged" provides bigger spare capacities to re-accommodate traffic from candidate bumps to "flatten".

Table 4.8. R-VTD Case: Number of transceivers (and reconfigurations) for each testing scenario

	N = 6; T=12			**Abilene; N = 11; T=24**			**Abilene; N = 11; T=168**		
ρ	**0.1**	**1**	**10**	**0.1**	**1**	**10**	**0.1**	**1**	**10**
LB	12.0	71.0	647.0	36	248	2385	39	278	2659
MILP	16.0 (0)	71.2 (0.2)	647.2 (2.9)	- (-)	- (-)	- (-)	- (-)	- (-)	- (-)
GARF	21.6 (**2.2**)	72.4 (**0.2**)	651.4 (**6.1**)	60 (6.8)	271 (**2.3**)	2400 (**8.0**)	**64** (4.4)	301 (**0.9**)	2671 (**2.6**)
TS	**16.4** (2.4)	**71.4** (3.5)	**648.6** (33.6)	**52** (8.4)	**260** (9.1)	**2393** (45.0)	66 (8.2)	**290** (11.6)	**2669** (53.8)
LRvSG	48.2 (4.8)	89 (2.1)	671.8 (34.7)	93 (**1.7**)	369 (4.0)	2497 (43.7)	108 (**2.4**)	396 (4.0)	2770 (51.2)
ICET	24.6 (2.6)	73.0 (3.2)	653.6 (33.5)	74 (10.7)	275 (0.8)	2405 (44.0)	88 (11.9)	303 (11.7)	2682 (54.1)
gap (%)	2.44%	0.28%	0.22%	30.77%	4.62%	0.33%	39.06%	4.14%	0.37%

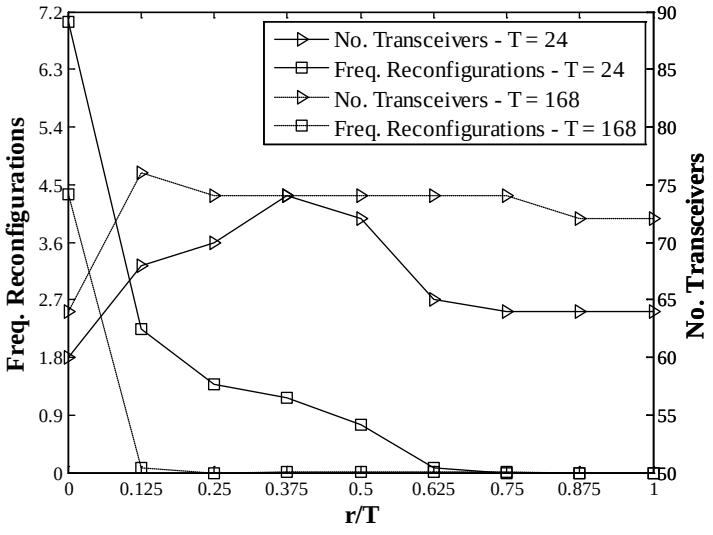

Fig. 4.6. Frequency of Reconfigurations (No. of Reconfigurations per Time slot) and Number of Transceivers vs. Quotient r/T for different test cases. Abilene traffic averaged on 1 day (T=24) and on 1 week (T=168) with ρ = 0.1.

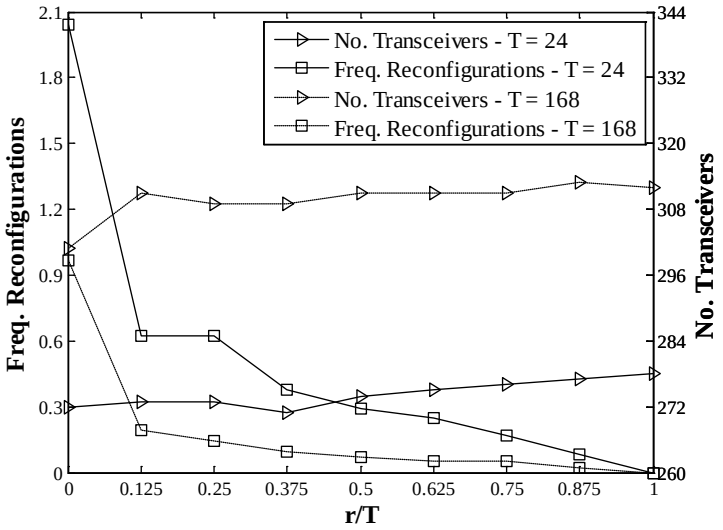

Fig. 4.7. Frequency of Reconfigurations (No. of Reconfigurations per Time slot) and Number of Transceivers vs. Quotient r/T for different test cases. Abilene traffic averaged on 1 day (T=24) and on 1 week (T=168) with ρ = 1.

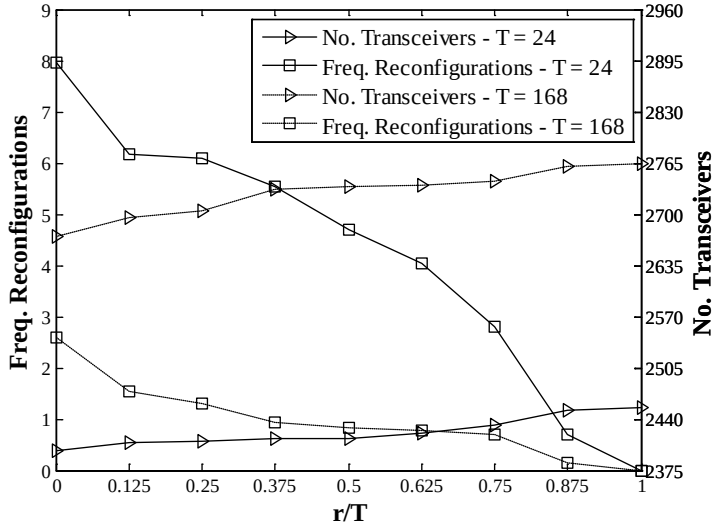

Fig. 4.8. Frequency of Reconfigurations (No. of Reconfigurations per Time slot) and Number of Transceivers vs. Quotient r/T for different test cases. Abilene traffic averaged on 1 day (T=24) and on 1 week (T=168) with ρ = 10.

The MH-VTD-NR problem

In this subsection we are interested on assessing the merits of the algorithms proposed in Section 4.4, for planning those networks in which the VT is constrained to be static along time (NR-VTD problem). Table 4.9 collects the obtained results where the rows correspond to:

- LB: Equal to that of the R-VTD case.
- MILP: Exact solution to the MILP formulation to the NR-VTD-VRs problem presented in Subsection 4.3.2.
- GARF: GARF algorithm presented in Subsection 4.4.5 with parameter $r = T$ in Step 3 of the algorithm, so that lightpath reconfigurations are prohibited.
- TS: The Tabu Search (TS) algorithm presented in Subsection 4.4.3 using the fitness function aimed the non reconfigurable case. The number of iterations without improvement and the tabu list size are set to the same values as GARF Step 2.
- LRvSG: The Lagrangean Relaxation-based algorithm, following the same technique as in [135], applied to the MILP formulation Subsection 4.3.2 for the NR-VTD-VRs problem. The total number of iterations is set to 50, the initial and the minimal value of the step-size parameter p to 2 and 0.005, respectively, and the maximum number of iterations without improvement to halve p is set to 10.
- 3-Step-D: The three-step domination based heuristic approach proposed for the NR-VTD-VRs problem in Subsection 4.4.2.
- UCMT: A design obtained by applying the Unique Configuration with Maximal Traffic (UCMT) strategy presented in [28]. It consists of (i) calculating the maximal element-wise traffic matrix from the traffic sequence, and then (ii) finding the minimum-cost VT which carries that traffic matrix. For the second step, the algorithm from [33] is used.
- Gap%: This row shows a bound to the GARF sub-optimality gap, calculated in a similar way as in Table 4.8.

We can see from Table 4.9 that in all the medium load and high load cases, GARF provided either the best heuristic solution or a solution within 2% of the best heuristic solution. In the low load case, the UCMT and 3-Step-H approaches provided better results, where GARF is 23%, 4% and 17% worse for the 6-node, Abilene-24 and Abilene-168 cases, respectively. Finally, in all the cases, the solutions from GARF improved those of the LRvSG and TS algorithms.

The GARF sub-optimality gap for the NR -VTD problem is in the order of 1% for the 6-node network in medium and high load cases, being the best among the heuristic algorithms. For the Abilene network, the sub-optimality gap is in the order of 10% for ρ=1 and 3%~4% for ρ=10. The true gaps should be presumably better since the lower bounds used are the same as those calculated for the reconfigurable case, i.e., they may be somewhat weaker for the static problem. The accuracy of GARF in the low load experiments cannot be easily assessed given the presumable weakness of the lower bound for those cases, as indicated in the previous subsection for the R-VTD problem.

Table 4.9. NR-VTD Case: Number of transceivers (and reconfigurations) for each testing scenario

	N = 6; T=12			**Abilene; N = 11; T=24**			**Abilene; N = 11; T=168**		
ρ	**0.1**	**1**	**10**	**0.1**	**1**	**10**	**0.1**	**1**	**10**
LB	12.0	71.0	647.0	36	248	2385	39	278	2659
MILP	**16.0**	**71.6**	**662.4**	- / -	- / -	- / -	- / -	- / -	- / -
GARF	23.2	**72.4**	**673.6**	58	**274**	2456	68	312	2778
TS	25.6	74.0	724.0	138	326	2552	216	406	3150
LRvSG	23.6	100.8	747.2	110	382	2652	168	430	3240
3-Step-H	19.2	76.4	686.4	58	276	**2454**	**58**	**308**	**2774**
UCMT	**18.8**	80.4	728	**56**	288	2576	62	346	3156
gap (%)	**31%**	**1.1%**	**1.7%**	**37.9%**	**9.5%**	**2.9%**	**42.6%**	**10.9%**	**4.3%**

Scalability

This Section compares the scalability properties of the GARF algorithm to that of the other heuristic algorithms. Table 4.10 shows the execution times of all the algorithms for each testing scenario. The results are obtained on an Intel Core2 Duo CPU P8400 2.26 GHz processor. In the reconfigurable case, GARF is more scalable than the TS and LRvSG algorithms, their true competitors in the cost of the solutions provided (but with much worse results in terms of reconfiguration frequency). The execution time of GARF grows with the number lightpaths (network load), and slightly grows with the number of time slots. In contrast, the complexity of the TS algorithm greatly increases with the number of time slots, and with lower loads. In average, GARF is several hundred times faster than TS. The LRvSG has a running time mostly insensitive to the network load but very dependent on the number of time slots. Its running time is approximately between 2 (high loads) and 20 times (low loads) higher than the execution time of GARF.

In the non-reconfigurable case, the same trends apply to GARF, TS and LRvSG. The execution time of the 3-Step-D algorithm is independent of the network load. The execution time of GARF is approximately one order of magnitude faster at medium and low loads, and in the same order at higher loads.

The ICET and UCMT algorithms are in general faster than GARF for the reconfigurable and non-reconfigurable cases, respectively. Nevertheless, ICET is not aimed to minimize the reconfigurations and was outperformed by GARF with respect to both network cost and reconfiguration frequency, while UCMT does not exhibit good performance characteristics at medium and high loads.

Table 4.10. Algorithms' Execution Times (Seconds)

	N = 6; T=12			Abilene; N = 11; T=24			Abilene; N = 11; T=168		
ρ	**0.1**	**1**	**10**	**0.1**	**1**	**10**	**0.1**	**1**	**10**
R-VTD									
GARF	1.5	1.2	4.7	25.9	35.7	253.0	165.7	222.3	2397.6
TS	518.7	162.9	70.7	140673.7	5398.3	1985.2	367141.2	104295.6	37923.4
LRvSG	16.3	16.3	16.3	409.0	413.6	422.6	6251.3	6257.9	6226.5
ICET	1.6	0.9	1.4	82.7	63.0	107.5	501.0	399.4	595.3
NR-VTD									
GARF	0.9	1.0	4.8	18.2	23.5	201.6	52.0	90.2	1481.5
TS	597.7	18.1	10.6	74302.7	17918.9	5306.0	235752.5	5878.0	5904.9
LRvSG	11.8	11.7	11.7	400.4	399.7	405.5	3749.6	3767.5	3876.9
3-Step-H	0.7	0.6	1.0	280.3	271.3	274.2	847.4	840.2	817.9
UCMT	0.4	0.3	0.5	5.7	5.1	9.3	16.6	15.0	36.5

Reconfigurable vs Non-reconfigurable VTD

The results of the conducted experiments motivate a discussion on the potential interest of a periodic virtual topology reconfiguration, as a valid method to reduce the transceivers cost. Table 4.11 summarizes them for this discussion. The *Upper bound* row contains the maximum theoretical cost saving that could be achieved, i.e. the maximum possible savings that periodic virtual topology reconfiguration could bring. For the 6-node networks the upper bound shown is in fact comparison of the optimal solutions of the exact MILPs for the two problem variants. For the Abilene network scenarios, the upper bound is calculated by comparing the best non-reconfigurable solution found, to the lower bound on the transceivers cost (valid for the reconfigurable case). Note that this bound is calculated using the lower bound on transceiver cost (Subsection 4.4.1) which is presumably weak for low loads. Consequently, the upper bound for the Abilene scenarios shown in the table may also be weak at low loads. The *Achieved savings* row shows the maximal savings actually achieved in the number of transceivers comparing the best solution obtained for the non-reconfigurable case and the best solution obtained for the reconfigurable case. These solutions come from the exact MILP in the 6-node network, and the best solutions among the heuristics in the Abilene experiments. Naturally, given the exact solutions of the MILP, the both rows are equal for the 6-node case.

Optimal results for the 6-node networks show that the transceiver cost benefits of reconfiguring increase with the network load. However, the upper bounds for the Abilene instances indicate the

opposite trend. Although it is inconclusive whether the bound or the solutions are weak for low loads, the fact that the achieved savings at medium loads is greater than the upper bound at high loads for both Abilene -24 and -168, seems to suggest that the possible savings decrease from medium to high loads. For both Abilene scenarios, the savings achievable are generally greater than for the 6-node network for all the loads, with a maximum achieved value of 7.14%. However the average achieved reduction over all cases seems marginal (3%) which may not be significant enough to justify the trade-off in the extreme case where transceiver cost is the primary objective allowing unlimited reconfiguration. The results shown in Fig. 4.6, Fig. 4.7 and Fig. 4.8 indicate that a more advantageous trade-off may be achieved by allowing for some (limited) reconfiguration while still comparably reducing transceivers cost. In these cases, a narrow but significant reduction in transceivers cost (e.g. 5%) could be achieved in some scenarios with a minimal number of reconfigurations (on average, less than one lightpath reconfiguration in the whole network per hour).

Table 4.11. Maximal cost savings achieved with R-VTD with respect to the NR –VTD.

	N = 6; T=12			**Abilene 24**			**Abilene 168**		
ρ	**0.1**	**1**	**10**	**0.1**	**1**	**10**	**0.1**	**1**	**10**
Upper bound	0%	0.56%	2.29%	35.71%	9.49%	2.81%	32.76%	9.74%	4.15%
Achieved savings	0%	0.56%	2.29%	7.14%	5.11%	2.49%	0%	5.84%	3.79%

Conclusion

Although the reconfigurable solution (R-VTD problem) can achieve a reduction in the number of transceivers needed to establish the VTD in relation to the non-reconfigurable solution, this comes at a cost. Namely, each reconfiguration implies increased signaling complexity and network service disruption. Consequently, we investigate the associated tradeoffs between transceiver reduction and increased reconfiguration frequency for the R-VTD problem variant. Exhaustive experiments are conducted to explore these tradeoffs. In the experiments, exact MILP formulations (Section 4.3), the heuristic proposals in Section 4.4 and the lower bounds from Subsection 4.4.1 are applied to the reconfigurable and non-reconfigurable MH-VTD problems.

Among the heuristic approaches, we must note the GARF (Greedy Approach with Reconfiguration Flattening) due its better results in terms of scalability and wellness of the suboptimal solutions found. Despite its simplicity, GARF obtains reconfigurable VTD solutions which improve or match the network transceiver cost with respect to other algorithms, while strongly reducing the number of reconfigurations and with better scalability than its closer competitors. For the non-reconfigurable case, GARF provides

designs with a similar cost to the some algorithms previously proposed in the literature, with similar or better scalability.

The exhaustive results obtained also motivate a discussion on the benefits of virtual topology reconfiguration to better adapt to traffic variations. Results suggest that the maximal transceiver cost reduction coming from unlimited lightpath reconfiguration may not be dramatic enough to justify the trade-off. However, we have observed that allowing just a limited amount of reconfiguration, provides still significant transceiver cost reduction.

Chapter 5

5 Conclusions and Future Work

ABSTRACT: In this chapter the main contributions of the present thesis to the topic are summarized. In addition, some possible future research lines are suggested.

5.1 Final Conclusions

Along this thesis, several planning problems in *WDM Transparent Optical Networks* have been investigated by means of a variety of optimization techniques: (a) exact ILP or MILP formulations; (b) classical heuristic approaches, such as tabu searches or greedy algorithms; (c) "smart" heuristic procedures combining (a) and (b) approaches; or, analytical bounds on the optimal costs.

All the planning problems were addressed following a similar methodology: first, modeling the problem as an exact ILP/MILP formulations; second, devising analytical bounds on the network costs; third, proposing heuristic algorithms to handle large-sized problems; fourth, assessing the performance of the proposals comparing its solution with bound or exact solutions (when network size allows it); and, finally, using the previous techniques to study tradeoffs on network costs among possible network configurations.

Two families of optical network problems have been more intensely researched, constituting the major focus of the thesis: *Physical Layer Impairment Aware (PLIA) Planning* and *Multihour Planning*. The former incorporates to the optimization problem the signal quality degradation due to the physical layer impairments (PLIs); the latter introduces the time variability of the traffic.

In the field of the *PLIA planning*, *RWA* problem in traditional 10 Gbps Single Line Rate (SLR) networks and multilayer *VTD* problem in 10/40 Gbps Mixed Line Rate (MLR) communications were investigated. In the *PLIA-RWA* problem, several algorithms were proposed to consider the PLIs affecting to 10 Gbps OOK modulated signals. These impairments were modeled by analytical formulae and collected in a global QoT evaluator called *Q-tool*. Two algorithmic approaches were presented: (i) an iterative global search driven by a set of BILP formulations whose problem complexity is limited by heuristic techniques; and, (ii) a sequential heuristic approach where lightpaths demands are sequentially processed according to different pre-orderings. Both strategies alternate network planning iterations with signal quality verifications; but, global optimization technique reroutes some of the lightpaths in the

current RWA solution depending on the *Q-tool* evaluations, meanwhile sequential algorithm simply adds new quality-verified lightpath routings to the current RWA solution. Moreover, the global optimization technique minimizes the number of invocations to *Q-tool* by making use of the precomputed *degradation matrix D* that collects the interactions between any two possible *lightpaths*. Several experiments were conducted, showing its results that global exploration algorithm outperforms the sequential scheme in larger topologies, although they have a similar performance in small topologies. Furthermore, the time complexity of the global search algorithm remained low, and approximately constant with network size and traffic demand in comparison with the sequential approach. The impact of BILP executions on the total execution time was negligible, in comparison to the running time of the QoT evaluation function. Therefore, it can be concluded that the global search method proposed is both effective and scalable. Conversely, the sequential approaches were penalized by the excessive utilization of time-consuming QoT evaluations. Finally, results suggest that a PLIA-RWA algorithm should *include rerouting techniques* to *increase their blocking rate performance*; and, *incorporate precomputed information* about *QoT degrading interactions* between *lightpaths to reduce the number of Q factor invocations*.

In the novel topic of *PLIA-VTD* in *MLR networks*, the non-linear interferences between neighboring lightpaths were studied. In Mixed Line Networks, traditional 10 Gbps intensity modulated signals coexist with higher bit rate (40 or 100 Gbps) phase modulated signals. Several studies [108],[109] have demonstrated that intensity modulated signals induce non linear interferences over the phase modulated ones. To cope with this, one option is to instruct the network planning to allocate empty guard wavelengths separating adjacent channels at different bit rates. The multilayer VTD problem was modeled as a MILP formulation; and, a heuristic algorithm was presented to solve large networks. Several experiments were conducted to analyze the tradeoffs between longer transparent reach of 10 Gbps transceivers, versus higher capacity and better cost per bps of 40 Gbps transceivers in MLR networks. From the results, it is possible to extract two different conclusions depending on the network load. In *low loaded networks*, *MLR networks* seem to be *efficient solutions* to reduce the transceiver network cost. However, in *heavy loaded networks*, the *non linear interferences* between 10 and 40 Gbps adjacent channels *dissuade to mix them*, despite the possible benefits of using longer-reach 10 Gbps lightpaths.

The other large family of problems addressed in the thesis was the multihour *planning*. Depending on the network configurations several approaches to satisfy the multihour traffic demands are possible: reconfigurable and non- reconfigurable optical equipment, time fixed and time varying high layer traffic routing on the VT, splittable and unsplittable routing, etc. These assumptions allow us to distinguish several problem variants with different advantages and drawbacks. The tradeoffs existing between them were broadly studied in this thesis. First, several tradeoffs in networks with non reconfigurable optical

equipment (*Non Reconfigurable VTD* problems) are investigated. Four problem variants have been considered assuming variable/fixed flow routing with splittable/unsplittable flows. For each one of these problem variants, exact MILP formulations, as well as a family of three-step algorithms based on the domination concept, have been proposed. The heuristic approaches apply the concept of traffic domination, providing a theoretical basis allowing us to devise a set of complexity reduction techniques for the problem.

Results support interesting conclusions regarding cost reduction (in terms of the number of transceivers used) that network operators can achieve depending on the network configurations. The results point out that the *migration from fixed to variable routing* is *justified only if splittable routing* is also allowed in the network, and only for medium or high loads. Analogously, the *splittable routing* approach is *solely cost-effective compared with unsplittable* routing for medium load scenarios, with a larger cost reduction *if variable routing* is *allowed*. In both comparisons, the reductions found are moderate: about 15% for variable vs fixed routing and about 20% for splittable vs unsplittable routing. On the other hand, we use the lower bound from Subsection 4.4.1 to guess some conclusions about the tradeoffs associated with replacing non-reconfigurable equipment with their reconfigurable counterparts. Since these lower bounds represent the minimal transceiver cost reachable in a fully reconfigurable VT with variable splittable routing, they can be compared with the results of the NR-VTD-VRs problem. In this comparison, the maximum cost reduction by using reconfigurable VT was not significant for medium and high load scenarios. On the contrary, values up to 40% and 65% were found for low load scenarios. Nevertheless, it should be noted that in these scenarios, as the number of lightpaths is low, the reduction in the number of transmitters in absolute value is also small. Therefore, it is difficult to state from these results whether the increase in cost caused by using reconfigurable optical equipment, at all or some nodes in the network, as well as the extra signaling complexity, could be compensated for by the cost reduction achieved by using fewer transceivers.

The previous inconclusive results about the cost reduction achievable in reconfigurable VTDs (R-VTD problem) motivated to study directly this multihour approach. When the optical equipment is assumed reconfigurable, the above indicated reduction in the number of transceivers required to establish the virtual topology, in relation to the non-reconfigurable case, comes at an extra cost: each lightpath reconfiguration implies increased signaling complexity and network service disruption. These tradeoffs between transceiver cost reduction and increased reconfiguration frequency for the R-VTD problems were investigated. An exact MILP formulation and several heuristic procedures were proposed to explore the tradeoffs. Among the heuristic proposals, GARF (Greedy Approach with Reconfiguration Flattening) algorithm has been proved as the best algorithm in terms of efficiency and scalability. Despite its simplicity, GARF obtained solutions with a clear higher reduction of the number of reconfigurations, a

similar or lower transceiver cost than other algorithms, and a better scalability than its closer competitors in transceiver cost performance.

Exhaustive experiments were conducted using all the R- and NR-VTD algorithms proposed along this thesis. Results suggest that the t*ransceiver cost saving by* using *unlimited lightpath reconfigurations may not be dramatic sufficient to justify its drawbacks*. Namely, maximal transceiver cost savings were found in the range between *5%* and *8%*. Even, we have observed that *an almost non-reconfigurable network* (e.g. allowing one lightpath reconfiguration in the whole network per hour) might provide still a *similar transceiver cost reduction* than a *fully-reconfigurable network*. In summary, a very limited use of lightpath reconfigurations is sufficient to provide the same performance as if very frequent reconfigurations were planned.

5.2 Future work

We briefly outline some possible further research lines continuing the work in this thesis: (a) *PLIA-VTD in Mixed Line Rate (MLR) Networks* [26],[107],[122],[123]; and (b) *robust planning under traffic uncertainty* [157]-[160].

The new equipments able to support 40 Gbps optical communications [4] are forcing to consider systems where signals at different bit rates (10, 40 Gbps) and modulated by different formats (OOK, duobinary, DQPSK, PMD-QPSK, …) may coexist. Moreover, the promising 100 Gbps bit rate has attracting more and more the interest of the network operators. These higher bit rates and the modulation formats associated to them introduce new challenges to the network planning since the physical layer impairments become more severe, and new degrading interactions between neighboring channels modulated with different formats arise. Consequently, future work could continue the research in MLR networks started in [27] so as to consider additional modulation formats (apart from DQPSK) suitable for 40 Gbps systems, and, as well, 100 Gbps systems.

In this thesis, we have assumed that the multihour traffic could be easily estimated from a large number of real traffic traces or modeled by traffic intensity variation models to obtain moderate-sized sets of perfectly known matrices. However, the diversity of communication services and applications, the user mobility or the existence of unpredictable variations due to special events are becoming more difficult to estimate or model traffic patterns suitable as input data to the planning process. Therefore, a promising research line could be to extend the work in the thesis to scenarios where the *traffic uncertainty* is captured in flexible models. Then, instead designing routings dependent on the exact traffic variations; we will plan *robust routings* valid for any traffic matrix meeting the flexible definitions of the traffic

uncertainty model. The research in this line would follow the adaptation of the traffic domination results and planning techniques presented, to the new scenario.

Annex A

A The MatPlanWDM Network Planning Tool

ABSTRACT: In this annex, the optical network planning tool MatPlanWDM, developed by the Technical University of Cartagena (*Universidad Politécnica de Cartagena, UPCT*) for educational and research purposes is briefly described.

A.1 Introduction to MatPlanWDM Network Tool

As we have introduced in the Chapter 1, the network planning and design is a critical process which must be performed before deploying new communication networks. Some of the basic methodologies employed in the network planning include measurement campaigns, analytical studies and computer simulations [44]. These methodologies allow the planners to evaluate the network performance. However, they present different advantages and drawbacks, making them suitable depending on the specific problem to solve. In general, measurements are superior since they provide real data, in comparison with the analytical studies and computer simulations based on theoretical models. Conversely, analysis and simulation permit to reduce the planning costs, since expensive campaigns of measurements are not required, different network configurations can be tested in parallel or rare error simulation scenarios can be studied. To perform the analytical studies and computer simulations, network planning tools must be developed. Network planners allow to simulate, analyze, dimension, optimize and evaluate the performance of the proposed network designs before of its deployment, providing us with the possibility of reaching a better understanding of the existing network systems, identifying flaws or features to improve and a fast development of new systems.

All the commented in the previous paragraph is also valid for optical WDM communications. The planning tools in the field of the optical communication systems and networks span a broad range of platforms, systems, languages, functionalities and applications. Some of the tools are oriented to the industry, whereas other ones are developed in the academy for educational and research purposes. Inside this last category, the Technical University of Cartagena (*Universidad Politécnica de Cartagena, UPCT, Spain*) has developed a optical planning tool called *MatPlanWDM* [44], [45], [46]. The researching work in thesis forms part of the development process of this planning tool, motivating this annex.

MatPlanWDM tool is an academic network planner devoted to designing and planning multilayer transparent and translucent WDM Networks. The tool is implemented as a *MATLAB*™ toolbox together

with a Graphical User Interface (GUI). The author's MSc Final Year Project [47] together with the MSc Final Year Project [48] constitute the foundations of the tool. The first version was distributed in January 2007 and it was presented in [49]. Current version of the tool (v0.60) can be freely downloaded from [46].

MatPlanWDM consists of four modes that allow different network planning and analysis in optical WDM networks. In any of the four modes, the tool addresses the aforementioned multilayer planning problem in Chapter 1: in the lower layer, the RWA problem is solved; whilst the routing of the traffic demand is computed on top of the virtual topology, in the upper layer. A snapshot of the four modes is provided below:

1. *Design Virtual Topology Layer and Flow Routing Mode ("Static" Mode).* This mode solves the static multilayer problem. In this case, the traffic demand is assumed to be constant along time. As a result, a fixed network plan (expected to be permanent in time) is produced. The input to the planning tool takes the form of a traffic matrix. The output of the tool is the virtual topology layer, defined by the RWA of the *lightpaths*, along with the upper traffic layer, where the routing of the traffic demands over the *lightpaths* is detailed.

2. *What-If Analysis Mode.* The *What If Analysis* functionality allows the user to launch a series of simulations varying the input parameters among a given range (v. g. number of optical transceivers installed at the nodes, number of wavelength channels available at the fibers, traffic load). That automates the realization of more exhaustive comparisons and performance tests. At the end of the simulations, a report is generated summarizing the results

3. *Multi-hour Analysis Mode*. In this mode, the traffic demand is multi-hour, that is, the traffic demand changes along time following a variation known in advance. Then, the traffic can be modeled as a temporal series of traffic matrices, corresponding to multiple time intervals, like hours. Therefore, in this scenario the traffic demand is entered as a sequence of matrices to the planning process.

4. *Dynamic Analysis Mode.* In this analysis, the traffic demand varies randomly with no *a priori* deterministic knowledge. For this case, a discrete event driven simulator invokes a traffic generator for scheduling the random connection requests arrivals and terminations

MATLAB™ was selected as the core platform to develop *MatPlanWDM* due to its powerful mathematical framework and flexibility. *MATLAB*™ allows the implementation, testing and execution of complex mathematical algorithms comparatively faster than other platforms. Its inherent flexibility eases the upgrading processes and the integration with other programming languages.

MatPlanWDM was specifically designed to permit the users to extend it by adding their own planning algorithms. This is a particularly useful feature in the research and academic world. To integrate a new planning algorithm into *MatPlanWDM*, the user has two options: i) starting from any of the classical planning algorithms included in the libraries freely distributed with the tool; or, ii) starting from scratch by developing his/her own planning algorithm. In any of both cases, the integration of the user's files requires solely to save them in specific directories.

In the next sections, a more detailed description is provided in those *MatPlanWDM* modes developed as a part of this thesis: *"Static" Mode*¸ *What-If Analysis Mode* and *Multi-hour Analysis Mode*. And, finally, an overview about other academic planning tools concludes this appendix.

A.2 "Static" mode

*"Static" (*or *Design Virtual Topology Layer and Flow Routing) Mode* addresses the static multilayer planning problem. This *MatPlanWDM* mode was presented in [49]. Fig. A.1 displays the GUI for this option. The workspace of the GUI is divided into three areas: input parameters area (left side), plot area (center), and results report area (right side).

The input parameters for the planning process are specified in three files:

1. ***Physical topology input parameters file*** (.xml file). This .xml file describes the physical network structure in a text format. The file contains the list of nodes and fiber links in the network. Per node information is composed of the node *X* and *Y* coordinates measured in kilometers over a Euclidean plane, number of E/O transmitters, O/E receivers, number of WCs (Wavelength Converters), node population, node type (or node level) and node time zone. Node level and node population information are used by the *Traffic generation GUI* included in MatPlanWDM, to generate realistic traffic matrices making use of population-distance models [104]. Per link information is the maximum number of wavelengths per link. MatPlanWDM incorporates a *GUI* in the *Tools* menu named *Topology Designer* to support the design of physical topology .xml files, in a graphical way. Fig. A.2 provides a snapshot of the physical topology generator workspace.

2. ***Traffic demand file*** (.traff file). The *.traff* file contains the traffic matrix used as traffic demand, stored in a text format. Each element of the traffic matrix represents the average traffic offered between each node pair (measured in Gbps). Random traffic matrixes can be generated with different distributions and stored into *.traff* files with the *Traffic generation GUI* accessible from the *Tools* menu. Fig. A.3 shows the *Traffic generation* interface window. A uniform distribution

from 1 to 10 Gbps for each matrix coordinate is employed in the figure example. In addition, the traffic matrixes can be normalized in different ways (see [46] for details). In the example of Fig. A.3, the Total Normalization to the value of 350 Gbps is applied. That means that the traffic matrix is multiplied by the appropriate constant so that the total traffic offered to the network sums 350 Gbps. *MatPlanWDM* supports the training of the students in the use of different types of traffic normalization, which is a common instrument to generate realistic traffic matrixes in network planning methodology.

3. ***Planning algorithm module*** (matlab .m file). A planning algorithm module is a *.m* file which implements the planning algorithm. The implementation by the user of new algorithms has been facilitated in *MatPlanWDM*, incorporating a set of libraries of classical network optimization algorithms. The user can observe the algorithms' codes in the toolbox and use them as templates in the development of their own proposals. The user can also select to use a MILP (Mixed Integer Linear Programming) search of the optimum solution instead of a heuristic planning algorithm. The MILP-optimization algorithm integrated in the tool can be tuned in two ways: allowing or not wavelength conversion, traffic losses, or multi-lightpath between nodes; and varying the different weights of the components of the objective function to optimize. Moreover, users can choose between the two different *solvers*: a commercial *solver* (*TOMLAB™/CPLEX*) [53] or an open-source one (GLPK, GNU Linear Programming Kit, included in the MatPlanWDM distribution) [54]. In the former case, optimum solutions have been obtained for topologies of up to 14 nodes, in an Intel© Core© i5 M430 2.27 GHz processor and 4 GB of RAM. In the example shown in Fig. A.1, we choose a "testing algorithm" without input parameter. The "testingAlgorithm1" is a built-in simple RWA algorithm. The reader can check [46] for a complete list of heuristic algorithms distributed with the tool.

Once input data have been entered, the user should click the *Design* button to trigger the algorithm execution. The planning algorithm must produce a *netState MATLAB™ struct*, and return it to the *MatPlanWDM* kernel. The detailed fields in this *struct* are described in [46]. In summary, the planning information returned is: (i) the set of lightpaths to establish together with their physical route in the network, and (ii) the routing of the higher-layer electronic traffic on top of the virtual topology of lightpaths.

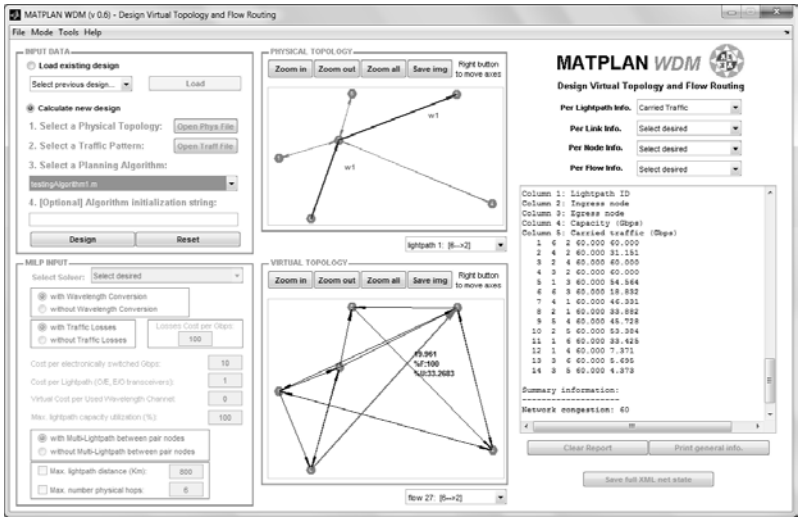

Fig. A.1. “Static” Mode GUI

After the algorithm completion, the solution can be observed in the GUI panels, or saved in a *.xml* results file for later use. In the GUI, the *Physical Topology* panel displays the solution to the RWA problem calculated by the planning algorithm: the set of planned lightpaths and its route on top of the optical fibers. User can select a planned lightpath. Then its traversing fibers and the transmission wavelengths in each hop are highlighted.

Below, the *Virtual Topology* panel shows the routing of the traffic flows on the top of the VT. The user can select a traffic flow. Then, the set of traversed lightpaths from flow ingress to egress node are highlighted. Interestingly, the comparison between both panels helps to comprehend the *multi-layer network* concept: the traffic flows are routed over the lightpaths (upper layer), and the lightpaths are routed over the optical fibers (lower layer).

The *Results Report Area* collects indicators of the WDM network cost and performance that allow the comparison among different solutions. The cost indicators inform about the number of used resources (i.e. number of transmitters, or converters). The performance indicators provide relevant values like the network congestion, measured as traffic carried by the highest loaded lightpath. Finally, physical impairment indicators give an insight into the optical signal impairments suffered by each lightpath: number of traversed fibers, propagation distance, number of wavelength conversions suffered. The three types of indicators are relevant in RWA planning. All this information is accessible from the different kinds of report provided by the tool.

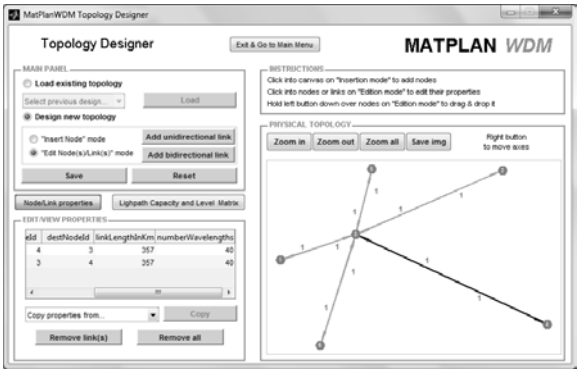

Fig. A.2. Snapshot of the topology designer workspace.

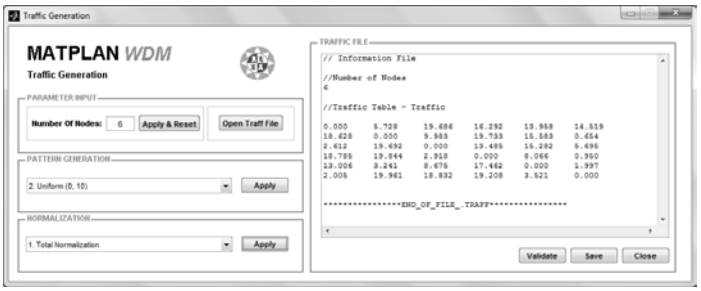

Fig. A.3. Snapshot of the of the traffic generator workspace.

A.3 What if analysis mode

The *MatPlanWDM What-if analysis* GUI can be used to design series of tests of one algorithm under different input parameters, and comparisons among different heuristic algorithms, or against optimum MILP algorithms (in small topologies). Algorithm comparison and exhaustive tests are a relevant part of the planning methodology.

Fig. A.4 displays the workspace window, which contains (i) an *input data* panel to define the series of tests, (ii) a *physical topology* panel to plot the physical topology, (iii) a text field for report, and (iv) the *performance curves* panel that will contain the performance curves generated.

Before launching a "What-If" analysis, the user must define the parameters simulation. Like in the previous Section, network topology, traffic demand matrix and planning algorithms must be entered by selecting the proper ***physical topology input parameters file*** (*.xml* file), ***traffic demand file*** (*.traff* file)

and one or more ***planning algorithm modules*** (matlab *.m* file), respectively, in the *input data panel*. In this mode, more than one planning algorithm can be selected for the test. That permits the user to compare the merits of different approaches to solve the same problem. Besides, these basic input data, it is necessary to select the parameters to sweep and set up the sweeping range for them. The tool allows sweeping up to two input parameters simultaneously. This can only happen for those analyses that select one unique planning algorithm. Otherwise, the *2nd parameter sweeping* is disabled.

The input parameters that can be varied as first or second sweep parameter are the number of transmitters, receivers or converters per node, the number of wavelengths per fiber, the lightpath capacity in Gbps, and a multiply factor to the traffic demand. The sweeping range is defined by setting up (i) the lower limit as a percentage over its current value, (ii) the sweep step as a percentage over its current value, again, and (iii) the number of sweep points. The total number of simulations to run is, trivially, the product of the number of points of the two sweeping parameters. In case of several planning algorithms are selected, the total number of simulation points is the product of the number of sweep points of the one unique parameter and the number of the planning algorithms.

Once that all the simulations of the *What-If* Analysis have been completed the details of the results obtained can be observed in the text report in the upper right text field. Nevertheless, the more intuitive manner to observe the comparison results is by the performance curves generated. The user can select 8 different graphs to plot 8 different performance metrics: (i) percentage of carried traffic, (ii) average number of virtual hops, (iii) network congestion, (iv) percentage of single hop traffic, (v) number of established lightpaths, (vi) average number of used wavelength channels, (vii) average number of used wavelengths per fiber, and (viii) average propagation delay. The user may use these graphs to assess the merits of the different algorithms. For instance, Fig. A.4 shows the performance curves generated for the metric of percentage of single-hop traffic (traffic that only traverses one lightpath). One curve is plotted for each algorithm, showing the evolution of the performance with the number of transmitters. Selecting different metrics may vary the performance observed in the algorithms. This functionality helps the user to study the trade-offs that appear in network planning, as optimizing one performance metric usually implies the sub-optimization of others.

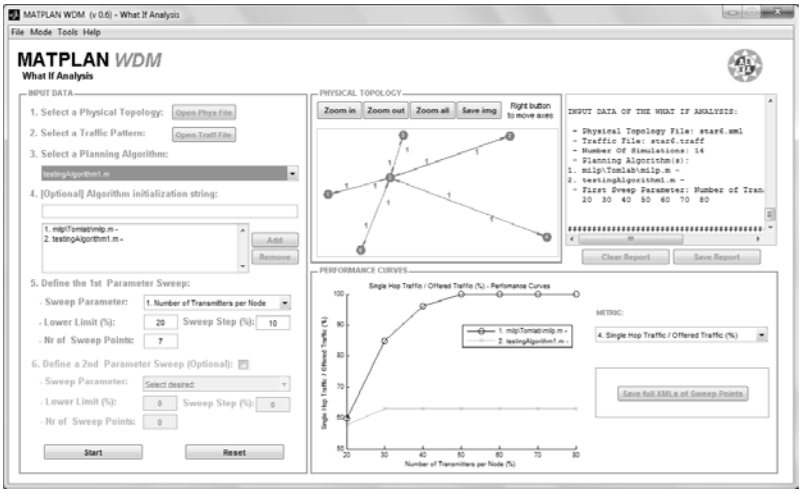

Fig. A.4. GUI of the What-If Analysis functionality.

A.4 Multihour analysis mode

In [50], the multi-hour planning mode of the *MatPlanWDM* was presented. This mode allows the user to test planning algorithms which react to changes in the traffic demands which follow a multi-hour pattern. In a trivial multi-hour traffic pattern, the traffic between every node-pair have the same peak-traffic times and low-traffic times. However, interesting traffic patterns where peak and low traffic times differ for different node pairs appear in backbone networks that span over large geographical areas, where network nodes are situated in different time zones. The Multi-hour analysis GUI in MatPlanWDM tool is devoted to illustrate and address these cases.

Fig. A.5 displays the multi-hour interface window, which contains (i) an *input data* panel to enter the input parameter of the multi-hour analysis, (ii) a *physical topology* panel to plot the physical topology, (iii) a *virtual topology* panel to plot the virtual topologies computed for each hour, and a (iii) a text field for reports.

In the input data panel (left-up side) the user selects (i) the ***physical topology input parameters file*** (.xml file), (ii) one single ***traffic demand file*** (.traff file), and (iii) the multi-hour ***planning algorithm module*** (matlab .m file). The information about the location of the nodes, that is, the time zone where the node is, is contained in the ***physical topology input parameters file*** (.xml file). The time zone of each node is represented as the time offset respecting to Universal Time Coordinated (UTC).

When all the input parameters have been entered and the user has pressed the *start* button, the multi-hour optimization proceeds following the next steps:

1. The multihour traffic ($H = \{ h^t , t \in T \}$) is computed as a sequence of 24 traffic matrices, one matrix per hour in a day, using the UTC as reference time zone. The traffic matrix for the current UTC hour (t) is computed from the traffic matrix contained in the .traff file, applying the Linearity to Provider and Consumer (LPCA) methodology in [156].
2. The planning algorithm is executed by passing as input parameters the selected physical topology, and the multihour traffic H. The algorithm is responsible for calculating the *netState MATLAB™ struct*. Note that algorithms that react to changes in the traffic matrixes in any way can be implemented and tested under this scheme. For instance, algorithms can favor solutions that do not reroute lightpaths, or that do not reroute flows, or any other constraint.

After the simulation is completed, per-hour reports can be examined in the *Performance reports* panel by selecting the appropriate time at the *Hourly metrics* selector. Per node information reports can be generated that summarize the evolution of one selected metric across the nodes and along time. That provides fast access to relevant information like the time evolution in the number of used transmitters, receivers or converters.

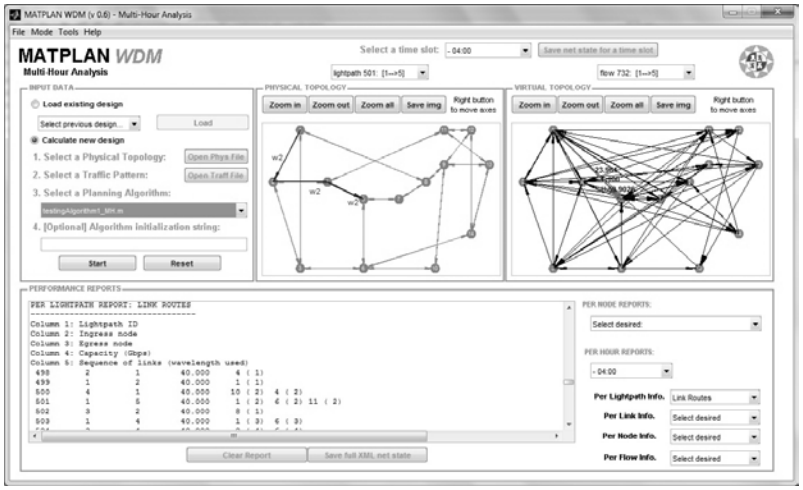

Fig. A.5. GUI of the Multi-hour Analysis mode.

A.5 State of the art in non commercial tools

This Section briefly overviews some relevant non-commercial planning tools, for WR networks, which can be used for educational purposes. Naturally, a wide range of commercial applications also

exists (i.e.[161], [162]and[163]). Nevertheless, these tools are not designed for academic use: their underlying algorithmic details are not publicly available, and cannot be extended by the students. Therefore, they are out of the scope of this thesis.

A notable educational tool is the *Optical WDM Network Simulator* (*OWns*)[164], developed at the Washington University, as a framework built on top of the well-known network simulator *ns*[165]. Unfortunately, *OWns* upgrading stopped in 2001. The *OWns* tool facilitates the study of switching and routing schemes in WDM networks. It tries to incorporate the key characteristics of WDM networks, such as optical switching architectures, virtual topology design, related switching schemes and routing algorithms. In opposition to *OWns*, the MatPlanWDM tool is specifically focused on the optimization algorithm design. When compared to MatPlanWDM, the benefits of our proposal are based on the more powerful framework that MATLAB provides due to its mathematical functionality and flexibility. All this helps to simplify the algorithm implementation and clarify to the student the planning concepts addressed.

A planning tool more focused on the field of the WDM Network Design is the GMPLS Lightwave Agile Switching Simulator (GLASS)[166], built as an evolution of the MERLiN (Modelling Evaluation and Research of Lightwave Network) project, which was discontinued in 2001[167]. The GLASS tool was developed at the National Institute of Standards and Technology (NIST). It is implemented in Java, and designed on top of the SSF/SSFNet [166] discrete event simulation framework. GLASS uses the Data Modeling Language (DML) [166] to design the topology and derive scripts for the different simulation scenarios and components. The GLASS core is designed as a command-line simulator that reads its simulation setup from a script and writes dumps in binary files that can be processed by customized readers. GLASS is of free use, and its last public version update occurred in March 2006. The MatPlanWDM approach offers some advantages when compared to GLASS tool. First, GLASS requires training in a complex class hierarchy of Java classes to allow the definition and testing of new optimization algorithms. Second, Java language does not offer the mathematical functionality that MATLAB provides for a fast implementation of complex algorithms. As a result, MatPlanWDM allows an easier and faster implementation of the simulations, concentrating on the essential skills required in network planning methodology.

Finally, Delite [104] is a non-WDM specific network planning educational tool. It follows a similar philosophy of the MatPlanWDM tool, offering a set of planning algorithms for evaluation and comparison, under different traffic patterns and network topologies. Delite is implemented in C language, it is open source, extensible, and purely designed for academic purposes. However, Delite tool neither consider the specifics of the RWA planning problem, nor provide any optimum search for comparison. In addition, when compared to MatPlanWDM tool, the advantages of the MATLAB language for the

implementation of more complex mathematical operations are again made evident.

Annex B

B Traffic Domination Applied to Multihour Planning

ABSTRACT: This annex summarizes the theoretical basis of traffic domination variants employed in the thesis and outlines a collateral contribution in general communication networks. First, the domination between two matrices is introduced, along its variants employed in the 3-Step-D algorithm presented in [30]. Next, the generalization of the previous domination types to apply to sets of traffic matrices is presented. Finally, the general scheme in [39] to apply the domination between sets of matrices in general communication network problems is outlined.

B.1 Domination between two traffic matrices

B.1.1 Notation

Let N be the set of nodes in a network graph $G(N,E)$, being E the set of unidirectional links in the network. The initial and end nodes of link e will be denoted by $a(e)$ and $b(e)$ respectively. Also, we denote as $\delta^+(n)$ and $\delta^-(n)$ the set of links outgoing from and incoming to node n respectively. Let D denote the set of traffic demands in the considered network. Each demand $d \in D$ is characterized by its end nodes $a(d)$ and $b(d)$, and its traffic volume h_d. The vector of traffic volumes for all demands is equal to $h=(h_d, d \in D)$ $(h \in R_+^{|D|})$. Note that in this notation, we use a vector representation of the concept of traffic matrix, with one coordinate per demand. This is a more general representation of the concept of traffic matrix (where one demand type would exist for each input-output node pair). Thus, in this Annex the expression *traffic vector* can be safely assumed by the reader to refer to the same traditional concept of *traffic matrix*.

A capacity allocation $u=(u_e, e \in E)$ in the graph $G(N,E)$ is a vector in $R_+^{|E|}$ that assigns a non-negative capacity u_e to every link $e \in E$. Both the traffic vector and the capacity vector are supposed to be measured in the same traffic units, which may depend on the underlying technology being modeled (e.g. Gbps, Erlangs). Given a network graph $G(N,E)$, and a set of demands D, we define a flow allocation pattern (i.e. a traffic flow routing) as a vector $x=(x_{de}, d \in D, e \in E) \in R_+^{|D||E|}$, where each x_{de} represents the fraction (in the interval [0,1]) of traffic volume of demand d traversing link e. Routing can be splittable or unsplittable. In this model, flow routing x is unsplittable if it is integer, that is, if $x_{de} = \{0,1\}$, $d \in D$, $e \in E$.

Finally, we say that a capacity vector *u supports* a traffic vector h if there exists a feasible routing

vector x which enables all the traffic in h to be carried over u. Then, the set of capacity vectors u supporting a given traffic vector h is denoted as $U(h)$, whereas set of capacity and routing pairs (u,x) supporting h is represented by $UX(h)$.

B.1.2 Definitions and Properties

Formal definitions of the types of domination between traffic matrices applied in this thesis, called *weak* and *total* domination, are extracted from [41]:

Definition B.1.1: Let h and h' be two traffic vectors. We say that traffic vector h *weakly dominates (*or simply *dominates)* h' if $U(h) \subseteq U(h')$. In other words, h *dominates* h' if for any capacity vector u supporting h, then there exists at least one routing x such that (u, x) also supports h'.

Proposition B.1.1*: Let h and h' be two traffic vectors, h dominates h' if and only if h (considered as capacity vector) supports h'. Considering h as a capacity vector means constructing a network G(N,D) with one link e, for every demand* $d \in D$*, so that the capacity* u_e *of link e is given by the demand volume* h_d*.*

Proof: See [41].

Definition B.1.2: Let h and h' be two traffic vectors. We say that traffic vector h *totally dominates* h' if $UX(h) \subseteq UX(h')$. In other words, h *totally dominates* h' if any capacity and routing pair (u, x) supporting h, also supports h'.

Proposition B.1.2*: Let h and h' be two traffic vectors, h totally dominates h' if and only if* $h_d \geq h'_d$*, for any demand* $d \in D$.

Proof: See [41].

The difference between *total* and *weak* domination comes from the flow routing perspective. If a traffic vector h totally dominates another traffic vector h', then any capacity and routing pair (u, x) that

supports *h* also supports *h'*. If the domination is weak, then finding a capacity *u* and a routing *x* supporting *h* guarantees that capacity *u* is enough to carry the traffic *h'*, but does not guarantee that it can be done with the same routing *x*. Naturally, *total* domination is a stronger condition, which implies *weak* domination.

A second variation of weak domination was also considered in [41], *weak domination with respect to unsplittable flows*:

Definition B.1.3: Let *h* and *h'* be two traffic vectors. We say that traffic vector *h* (*weakly*) *dominates h with respect to unsplittable flows* if for any capacity vector *u* supporting *h* with unsplittable flows, then there exists at least one unsplittable routing vector *x* such that (*u*, *x*) also supports *h'*.

Proposition B.1.3*: Let h and h' be two traffic vectors, h (weakly) dominates h' with respect to unsplittable flows if and only if h (considered as capacity vector) supports h' by unsplittable flows.*

Proof: See [41].

Note that the general (*weak*) domination case applies to general (and, thus, splittable) routing. Also, note that if a traffic vector *h* totally dominates another vector *h'*, the capacity *u* and routing *x* which is feasible for *h* is also feasible for *h'*, whether the routing is splittable or not.

B.2 Domination between sets of traffic matrices

B.2.1 Notation

The same notation as B.1 is assumed, and some definitions related to set of traffic matrices (or vectors) are added.

A MH traffic demand is a finite set of traffic vectors $H=\{h^1, h^2, \ldots, h^T\}$. Such a set can represent traffic vectors that have to be supported by the network at different time intervals $t=1,\ldots,T$. We denote as *conv*(*H*) the convex hull of *H*: the set of traffic vectors composed as a convex combination of the vectors

in H. For every time interval t, its traffic volume for demand type $d \in D$ is denoted h_d^t, so that $h^t = (h_d^t, d \in D)$.

Given a network graph $G(N,E)$, and a set of demands D, we define now a *static* flow allocation pattern as a vector $x=(x_{de}, d \in D, e \in E) \in R_+^{|D||E|}$, where each x_{de} represents the fraction of traffic volume of demand d traversing link e. Similarly, a *dynamic* flow allocation pattern is a vector $x=(x_{det}, d \in D, e \in E, t \in T) \in R_+^{|D||E||T|}$. We denote as x^t the flow allocation vector at time interval t, $x^t=(x_{det}, d \in D, e \in E) \in R_+^{|D||E|}$.

B.2.2 *Generalized* Multi-Hour Static Routing (MHSR) problem

The so-called *generalized* MHSR problem may be described by (B.1)-(B.4):

$$\text{Find } (u,x), u \in \Re_+^{|E|}, x \in \Re_+^{|D||E|}$$

$$\text{Min } g(u,x), \text{s.t.} \tag{B.1}$$

$$\sum_{d \in D} x_{de} h_d^t \le u_e, e \in E, t = 1,...,T \tag{B.2}$$

$$\sum_{e \in \delta^+(n)} x_{de} - \sum_{e \in \delta^-(n)} x_{de} = w_{dn}, d \in D, n \in N \tag{B.3}$$

$$(u,x) \in Y \tag{B.4}$$

Initially, no assumption is made about the cost function g in (B.1). Constraint (B.2) represents capacity requirements: capacity of every link must be sufficient to support the traffic load induced by any traffic vector in H. Constraint (B.3) is the flow conservation constraint. The expression w_{dn} is given by (B.5):

$$w_{dn} = \begin{cases} 1 \text{ if } n = a(d), \\ -1 \text{ if } n = b(d), \\ 0 \text{ otherwise} \end{cases}, d \in D, n \in N \tag{B.5}$$

Finally, constraint (B.4), where Y is some subset (proper or not) of $R_+^{|E|} \times R_+^{|D||E|}$, is a placeholder for possible extra constraints that could be defined for the problem, limiting the set of feasible solutions $(u; x)$. As an example, non-bifurcated routing can be defined through $Y=R_+^{|E|} \times \{0,1\}^{|D||E|}$, and integral capacity through $Y=Z_+^{|E|} \times R_+^{|D||E|}$. When no additional constraints are assumed, i.e., when $Y=R_+^{|E|} \times R_+^{|D||E|}$, constraint

(1d) is skipped.

B.2.3 *Generalized* Multi-Hour Dynamic Routing (MDSR) problem

The *generalized* MHDR problem is defined in (B.6)-(B.9):

$$\text{Find } (u,x) = (u, x^1, ..., x^T), u \in \Re_+^{|E|}, x^t \in \Re_+^{|D||E|}, t = 1,...,T$$

$$\text{Min } g(u,x), \text{s.t.} \tag{B.6}$$

$$\sum\nolimits_{d \in D} h_d^t x_{\text{det}} \le u_e, e \in E, t = 1,...,T \tag{B.7}$$

$$\sum\nolimits_{e \in \delta^+(n)} x_{\text{det}} - \sum\nolimits_{e \in \delta^-(n)} x_{\text{det}} = w_{dn}, d \in D, n \in N, t = 1,...,T \tag{B.8}$$

$$u \in Y \tag{B.9}$$

The expressions in (B.6)-(B.8) are a trivial adaptation of (B.1)-(B.3) to the case in which the flow allocation *x* can change along time. A more significant difference appears in (B.9). This extra constraints in (B.6)-(B.9) affect uniquely to the capacity variables. This is a technical requirement for the sufficient condition for traffic domination shown later to hold. Note that (B.9) prevents the application of these techniques to the non-bifurcated routing variant of the MHDR problem.

B.2.4 Definitions and Properties

Formal definitions of the types of domination between set of traffic matrices applied in this thesis are extracted from [42],[43]:

Definition B.2.1: Let *H* and *H*' be two MH traffic demands for a given generalized MHSR problem (B.1)-(B.4), defined by a set of demands *D* and a set *Y* of extra constraints. We say that *H totally dominates H*' if, and only if every network design (*u*,*x*) suitable for MH demand *H* is also a valid design for the MH demand *H*' in problem (B.1)-(B.4).

The following proposition from [42],[43] states a *sufficient condition* for *total* domination to occur in generalized MHSR problems.

Proposition B.2.1*: In the same conditions described above, if for every vector h'∈H' there exists a vector* $h^* \in conv(H)$ *such that* $h^* \geq h'$*, then H totally dominates H'.*

Proof: See [42],[43].

In [43], it is shown that if certain technical properties are met, the condition in the previous proposition is also necessary.

We illustrate the geometrical interpretation of the concept of total domination between MH traffic demand sets with an example in Fig. B.1. Let $H = \{h^1, h^2, h^3, h^4, h^5\}$ be a set of 5 traffic vectors for a network $G(N, E)$. To ease the graphical representation, let us suppose that all the traffic vectors in H are exactly equal, except for the different values observed in the coordinates of two particular demands $d_1, d_2 \in D$ (which correspond e.g. to two different input-output node pairs). For a traffic vector h^i, the values in the d_1 and d_2 demands are represented in the pair of coordinates (a_i, b_i) in Fig. B.1. Fig. B.1 plots in a plane the (a_i, b_i) points, $i = 1,...,5$, corresponding to the 5 vectors of the set. Also, the points $P^i = (0, \max\{b_i\})$ and $P^{i'} = (\max\{a_i\}, 0)$ represent the maximum values in the two coordinates of the traffic vector h^i.

In this example, the vectors which are totally dominated by a traffic vector h^i are those whose (a_i, b_i) positions fall within the rectangle of vertices $\{(a_i, b_i), (0, b_i), (a_i, 0), (0, 0)\}$. For instance, traffic vector h^4 is totally dominated by h^1 and also is totally dominated by h^2. There is no single traffic vector in the set $\{h^1, h^2, h^3, h^4\}$ which totally dominates the vector h^5. However, note that h^5 is totally dominated by the set of traffic vectors $\{h^1, h^2, h^3\}$, as there is a convex combination of the vectors $\{h^1, h^2, h^3\}$ that totally dominates h^5. In the figure, we see that the traffic vector $0h^1+0.5h^2+0.5h^3$ totally dominates h^5. The shaded area in Fig. B.1 delimits the traffic vectors that are totally dominated by the set $\{h^1, h^2, h^3\}$. Considering the proposition 1, if the shaded area contained each of the traffic vectors of a set (e.g. set $\{h^4, h^5\}$), the set is totally dominated by the set $\{h^1, h^2, h^3\}$.

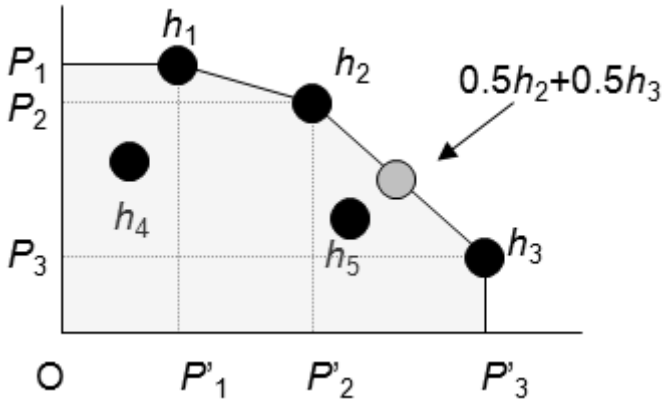

Fig. B.1. Graphical representation of the total domination relation

Definition B.2.2: Let *H* and *H*' be two MH traffic demands for a given generalized MHDR problem (B.6)-(B.9), defined by a set of demands *D*, and a set *Y* of extra constraints. We say that *H dominates H*' if and only if every capacity vector *u* for which a valid time varying flow allocation *x* exists so that (*u*,*x*) supports the MH demand *H*, is also a valid capacity vector for the MH demand *H*' in problem, potentially using a different time varying flow allocation *x*'.

The following proposition from [42] states a *sufficient condition* for traffic domination to occur.

Proposition B.2.2: *For general MH traffic demands H and H', if* $\forall h' \in H'$*, there is a (potentially different) traffic matrix* $h^* \in conv(H)$ *so that* h^* *dominates h', then H dominates H'.*

Proof: See [42].

B.3 Application of the domination between sets of traffic matrices to the multihour planning

This Section presents the basic foundations of the reduction complexity techniques proposed in [39] to address multihour network planning, such as the MHSR and MHDR problems presented in Subsections B.2.2 and B.2.3, respectively. These techniques take advantage of the domination relation between sets of traffic: (i) the *total domination* as defined in **Definition B.2.1** is used for the MHSR problem; and, (ii) the (*weak*) *domination* as defined in **Definition B.2.2** is applied to the MHDR problem.

The domination concepts are applied to transform huge multihour traffic demands into sets with a small number of matrices, but guarantying that the network designed for the simplified series is suitable for the original one. Also, the domination relation may be used to derive lower bounds to the suboptimality incurred by simplifying the traffic demand.

B.3.1 Network design using an Upper Bound Traffic Demand

Multihour network design is fed by series of traffic matrices with a potentially large number of matrices. It can be of interest to replace such large set of traffic matrices by a smaller set with a lower number of elements. That smaller set could be used as an input to an algorithm solving the MHSR or MHDR problem, but allowing some potential suboptimality to arise.

The domination property helps us in this task. Given a potentially large set of traffic vectors H, we could search for a smaller set of vectors H^U (usually, $|H^U|<<|H|$) that *totally* (or *weakly*) dominates H. Then, any design obtained in the MHSR (or MHDR) problem for the reduced set H^U is a suitable planning design for the original traffic H.

If g is a cost function not directly dependent on the traffic vectors (for instance, an arbitrary function on the capacity planned u), then it holds that the cost of any design suitable for the H^U set is an upper bound to the optimal cost of the original problem. For this reason, we name the MH demand H^U as an *upper bound traffic demand* (UBTD) belonging to the *upper bound traffic demand* set of H ($H^U \in UBTD(H)$).

B.3.2 Cost lower bound using a Lower Bound Traffic Demand

Again, let H be a MH traffic demand and g be a cost function not directly dependent on the traffic matrices H. It is possible to use the domination property to derive lower bounds to the optimal cost of the MHSR or MHDR planning problems.

The method is based on calculating a new multi-hour traffic demand set H^L, so that H^L is dominated by the original set H (usually, $|H^L|<<|H|$). Again, total domination is required in the MHSR problem, while (weak) domination applies to the MHDR problem. Thanks to the domination property, every solution to the original problem is also a solution to the reduced problem, although the opposite statement is not necessarily true. Furthermore, under the same conditions showed in the previous subsection, the optimal cost of the MH problem for the demand H^L is a lower bound to the optimal cost of the original problem. Thus, the design obtained for the MH demand H^L is an infeasible solution for the original problem, but its optimal cost is a suitable lower bound for the optimal cost of the original problem. For this reason, we name the MH demand H^L as a *lower bound traffic demand* (LBTD), an element in the

lower bound traffic demand set of H ($H^L \in LBTD(H)$).

B.3.3 Bound to the suboptimality caused by the transformation of the demand set

The Subsection B.3.1 provides a technique for solving the MHSR and MHDR problems for a demand H, by first calculating a simplified demand $H^U \in UBTD(H)$, and then solving the target problem for the demand H^U. As a general rule, H^U demands with a small number of traffic vectors are preferred, as they imply less computational resources for solving the target problem. This raises the interest on measuring the maximum suboptimality we are incurring. That is, an upper bound to the extra planning cost that is directly caused by using the H^U demand instead of the original H demand. Herein we provide a technique for this case.

Let H^U and H^L be respectively an UBTD and a LBTD for a given MH traffic demand H, so that $|H^U| = |H^L|$. Let g be an arbitrary subadditive function of the planned capacity. That is: $g(u_1+u_2) \leq g(u_1)+g(u_2)$, u_1,u_2 capacity vectors in (B.1)-(B.4) or (B.6)-(B.9). Linear functions, norms and square roots are examples of such subadditive functions. Moreover, the conventional cost models that reflect the economy of scale principle for the capacity in the links fall into this category.

Let u_D^*, u_U^* and u_L^* be optimal capacities for the MH problems with H, H^U and H^L demands respectively, and let $c_D^* = g(u_D^*)$, $c_U^* = g(u_U^*)$ and $c_L^* = g(u_L^*)$ be their associated optimal costs. Then, the extra suboptimality we are incurring because of the simplification of the traffic demand is given by $\Delta c^* = c_U^* - c_D^*$.

In the following, we present a technique which is suitable for giving a bound to Δc^* even when only approximated solutions to the MHSR (MHDR) can be calculated for the simplified demands.

We say that a MH traffic demand H^E is an *excess traffic demand* (ETD) for the demands H^U and H^L, and we denote it as $H^E \in ETD(H^U,H^L)$, if and only if (i) $|H^E| = |H^U| = |H^L|$, and (ii) H^L+H^E (*totally* or *weakly*) dominates H^U. Note that the addition operation applies in this context to *sets of traffic vectors*. This assumes that the traffic vectors in the sets H^U, H^L and H^E are ordered in a series, and that the i-th vector of the aggregated series H^L+H^E is equal to the sum of the i-th vector of H^L ($h^L{}_i$) and the i-th vector of H^E ($h^E{}_i$). In short words, H^E is a traffic demand, that when aggregated to the lower bound demand, (*totally* or *weakly*) dominates the upper bound demand. The following proposition shows that, once H^E is calculated, it can be used to bind the suboptimality Δc^*.

Proposition B.3.1*: The cost gap Δc^* is lower than the cost $c_E = g(u_E)$, being u_E a (non-necessarily optimal) capacity solving the MHSR (MHDR) problem for the excess traffic demand H^E.*

Proof: See [39].

B.3.4 General structure of the algorithms

The basic notions introduced above are used in [39] to implement heuristic algorithms able to generate the simplified sets of traffic matrices UBTD, LBTD and ETD from a given MH traffic demand *H*. This subsection outlines the general structure of these methods. A detailed description of them along with the results of the experiments conducted to assess its performance may be consulted by the interested reader in [39].

Given a MH traffic demand *H*, we are interested in calculating convenient UBTD, LBTD and ETD demands composed of *K* matrices each. The algorithms are based on (i) the distribution of the traffic matrices into *K* clusters, and then (ii) iteratively adapting the centroids of the clusters till they (totally) dominate/are dominated by the original traffic series. A similar sequence of four steps is proposed for the MHSR and the MHDR case:

- Step 1: Partition the MH traffic demand *H* into *K* clusters C^1, ..., C^K (with possibly different number of vectors each), according to a clustering technique, such as the Criticalness Aware Clustering Algorithm (CritAC) [168] or conventional clustering techniques like *K*-means. For each cluster C^k, $k = 1, ..., K$ we compute its representative traffic vector c^k, named *centroid*. The centroid is calculated as the convex combination of the vectors in the cluster with the same coefficient $(1/|C^k|)$ for each term. The set of centroids is denoted as *C* (note that $|C| = K$).
- Step 2: Generate the MH demand H^U by iteratively modifying the *K centroids* until they totally dominate *H*.
- Step 3: Generate the MH demand H^L by iteratively modifying the *K centroids* until they are totally dominated by *H*.
- Step 4: Compute a convenient excess traffic demand $H^E \in ETD(H^U, H^L)$.

Fig. B.2 illustrates graphically the steps 2 and 3 of the process in the MHSR case (total domination). The shaded area corresponds to the traffic vectors totally dominated by the original MH traffic demand.

The target of the method is the modification of the initial centroids $\{c_1, c_2\}$, to obtain the LBTD $H^L = \{h^{L1}, h^{L2}\}$ (Fig. B.2 (a)) and the UBTD $H^U = \{h^{U1}, h^{U2}\}$ (Fig. B.2(b)).

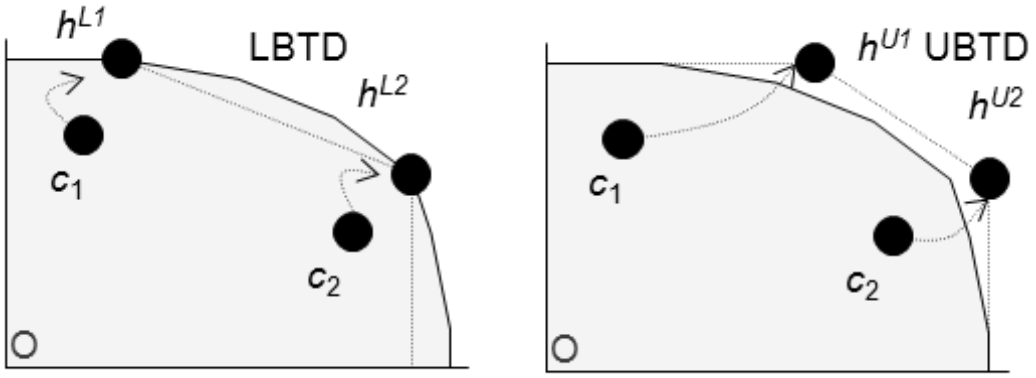

(a) (b)

Fig. B.2. Graphical representation of the centroid movement in the algorithm, (a) LBTD, (b) UBTD

References

[1] B. Mukherjee, *Optical WDM Networks*, Springer Science+Business Media, Inc., New York, 2006.

[2] NTT, "World Record 69-Terabit Capacity for Optical Transmission over a Single Optical Fiber," NTT Press release, March 2010, http://www.ntt.co.jp/news2010/1003e/100325a.html.

[3] R. S. Tucker, "The role of optics and electronics in high-capacity routers," J. Lightw. Technol., vol. 24, pp. 4655–4673, Dec. 2006.

[4] Cisco Systems, Inc., "Cisco CRS Carrier Routing System 16-Slot Line Card Chassis System Description," Cisco Systems, Inc., October 2010

[5] T. S. El-Bawab, Optical Switching, Springer Science+Business Media, Inc., New York, 2006.

[6] B. Ramamurthy, D. Datta, H. Feng, J. P. Heritage, and B. Mukherjee, "Transparent vs. opaque vs. translucent wavelength-routed optical networks," in Proc. .OFC, 1999, pp. 59–61.

[7] H. Zang, J. P. Jue, and B. Mukherjee, "A Review of Routing and Wavelength Assignment Approaches for Wavelength-Routed Optical WDM Networks," *Optical Network Magazine*, pp. 47-59, Jan. 2000.

[8] B. Mukherjee, S. Ramamurthy, D. Banerjee, A. Mukherjee. "Some Principles for Designing a Wide-Area WDM Optical Network," *IEEE/ACM Transactions on Networking*, Vol. 4, No. 5, pp. 684-696, October 1996.

[9] Gagnaire, M. Koubaa, M. Puech, N.: Network Dimensioning under Scheduled and Random Lightpath Demands in All-Optical WDM Networks. *IEEE Journal on Selected Areas in Communications*. Vol 25, issue 9, pag. 58-67. December 2007.

[10] S. Baroni, P. Bayvel, R.J. Gibbens, S.K. Korotky, "Analysis and design of resilient multifiber wavelength-routed optical transport networks," *IEEE/OSA Journal of Lightwave Technology*, vol. 17, no. 5, pp 743-758, May 1999

[11] L. Li, A. K. Somani, "A New Analytical Model for Multifiber WDM Networks," *IEEE Journal on Selected Areas in Communications*, vol. 18, no. 10, pp. 2138-2145, Oct. 2000

[12] M. Saad, Z. Luo, "Reconfiguration With No Service Disruption in Multifiber WDM Networks," *J. Lightwave Technol.*, vol. 23, no. 10, pp. 3092–3104, Oct. 2005

[13] P. Pavon-Marino, R. Aparicio-Pardo, B. Garcia-Manrubia, J. Fernandez-Palacios, O. Gonzalez, F. Martin, and J. Garcia-Haro, "Balancing multifibre and wavelength converter cost in wavelength routing networks," in *Proc. 34th European Conference on Optical Communication, ECOC 2008*, vol. 5, Brussels, Belgium, Sept. 2008, pp. 185-186.

[14] M. Farahmand, D. Awduche, S. Tibuleac, "Characterization and representation of impairments for routing and path control in all-optical networks", D Atlas - Proc., NFOEC, 2002

[15] J. Strand, A. Chiu, "Impairments and Other Constraints on Optical Layer Routing," *Request For Comments 4054*, Network Working Group, At&T, May, 2005.

[16] Phosphorus –Deliverable D 5.3. "Grid Job Routing Algorithms," June 2007, http://www.ist-phosphorus.eu/files/deliverables/Phosphorus-deliverable-D5.3.pdf

[17] S. Azodolmolky, M. Klinkowski, E. Marin, D. Careglio, J. Solé Pareta, and I. Tomkos, "A Survey on Physical Layer Impairments Aware Routing and Wavelength Assignment Algorithms in Optical Networks," in *Comp. Netw.*, vol. 53, no. 7, pp. 926–944, 2009.

[18] G. P. Agrawal, *Fiber-optic communications systems*, 3rd ed. New York:, John Wiley & Sons, Inc., 2002.

[19] S. D. Personick, "Receiver Design for Digital Fiber Optic Communication Systems, I," *Bell Syst. Tech. J*, vol. 52, no. 6, pp. *843-874, July-August* 1973.

[20] B. Garcia-Manrubia, P. Pavon-Marino, R. Aparicio-Pardo, M. Klinkowski, and D. Careglio, "Offline impairment-aware RWA and regenerator placement in translucent optical networks," *IEEE/OSA Journal of Lightwave Technology*, to be published.

[21] P. Pavon-Marino, S. Azodolmolky, R. Aparicio-Pardo, B. Garcia-Manrubia, Y. Pointurier, M. Angelou, J. Sole-Pareta, J. Garcia-Haro, and I. Tomkos, "Offline Impairment Aware RWA Algorithms for Cross-Layer Planning of Optical Networks," *IEEE/OSA Journal of Lightwave Technology*, vol. 27, no. 12, pp. 1763-1775, June 2009.

[22] S.W. Kim and S.W. Seo, "Regenerator placement algorithms for connection establishment in all-optical networks", *IEEE Pro. Commun*, vol. 148, no.1, February 2001.

[23] Xi Yang, Byrav Ramamurthy, "Sparse Regeneration in Translucent Wavelength-Routed Optical Networks: Architecture, Network Design and Wavelength Routing", *Photonic Network Communications*, vol. 10, no. 1, pp 39-53, 2005.

[24] K. Manousakis, K. Christodoulopoulos, E. Kamitsas, I. Tomkos, and E.A. Varvarigos, "Offline impairment-aware routing and wavelength assignment algorithms in translucent WDM optical networks," *IEEE/OSA J. Lightw. Technol.*, vol. 27, no. 12, pp. 1866–1877, Jun. 2009.

[25] G. Charlet, S. Bigo, S., "Upgrade of 10Gb/s network to 40Gb/s, challenges and enabling technologies," in *Proc. ECOC'06*, Cannes, France, Sept., 2006, paper Th.1.6.1

[26] A. Nag, M. Tornatore, B. Mukherjee, "Optical network design with optical with mixed line rates and multiple modulation formats," *IEEE J. Lightw. Technol.*, Vol. 28, No. 4, pp. 466-475, Feb. 2010

[27] R. Aparicio-Pardo, P. Pavon-Marino, S. Zsigmond, "Mixed line rate virtual topology design considering non linear interferences between amplitude and phase modulated channels," *Photonic Network Communications*, under review.

[28] F. Ricciato, S. Salsano, A. Belmonte, and M. Listanti, "Off-line Configuration of a MPLS over WDM Network under Time-Varying Offered Traffic," *IEEE Infocom*, pp. 57-65, 2002.

[29] G. Agrawal and D. Medhi, "Lightpath Topology Configuration for Wavelength-Routed IP/MPLS Network for Time-Dependent Traffic", *Proc. of IEEE Globecom 2006*, San Francisco, Nov-Dec 2006.

[30] P. Pavon-Marino, R. Aparicio-Pardo, B. Garcia-Manrubia, and N. Skorin-Kapov, "Virtual topology design and flow routing in optical networks under multihour traffic demand," *Photonic Network Communications*, vol. 19, no. 1, pp. 42-54, Feb. 2010.

[31] M. Pioro and D. Medhi, *Routing, Flow and Capacity Design in Communication and Computer Networks*. San Francisco, CA: Morgan Kaufmann, 2004, pp. 455–474.

[32] TOTEM Project: Toolbox for Traffic Engineering Methods [Online]. Available: http://totem.run.montefiore.ulg.ac.be/datatools.html

[33] V.R. Konda, T.Y Chow, "Algorithm for traffic grooming in optical networks to minimize the number of transceivers," in *Proc. IEEE Workshop on High Performance Switching and Routing*, Dallas, TX, 2001, pp. 218–221.

[34] K. Zhu, H., Zhu, B., Mukherjee, "Traffic engineering in multigranularity heterogeneous optical WDM mesh networks through dynamic traffic grooming," *IEEE Netw.*, vol. 17, no. 2, pp. 8–15, 2003.

[35] N. Srinivas, C. Siva Ram Murthy, "Design and dimensioning of a WDM mesh network to groom dynamically varying traffic," *Photon. Netw. Commun.*, vol. 7, no. 2, pp. 179–191, 2004.

[36] B. Garcia-Manrubia, R. Aparicio-Pardo, P. Pavon-Marino, N. Skorin-Kapov, and J. Garcia-Haro, "MILP Formulations for Scheduling Lightpaths under Periodic Traffic," in *Proc. 11th International Conference on Transparent Optical Networks, ICTON 2009,* Island of São Miguel, Azores, Portugal, June 2009, p. Tu.C3.4, invited paper.

[37] N. Skorin-Kapov, P. Pavon-Marino, B. Garcia-Manrubia, and R. Aparicio-Pardo, "Scheduled Virtual Topology Design Under Periodic Traffic in Transparent Optical Networks," in *Proc. 6th*

ICST International Conference on Broadband Communications, Networks and Systems, BROADNETS 2009, Madrid, Spain, Sept. 2009.

[38] R. Aparicio-Pardo, P. Pavon-Marino, N. Skorin-Kapov, B. Garcia-Manrubia, and J. Garcia-Haro, "Algorithms for virtual topology reconfiguration under multi-hour traffic using Lagrangian relaxation and Tabu Search approaches," in *Proc. 12th International Conference on Transparent Optical Networks, ICTON 2010*, Munich, Germany, June 2010, p. We.B1.2, invited paper.

[39] P. Pavon-Marino, B. Garcia-Manrubia, and R. Aparicio-Pardo, "Multi-hour network planning based on domination between sets of traffic matrices," *Computer Networks*, vol. 55, no. 3, pp. 665-675, Feb. 2011.

[40] R. Aparicio-Pardo, N. Skorin-Kapov, P. Pavon-Marino, and B. Garcia-Manrubia, "(Non)-Reconfigurable Virtual Topology Design under Multi-hour Traffic in Optical Networks," *IEEE/ACM Transactions On Networking*, under review.

[41] G. Oriolo, "Domination between traffic matrices," *Mathematics of Operations Research*, vol. 33, no. 1, pp. 91-96, Feb. 2008.

[42] S. E. Terblanche, "Contributions towards survivable Network Design with Uncertain Traffic Requirements," Ph.D. dissertation, School of Computer, Statistical and Mathematical Sciences, Potchefstroom Campus, North-West University, South Africa, 2008.

[43] P. Pavon-Marino, M. Pioro, "On total traffic domination in non-complete graphs", *Operations Research Letters* vol. 39, no. 1, pp. 40-43, January 2011.

[44] S. Rumley, C. Gaumier, R. Aparicio-Pardo, C. H. Chang, W. Colitti, B. Garcia-Manrubia, P. Kourtessis, J. Martinez-Leon, A. Nowe, P. Pavon-Marino, J. Scharf, and K. Steenhaut, "Software Tools and Methods for Research and Education in Optical Networks," in *Lecture Notes in Computer Science*, vol. 5412, Towards Digital Optical Networks, C*OST Action 291 Final Report. I. T*omkos, M. Spyropoulou, K. Ennser, M. Köhn, and B. Mikac, Eds. Springer Berlin / Heidelberg, 2009, pp. 331-364.

[45] P. Pavon-Marino, R. Aparicio-Pardo, B. Garcia-Manrubia, and J.-L. Izquierdo-Zaragoza, "MatPlanWDM: A MATLAB-based educational tool for Communication Networks Planning courses," *Computer Applications in Engineering Education*, 2011, submitted.

[46] MatPlanWDM, Web Site, [Online], Available: http://ait.upct.es/~ppavon/matplanwdm/ Accessed 18 January 2011.

[47] R. Aparicio-Pardo, *Optimización de redes WDM de conmutación de lightpaths mediante modelos de programación lineal entera-mixta*, MSc Final Year Project, Universidad Politécnica de Cartagena, 2006.

[48] G. Moreno-Munoz, *Herramienta MATPLANWDM para Optimización en Redes WDM de Conmutación de Lightpaths*, MSc Final Year Project, Universidad Politécnica de Cartagena, 2006.

[49] P. Pavon-Marino, R. Aparicio-Pardo, G. Moreno-Munoz, J. Garcia-Haro, and J. Veiga-Gontan, "MatPlanWDM: An Educational Tool for Network Planning in Wavelength-Routing Networks," in *Lecture Notes in Computer Science*, vol. 4534, *Optical Network Design and Modeling, 11th International IFIP TC6 Conference, ONDM 2007, Athens, Greece, May 29-31, 2007. Proceedings*. I. Tomkos, F. Neri, J. Solé-Pareta, X. Masip-Bruin, and S. Sánchez-López, Eds. Springer Berlin / Heidelberg, 2007, pp. 58-67.

[50] P. Pavon-Marino, R. Aparicio-Pardo, B. Garcia-Manrubia, and J. Garcia-Haro, "WDM networks planning under multi-hour traffic demand with the MatPlanWDM tool," in *Proc. Industry Track "Simulation Works" collocated with 1st International ICST Conference on Simulation Tools and Techniques for Communications, Networks and System*, Marseille, France, Mar. 2008.

[51] P. Pavon-Marino, B. Garcia-Manrubia, R. Aparicio-Pardo, J. Garcia-Haro, and G. Moreno-Munoz, "An educational RWA network planning tool for dynamic flows," in *Proc. 12th International IFIP Conference on Optical Network Design and Modeling, ONDM 2008*, Vilanova i la Geltru, Spain, Mar. 2008, pp. 235-240.

[52] B. Garcia-Manrubia, *Planificación de redes ópticas wavelength-routing con demanda dinámica de tráfico*, MSc Final Year Project, Universidad Politécnica de Cartagena, 2007.

[53] TOMLAB Optimization, Web Site, [Online], Available: http://tomopt.com/ Accessed 09 December 2010.

[54] GNU Linear Programming Kit, Web Site, [Online], Available: http://www.gnu.org/software/glpk/ Accessed 09 December 2010.

[55] X. Zhang, C. Qiao, "Wavelength Assignment for Dynamic Traffic in Multi-fiber WDM Networks," in *Proc. 7th Int. Conference on Computer Communications and Networks*, pp. 479-485, Lafayette, LA, USA, Oct 1998.

[56] S. Xu, L. Li and S. Wang, "Dynamic routing and assignment of wavelength algorithms in multifiber wavelength division multiplexing networks," *IEEE J. Select Areas Commun.*, vol. 18, no. 10, Oct. 2000, pp. 2130–2137.

[57] L. Li, A. K. Somani, "Blocking performance of fixed-paths least-congestion routing in multifibre WDM networks," *International Journal of Communication Systems*, vol. 15, pp. 143–159, 2002.

[58] D. Zhemin and M. Hamdi, "On the Application of the Blocking Island Paradigm in All-Optical Networks," *IEEE Transactions on Communications*, vol. 51, no. 10, pp. 1690-1699, Oct. 2003.

[59] A. Jaekel and Y. Chen, "Dynamic Lightpath Allocation in Survivable Multifiber WDM Netwoks," in *Proc. 3rd International Conference on Broadband Communications, Networks and Systems (BROADNETS)*, San Jose, CA, Oct. 2006.

[60] Jong-Seon Kim, D. C. Lee, J. Sridhar, "Route-Metric-Based Dynamic Routing and Wavelength Assignment for Multifiber WDM Networks," *IEEE J. Select Areas Commun.*, vol. 24, no. 12, pp. 56-68, Dec. 2006

[61] S. Baroni and P. Bayvel, "Wavelength requirements in arbitrarily connected wavelength-routed optical networks," J. Lightwave Technol., vol. 15, pp. 242–251, Feb. 1997.

[62] I. de Miguel, F. González, J. C. Aguado, P. Fernández, R. M. Lorenzo, J. Blas, E. J. Abril, M. López, "An iterative algorithm for routing and wavelength assignment in multifiber WDM optical networks," in *Long-Haul and Access Networks, Optical Metro and WDM*, IOS-Press, 2001, pp. 79-85.

[63] A. Dacomo, S. De Patre, G. Maier, A. Pattavina, M. Martinelli, "Design of Static Resilient WDM Mesh Networks with Multiple Heuristic Criteria," in *Proc. IEEE INFOCOM 2002*, vol. 3, pp. 1793-1802, New York, June 2002.

[64] M. Tornatore, G. Maier, and A. Pattavina, "WDM network optimization by ILP based on Source Formulation," in *Proc. IEEE INFOCOM 2002*, vol. 3, pp. 1813-1821, New York, June 2002.

[65] A. Zalesky, H. Vu, M. Zukerman, C. Leckie and I. Ouveysi, "Routing and Wavelength Assignment over Multi-Fiber Optical Networks with No Wavelength Conversion," in *Proc. Proceedings of the Seventh IFIP Working Conference on Optical Network Design & Modeling (ONDM 2003)*, pp. 3-5, Feb, 2003, Budapest, Hungary.

[66] M. Saad and Zhi-Quan Luo, "On the Routing and Wavelength Assignment in Multifiber WDM Networks," *IEEE Journal on Selected Areas in Communications*, vol. 22, no. 9, pp. 1708-1717, Nov. 2004.

[67] A. Concaro, S. De Patre, G. Maier, M. Tornatore, "Optimization algorithms for WDM optical network dimensioning," in *Proc. Conference on Optical Network Design and Modeling (ONDM'05)*, Milan, Italy, Feb. 2005, pp. 141- 151.

[68] Z.M. Wali, K.M.F. Elsayed, A.-K.S.O. Hassan, "Static RWA in All-Optical Network under Multifiber, Multiple Requests Assumption," in *Proc. Intl. Conference on Computer Engineering and Systems*, Nov. 2006, pp. 172-177.

[69] M Tornatore, G Maier, A Pattavina, "Variable Aggregation in the ILP Design of WDM Networks with Dedicated Protection", *Journal of Communications and Networks*, Vol.9, No. 4, pp. 419-427, Dec. 2007.

References

[70] NOBEL phase 2 –Deliverable D 2.4. “Migration Guidelines with Economic Assessment and New Business Opportunities Generated by NOBEL phase 2”: http://www.ist-nobel.org/Nobel2/imatges/D2.4_final%20version.pdf.

[71] S. Pachnicke, T. Paschenda, and P. Krummrich, “Assessment of a constraint-based routing algorithm for translucent 10 Gbits/s DWDM networks considering fiber nonlinearities”, *OSA Journal of Optical Networking*, Vol. 7, No. 4, pp. 365-377, April 2008.

[72] K. Christodoulopoulos, K. Manousakis, and E. Varvarigos, "Offline Routing and Wavelength Assignment in Transparent WDM Networks," *IEEE/ACM Transactions on Networking*, vol. 18, no. 5, pp. 1557-1570, Oct. 2010

[73] J. Strand, A., Chiu and R. Tkach, "Issues for Routing in the Optical Layer", *IEEE Communications Magazine*, vol. 39, no. 2, pp. 81-88, Feb. 2001.

[74] B. Ramamurthy, D. Datta, H. Feng, J. P. Heritage, and B. Mukherjee, “Impact of transmission impairments on the teletraffic performance of *w*avelength-routed optical networks,” *IEEE Journal of Lightwave Technology*, vol. 17, no. 10, pp. 1713–1723, Oct. 1999.

[75] B. Mukherjee, *Optical WDM Networks*, Springer Science+Business Media, Inc., New York, 2006, pp. 729-732

[76] R. Cardillo, V. Curri, and M. Mellia, “Considering transmission impairments in wavelength routed optical networks,” in*Proc. Conference on Optical Network Design and Modeling (ONDM’05)*, Milan, Italy, Feb. 2005, pp. 421–429.

[77] T. Tsuritani et al., “Optical path computation element interworking with network management system for transparent mesh networks,” in *Proc. OFC/NFOEC 2008*, San Diego, USA, Mar. 2008.

[78] P. Kulkarni, A. Tzanakaki, C. Mas Machuka, and I. Tomkos, “Benefits of Q-factor based routing in WDM metro networks,” in *Proc. European Conference Optical Communications*, Glasgow, U.K., 2005, vol. 4, pp. 981- 982.

[79] G. Markidis, S. Sygletos, A. Tzanakaki, and I. Tomkos, “Impairment Aware Based Routing and Wavelength Assignment in Transparent Long Haul Networks,” in *Proc. IFIP Int. Conf. Optical Network Design and Modelling*, Athens, Greece, 2007, pp. 48-57.

[80] M. A. Ezzahdi, S. A. Zahr, M. Koubaa, N. Puech, and M. Gagnaire, “LERP: A Quality of transmission dependent heuristic for routing and wavelength assignment in hybrid WDM networks,” in *Proc. ICCCN 2006*, Virginia, USA, 2006, pp. 125–136.

[81] A. Morea, N. Brogard, F. Leplingard, J.C. Antona, T. Zami, B. Lavigne, and D. Bayart, “QoT function and A* routing an optimized combination for connection search in translucent networks,” *OSA Journal of Optical Networking*, vol. 7, no. 1, pp. 42-61, Jan. 2008.

[82] M. Yannuzzi, M. Quagliotti, G. Maier, E. Marin-Tordera, X. Masip-Bruin, S. Sanchez-Lopez, J. Sole-Pareta, W. Erangoli, and G. Tamiri, “'Performance of translucent optical networks under dynamic traffic and uncertain physical-layer information,” in *Proc. IFIP/IEEE ONDM 2009*, Braunschweig, Germany, Feb. 2009.

[83] K. Christodoulopoulos, K. Manousakis, E. Varvarigos, “Cross Layer Optimization of Static Lightpath Demands in Transparent WDM Optical Networks,” in *Proc. IEEE ITW Netw. Inf. Theory*, pp. 115-119 , Greece, June 2009.

[84] V. T. Cartaxo, “Cross-phase modulation in intensity modulation-direct detection WDM systems with multiple optical amplifiers and dispersion compensators,” *IEEE Journal of Lightwave Technology*, vol. 17, no. 2, pp. 178–190, Feb. 1999.

[85] S. Pachnicke, J. Reichert, S. Spälter, E. Voges, “Fast analytical assessment of the signal quality in transparent optical networks”, *IEEE/OSA Journal of Lightwave Technology*, vol. 24, no. 2, pp. 815–824, Feb. 2006.

[86] W. Zeiler, F. Di Pasquale, P. Bayvel, and J. E. Midwinter, “Modelling of four-wave mixing and gain peaking in amplified WDM optical communication systems and networks,” *IEEE Journal of Lightwave Technology*, vol. 14, no. 9, pp. 1933–1942, Sep. 1996.

[87] K. Inoue, K. Nakanishi, and K. Oda, "Crosstalk and power penalty due to fiber four-wave mixing in multichannels transmissions," *IEEE Journal of Lightwave Technology*, vol. 12, no. 8, pp. 1423–1439, Aug. 1996.

[88] C. D. Cantrell, "Transparent optical metropolitan-area networks," in *Proc. 16th Annual Meeting IEEE/Laser Electro Optics Society*, Tucson, AZ, 2003, vol. 2, pp. 608–609.

[89] S. Norimatsu and M. Maruoka, "Accurate Q-factor estimation of optically amplified systems in the presence of waveform distortion," *IEEE Journal of Lightwave Technology*, vol. 20, no. 1, Jan. 2002.

[90] M. Gagnaire and S. Al Zahr, "Impairment-aware routing and wavelength assignment in translucent networks: State of the Art," *IEEE Communications Magazine*, vol. 47, no. 5, pp. 55–61, May 2009.

[91] Y. Huang, J. Heritage, and B. Mukherjee, "Connection provisioning with transmission impairment consideration in opticalWDMnetworks with high-speed channels," *J. Lightw. Technol.*, vol. 23, no. 3, pp. 982–993, Mar. 2005.

[92] R. Cardillo, V. Curri, and M. Mellia, "Considering transmission impairments in wavelength routed optical networks," in *Proc. ONDM*, 2005, pp. 421–429.

[93] T. Deng, S. Subramaniam, and J. Xu, "Crosstalk-aware wavelength assignment in dynamic wavelength-routed optical networks," in *Proc. Broadnets*, 2004, pp. 140–149.

[94] V. Anagnostopoulos, C. Politi, C. Matrakidis, and A. Stavdas, "Physical layer impairment aware wavelength routing algorithms based on analytically calculated constraints," *Opt. Commun.*, vol. 270, no. 2, pp. 247–254, Feb. 2007.

[95] J. He, M. Brandt-Pearce, Y. Pointurier, and S. Subramaniam, "QoT aware routing in impairment-constrained optical networks," in Proc. *IEEE Globecom*, 2007, pp. 2269–2274.

[96] I. Tomkos, D. Vogiatzis, C. Mas, I. Zacharopoulos, A. Tzanakaki, and E. Varvarigos, "Performance engineering of metropolitan area optical networks through impairment constraint routing," *IEEE Communications Magazine*, vol.42, no.8, Aug. 2004.

[97] A.M. Hamad, and A.E. Kamal, "Routing and wavelength assignment with power aware multicasting in WDM networks," in *Proc. Int. Conf Broadband Networks*, Boston, MA, 2005, vol.1, pp. 31-40.

[98] A. Szodenyi, S. Zsigmond, B. Megyer, and T. Cinkler, "Design of traffic grooming optical virtual private networks obeying physical limitations," in *Proc. IFIP/IEEE Int. Conf. Wireless and Optical Communications Networks*, Dubai, United Arab Emirates, 2005, pp. 221-225.

[99] F. Cugini, F. Paolucci, L. Valcarenghi, and P. Castoldi, "Implementing a Path Computation Element (PCE) to encompass physical impairments in transparent networks," in *Proc. Optical Fiber Communication Conf. and Exposition and Nat. Fiber Optic Engineers Conf.* Anaheim, CA, 2007, pp. 1-3.

[100] A. E. Ozdaglar and D. P. Bertsekas, "Routing and wavelength assignment in optical networks," *IEEE/ACM Trans. Netw.*, vol. 11, no. 2, pp. 259–272, Apr. 2003.

[101] K. Christodoulopoulos, K. Manousakis, and E. Varvarigos, "Comparison of routing and wavelength assignment algorithms in WDM networks,"in *Proc. IEEE Globecom*, New Orleans, Dec. 2008, pp. 1–6.

[102] Internet 2 Global Research Network Operations Center, Web Site, [Online], Available: http://www.abilene.iu.edu/

[103] L. Wuttisittikulkij, M.J. O'Mahony, "Design of a WDM network using a multiple ring approach", in *Proc. IEEE Global Telecommunications Conference*, Phoenix, AZ, 1997, vol. 1, pp. 551-555.

[104] R.S. Cahn, *Wide Area Network design. Concepts and tools for optimization*, San Francisco, CA: Morgan Kaufmann Publishers Inc., 1998.

[105] J. Berthold, A. A. M. Saleh, L. Blair, and J. M. Simmons, "Optical Networking: Past, Present, and Future," *Journal of Lightwave Technology*, vol. 26, no. 9, pp.1104-1118, May 2008.

References

[106] A. Lemus, "Optical Digital Communications Technology and Modulation Formats," Resource document. Strata light Communications, 2008: http://www.nsc.liu.se/nsc08/pres/lemus.pdf. Accessed 09 December 2010.

[107] A. Nag, M. Tornatore, "Optical network design with mixed line rates," *Optical Switching and Networking*, vol. 6, no. 4, pp. 227–234, 2009

[108] G. Charlet, H., Mardoyan, P., Tran, M., Lefrancois, S., Bigo, "Nonlinear Interactions Between 10Gb/s Channels and 40Gb/s Channels with either RZ-DQPSK or PSBT Format, over Low-Dispersion Fiber," in *Proceedings of ECOC'06*, paper Mo.3.2.6, Cannes, France, 2006

[109] M. Lefrancois, F., Houndonougbo, T., Fauconnier, G., Charlet, S., Bigo, "Cross comparison of the nonlinear impairments caused by 10Gbit/s neighboring channels on a 40Gbit/s channel modulated with various formats, and over various fiber types," in *Proceedings of OFC/NFOEC'07*, paper JThA4p4, Anaheim, CA, 2007

[110] T. Wuth, M. Chbat, V. Kamalov, "Multi-rate (100G/40G/10G) transport over deployed optical networks," in *Proc. OFC/NFOEC'08*, San Diego, CA, 2008, paper NTuB3

[111] A. Tan, E. Pincemin, "Performance Comparison of Duobinary Formats for 40 Gbps and Mixed 10/40 Gbps Long-Haul WDM Transmission on SSMF and LEAF Fibers," *IEEE J. Lightw. Technol.*, vol. 27, no. 4, pp. 396-408, 2009

[112] J.P. Faure, B. Lavigne, C. Bresson, O. Bertran-Pardo, A.C. Colomer, R. Canto, "40G and 100G deployment on 10G Infrastructure: market overview and trends, Coherent versus Conventional technology," in *Proc. OFC/NFOEC'10*, San Diego, CA, 2010, paper OThE3

[113] J. Renaudier, O. Bertran-Pardo, H. Mardoyan, P. Tran, G. Charlet, S. Bigo, M. Lefrancois, B. Lavigne, J.L. Auge, L. Piriou, O. Courtois, "Performance comparison of 40G and 100G coherent PDM-QPSK for upgrading dispersion managed legacy systems," in Proc. *OFC/NFOEC'09*, San Diego, CA, 2009, paper NWD5

[114] O. Rival, A. Morea, "Elastic optical networks with 25–100G format-versatile WDM transmission systems," in Proc. *IEICE OptoElectronics and Communications Conference* (*OECC'10*), Sapporo, Japan, 2010, pp. 100-101

[115] Next-generation Electro-Optics Technology with Coherent Detection: Addressing the Challenge of Capacity Growth in Optical Networks. Technology white paper. Alcatel Lucent (2010). http://www.alcatel-lucent.com/wps/PA_1_A_9C1/DocumentDownloadFormServlet?LMSG_CABINET=Docs_and_Resource_Ctr&LMSG_CONTENT_FILE=White_Papers/100G_Next_Generation_Coherent_Technology_TechWhitePaper.pdf&lu_lang_code=en_WW. Accessed 19 January 2011.

[116] G. Charlet, J. Renaudier, P. Brindel, P. Tran, H. Mardoyan, O. Bertran-Pardo, M. Salsi, S. Bigo, "Performance comparison of DPSK, P-DPSK, RZ-DQPSK and coherent PDM-QPSK at 40Gb/s over a terrestrial link," in *Proc. OFC/NFOEC'09*, San Diego, CA, 2009, paper JWA40

[117] O. Vassilieva, T. Hoshida, J. C. Rasmussen, T. Naito: Symbol rate dependency of XPM-induced phase noise penalty on QPSK-based modulation formats, in *Proc. ECOC'08*, Brussels, Belgium, 2008, paper We.1.E.4

[118] M. R. Phillips, S. L. Woodward, R. L. Smith, "Cross-Polarization Modulation: Theory and Measurement in Subcarrier-Modulated WDM Systems," *IEEE J. Lightw. Technol.*, vol. 24, no. 11, pp. 4089-4099, 2006

[119] A. Bononi, P. Serena, N. Rossi, D. Sperti, "Which is the Dominant Nonlinearity in Long-haul PDM-QPSK Coherent Transmissions?", in *Proc. ECOC'10*, Torino, Italy, 2010, paper Th.10.E.1.

[120] S. Zsigmond, D. Mazroa, H. Furukawa, N. Wada, "Limitation of Spectral Efficient Modulation Formats for Circuit and Packet Switched Networks," in *Proc. IEICE OptoElectronics and Communications Conference (OECC'10)*, Sapporo, Japan, 2010, pp. 598-599

[121] N. Zulkifli, K. Guild, "Moving towards upgradeable all-optical networks through impairment-aware RWA algorithms," in *Proc. OFC/NFOEC'07*, Anaheim, CA, 2007, paper OWR3

[122] M. Batayneh, D.A. Schupke, M. Hoffmann, A. Kirstadter, B. Mukherjee, "Optical Network Design for a Multiline-Rate Carrier-Grade Ethernet Under Transmission-Range Constraints," *IEEE J. Lightw. Technol.*, vol. 26, no. 1, pp. 121-130, 2008.

[123] M. Liu, M. Tornatore, B. Mukherjee, "New and Improved Strategies for Optical Protection in Mixed-Line-Rate WDM Networks," in *Proc. of OFC/NFOEC'10*, paper OWH2, San Diego, CA, 2010.

[124] R. K. Ahuja, T. Magnanti, and J. B. Orlin, *Network Flows: Theory, Algorithms, and Applications*, Prentice Hall, 1993, pp. 4–8

[125] L. Kleinrock, *Queueing systems: Computer applications*, vol. 2, Wiley, New York, 1976.

[126] S. Uhlig, B. Quoitin, J. Lepropre, S. Balon, "Providing public intradomain traffic matrices to the research community," *ACM SIGCOMM Computer Communication Review*, vol. 36, no. 1, pp. 83-86, January 2006

[127] I. Baldine and G. N. Rouskas, "Traffic adaptive WDMnetworks:A study of reconfiguration issues," *Journal of Lightwave Technology*, vol. 19, pp. 433–455, Apr. 2001.

[128] G. R. Ash, R. H. Cardwell, and R. P. Murray, "Design and optimization of networks with dynamic routing," *Bell Systems Technical Journal*, vol. 60, pp. 1787-1820, Oct. 1981.

[129] E. Rosenberg, "A nonlinear programming heuristic for computing optimal link capacities in a multi-hour alternate routing communications network," *Operations Research*, vol. 35, no. 3, pp. 354-364, May 1987.

[130] A. Girard, P. D. Lansard, B. Liau, A. M. Mongeon, and J. L. Thibault, "Multihour engineering and traffic routing optimization in hierarchical telephone networks," *Annals of Telecommunications*, vol. 46, no. 5, pp. 335-350, May 1991.

[131] D. Medhi and S. Guptan, "Network dimensioning and performance of multiservice, multirate loss networks with dynamic routing," *IEEE/ACM Transactions on Networking*, vol. 5, no. 6, pp. 944-957, Dec. 1997.

[132] A. Amiri, "The multi-hour bandwidth packing problem with response time guarantees," *Information Technology and Management*, vol. 4, no. 1, pp. 113-127, Jan. 2003.

[133] A. Dutta, "Capacity planning of private networks using DCS under multibusy-hour traffic," *IEEE Transactions on Communications*, vol. 42, no. 7, pp. 2371-2374, Jul. 1994.

[134] D. Medhi, "Multi-hour, multi-traffic class network design for virtual path-based dynamically reconfigurable wide-area ATM networks," *IEEE/ACM Transactions on Network*, vol. 3, no. 6, pp. 809-818, 1995.

[135] D. Medhi and D. Tipper, "Some approaches to solving a multihour broadband network capacity design problem with single-path routing," *Telecommunication Systems*, vol. 13, no. 2-4, pp. 269-291, Jul. 2000.

[136] I. Ouveysi and Y. K. Tham, "Network design for multi-hour traffic profile," in *Proc. Australian Telecommunication Networks and Applications Conference '95*, Clayton, Victoria, Australia, pp. 1-6, Dec. 1995.

[137] K. Chari, "Multi-hour design of computer backbone networks," *Telecommunication Systems*, vol. 6, no. 1, pp. 347-365, Dec. 1996.

[138] W. Ben-Ameur, "Multi-hour design of survivable classical IP networks," *International Journal of Communication Systems*, vol. 15, no. 6, pp. 553-572, Jun. 2002.

[139] B. G. Józsa, D. Orincsay, and L. Tamasi, "Multi-hour design of dynamically reconfigurable MPLS networks, D. Hutchison, T. Kanade, J. Kittler, J. Kleinberg, A. Kobsa, F. Mattern, J. C. Mitchell, M. Naor, O. M. Nierstrasz, C. Pandu Rangan, B. Steffen, M. Sudan, D. Terzopoulos, J. D. Tygar and G. Weikum, Eds. *Lecture notes in computer science*, vol. 3042, pp. 502-513, Apr. 2004.

[140] N. Maxemchuk, I. Ouveysi, and M. Zukerman, "A Quantitative Measure for Telecommunications Networks Topology Design," IEEE/ACM Transactions on Networking, vol. 13, no. 4, pp. 731-742, Aug. 2005.

References

[141] G. Rouskas, M. H. Ammar, “Dynamic Reconfiguration in Multihop WDM Networks,” *Journal of High Speed Networks*, vol. 4, no. 3, pp. 221-238, 1995.

[142] A. Gencata, B. Mukherjee, “Virtual-Topology Adaptation for WDM Mesh Networks under Dynamic Traffic,” *IEEE/ACM Transactions on Networking*, vol. 11, no. 2, pp. 236-247, Apr. 2003.

[143] D. Banerjee, B. Mukerjee, “Wavelength-Routed Optical Networks: Linear Formulation, Resource Budgeting Tradeoffs, and a Reconfiguration Study,” *IEEE/ACM Transactions on Networking*, vol. 8, pp. 598-607, 2000.

[144] B. Ramamurthy, A. Ramakrishnan, “Virtual Topology Reconfiguration of Wavelength-Routed Optical WDM Networks,” *IEEE Globecom 2000*, 2000.

[145] K. Liu, C. Liu, J. Pastor, A. Roy, J. Wei, “Performance and Testbed Study of Topology Reconfiguration in IP over Optical Networks,” *IEEE Transactions on communications*, vol. 50, no. 10, pp. 1662-1679, Oct. 2002.

[146] J. Kuri, N. Puech, M. Gagnaire, E. Dotaro, and R. Douville, “Routing and wavelength assignment of scheduled lightpath demands,” *IEEE Journal on Selected Areas in Communications*, vol. 21, pp. 1231–1240, Oct. 2003.

[147] N. Skorin-Kapov, “Heuristic algorithms for the routing and wavelength assignment of scheduled lightpath demands in optical networks,” *IEEE Journal on Selected Areas in Communication*, vol. 24, pp. 2–15, 2006.

[148] J. Kuri, N. Puech, and M. Gagnaire, “Diverse routing of scheduled lightpath demands in an optical transport network,” in *Proc. Design of Reliable Communication Networks (DCRN2003)*, pp. 69–76, Oct. 2003.

[149] C. V. Saradhi, L. K. Wei, and M. Gurusamy, “Provisioning fault-tolerant scheduled lightpath demands in WDM mesh networks”, in *Proc. of BroadNets 2004*, San Jose, Cal. USA, pp. 150-159, Oct. 2004.

[150] B. Wang, T. Li., C. Xin, X. Zhang, “On survivable service provisioning in WDM networks under a scheduled traffic model”, in *Proc. of Globecom 2005*, St. Louis, MO, USA , pp. 1900-1904, Nov.-Dec. 2005.

[151] B. Wang, T. Li., X. Luo, Y. Fan and C. Xin, ”On service provisioning under a scheduled traffic model in reconfigurable WDM optical networks“ in Proc. Of BroadNets 2005, Boston, USA, pp 13-22, Oct. 2005.

[152] C. V. Saradhi, M. Gurusamy,and R. Piesiewicz, “Routing fault-tolerant sliding scheduled traffic in WDM optical mesh networks” in *Proc. of BroadNets 2008*, London, UK, pp.197-202, Sept. 2008.

[153] A. Jaekel, Y. Chen, “Resource provisioning for survivable WDM networks under a sliding cheduled traffic model”, *Optical Switching and Networking*, Vol. 6, pp. 44-54, 2009.

[154] A. Aggarwal, A. Bar-Noy, D. Coppersmith, R. Ramaswami, B. Schieber, M. Sudan, "Efficient routing and scheduling algorithms for optical networks," in *Proceedings of 5th annual ACM-SIAM symposium on Discrete algorithms*, Arlington, VA, USA, 2004, pp. 412-423.

[155] M. Pioro and D. Medhi, *Routing, Flow and Capacity Design in Communication and Computer Networks*. San Francisco, CA: Morgan Kaufmann, 2004, pp. 178–184.

[156] J. Milbrandt, M. Menth, S. Kopf, “Adaptive Bandwidth Allocation: Impact of Traffic Demand Models for Wide Area Networks,” in *Proc. 19th International Teletraffic Congress* (*ITC19*), Beijing, China, 2005.

[157] W. Ben-Ameur, H. Kerivin, "Routing of uncertain traffic demands," Optimization and Engineering, vol. 6, no. 3, pp. 283-313, 2005.

[158] C. Chekuri, F.B. Shepherd, G. Oriolo, M.G. Scutella, "Hardness of robust network design," Networks, vol. 50, no. 1, pp. 50-54, August 2007

[159] W. Ben-Ameur, "Between fully dynamic routing and robust stable routing," in Proc. of Design and Reliable Communication Networks (DRCN’2007), La Rochelle, France, Oct. 2007.

[160] N. Goyal, N. Olver, F.B. Shepherd, "Dynamic vs. Oblivious routing in network design," in Proc. ESA, Copenhagen, Denmark, 2009, pp. 277-288.

[161] OPNET Technologies, Inc, http://www.opnet.com (last access: 11th January, 2011).

[162] http://www.rsoftdesign.com/products.php?itm=MetroWAND (last access: 11th January, 2011).

[163] http://www.optiwave.co.kr/product/optisystem.htm (last access: 11th January, 2011).

[164] B. Wen, N.M. Bhide, R.K. Shenai and K.M. Sivalingam, Optical Wavelength Division Multiplexing (WDM) Network Simulator (OWns): Architecture and Performance Studies, *SPIE Optical Networks Magazine Special Issue on Simulation, CAD, and Measurement of Optical Networks* **2** (2001), 1-21.

[165] http://www.isi.edu/nsnam/ns/, (last access: 11th January, 2011).

[166] http://www-x.antd.nist.gov/glass/ (last access: 11th January, 2011).

[167] F. Mouveaux, F. Lapeyrere and N. Golmie, *MERLIN, User's Manual and Programmer's Guide. Vs 1.0*. National Institute of Standards and Technology, (2000). Available: http://w3.antd.nist.gov/Hsntg/prd_merlin.html (last access: 11th January, 2011).

[168] Y. Zhang and Z. Ge, Finding critical traffic matrices, Proceedings of DSN'05, Yokohama, Japan, pp. 188- 197, Jun. 2005.

Durante esta tesis, el autor ha disfrutado de una ayuda predoctoral con referencia BES-2008-002437, dentro del Subprograma de Formación de Personal Investigador del Ministerio de Ciencia e Innovación, cofinanciado por el Fondo Social Europeo, en el marco del Plan Nacional de Investigación Científica, Desarrollo e Innovación 2008-2011.

El trabajo descrito en esta tesis ha sido realizado con el apoyo de los proyectos *BONE ("Building the Future Optical Network in Europe")*, una Red de Excelencia financiada por la Comisión Europea a través del 7º Programa Marco; el proyecto TEC2007-67966-01/TCM CONPARTE-1, financiado por el Ministerio de Ciencia e Innovación; y finalmente, ha sido desarrollado en el marco del "Programa de Ayudas a Grupos de Excelencia de la Región de Murcia" financiado por la Fundación Séneca, Agencia de Ciencia y Tecnología de la Región de Murcia (Plan Regional de Ciencia y Tecnología 2007/2010).

During the present thesis, the author has been granted a Ph D student fellowship with reference BES-2008-002437 of the Spanish Personnel Research Training Programme, in the framework of Spanish Plan of Research, Development and Innovation 2008-2011, funded by the Ministry of Science and Innovation of Spain and the European Social Fund.

The work described in this thesis was carried out with the support of the BONE-project ("Building the Future Optical Network in Europe"), a Network of Excellence funded by the European Commission through the 7th ICT-Framework Programme and the support of the Spanish project TEC2007-67966-C03-01/TCM (CON-PARTE-1), funded by the Ministry of Science and Innovation of Spain, and also developed in the framework of "Programa de Ayudas a Grupos de Excelencia de la Región de Murcia," funded by Fundación Séneca, (Plan Regional de Ciencia y Tecnología 2007/2010).